6-30-2016

Engineered Earthen Masonry Structures For Extreme Wind Loads

Mabel Cristina Cuellar-Azcarate
University of South Carolina

ENGINEERED EARTHEN MASONRY STRUCTURES FOR EXTREME WIND LOADS

by

Mabel Cristina Cuéllar-Azcárate

Bachelor of Science
Universidad del Valle, 2007

Master of Science
Universidad del Valle, 2010

Submitted in Partial Fulfillment of the Requirements

for the Degree of Doctor of Philosophy in

Civil Engineering

College of Engineering and Computing

University of South Carolina

2016

Accepted by:

Fabio Matta, Major Professor

Ece Erdogmus, Committee Member

Juan M. Caicedo, Committee Member

Sarah Gassman, Committee Member

Lacy Ford, Senior Vice Provost and Dean of Graduate Studies

DEDICATION

To God that was with me in each step of the way. He never left my side and helped me to overcome each obstacle. He put in my way all the tools and people that made this process easier.

To my parents for their unconditional love, tireless support, and constant encouragement. None of my life's successes would have been possible without you. I love you. (A mis padres por su amor sin condicion, su incansable apoyo y su constante estimulo. Nada de lo que he logrado en mi vida hubiera sido possible sin ustedes. Los amo)

To my wonderful husband, who is the best and has supported me in every step. Our beautiful little family is what gives me strength. To my son Connor that came at the end of this process to make my life full and happier.

To my parents in law for all your love and support.

ACKNOWLEDGEMENTS

I would like to express my deepest gratitude to my advisor, Dr. Fabio Matta, for dedication, patience, and support throughout these years. His valuable lessons in work and life have helped me to culminate this process with success.

I would like to thank my committee members, Dr. Ece Erdogmus, Dr. Juan M. Caicedo, and Dr. Sarah Gassman for their advice and taking the time to be active part of my PhD Committee.

The research presented in this dissertation is based upon work supported by the National Science Foundation under grants No. 1131161 and No. 1321489. The support of the University of South Carolina (USC) and the USC Department of Civil and Environmental Engineering through the Structures and Materials Laboratory, a SPARC Graduate Fellowship, a M. Bert Storey Endowed Graduate Fellowship, an ASPIRE-I award, and the Magellan Scholar Program, is gratefully acknowledged. Special thanks are extended to Dr. Michael Sutton and Mr. Sreehari Rajan (Ph.D student), Dr. Enrico Garbin (formerly Postdoctoral Fellow), and undergraduate research assistants Bradford DiFranco, Aaron Marshall, Tyler McElroy, Naron Phal and Christopher Boyer, for their assistance in preparing and conducting the experiments.

ABSTRACT

Stabilized earthen masonry (SEM), which is built with compressed stabilized earthen blocks (CSEB) and mortar, is emerging as a construction system for affordable, sustainable and high-quality dwellings. Compelling features of earthen masonry are local availability of suitable soils, thermal insulation properties, humidity control within healthy ranges, and relatively low carbon footprint. SEM is also appealing for the construction of affordable houses in rural areas and farmlands, where underrepresented and underprivileged groups often live. In fact, the lack of affordable housing is an issue across the United States where low-income families are most affected, often committing more than half of their income on housing. In addition, the low-income population tends to be more vulnerable to hazard events. For example, in the United States, high wind events, such as tornadoes and hurricanes, cause casualties and property damage. This is often due to the lack of adequate construction systems and practices. Although SEM has been used around the world for the construction of modest as well as high-end housing, the non-engineered nature of SEM materials and structures limits the use of SEM as a mainstream construction system, even more so for hazard-resistant dwellings. Filling the knowledge gap related to the structural behavior of the SEM, with an emphasis on extreme loads, is necessary to increase the confidence in and facilitate the acceptance of this affordable and sustainable masonry system.

Recent literature reported on the feasibility of using SEM in low-rise dwellings to withstand high wind loads. In addition, the lack of data on the mechanical and structural properties of stabilized earthen masonry, and the need for an experimentally characterized masonry prototype where strength and deformability properties and failure modes are verified, have been highlighted.

In this research, theoretically determined target strength ranges are used to guide the engineering and prototyping of an affordable and "green" SEM prototype. First, stabilized earthen blocks are prototyped using a silty loam soil, which is locally available in South Carolina as well as throughout the US "Tornado Alley". The blocks are stabilized with ordinary Portland cement (OPC) in amounts of 0%, 6% and 9% in weight of soil (wt%). Stabilization is required to ensure sufficient erosion resistance and, in general, durability. In addition, randomly distributed non-biodegradable and recyclable plastic fibers are incorporated in the soil matrix as a sustainable means to radically enhance the toughness of the earthen blocks, thereby making them attractive for toughening against the localized impact of wind-borne debris. The amount of fiber reinforcement was kept to a value of 0.5 wt%. It was shown that the addition of plastic fiber reinforcement radically changes the damage tolerance of the compressed and stabilized earth blocks (CSEBs). In fact, unreinforced CSEBs were transformed into earthen blocks with significant post-cracking deformability and residual strength due to the crack-bridging effect of well-distributed and embedded plastic fibers.

Once the block strength requirements were met, the designing of a compatible mortar that provides sufficient bond strength at the block-mortar interface was carried out. Then, two SEM prototypes that are engineered for high-wind resistance were

developed. The salient mechanical properties, obtained by load-testing masonry subassemblies, were used for the prototyping and mechanical characterization of SEM. First, a prototype built with unreinforced compressed earthen blocks and mortar that meets the strength requirements for high wind pressures is presented. The unreinforced SEM specimens were physically tested to characterize their structural response under compression, flexure and shear loading. Compressed earthen blocks with OPC in amounts of 0 wt%, 6 wt% and 9 wt% were combined with the selected mortar for the compression characterization of prisms and wallettes. The results from the compression tests were used to determine the combination of earthen blocks and mortar that provides the required strength to withstand high wind loads while minimizing the amount of OPC. Next, the selected combination of CSEB and mortar was characterized in flexure and shear. As a proof of concept, the strength values obtained for the unreinforced SEM are used for the analysis of a realistic EF3 tornado-resistant dwelling structure.

The second prototype, which is made with the plastic fiber-reinforced CSEBs paired with a mortar reinforced with low-cost plastic microfibers, aims to radically enhance the SEM damage tolerance and resist the impact of wind-borne debris. Subassemblies of fiber reinforced and stabilized earthen masonry (SREM) were used to evaluate the effect of fiber reinforcement on the in-plane and out-of-plane behavior of the masonry. The plastic fibers radically enhanced the tensile and shear strength of the block mortar interface, and the overall toughness of the earthen masonry. Finally, the results of two high-velocity flying-debris impact tests are presented to offer preliminary evidence of the impact resistance of the SREM prototype vis-à-vis its SEM counterpart.

TABLE OF CONTENTS

LIST OF TABLES

LIST OF FIGURES

LIST OF SYMBOLS

A	Transverse area of diagonal compression panel, in m^2
f_b	Compressive strength of earthen block, in MPa
f_c	Compressive strength of earthen masonry, in MPa
$f_{c,if}$	Compressive strength of masonry for in-plane flexural failure, in Pa
f_{es}	Shear strength of earth (mansonry), in MPa
f_m	Compressive strength of earthen mortar masonry, in MPa
f_s	Shear strength of masonry, in MPa
$f_{s,if}$	Shear strength of masonry for in-plane shear failure, in Pa
f_t	Tensile strength of masonry, in Pa
$f_{t,of}$	Tensile strength of masonry for out-of-plane flexural failure, in Pa
f_{vk}	Shear strength from diagonal triplet test, in MPa
f_{vo}	Shear strength at zero pre-compression, in MPa
H	Height of MWFRS walls, in m
K	Constant for the calculation of masonry compressive strength CEN (2005), in MPa
k_v	Shear factor indicating friction resistance along mortar bed joint
L_i	Length of wall i, in m
P	Compression load for diagonal compression test (assumed positive), in N
p_s	Net wind pressure, in Pa
t	Thickness of wall, in m

V Basic wind speed (3-s gust speed at 10 m above ground in Exposure C), in m/s

V_f Fiber volume fraction

ϕ Design strength reduction factor for designated failure mode

γ Specific weight of earthen masonry, in N/m^3

μ_c friction coefficient of the masonry

σ_D Axial compressive stress produced by self-weight of diaphragm and roof, in Pa

σ_i Combined axial stress produced by self-weight of masonry, diaphragm and roof, and wind uplift force in reference section of wall i, in Pa

σ_M Axial compressive stress produced by self-weight of masonry, in Pa

σ_W Axial tensile stress produced by wind uplift force, in Pa

σ_x compressive stress, in Pa

σ_o Compressive stress perpendicular to shear, in Pa

τ_i Shear stress produced by horizontal wind load in wall i, in Pa

τ_{xy} Shear stress, in Pa

List of Abbreviations

C ..... Unstabilized compressed earthen blocks (0wt% cement content)

CS6 ..... Compressed and stabilized earthen block with 6wt% cement content

CS9 ..... Compressed and stabilized earthen block with 9wt% cement content

CSEB ..... Compressed and stabilized earthen block

CRS6 ..... Compressed, stabilized and reinforced earthen blocks 6wt% cement content

CRS9 ..... Compressed, stabilized and reinforced earthen blocks 9wt% cement content

EDX ..... Energy-dispersive X-ray spectroscopy

MWFRS ..... Main wind force resisting system

OMC ..... Optimum moisture content

OPC ..... Ordinary Portland cement type I

PET ..... Polyethylene terephthalate

PVA ..... Polyvinyl alcohol

SEM (Masonry) ..... .Stabilized earthen masonry

SEM (Microscopy) ..... Scanning electron microscopy

SREM..Stabilized and reinforced earthen masonry

CHAPTER 1
INTRODUCTION

1.1 BACKGROUND

Stabilized earthen masonry, which is made of compressed and stabilized earthen blocks (CSEBs) and stabilized earthen mortar, is emerging as a construction material that pairs sustainability with durability, energy efficiency, and affordability. The appeal of stabilized earthen masonry (SEM) has prompted its use in numerous applications in developed countries ranging from modest to high-end houses (e.g., Germany, Italy, New Zealand, Switzerland, UK and US), including structural walls and vaults. Compelling features of SEM include the local availability and affordability of suitable soils (including well dispersed clay-rich soil in the U.S.), thermal insulation properties, humidity control and relatively small carbon footprint (Morton 2008). SEM is an alternative material for masonry construction that maximizes the use of local materials, minimizes transportation costs, and creates jobs. In the US, SEM is particularly appealing as a viable response to the lack of affordable housing that affects especially low-income families (Enterprise 2014). A striking example is the "Good Earth Lodges" program of the Crow Tribe of Native Americans in Montana, U.S (Figure 1.1). This initiative is the Crow Tribe's response to the energy-efficient housing demand of over 1,500 units (Good Earth Lodges 2012).

(a)

(b)

(c)

Figure 1.1 Crow Tribe's Good Earth Lodges operation: (a) block fabrication in local facility, MT; (b) construction; and (c) finished dwelling structure (right) replacing nearby trailer home (left). Credit: Thomas Bowen (a-b) and Patrick Bresnan (c).

SEM is often used for non-structural elements due to the lack of understanding of structural response, which is mainly due to the limited availability of hard evidence from

research on structural assemblies. Matta et al. (2015) found that it is feasible to use SEM for high-wind resistance in low-rise dwellings having wall thicknesses up to 400 mm, and providing rigid floor or roof diaphragms. This study intends to demonstrate that it is possible to manufacture SEM that is suitable for hazard mitigation in extreme wind regions. However, Matta et al. (2015) also highlighted the need to prototype and experimentally characterize a hazard-resistant SEM, where the defined target strength and failure modes are verified. Strength parameters are maximized by modifying the material and designing a combination of earthen blocks and mortar that yields an earthen masonry whose mechanical properties lend themselves to hazard resistant designs. For example, a low-performance earthen masonry can be transformed into a resilient and affordable system for low-rise dwellings in territories prone to extreme winds (including Florida, the Carolinas, and the "Tornado Alley"). These regions often include rural areas and farmlands, where underrepresented and underprivileged groups live and require sustainable and affordable dwellings.

The incorporation of small amounts of stabilizers, such as OPC, in the soil mix improves durability and strength. The post-cracking strength and deformability can be increased by incorporating well-dispersed fiber reinforcement (Yetgin et al. 2008; Lenci et al. 2011; Aymerich et al. 2012). Both structural strength and deformability are needed to withstand extreme wind loads where most casualties are due to the impact of wind-born debris (Marchigiani et al. 2014). Flying debris may impact walls at speeds up to 100 mph, with disastrous consequences especially on wood-frame and hollow-block masonry walls (Boruff et al. 2003; Li and Ellingwood 2006).

This study consists of three projects: (1) the first project aims at radically enhancing the strength and deformability of earthen blocks, through the addition of a small amount of ordinary Portland cement (OPC) and recyclable plastic fibers. (2) The second project aims at prototyping a combination of earthen blocks and mortar that provides suitable masonry strength based on theoretically set targets. Once the strength of the prototyped masonry is verified, the actual mechanical properties are used in the structural analysis of a representative low-rise dwelling subject to extreme wind pressures. (3) The third project aims at experimentally demonstrating the transformation of the masonry system as a result of incorporating low-cost plastic fiber reinforcement in the blocks and mortar, and verifying the earthen masonry resistance against the impact of flying debris.

1.2 OBJECTIVES

The overall goal of the research is to engineer and prototype an affordable and sustainable stabilized reinforced earthen masonry whose structural behavior makes it suitable for dwellings in high-wind prone areas. The specific objectives are:

1. Engineering compressed and stabilized earthen blocks through the addition of small amounts of cement and non-biodegradable plastic fibers, such that the strength and deformability of earthen masonry are transformed to resist extreme wind loads.
2. Prototyping and characterizing a SEM system using widely available local South Carolina soil to attain strength values that meet or exceed those required to resist extreme wind pressures.

3. Demonstrating the applicability of the prototype earthen masonry based on the structural analysis of representative low-rise dwellings subject to extreme wind loads, using experimentally validated mechanical properties.
4. Verifying damage tolerance of the prototype earthen masonry based on evidence from flexural, shear and wind-borne debris impact tests.

1.3 STATE OF THE ART

The main components of SEM are the earthen blocks and mortar, which should be produced with local soils. Feasibility depends on the availability of suitable soils. For the selection of suitable soils, some recommendations about the texture or particle distribution, plasticity and compressibility have been reported. The soil should have an adequate balance of clay, sand and silt in the range 5 - 70%, 20 - 80% and 10 - 35%, respectively (Jiménez Delgado and Guerrero 2007; Galan-Marin et al. 2010; Muntohar 2011). The plastic index and liquid limit are recommended in the ranges 16 - 28 and 32 - 46, respectively (Jiménez Delgado and Guerrero 2007).

As any other earth-based material, the main weaknesses of compressed earthen blocks are their susceptibility to shrinkage during the drying process, low durability, and low compressive and flexural strength. Additives, stabilizers and compaction (densification) processes are often used (Rafalko et al. 2007; Galan-Marin et al. 2010) for the enhancement of soil materials. A wide range of modifiers such as cement, lime, bitumen, organic products and natural and artificial fibers have been utilized (Bell 1996; Achenza and Fenu 2006; Venny Riza et al. 2010). Densification is necessary for the soil particles to form chemical bonds with the stabilizer (Horpibulsuk et al. 2010). In the study presented in this dissertation, ordinary Portland cement (OPC) was selected for the soil

stabilization. OPC is mistakenly assumed to be effective to stabilize soils with low plasticity, but it has been found that OPC is at least as effective as lime in stabilizing clayey soils having moderate to high plasticity (Prusinski and Bhattacharja 1999). The stabilization of CSEB is commonly done with small amounts of ordinary Portland cement (OPC). Research results on the stabilization of earthen blocks suggested that the compressive strength and durability of earthen blocks are improved by increasing the OPC content (Morel et al. 2007; Walker and Stace 1997). There is a tendency to use less than 10% of OPC content to control the costs and carbon footprint of the earthen blocks (Walker and Stace 1997, Venny Riza et al. 2010, Taallah et al. 2014). To complement the work of the cement stabilization, fibers are added to the soil mixture to limit the movement of the soil particles and control the cracking of the soil matrix caused by mechanical and thermal loads, and water erosion and penetration (Houben and Guillaud 1994).

The incorporation of fiber reinforcement to strengthen soils has been extensively investigated. In general, the addition of fibers in the soil matrix reduces cracking due to shrinkage and transverse expansion due to Poisson's effects (Ghavami et al. 1999; Binici et al. 2005; Bouhicha et al. 2005). Also, the fiber reinforcement improves the engineering properties of the soil composites in terms of post-cracking strength and deformability (Achenza and Fenu 2006; Tang et al. 2007; Aymerich et al. 2012). Natural fibers such as straw, coconut strands and sisal may result in significant water absorption and expansion during the mixing process. Consequently, the water content needs to be increased, which results in a less efficient load transfer between the fibers and the soil matrix, and strength reduction (Yetgin et al. 2008). The water absorbed by the fibers is

released at the end of the drying process, facilitating the formation of voids that negatively affect the strength of the fiber-soil interface, and the overall durability of the block. In addition, the use of water repellent materials to reduce absorption of water by natural fibers has been reported to be ineffective in improving bonding with the soil matrix (Ghavami et al. 1999).

In the study presented in this dissertation, non-biodegradable polyethylene terephthalate (PET), similar to that of plastic bottles, is selected for the fiber reinforcement for the earthen blocks. The beverage industry has widely spread the use of PET, of which only 31% is recycled in the U.S. (NAPCOR 2015). Therefore, the recycling of post-consumer PET bottles seems to be a viable source of low-cost non-biodegradable fiber reinforcement. Waste materials have been used previously to reinforce earthen blocks. Eko et al. (2012) observed that, when using salvaged steel fibers from used tires, reinforced earthen blocks subject to flexural loading display an enhanced post-cracking behavior. Subramania Prasad et al. (2012) reinforced stabilized earthen blocks with chopped plastic carry bags and beverage bottles. The former showed a beneficial effect on the compressive strength by increasing it up to 10%; while the fibers obtained from water bottles were found to be ineffective in enhancing the compressive strength. This was attributed to the dimensions and surface finish of the fibers, which result in insufficient bonding with the surrounding soil matrix. A plastic fiber content of 0.8% in weight of soil (wt%) is recommended as the maximum practical limit, due to a negative effect on the workability and uniform distribution in the soil matrix (Miller and Rifai 2004). With other fiber materials this number is found to be limited to 0.5 wt% due to reduction in the compressive strength when larger fiber

contents are used, introducing excessive discontinuities and possibly defects (Yetgin et al. 2008).

The selection of the mortar is a critical factor to obtain a high-performance earthen masonry system. It has been found that soil or lime mortars are more suitable for earthen block than conventional cement mortars (Walker and Stace 1997; Walker 1999; Sarangapani et al. 2005). Soil mortars offer better water retention and an improved contact due to better flow properties, which lead to better block-mortar interfaces. Sarangapani et al. (2005) concluded that masonry compressive strength increases when both flexural bond and shear bond strength are improved. This study suggests that the masonry compressive strength is more sensitive to the bond strength between blocks and mortar than the compressive strength of the mortar. Increasing the mortar compressive strength does not necessarily result in increased bond strength as much as other factors such as mortar type, clay content and block moisture content (Walker 1999).

Although the SEM components, earthen blocks and mortar, have been the subject of different investigations, the limited evidence on the behavior of earthen masonry assemblages somewhat restricts their use to non-structural elements. In this study, results of masonry compression tests are used to select the combination of earthen blocks and mortars that offers the better compromise between strength and carbon footprint (i.e., OPC content). Masonry compressive strength is the key parameter for the design of load bearing structures. In fact, design codes and standards, such as the MSJC (MSJC 2013) code in the US, the Eurocode 6 in Europe (CEN 2005), and the New Zealand NZS 4297 design code (NZS 4297 1998), express the masonry tensile and shear strength as a function of the masonry compressive strength. The SEM compressive strength depends

on the compressive strength of the earthen blocks and mortar. However, it has been reported that the mortar compressive strength has little influence on the masonry compressive strength. Walker (2004) observed that while the prism compressive strength can be correlated with the block strength, the mortar compressive strength has little influence on the prism compressive strength. Similar results were obtained by Venkatarama Reddy and Gupta (2006), where it was concluded that there is not a definite relationship between the mortar and masonry compressive strengths. In addition, the in-plane and out-of-plane behavior of earthen masonry are evaluated through shear and flexural tests, repectively. Triplet tests have been used to evaluate the effect of fiber reinforcement (Morel et al. 1999) and soil composition (Venkatarama Reddy et al. 2007) on the shear-bond strength. On the other hand, the diagonal compression test has been used on earthen masonry assemblies to evaluate the effect of different reinforcement alternatives. Turanli and Saritas (2011) found that adding a reinforcement mesh in the mortar joint results in increased shear strength in adobe panels. Lima et al. (2012) tested the effect sugar bagasse ash, added to the blocks and mortar, on earthen masonry, finding that it improves the compressive and shear strengths of the panels in comparison to the unreinforced specimens. Miccoli et al. (2014) evaluated the mechanical behavior of three types of earthen construction systems, based on diagonal compression tests. For the earth masonry, the authors found that wetting the earthen blocks, which in turn improves the integrity of the block-mortar interface, increases the diagonal compression strength in more than three times. The flexural test of the earthen masonry is key to study the behavior against out-of-plane loads, such as wind pressure. Often, masonry building codes recommend neglecting the flexural strength due its small value and high variability

(Walker 1999). However, Tennant et al. (2013) suggests allowing the use of experimental data for the flexural strength, since the earthen masonry resembles the behavior of traditional masonry. Similarly, Jayasinghe and Mallawaarachchi (2009) found that the flexural strength of earthen masonry has similar values to the recommended for burnt clay masonry. In fact, it is recommended considering the earthen masonry for external and internal load bearing walls. Although the earthen masonry shear and flexural strength have been characterized previously, the ratios between the shear and compressive strength, and flexural and compressive strength have not been studied for earthen masonry. Also, to the best of the authors' knowledge, no literature is available on CSEB masonry subjected to impact test.

1.4 METHODOLOGY

The methodology followed to engineer an affordable and energy efficient fiber reinforced earthen masonry for high wind regions is summarized in this section (Figure 1.2) and presented more extensively in the "Methodology" section of each chapter.

The results from the material characterization of compressed and stabilized earthen blocks are used to evaluate if the strength targets can be attained using a locally available soil that is also widely available in the U.S. (e.g., in the "Tornado Alley"). In addition, reinforcing fibers made of recyclable and non-biodegradable plastic are added to radically enhance the otherwise brittle post-cracking behavior of the blocks. The strengthening effect of stabilization and the toughening effect of the reinforcement are assessed through mechanical tests, scanning electron microscopy (SEM) images, and Energy Dispersive X-Ray Analysis (EDX) analysis.

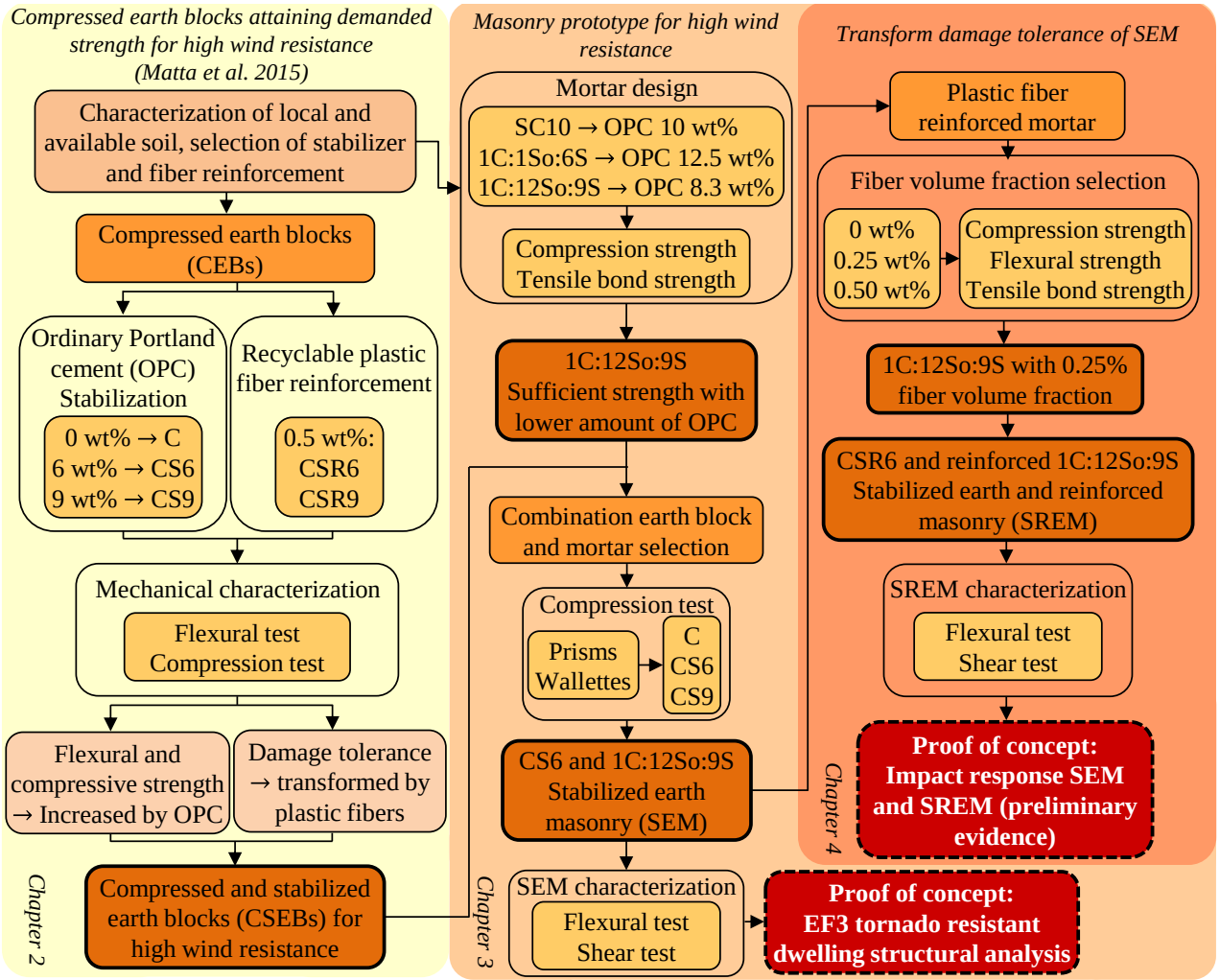

C: compressed. CS: compressed and stabilized. CSR: compressed, stabilized and reinforced. C:So:S (Cement:Soil:Sand)

Figure 1.2 Procedure for engineering an affordable and energy efficient fiber reinforced earthen masonry for high wind regions.

Once the required block strength is attained, a stabilized earthen masonry for high wind loads is prototyped. The prototyping process included the design and selection of a compatible mortar that provides quality bond. From the compressive strength characterization of the masonry, the best combination of block and mortar is selected. The resulting stabilized earthen masonry is mechanically characterized in flexure and shear. The strength results are then used as input for the analysis of a single-story dwelling structure subject to tornado loads based on the analytical framework introduced by Matta et al. (2015).

The plastic fiber reinforcement is incorporated in the SEM system to transform its post-cracking behavior, and thus its damage tolerance. Low-cost polyvinyl alcohol (PVA) microfibers are incorporated in the mortar. PVA microfibers have been previously used in the reinforcement of mortars, presenting a beneficial effect on the post-cracking behavior without affecting the compressive strength (Fanella and Naaman 1985, Skourup and Erdogmus 2010, Armwood et al 2011). The selection of the fiber volume fraction for the mortar is made based on the strength results from flexure, compression and shear bond tests. Then, the effect of the reinforcement on the in-plane and out-of-plane responses of the earthen masonry is assessed through shear and flexural load tests on masonry subassemblages, respectively. The proof of concept for transforming damage tolerance is demonstrated through preliminary evidence from high-velocity impact tests.

1.5 RESEARCH NOVELTY AND SIGNIFICANCE

The novel contributions of this study are offered by:

1. Radical transformation of the post-cracking behavior of compressed and stabilized earthen blocks by incorporating recyclable plastic fibers. The earthen blocks are produced utilizing a widely available soil in the US, and are stabilized with small amounts of OPC to enhance strength and durability. A novel and practical reinforcement based on non-biodegradable recycled plastic fibers, having dimensions that are suitable to effectively toughen the earthen blocks, is presented. The earthen blocks are transformed into a material that is capable to absorb energy after cracking, which is a key feature for the local and global behavior of hazard-resistant earthen masonry.

2. Prototyping and verifying a novel earthen masonry system that is designed to meet the load demands of a high wind event. Two novel masonry prototypes are proposed. This study is the first attempt to create an earthen masonry prototype with comprehensive and well-defined mechanical properties for load-bearing walls. The first prototype consists of stabilized earthen blocks with 6 wt% and mortar with 8.3 wt% of OPC. Then, the masonry system is reinforced with non-biodegradable and recyclable plastic fibers for transformed damage tolerance.

3. Radical enhancement of in-plane load capacity and post-cracking strength of the masonry due to the plastic reinforcement. The addition of plastic reinforcement in blocks and mortar results in the transformation of the in-plane behavior of the earthen masonry. The shear peak and post-cracking strength radically increase due primarily to the effect of the PVA fibers on the integrity of the block-mortar interface, and of the PET fibers

bridging the cracks, respectively. This makes the prototype masonry suitable to withstand other hazardous loads that require energy dissipation, such as earthquake loads. In addition, the ability to withstand loads after cracking makes the prototype fiber reinforced earthen masonry attractive also because it can provide additional post-hazard safety (e.g., against collapse).

4. Implementation of a framework for the structural analysis of an earthen masonry low rise dwelling. The framework proposed by Matta et al. (2015) is verified, refined with respect to the relation between masonry compressive, tensile and shear strength, and then used for the structural analysis of a low-rise tornado-resistant dwelling. The experimental data obtained for the SEM characterization are used to present a realistic example.

5. Experimental evidence on the earthen masonry response against wind-borne debris. For the first time, the results of impact experiments using 15-lb 2 x 4 in. studs launched at 137 km/h (85 mph) on SEM and SREM walls are presented as preliminary evidence of the earthen masonry performance against wind-borne debris.

1.6 OUTLINE OF DISSERTATION

In Chapter 2, earthen block prototypes produced with a locally available soil, are introduced based on results from load testing in flexure and compression to understand if the target strength for high-wind resistance is attained. The effect of incorporating plastic fibers, which are added to the soil matrix to transform the block toughness, is evaluated. Chapter 3 focuses on prototyping a compressed and stabilized earthen masonry for high-wind resistant dwelling structures. The salient mechanical properties are characterized

and compared with the requirements from available building codes. In addition, the experimental results are used as inputs for the structural analysis of a realistic low-rise tornado-resistant dwelling. The focus of Chapter 4 is on transforming the damage tolerance of the stabilized earthen masonry by incorporating recyclable plastic fiber reinforcement. The out-of-plane and in-plane structural behavior are evaluated based on physical experiments. Then, preliminary results from high-velocity impact tests are presented as a proof of concept for the transformation of the toughness of the earthen masonry system. Chapter 5 summarizes the conclusions drawn from the findings reported in Chapters 2 through 4, and offers recommendations for future research.

1.7 REFERENCES

Achenza, M., and Fenu, L. (2006). "On earth stabilization with natural polymers for earth masonry construction." *Materials and Structures*, 39(1), 21-27.

Armwood, C. K., Erdogmus, E., and Haider, H. (2011). "Effect of fibers on the flexural strength of masonry mortars." *The Masonry Society Journal*, 29(1), 18–32.

Aymerich, F., Fenu, L., and Meloni, P. (2012). "Effect of reinforcing wool fibres on fracture and energy absorption properties of an earthen material." *Construction and Building Materials*, 27(1), 66-72.

Bell, F. G. (1996). "Lime stabilization of clay minerals and soils." *Engineering Geology*, 42(4), 223-237.

Binici, H., Aksogan, O., and Shah, T. (2005). "Investigation of fibre reinforced mud brick as a building material." *Construction and Building Materials*, 19(4), 313-318.

Boruff, B.J., Easoz, J.A., Jones, S.D., Landry, H.R., Mitchem, J.D., and Cutter, S.L. (2003). "Tornado hazards in the United States." *Climate Research*, 24, 103-117.

Bouhicha, M., Aouissi, F., and Kenai, S. (2005). "Performance of composite soil reinforced with barley straw." *Cement and Concrete Composites*, 27(5), 617-621.

CEN (2005). "European Committee for Standardization. Eurocode 6 – Design of masonry structures – Part 1-1: General rules for reinforced and unreinforced masonry structures." BS EN 1996-1-1:2005. Brussels, Belgium:

Eko, R. M., Offa, E. D., Ngatcha, T. Y., and Minsili, L. S. (2012). "Potential of salvaged steel fibers for reinforcement of unfired earth blocks." *Construction and Building Materials*, 35, 340-346.

Enterprise (2014). " Impact of affordable housing on families and communities: a review of the evidence base." Enterprise Community Partners Inc, Columbia, MD 21044.

Fanella, D. A., and Naaman, A. E. (1985). "Stress-strain properties of fiber reinforced mortar in compression." *ACI Journal*, 82(4), 475–483.

Galán-Marín, C., Rivera-Gómez, C., and Petric, J. (2010). "Clay-based composite stabilized with natural polymer and fibre." *Construction and Building Materials*, 24(8), 1462-1468.

Ghavami, K., Toledo, R. D., and Barbosa, N. P. (1999). "Behaviour of composite soil reinforced with natural fibres." *Cement and Concrete Composites*, 21(1), 39-48.

Good Earth Lodges (2012). "The Crow Tribes – Compressed Earth Blocks Program, " http://goodearthlodges.crowtribe.com/ (accessed January 28, 2013).

Horpibulsuk, S., Rachan, R., Chinkulkijniwat, A., Raksachon, Y., and Suddeepong, A. (2010). "Analysis of strength development in cement-stabilized silty clay from microstructural considerations." *Construction and Building Materials*, 24(10), 2011-2021.

Houben, H., and Guillaud, H. (1994). *Earth construction: a comprehensive guide*, Intermediate Technology Publications, London, UK.

Jayasinghe, C., and Mallawaarachchi, R. S. (2009). "Flexural strength of compressed stabilized earth masonry materials." *Materials and Design*, 30, 3859-3868.

Jiménez Delgado, M. C., and Guerrero, I. C. (2007). "The selection of soils for unstabilised earth building: a normative review." *Construction and Building Materials*, 21(2), 237-251.

Lenci, S., Piattoni, Q., Clementi, F., and Sadowski, T. (2011). "An experimental study on damage evolution of unfired dry earth under compression." *International Journal of Fracture*, 172(2), 193-200.

Li, Y., and Ellingwood, B.R. (2006). "Hurricane Damage to Residential Construction in the US: Importance of Uncertainty Modeling in Risk Assessment." *Engineering Structures*, 28, 1009-1018.

Lima, S. A., Varum, H., Sales, A., and Neto, V. F. (2012). "Analysis of the mechanical properties of compressed earth block masonry using the sugarcane bagasse ash." *Construction and Building Materials*, 35(0), 829-837.

Marchigiani, R., Gordy, S., Cipolla, J., Adams, R. C., Evans, D. C., Stehly, C., Galwankar, S., Russell, S., Marco, A. P., Kman, N., Bhoi, S., Stawicki, S. P. S., and Papadimos, T. J. (2014). "Wind disasters: a comprehensive review of current management strategies." *International Journal of Critical Illness and Injury Science*, 3(2), 130-142.

Matta, F., Cuéllar-Azcárate, M. C., and Garbin, E. (2015). "Earthen masonry dwelling structures for extreme wind loads." *Engineering Structures*, 83, 163-175.

Miccoli, L., Müller, U., and Fontana, P. (2014). "Mechanical behaviour of earthen materials: a comparison between earth block masonry, rammed earth and cob." *Construction and Building Materials*, 61, 327-339.

Miller, C. J., and Rifai, S. (2004). "Fiber reinforcement for waste containment soil liners." *ASCE Journal of Environmental Engineering*, 130(8), 891-895.

Mitchell, J. K., and Soga, K. (2005). *Fundamentals of soil behavior*, Wiley, New York, US.

Morel, J.C., Ghavami, K., and Mesba, A. (1999). "Theoretical and experimental analysis of composite soil blocks reinforced with sisal fibres subjected to shear." *Masonry International*, 13, 54-62.

Morel, J.C., Pkla, A., and Walker, P. (2007). "Compressive strength testing of compressed earth blocks." *Construction and Building Materials*, 21(2), 303-309.

Morton, T. (2008). *Earth masonry design and construction guidelines*, IHS BRE Press, Garston, Watford.

MSJC (2013). "Building code requirements and specification for masonry structures (TMS 402-13 / ACI 530-13 / ASCE 5-13) and specification for masonry structures (TMS 602-13/ACI 530.1-13/ASCE 6-13) and companion commentaries." Farmington Hills, MI: American Concrete Institute; Reston, VA: American Society of Civil Engineers; Longmont, CO: The Masonry Society; 2011.

Muntohar, A. S. (2011). "Engineering characteristics of the compressed-stabilized earth brick." *Construction and Building Materials*, 25(11), 4215-4220.

NAPCOR (2015). "Report on postconsumer PET container recycling activity in 2014." National association for PET container resources, and APR The association of postconsumer plastic recyclers.

<http://www.napcor.com/pdf/NAPCOR_2014RateReport_FINAL.pdf> (Mar. 29, 2016)

NZS 4297 (1998). "Standards New Zealand. Engineering design of earth buildings." Wellington, New Zealand.

Prusinski, J. R., Bhattacharja, S., and Nrc (1999). "Effectiveness of Portland cement and lime in stabilizing clay soils." *Transportation Research Record*, 1652, 215-227.

Rafalko, S. D., Brandon, T. L., Filz, G. M., and Mitchell, J. K. (2007). "Fiber reinforcement for rapid stabilization of soft clay soils." *Transportation Research Record*, 2026, 21-29.

Sarangapani, G., Venkatarama Reddy, B., and Jagadish, K. (2005). "Brick-mortar bond and masonry compressive strength." *Journal of Materials in Civil Engineering*, 17(2), 229–237.

Skourup, B. N., and Erdogmus, E. (2010). "Polyvinyl alcohol fiber-reinforced mortars for masonry applications." *ACI Materials Journal*, 107(1), 57–64.

Subramania Prasad, C., Kunhanandan Nambiar, E., and Benny Mathews Abraham (2012). "Plastic fibre reinforced soil blocks as a sustainable building material." *International Journal of Advancements in Research and Technology*, 1(5), 42-45.

Taallah, B., Guettala, S., Guettala, S., and Kriker, A. (2014). "Mechanical Properties and Hygroscopicity Behavior of Compressed Earth Block Filled by Date Palm Fibers." Construction and Building Materials, 59, 161–168.

Tang, C., Shi, B., Gao, W., Chen, F., and Cai, Y. (2007). "Strength and mechanical behavior of short polypropylene fiber reinforced and cement stabilized clayey soil." *Geotextiles and Geomembranes*, 25(3), 194-202.

Tennant, A. G., Foster, C. D., and Venkatarama Reddy, B. V. (2013). "Verification of masonry building code to flexural behavior of cement-stabilized soil block." *Journal of Materials in Civil Engineering*, 25(3), 303-307.

Turanli, L., and Saritas, A. (2011). "Strengthening the structural behavior of adobe walls through the use of plaster reinforcement mesh." *Construction and Building Materials*, 25(4), 1747-1752.

Venkatarama Reddy, B. V., and Gupta, A. (2006). "Tensile bond strength of soil-cement block masonry couplets using cement-soil mortars." *Journal of Materials in Civil Engineering*, 18(1), 36-45.

Venkatarama Reddy, B. V., Lal, R., and Nanjunda Rao, K. S. (2007). "Enhancing bond strength and characteristics of soil-cement block masonry." *Journal of Materials in Civil Engineering*, 19(2), 164-172.

Venny Riza, F., Rahman, I. A., and Zaidi, A. M. A. (2010). "A brief review of compressed stabilized earth brick (CSEB)." *Science and Social Research (CSSR), 2010 International Conference*, IEEE Xplore, Kuala Lumpur, Malaysia, 999 - 1004.

Walker, P. (1999). "Bond characteristics of earth block masonry." *Journal of Materials in Civil Engineering*, 11(3), 249-256.

Walker, P. J. (2004). "Strength and erosion characteristics of earth blocks and earth block masonry." Journal of Materials in Civil Engineering, 16(5), 497-506.

Walker, P., and Stace, T. (1997). "Properties of some cement stabilised compressed earth blocks and mortars." *Materials and Structures*, 30(203), 545-551.

Yetgin, Ş., ÇAvdar, Ö., and Çavdar, A. (2008). "The effects of the fiber contents on the mechanic properties of the adobes." *Construction and Building Materials*, 22(3), 222-22

CHAPTER 2

COMPRESSED AND STABILIZED EARTHEN BLOCKS WITH RECYCLABLE PLASTIC FIBER REINFORCEMENT

ABSTRACT. Compressed and stabilized earthen block (CSEB) masonry is a sustainable and affordable construction material that is attracting widespread interest. This masonry system is especially appealing for high-quality and energy-efficient dwellings in areas where access to mainstream construction materials is more difficult, for example due to local availability and cost. In addition, recent studies have found that earthen masonry is a viable option to build dwelling structures that can withstand extreme wind loads, such as the tornadoes that periodically scourge vast areas of the U.S. In this chapter, a soil that is widely available in the U.S. is used to prototype CSEBs. In order to stabilize the soil matrix, small amounts of ordinary Portland cement (OPC) are used. Then, recyclable non-biodegradable polyethylene terephthalate (PET) is added to the stabilized soil matrix in the form of reinforcing fibers. These fibers are considered a sustainable reinforcement alternative since just a 31% of the PET bottles produced in the U.S. is recycled. The earthen blocks are tested in flexure and compression to characterize their mechanical properties and discuss the effects of the plastic fibers on the strength and deformability of the stabilized soil matrix.

Based on the experimental evidence, the addition of small amounts of OPC (less than 10% in weight of soil, wt%) increases the peak strength and the stiffness of the earthen block in compression and flexure as a result of the formation of cement hydrates.

In addition, the incorporation of randomly distributed plastic fibers (0.5 wt%) results post-cracking strength and deformability that cannot be attained by the brittle unreinforced blocks.

2.1 INTRODUCTION

Earthen construction has been used around the world in different ways due to its many benefits, such as: local availability, thermal mass, humidity control and low carbon footprint (Morton 2008) compared to alternative masonry materials such as fired clay bricks. Earthen masonry is emerging as an alternative construction system that maximizes the use of local materials and minimizes transportation cost. The availability of suitable soils in the U.S. makes CSEB masonry particularly appealing for high performance dwellings in rural areas, where the access to mainstream construction materials is often more difficult. In fact, traditional construction systems (e.g., wood-frame) often do not offer hazard resistance, increasing vulnerability to natural hazards, such as extreme wind events (tornadoes and hurricanes). Besides resisting the lateral forces produced by high winds, a hazard-resilient dwelling is required to withstand the impact from wind-borne debris, which is often the cause of many injuries and property damages (Marchigiani et al. 2014). Thus, it is also necessary to modify the post-cracking strength and toughness of the masonry to ensure impact resistance.

Recently, Matta et al. (2015) showed that CSEB masonry is a viable option for high wind-resistant dwellings assuming, among other conditions, a CSEB compressive strength of at least 3 MPa. Therefore, it is necessary to study if, using a locally available soil representative of tornado-prone areas in the U.S., such strength can be achieved.

As for any other earth-based material, the main weaknesses of compressed earthen blocks are their susceptibility to shrinkage during the drying process, low durability, and low compressive and flexural strengths (Venny Riza et al. 2010). To enhance strength and durability, additives, stabilizers and compaction processes (densification) are recommended. Densification is necessary for the particles of soil to form chemical bonds with the stabilizer (Horpibulsuk et al. 2010). A wide range of modifiers such as cement, lime, bitumen, organic products and natural and artificial fibers have been utilized (Bell 1996; Achenza and Fenu 2006; Jiménez Delgado and Guerrero 2007; Riza et al. 2010). From the listed stabilizers, ordinary Portland cement (OPC) has a relatively low cost, and it is a widely available and accepted alternative for soil stabilization.

The addition of OPC significantly improves the workability and mechanical properties of clayey soils (Mitchell 1981; Horpibulsuk et al. 2010). The reactions between the calcium ions from the OPC and the clay particles work in two different phases. First, the water absorption and the plastic index of the soil are reduced modifying the workability of the mixture (Chew et al. 2004). Second, the calcium ions from the OPC and the silica and aluminum from the clay react generating cement hydrates, stabilizing the mixture and increasing the strength of the soil matrix (Herzog and Mitchell 1963; Mitchell 1981; Horpibulsuk et al. 2010). The cementitious phases in the soil mixture depend on the soil components, which actively participate in the chemical reactions (Herzog and Mitchell 1963; Croft 1967). The influence of soil components can be appreciated in different results reported in the literature on stabilization using similar amounts of OPC in the presence of different clay minerals. The benefits of the

stabilization depend on the type of soil, type and amount of stabilizer (Kolias et al. 2005; Oti et al. 2009b).

OPC is a recommended stabilizing agent for the manufacture of CSEBs due to both its binding abilities with larger soil particles and its availability (Rigassi 1985). OPC is mistakenly assumed to be effective for stabilizing soils with low plasticity, but it has been found that it can be as effective as lime in stabilizing moderate to high-plasticity clayey soils (Prusinski and Bhattacharja 1999). The optimum content of OPC varies between 4% and 10% in weight of soil (Rigassi 1985; Walker and Stace 1997; Morel et al. 2007; Riza et al. 2010). The effects of a particular amount of OPC in the soil matrix depend on different parameters, such as: type of soil, compaction method, climate conditions, and curing process (Walker and Stace 1997; Haghi et al. 2007; Muntohar 2011).

For an effective enhancement of the soil material, a viable strategy can be to use a combination of stabilizer and fibers. The former contributes to increasing strength and stiffness properties while the latter contributes to toughness (Rafalko et al. 2007; Galán-Marín et al. 2010). The inclusion of fiber reinforcement in stabilized soils has been widely investigated. In general, it is concluded that the addition of fibers in the soil matrix reduces shrinkage cracking and transverse expansion due to Poisson's effect (Ghavami et al. 1999; Binici et al. 2005; Bouhicha et al. 2005; Haghi et al. 2007). In addition, the fiber reinforcement contributes to improving deformability, post-cracking strength and energy absorption of the soil matrix (Achenza and Fenu 2006; Tang et al. 2007; Yetgin et al. 2008; Lenci et al. 2011; Aymerich et al. 2012). However, the effects of fibers in the soil matrix depend on their particular characteristics. For instance,

uncoated natural fibers such as straw, coconut and sisal are susceptible to water absorption and expansion during the mixing process. Consequently, the water content needs to be increased to ensure workability, eventually resulting in less efficient load transfer between the fibers and the clay particles due to the lubrication effect of the water. This phenomenon causes a reduction of the strength of the blocks (Maher and Ho 1994; Yetgin et al. 2008). Then, the absorbed water is partially released during the drying process, leaving voids that affect fiber embedment in the surrounding soil, and reduce the durability of the blocks (Ghavami et al. 1999; Bouhicha et al. 2005; Yetgin et al. 2008). Furthermore, the alternative of using water repellent materials to reduce water absorption in natural fibers has been shown to be ineffective in improving the bonding with the soil matrix due to reduction of friction at the fiber-soil interface (Ghavami et al. 1999). In contrast, plastic fibers are not susceptible to water absorption and have been found to increase the blocks compressive strength (Binici et al. 2005). The use of fiber reinforcement from recycled materials is often considered for composites having a cementitious matrix, such as earthen blocks. Eko et al. (2012) noted that by using steel fibers from salvaged tires the reinforced earthen blocks display a post cracking behavior. They concluded that the contribution of the steel fibers in the soil matrix becomes apparent after cracking has occurred, resulting in enhanced deformability and associated plastic energy. Similarly, Subramania Prasad et al. (2012) reinforced stabilized earthen blocks with chopped plastic bags and beverage bottles. The former showed a beneficial effect on the compressive strength by increasing it up to 10%; while the fibers obtained from water bottles were found to be ineffective in enhancing the compressive strength.

This was attributed to the dimensions and surface finish of the fibers, which result in lack of boding with the surrounding soil matrix.

In this study, non-biodegradable plastic fibers obtained from recyclable PET (polyethylene terephthalate) are used to reinforce an OPC-stabilized soil matrix. PET fibers were selected as the reinforcement because at least 69% of PET bottles in the United States are not recycled (NAPCOR 2015).

The transformation of the post-cracking behavior of CEBs is attained by incorporating OPC and PET fibers. The effects of OPC stabilization and plastic fiber reinforcement in CEBs is analyzed based on the results of compression and flexural load tests. Supporting evidence is also provided by means of scanning electron microscopy (SEM) and energy-dispersive X-ray spectroscopy (EDX) analysis performed on soil matrix samples.

2.2 MATERIAL AND METHODS

2.2.1 Materials

2.2.1.1 Soil

The soil selected for the CEBs should have an adequate balance of three main components, namely, clay, sand and silt in the range 5 - 40%, 25 - 80% and 10 - 30%, respectively (Rigassi 1985; Jiménez Delgado and Guerrero 2007). The plasticity indices, which are defined by the Atterberg limits, provide a measure of the ability of the soil to deform without cracking or crumbling. A soil with a plastic index in the range 16 - 28 and a liquid limit in the range 32 - 46 is recommended (Jiménez Delgado and Guerrero 2007).

A soil from the piedmont residuum of North America was used in this study (located in Lexington, South Carolina). The particle size distribution of the soil, which was analyzed in accordance with ASTM D422 (ASTM 2007), showed the soil can be defined as silt (52%) with fine and medium sand (22%) and around 26% of clay particles (Figure 2.1).

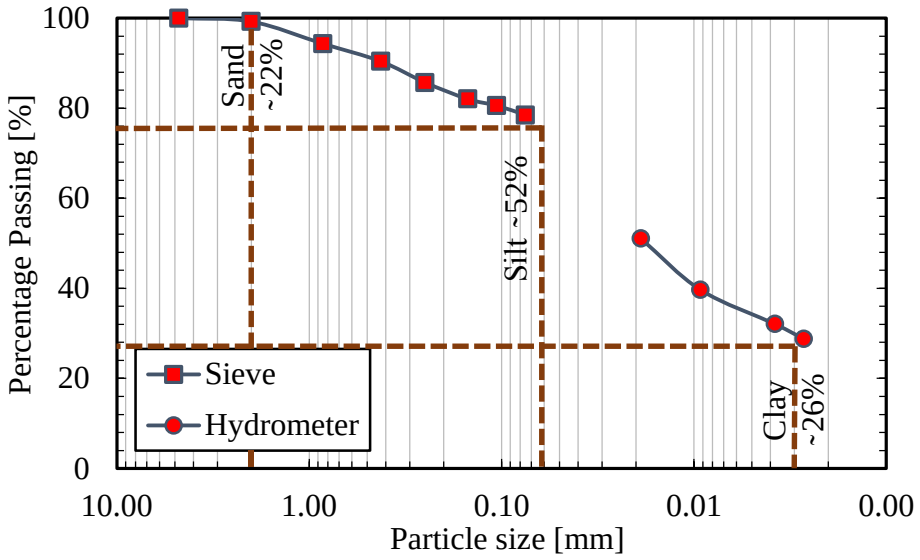

Figure 2.1 Particle size distribution for selected soil.

Using the standard ASTM D4318 (ASTM 2010), the plastic limit (PL = 14.4%), liquid limit (LL = 37.5%), and plasticity index (PI = 24.0%) were calculated. Then, in accordance with Casagrande's plasticity chart, the soil was classified as an inorganic clay of medium plasticity (Mitchell and Soga 2005). This is the case of most soils used in earthen construction (Jiménez Delgado and Guerrero 2007). The optimum moisture content (OMC) required for the compaction process of the earthen blocks, was estimated per ASTM D698 (2003). The OMC of the soil is approximately 17%. However, the water was added until a good workability of the mixture was attained. The final amount of water was approximately 20 wt%.

2.2.1.2 Stabilizer

The blocks were fabricated using Type I OPC as the stabilizer. The amount of OPC was fixed to 0 wt%, 6 wt% and 9 wt%.

2.2.1.3 Fibers

The fiber reinforcement is intended to mechanically stabilize the soil, limiting the movement of the soil particles and controlling cracking caused by compression and tension stresses, and water intrusion (Houben and Guillaud 1994). In this study, non-biodegradable and recyclable plastic was used as fiber reinforcement. The use of plastic fibers eliminates the issue of water absorption that affects natural fibers, which typically require special treatments and coating.

The plastic fibers were obtained from PET sheets, which is the same kind of plastic used to produce bottles for water and soft drinks. PET, which is the most widespread recycled plastic material, has a Young's modulus of approximately 2000 MPa, and an elongation at break larger than 100% (Torres et al. 2000). The amount of PET bottles that is not recycled is still dramatic (NAPCOR 2015). Therefore, the recycling of post-consumer PET bottles seems to be a reasonable source of non-biodegradable fiber reinforcement for the proposed use.

2.2.2 Specimens

In this study, the specimens selected are solid blocks with nominal dimensions of 355 mm × 254 mm × 89 mm. After 30 days, the blocks have an average specific weight of 1670 kg/m^3.

2.2.2.1 Test matrix

Five different specimens were fabricated. Unstabilized compressed earthen blocks were used as control specimens (C). Then, OPC was added in two different amounts, 6% and 9% in weight of soil, to evaluate the effect of stabilization (CS6 and CS9, respectively). To evaluate the effects of the fiber reinforcement, randomly distributed fibers were mixed with 6% and 9% of OPC in weight of soil (CSR6 and CSR9).

2.2.2.2 Production and manufacturing

The manufacturing of the blocks starts with the preparation and classification of the soil. To attain the desired soil particle size distribution, the natural soil was air dried, crushed using steel balls in a mechanical mixer and then sieved using a No. 8 sieve (opening 2.4 mm). Also, characterization tests were performed on the soil (ASTM D698 2003) to inform the mixture design to be considered for the blocks (e.g., water content). The mixture of the blocks was made in two phases. The first step consisted of dry mechanical mixing, where the dry elements (soil, OPC and fibers) were combined. Then, the water was added and the mixing was done by hand, carefully avoiding the formation of lumps (Figure 2.2a). The amount of soil that was mixed at one time was sufficient to produce three specimens.

The blocks were manufactured using a commercial hydraulic press (model EPH-2008, Fernco Metal Products, Capitan, NM) that can produce blocks with nominal dimensions of 355 mm × 254 mm × 89 mm, with a compaction pressure of 10.3 MPa (Figure 2.2b).

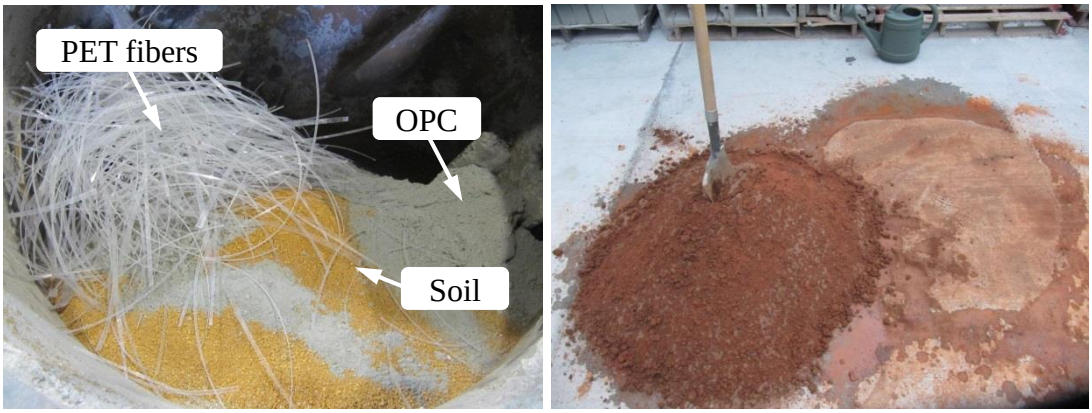

(a)


(b)


(c)

Figure 2.2 Manufacturing process: (a) Mechanical dry mixing and manual wet mixing, (b) casting and compression in hydraulic press, and (c) wet and dry curing.

The curing process was conducted in two phases, including: (a) "wet" curing for 14 days, where the blocks were wrapped in a plastic sheet indoors to create a relatively humid environment to offset rapid evaporation and formation of shrinkage cracks (Rigassi 1985); and (b) dry curing, where the plastic sheet was removed and the blocks were cured indoors for 14 days, without being directly exposed to sun and wind that may change the humidity conditions (Figure 2.2c).

2.2.2.3 Type of reinforcement

Fibers from PET bottles have been used to reinforce CEB blocks previously with no success. Subramania Prasad et al. (2012) found that the addition of chopped plastic fibers from water bottles does not result in enhanced compressive strength. This was attributed to the lack of bonding with the soil matrix, which is due to the surface finish and small dimensions of the fibers.

In this study, the PET fibers were obtained from a PET sheet with a thickness of 0.25 mm, which is an average value for the thickness of PET beverage bottles. The surface lightly roughened using sand paper. The fibers were cut with a length of 152 mm and width of 2 mm. The length of the fibers was comparable with the dimensions the blocks and did not affect the workability of the mixture. A plastic fiber content of 0.8% in weight of soil is recommended as the maximum practical limit to provide adequate workability and uniform fiber distribution in the soil matrix (Miller and Rifai 2004). For other fiber materials this number is found to be limited to 0.5% by weight due to a reduction in the compressive strength when a larger fiber content is used (Yetgin et al. 2008). Therefore, the amount of PET fibers selected was 0.5% in weight of soil (V_f =

0.6%). Through the mixing procedure presented above, the fiber reinforcement was randomly distributed in the soil mixture to facilitate the bridging of cracks along random planes, as it has been reported in previous studies for other types of fibers (Ghavami et al. 1999; Galán-Marín et al. 2010).

2.2.3 Set up and protocol

2.2.3.1 Instrumentation

A load test frame with a load capacity of 220 kN was used. For the flexural tests, a three-point bending setup was used (Figure 2.3a). The specimens consisted of five earthen blocks with nominal dimensions of 355 mm × 254 mm × 89 mm. The test was carried out under displacement control with a rate of 1.2 mm/min. The setup for the flexure test includes a rigid steel frame with two cylindrical hinges acting as supports for the earthen block specimens, resulting in a clear span of 279 mm. Two plastic foils with a low friction coefficient were placed between each cylindrical support and the earthen block to minimize horizontal reactions, and thus arching effects. The load was imparted using universal hydraulic machine and it was recorded through a dedicated 40 kN load cell. The midspan displacement was recorded through two displacement transducers placed underneath the centerline of the earthen block specimen.

For the compression test, the specimens consisted of five earthen blocks with nominal dimensions of 127 mm × 127 mm × 89 mm. The load was applied uniaxially with displacement rate of 1.8 mm/min. To record the displacement of the specimens, four transducers with a stroke of 50 mm were used, each placed at mid-length along a given side of the specimen. The test set up included two rigid loading steel plates and a

spherical hinge to evenly distribute the compressive force onto the surface of the blocks (Figure 2.3b).

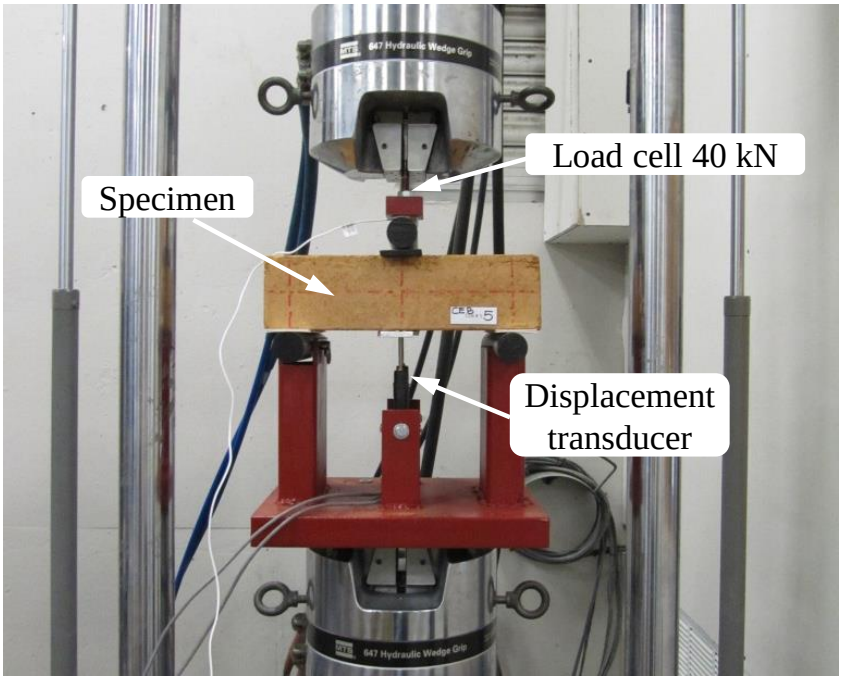

(a)

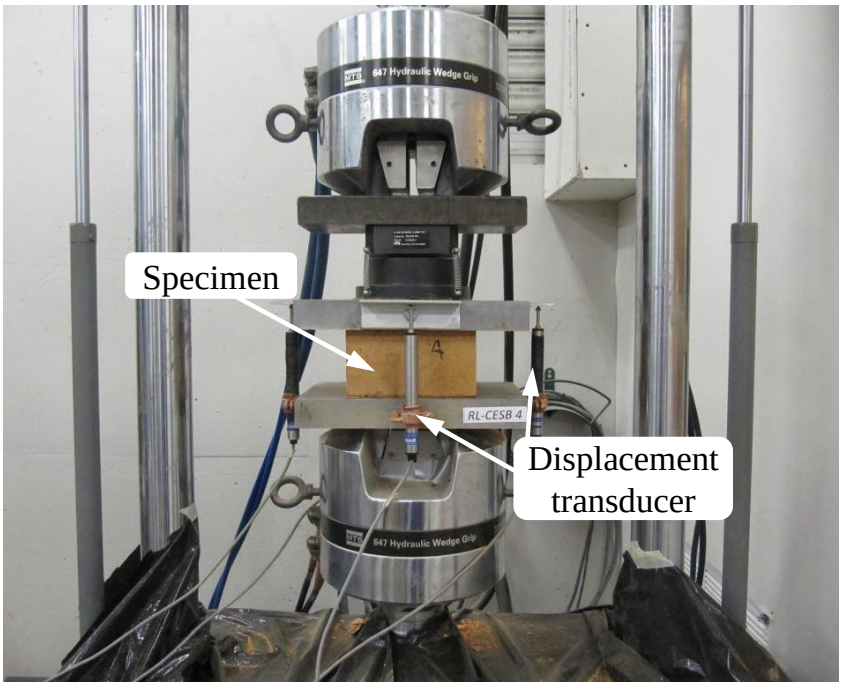

(b)

Figure 2.3 Test setup for: (a) Flexure, and (b) compression.

2.2.3.2 Protocol

The flexural and compressive tests were carried out in general conformance with ASTM C67 (ASTM 2013b) and ASTM C140 (ASTM 2013a). These standards apply to clay brick and concrete masonry units but, here, they were used as reasonable protocols in the absence of specific standards for earthen blocks. The flexural and compression tests were performed by applying vertical loads under displacement control. For the former, the specimens were tested at an age of 28 days in flexure at a displacement rate of 0.02 mm/sec. The specimens for the uniaxial compression tests were obtained from the halves of the specimens tested for flexural strength by cutting the material with a wet tile saw, the thickness remained the same. The average dimension of the compression test specimens were 127 mm x 127 mm x 89 mm. For the latter, the specimens were tested at an age of 28 days in uniaxial compression at a displacement rate of 0.03 mm/sec.

2.3 RESULTS AND DISCUSSION

2.3.1 Flexural and compressive strength and deformability

For each specimen series, the average compressive and flexural strength and the corresponding standard deviation are presented in Figure 2.4 (a) and (b). Table 2.1 summarizes the test matrix and results (See detailed results in Appendix D).

The addition of OPC results in an increase in the flexural and compressive strength by over 70% and 290% on average, respectively. The flexural strength is slightly reduced by the presence of plastic fibers. This is attributed to the introduction of discontinuities in the soil matrix.

Table 2.1 – Test matrix and summary of bending and compression test results.

Specimen series	OPC content [% wt]	PET fiber content [% wt]	Flexural strength			Compressive strength		
			Avg [MPa]	St. dev [MPa]	Δ [%]	Avg [MPa]	St. dev [MPa]	Δ [%]
C	-	-	0.31	0.01	0	1.16	0.14	-
CS6	6	-	0.67	0.12	116	4.62	0.48	298
CSR6	6	0.5	0.53	0.08	70	4.80	0.41	314
CS9	9	-	1.01	0.10	227	6.09	0.38	425
CSR9	9	0.5	0.90	0.10	191	5.90	0.43	409

In addition, the load/stress – deformation response for representative specimens in flexure and compression are presented in Figure 2.5a and Figure 2.5b, respectively. The OPC stabilization substantially increased the stiffness of the specimens, which was marginally reduced by the addition of the fibers. However, the addition of plastic fibers radically transformed the post-cracking behavior of the blocks. The effect of OPC stabilization and plastic fiber reinforcement are discussed in the following sections.

2.3.2 Effect of stabilization

The experimental results show that the addition of OPC as a stabilizer results in higher strength and stiffness of the earthen blocks (Figure 2.5). OPC supplies the necessary calcium for the initial stabilization, and enables the clayey soil stabilization through the following processes (Prusinski and Bhattacharja 1999):

- Cation exchange, due to the presence of a calcium-based stabilizer in the clayey soil matrix.
- Flocculation and agglomeration of clay particles, resulting in a textural change from fine-grained and plastic material to granular soil.

- Cement hydration, where OPC hydrates form and contribute to the chemical stabilization of the flocculated clay particles.
- Pozzolanic reaction, which is a secondary and relatively slow process where additional cement hydrates are formed, resulting in a progressive strength gain.

When the OPC reacts with water, cement hydrates form, such as calcium silicate hydrate (C-S-H). These cementitious materials form a network and act as binders, enhancing the strength of the soil matrix (Prusinski and Bhattacharja 1999; Oti et al. 2009a). Stabilization results in an enhancement of the mechanical properties of the blocks by filling pores and voids with hydration products, and binding the soil particles (Horpibulsuk et al. 2010).

SEM and Energy Dispersive X-ray (EDX) analysis were carried out to study the micro-structure and composition of the stabilized soil matrix vis-à-vis its unstabilized counterpart. Representative SEM micrographs of the unstabilized specimens show the morphology of the natural soil (Figure 2.6). It is noted that the soil is composed of particles with different shapes and sizes, which create a discontinuous matrix with numerous visible voids. The discontinuous structure is, in part, the result of residual water evaporation and shrinkage occurring during the drying process.

EDX analysis serves to identify the components of the type of clay present in the natural soil. This becomes a key parameter in the prediction of the behavior of the compacted earthen blocks. For unstabilized specimens, the type of clay controls the dimensional stability and shrinkage of the formed block. Similarly, in soil stabilization

the clay particles influence the chemical reactions with the OPC, and thus the type of cement hydrates that are present in the stabilized matrix (Croft 1967).

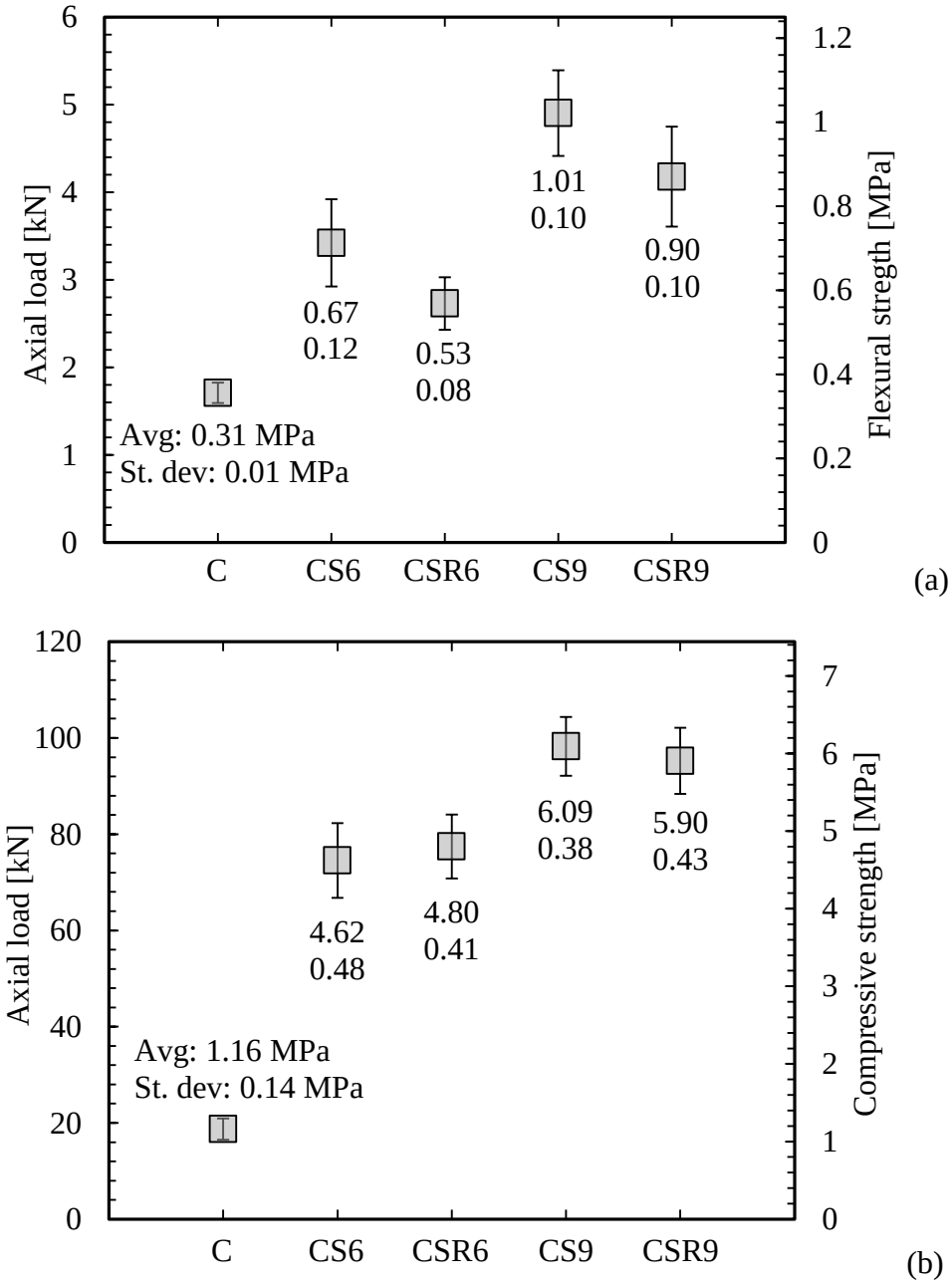

Figure 2.4 Maximum strength: (a) flexural strength and, (b) compressive strength.

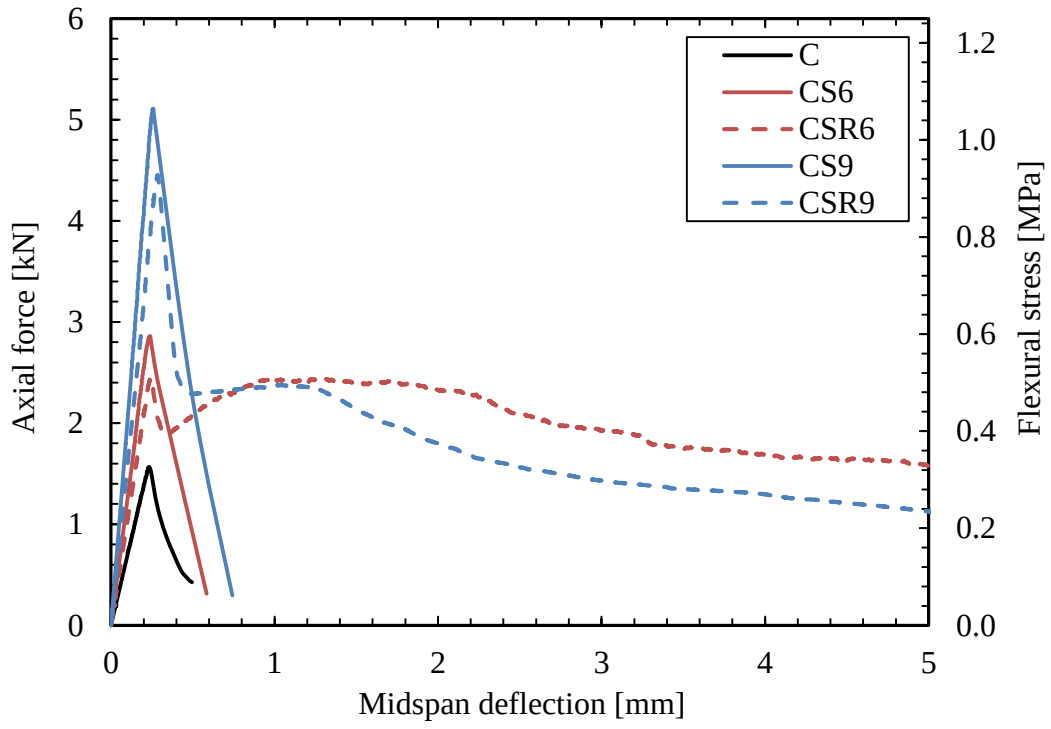

(a)

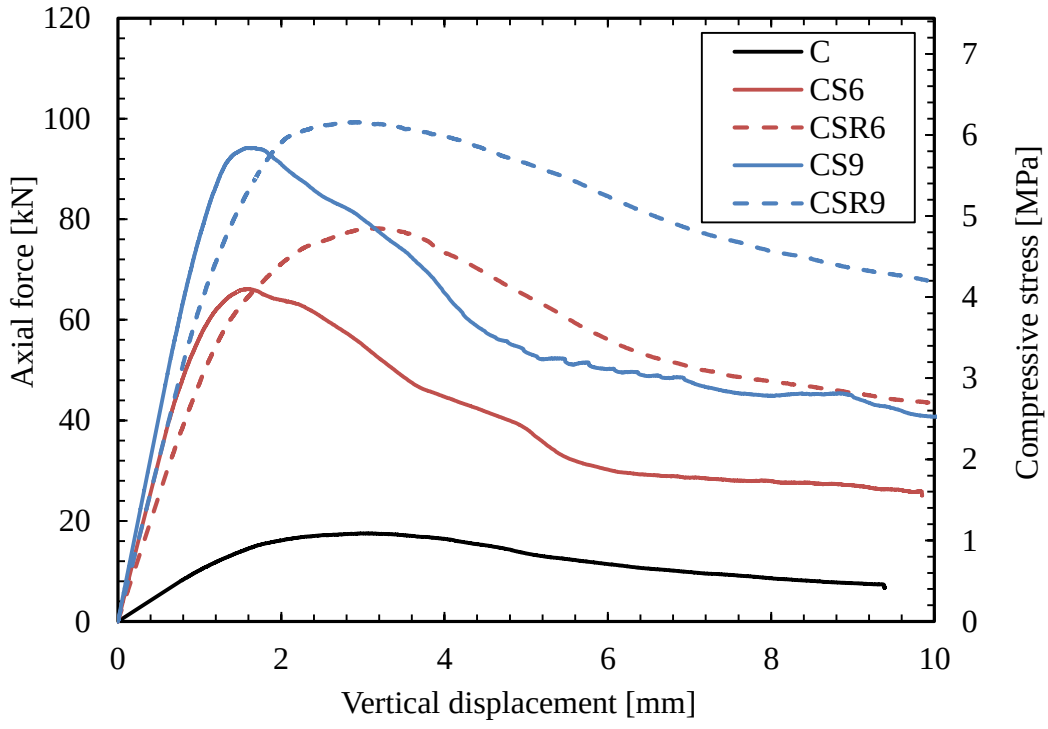

(b)

Figure 2.5 Representative load-displacement curves: (a) three point bending test, (b) compression test.

The EDX for the natural soil shows a majority of oxygen (O), silicon (Si) and aluminum (Al) with some amounts of potassium (K) and iron (Fe). The gold (Au) peaks are due to the gold sputter coating used to make the samples electronically conductive (Figure 2.7).

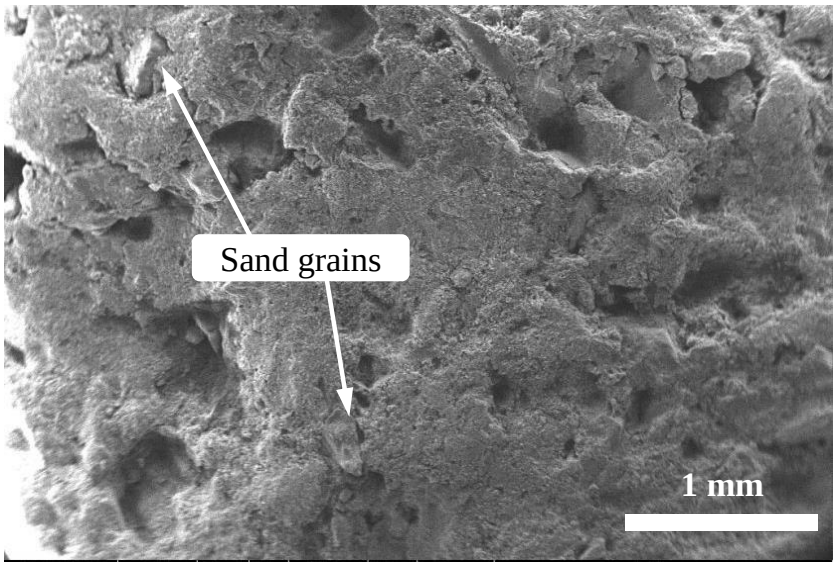

(a)

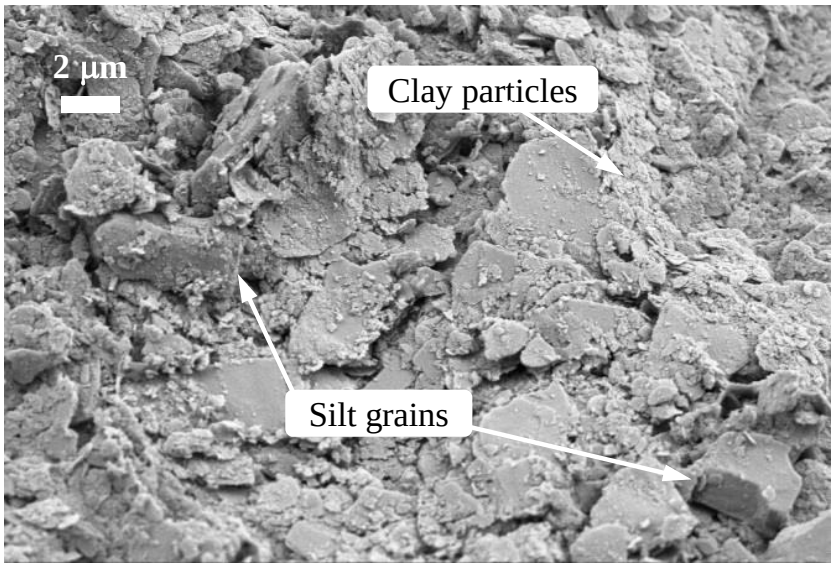

(b)

Figure 2.6 SEM micrographs showing discontinuous structure and voids of the unstabilized specimens (natural soil).

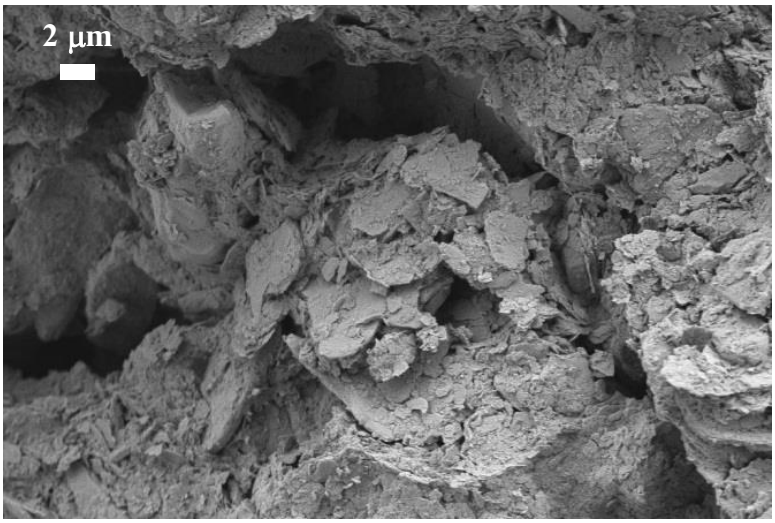

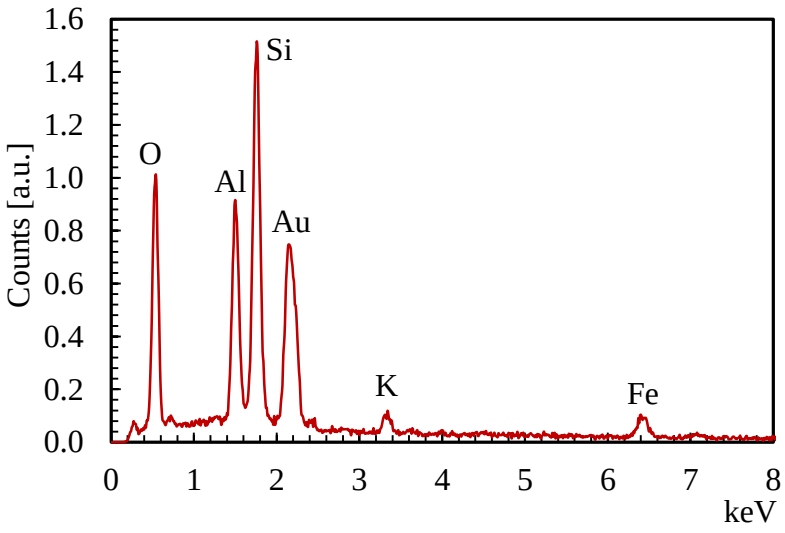

C	8.3%	Al	14.1%	K	1.9%
O	47.9%	Si	22.6%	Fe	5.1%

Figure 2.7 SEM micrographs and EDX analysis of C specimen.

Although the results are influenced by the presence of other soil particles that are present in the natural soil, it is possible to identify components that are representative of a particular type of clay. According to these results, the soil has clay particles with similar components to illite or kaolinite. Both minerals include aluminum and silicon and a relatively low tendency to shrink-swell. Illite has an interlayer space occupied by hydrated potassium, which is responsible for the non-expansive nature of this clay

mineral, and some traces of magnesium (Mg). On the other hand, kaolinite is a better fit since the raw soil is from piedmont, often known as red clay. In this type of soils, the dominant mineral is kaolinite and the iron (Fe) is what determines the particular reddish color.

Figure 2.8 and Figure 2.9 show the microstructure and the EDX analysis of the stabilized specimens CS6 and CS9, respectively. When compared with the natural soil, the micrographs in Figure 2.6 and Figure 2.7 highlight significant changes in morphology. The natural soil has a discontinuous structure where the voids are more visible because of the absence of hydration products, whereas the stabilized soil displays a denser and more continuous structure. The soil particles are bound by ~2-4 μm rod-like crystals (ettringite) that are formed as a result of OPC hydration (Day 1992, PCA 2001). In fact, in commercially available OPC, the sulfate (which is necessary for ettringite to form) is provided by the gypsum, which is typically added to control the rate of setting.

Ettringite is often observed in stabilized clayey soils as a result of the reactions between OPC and calcium, aluminum, iron, and water in the soil (Rajasekaran 2005). The presence of ettringite has also been reported in stabilized clayey soils (Horpibulsuk et al. 2010; Kolias et al. 2005; Oti et al. 2009b). Here, the formation of ettringite results in an increase in the compressive and flexural strength of the earthen blocks by binding and partially densifying (i.e., filling voids and defects) the soil matrix (Figure 2.8, Figure 2.9). The formation of cement hydration products was confirmed by evidence from EDX analysis where calcium (Ca) is observed in both stabilized (CS6 and CS9) specimens.

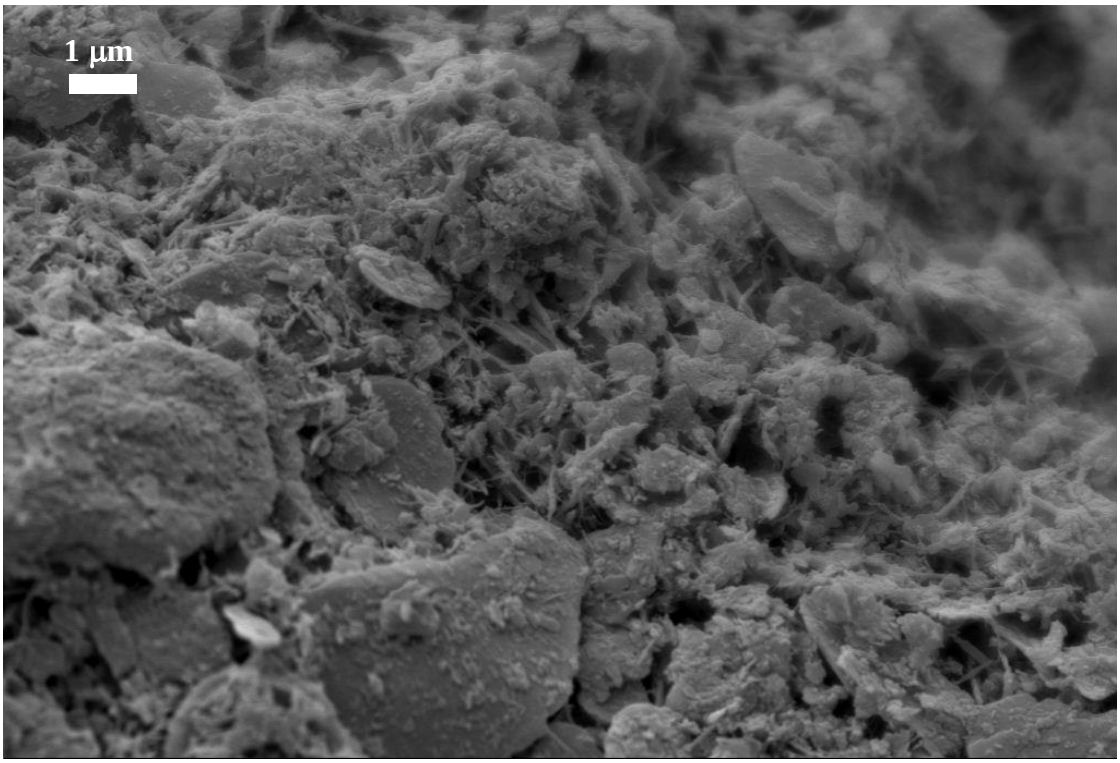

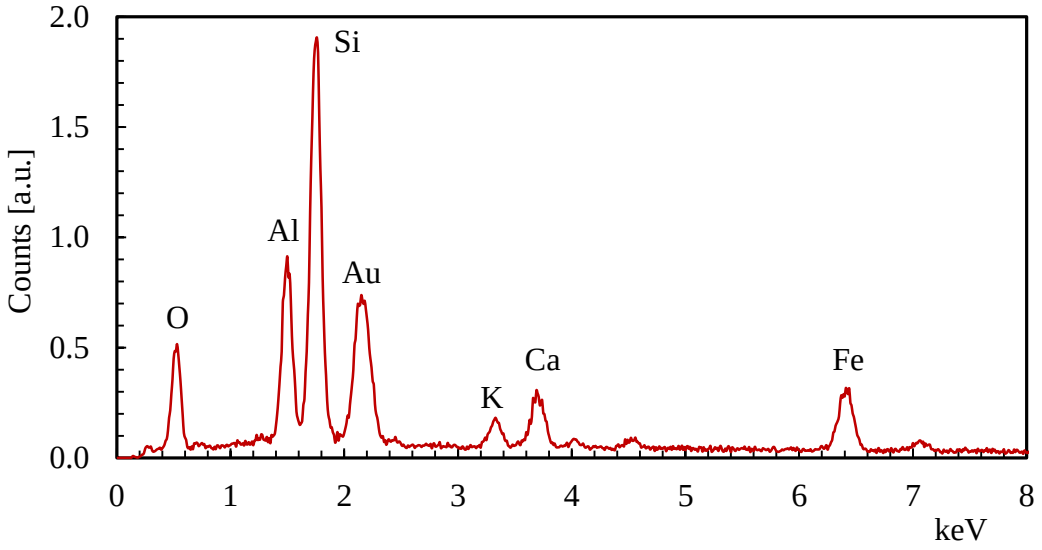

C	12.7%	Si	28.2%	Ti	0.6%
O	37.0%	K	1.5%	V	0.1%
Al	12.3%	Ca	2.7%	Fe	4.9%

Figure 2.8 SEM micrographs and EDX analysis of CS6 specimens (elements wt%).

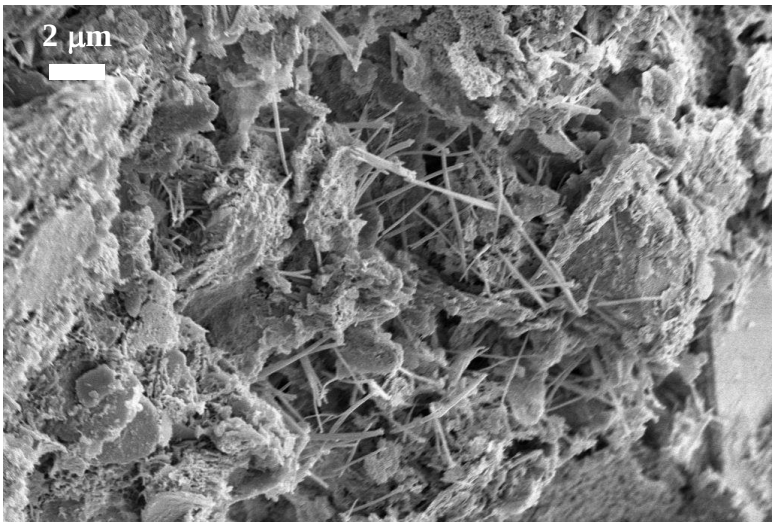

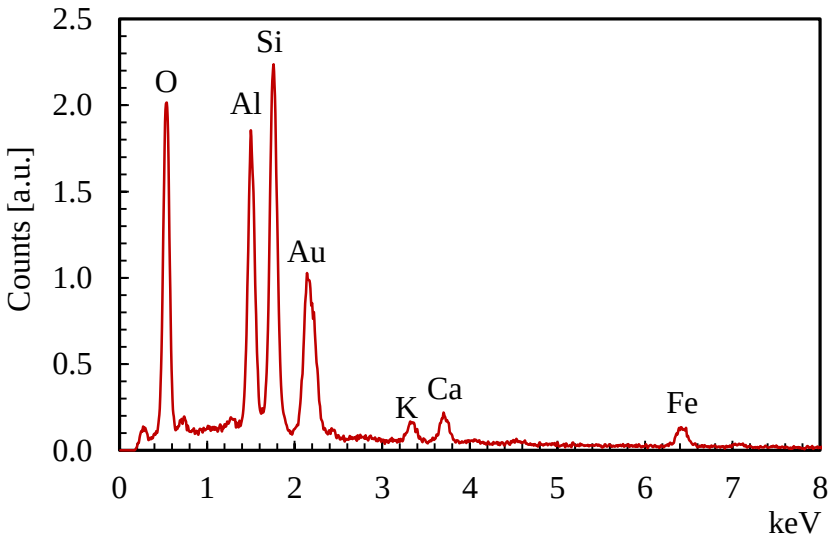

C	6.3%	Si	14.4%	Fe	3.1%
O	38.5%	K	1.2%	Au	23.6%
Al	11.3%	Ca	1.7%		

Figure 2.9 SEM micrographs and EDX analysis of CS9 specimens (elements wt%).

By adding 50% more OPC (i.e., from 6 wt% to 9 wt%), the compressive and flexural peak stress increased on average by 1.42 and 1.96 times, respectively. However, as expected, the brittle behavior of the earthen blocks is not modified by increasing the cement content.

2.3.3 Effect of fiber-reinforcement

The introduction of PET fibers results in a slight reduction in the flexural strength and the stiffness of the blocks (Figure 2.4 and Figure 2.5). However, the fibers transform the brittle behavior of the material. The residual (post-cracking) strength is attributed to the mechanical interaction (friction) between the PET fibers and the surrounding soil. Both CSRs specimens presented similar behavior; after attaining the peak load, the reinforced specimens experienced a drop in strength as the PET fibers bridging the crack at midspan were fully engaged. The maximum load drop in flexure for the CSR6 and CSR9 specimens was on average 28% and 55%, respectively. The post-cracking part of the load-displacement curves show a small recovery of flexural strength, which is attributed to the bridging action (i.e., load carrying contribution) of the fully-engaged and well-embedded PET fibers (Figure 2.5a). The post-cracking behavior was controlled by the progressive pull-out and (in some instances) rupture of the PET fibers. This was noted when inspecting the specimens after failure (Figure 2.10).

It was noted that, after the soil matrix cracked, the reinforced specimens reached a similar load level. It implies that the embedment of the fibers is not enhanced by increasing the strength of the soil matrix, and thus the amount of OPC. To study the deformability enhancement of the CSEBs through the incorporation of PET fiber reinforcement, the cumulative energy trend for the reinforced specimens (CSR6 and CSR9) is presented Figure 2.11 as a function of the vertical midspan displacement. Salient values are summarized in Table 2.2.

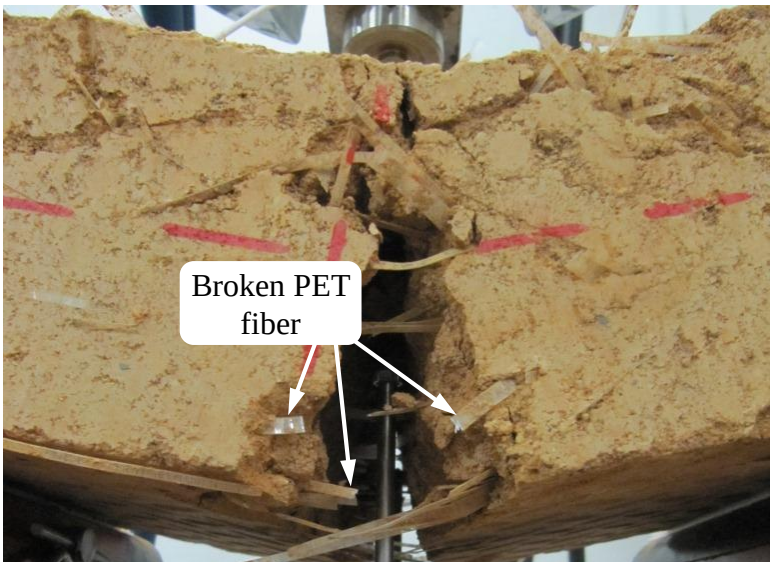

Figure 2.10 Failure details for CSREBs: fibers bridging the crack with a detail of a broken fiber.

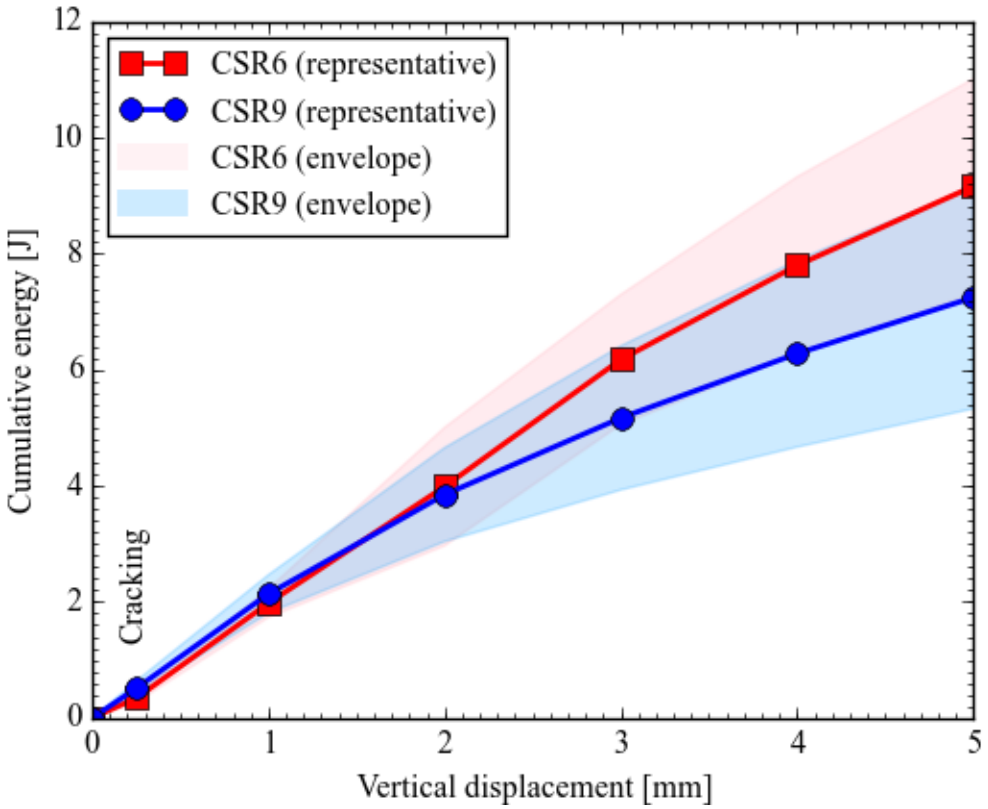

Figure 2.11 Average cumulative energy as function of vertical displacement for blocks tested in flexure.

Table 2.2 – Cumulative energy for PET fiber reinforced CSEBs.

Displacement [mm]	Cumulative energy [J]				Δ [%]
	CSR6		CSR9		
	Avg	St. dev.	Avg	St. dev.	
0.25 (cracking)	0.3	0.1	0.5	0.1	-49.6%
1	2.0	0.2	2.1	0.3	-8.1%
2	4.0	1.0	3.8	0.8	3.5%
3	6.2	1.1	5.2	1.2	16.3%
4	7.8	1.5	6.3	1.6	19.5%
5	9.2	1.9	7.2	1.9	20.9%

Up to the cracking point, the maximum cumulative energy is achieved by the CSR9 group due to the higher peak strength. After failure, the difference between the fiber reinforced groups (CSR6 and CSR9) behavior is smaller, dropping from 50% to 20%. This result confirms that the energy deformation is a function of the fiber reinforcement and not of the strength of the soil matrix (i.e., OPC content). After cracking, the energy absorption depends on the PET fibers (distribution and possibly amount) and their interaction with the surrounding soil matrix.

2.4 CONCLUSIONS

Based on the data of the flexure and compression tests and the SEM and EDX analysis presented in this chapter, the following conclusions are drawn:

1. The addition of OPC affects the micro-structure of the blocks. A small amount of OPC for the stabilization of the soil matrix (6% and 9% of soil weight) enhances the flexural and compressive strengths of compressed earthen blocks as well as their elastic stiffness. This effect is attributed to microstructural changes in the clay soil

resulting from the formation of cement hydrates. As expected, the brittle behavior of the unreinforced specimens is not changed by increasing the amount of OPC.

2. Using a locally available soil stabilized with a small amount of OPC, it is possible to attain a CSEB compressive strength well above the minimum value hypothesized by Matta et al. (2015) for stabilized earthen masonry subject to high wind-loads.

3. The presence of PET fibers results in a transformation of the post-cracking behavior (deformability) of stabilized earthen blocks subject to flexure. The fibers bridging the cracks allowed for the blocks to exhibit residual strength after the maximum load was attained.

4. The fibers introduce defects in the matrix increasing the amount of voids present, which reduces the density of the matrix and affecting the peak strength and elastic stiffness. However, the post-cracking behavior, which shows an enhanced damage tolerance, shows that the random distribution and the dimensions of the fibers were suitable to provide sufficient interaction with the stabilized soil matrix to offset the effect of the defects. Some fibers were sufficiently well embedded to reach their tensile strength.

5. The cumulative energy comparison showed that CSR specimens display a similar behavior after cracking, indicating that the strength of the fiber-matrix interface is not affected by the OPC content. Besides strength, increasing 50% of the cement content does not affect the mechanical behavior of the blocks. This is relevant to users to decide on a design mixture that offers a certain level of strength, deformability, and sustainability features.

2.5 REFERENCES

ASTM (2003). "Standard test methods for laboratory compaction characteristics of soil using standard effort (12,400 ft-lbf/ft3 (600 kN-m/m3)), D698." American Society for Testing and Materials, West Conshohocken, PA.

ASTM (2007). "Standard Test Method for Particle-Size Analysis of Soils, D422." American Society for Testing and Materials, West Conshohocken, PA.

ASTM (2010). "Standard Test Methods for Liquid Limit, Plastic Limit, and Plasticity Index of Soils, D4318." American Society for Testing and Materials, West Conshohocken, PA.

ASTM (2013a). "Sampling and testing concrete masonry units and related units, C140M." American Society for Testing and Materials, West Conshohocken, PA.

ASTM (2013b). "Standard test methods for sampling and testing brick and structural clay tile, C67." American Society for Testing and Materials, West Conshohocken, PA.

Achenza, M., and Fenu, L. (2006). "On earth stabilization with natural polymers for earth masonry construction." *Materials and Structures*, 39(1), 21-27.

Aymerich, F., Fenu, L., and Meloni, P. (2012). "Effect of reinforcing wool fibres on fracture and energy absorption properties of an earthen material." *Construction and Building Materials*, 27(1), 66-72.

Bell, F. G. (1996). "Lime stabilization of clay minerals and soils." *Engineering Geology*, 42(4), 223-237.

Binici, H., Aksogan, O., and Shah, T. (2005). "Investigation of fibre reinforced mud brick as a building material." *Construction and Building Materials*, 19(4), 313-318.

Binici, H., Aksogan, O., Bodur, M. N., Akca, E., and Kapur, S. (2007). "Thermal isolation and mechanical properties of fibre reinforced mud bricks as wall materials." *Construction and Building Materials*, 21(4), 901-906.

Binici, H., Aksogan, O., Bakbak, D., Kaplan, H., and Isik, B. (2009). "sound insulation of fibre reinforced mud brick walls." *Construction and Building Materials*, 23(2), 1035-1041.

Bouhicha, M., Aouissi, F., and Kenai, S. (2005). "Performance of composite soil reinforced with barley straw." *Cement & Concrete Composites*, 27(5), 617-621.

Chew, S. H., Kamruzzaman, A. H. M., and Lee, F. H. (2004). "Physicochemical and engineering behavior of cement treated clays." *Journal of Geotechnical and Geoenvironmental Engineering*, 130(7), 696-706.

Croft, J. B. (1967). "The influence of soil mineralogical composition on cement stabilization." *Géotechnique*, 17(2), 119-135.

Day, R. L. (1992). "The effect of secondary ettringite formation on the durability of concrete: a literature analysis." Portland Cement Association Research and Development Bulletin.

Eko, R. M., Offa, E. D., Ngatcha, T. Y., and Minsili, L. S. (2012). "Potential of salvaged steel fibers for reinforcement of unfired earth blocks." *Construction and Building Materials*, 35, 340-346.

Galán-Marín, C., Rivera-Gómez, C., and Petric, J. (2010). "Clay-based composite stabilized with natural polymer and fibre." *Construction and Building Materials*, 24(8), 1462-1468.

Ghavami, K., Toledo, R. D., and Barbosa, N. P. (1999). "Behaviour of composite soil reinforced with natural fibres." *Cement & Concrete Composites*, 21(1), 39-48.

Haghi, A. K., Sadrmomtazi, A., Bastani, A. F., Amiralyan, N., and Haghi, R. K. (2007). "Evaluation of reinforcement on the mechanical behavior of partially bonded fiber/matrix interface." *Composite Interfaces*, 14(7-9), 647-668.

Herzog, A., and Mitchell, J. K. (1963). "Reactions accompanying stabilization of clay with cement." *Highway Research Record* (36), 146-171.

Horpibulsuk, S., Rachan, R., Chinkulkijniwat, A., Raksachon, Y., and Suddeepong, A. (2010). "Analysis of strength development in cement-stabilized silty clay from microstructural considerations." *Construction and Building Materials*, 24(10), 2011-2021.

Houben, H., and Guillaud, H. (1994). *Earth construction: a comprehensive guide*, Intermediate Technology Publications, London, UK.

Jiménez Delgado, M. C., and Guerrero, I. C. (2007). "The selection of soils for unstabilised earth building: a normative review." *Construction and Building Materials*, 21(2), 237-251.

Kolias, S., Kasselouri-Rigopoulou, V., and Karahalios, A. (2005). "Stabilisation of clayey soils with high calcium fly ash and cement." *Cement and Concrete Composites*, 27(2), 301-313.

Lenci, S., Piattoni, Q., Clementi, F., and Sadowski, T. (2011). "An experimental study on damage evolution of unfired dry earth under compression." *International Journal of Fracture*, 172(2), 193-200.

Maher, M. H., and Ho, Y. C. (1994). "Mechanical-properties of kaolinite fiber soil composite." *ASCE Journal of Geotechnical Engineering*, 120(8), 1381-1393.

Marchigiani, R., Gordy, S., Cipolla, J., Adams, R. C., Evans, D. C., Stehly, C., Galwankar, S., Russell, S., Marco, A. P., Kman, N., Bhoi, S., Stawicki, S. P. S., and Papadimos, T. J. (2014). "Wind disasters: a comprehensive review of current management strategies." *International Journal of Critical Illness and Injury Science*, 3(2), 130-142.

Matta, F., Cuéllar-Azcárate, M. C., and Garbin, E. (2015). "Earthen masonry dwelling structures for extreme wind loads." *Engineering Structures*, 83, 163-175.

Miller, C. J., and Rifai, S. (2004). "Fiber reinforcement for waste containment soil liners." *ASCE Journal of Environmental Engineering*, 130(8), 891-895.

Mitchell, J. K., and Soga, K. (2005). *Fundamentals of soil behavior*, Wiley, New York, US.

Mitchell, J. K. (1981). "Soil improvement - state-of-the-art repor." *Tenth International Conference on Soil Mechanics and Foundation* Engineering, Stockholm, Sweden, 15-19.

Morel, J.C., Pkla, A., and Walker, P. (2007). "Compressive strength testing of compressed earth blocks." *Construction and Building Materials*, 21(2), 303-309.

Morton, T. (2008). *Earth masonry design and construction guidelines*, IHS BRE Press, Garston, Watford.

Muntohar, A. S. (2011). "Engineering characteristics of the compressed-stabilized earth brick." *Construction and Building Materials*, 25(11), 4215-4220.

NAPCOR (2015). "Report on postconsumer PET container recycling activity in 2014." National association for PET container resources, and APR The association of postconsumer plastic recyclers.

<http://www.napcor.com/pdf/NAPCOR_2014RateReport_FINAL.pdf> (Mar. 29, 2016)

Oti, J. E., Kinuthia, J. M., and Bai, J. (2009a). "Engineering properties of unfired clay masonry bricks." *Engineering Geology*, 107(3-4), 130-139.

Oti, J. E., Kinuthia, J. M., and Bai, J. (2009b). "Compressive strength and microstructural analysis of unfired clay masonry bricks." *Engineering Geology*, 109(3-4), 230-240.

PCA (2001). "Ettringite formation and the performance of concrete." Portland Cement Association.

Prusinski, J. R., and Bhattacharja, S. (1999). "Effectiveness of Portland cement and lime in stabilizing clay soils." *Transportation Research Record*, 1652, 215-227.

Quagliarini, E., and Lenci, S. (2010). "The influence of natural stabilizers and natural fibres on the mechanical properties of ancient Roman adobe bricks." *Journal of Cultural Heritage*, 11(3), 309-314.

Rafalko, S. D., Brandon, T. L., Filz, G. M., and Mitchell, J. K. (2007). "Fiber reinforcement for rapid stabilization of soft clay soils." *Transportation Research Record*, 2026, 21-29.

Rajasekaran, G. (2005). "Sulphate attack and ettringite formation in the lime and cement stabilized marine clays." *Ocean Engineering*, 32(8–9), 1133-1159.

Rigassi, V. (1985). "Compressed earth blocks: manual of production." *CRATerre-EAG*, Germany.

Riza, F. V., Rahman, I. A., and Zaidi, A. M. A. (2010). "A brief review of compressed stabilized earth brick (CSEB)." *Science and Social Research (CSSR), 2010 International Conference*, IEEE Xplore, Kuala Lumpur, Malaysia, 999 - 1004.

Subramania Prasad, C., Kunhanandan Nambiar, E., and Benny Mathews Abraham (2012). "Plastic fibre reinforced soil blocks as a sustainable building material." *International Journal of Advancements in Research and Technology*, 1(5), 42-45.

Tang, C., Shi, B., Gao, W., Chen, F., and Cai, Y. (2007). "Strength and mechanical behavior of short polypropylene fiber reinforced and cement stabilized clayey soil." *Geotextiles and Geomembranes*, 25(3), 194-202.

Torres, N., Robin, J. J., and Boutevin, B. (2000). "Study of thermal and mechanical properties of virgin and recycled poly(ethylene terephthalate) before and after injection molding." *European Polymer Journal*, 36(10), 2075-2080.

Venny Riza, F., Abdul Rahman, I., and Ahmad Zaidi, A. M. (2010). "A brief review of compressed stabilized earth brick (CSEB)." *2010 International Conference on Science and Social Research (CSSR 2010)*, December 5-7, Kuala Lumpur, Malaysia.

Walker, P., and Stace, T. (1997). "Properties of some cement stabilised compressed earth blocks and mortars." *Materials and Structures*, 30(203), 545-551.

Yetgin, Ş., ÇAvdar, Ö., and Çavdar, A. (2008). "The effects of the fiber contents on the mechanic properties of the adobes." *Construction and Building Materials*, 22(3), 222-227

CHAPTER 3

STABILIZED EARTHEN MASONRY PROTOTYPE FOR TORNADO LOADS

ABSTRACT. In the U.S., where suitable soils for earthen construction are widely available, stabilized earthen masonry (SEM) is an attractive option for dwellings in rural areas and farmlands, which are often located in tornado-prone regions. Recent tragic tornado events, and post-hazard reconstruction, have highlighted the need for a more affordable and hazard-resilient construction system that allows to build with locally available materials and conventional practices. Although SEM appears a suitable choice for affordable and hazard-resilient dwellings, it is often faced with skepticism.

This chapter reports on the prototyping of a SEM that is fabricated using a widely available soil in tornado-prone areas, and is designed to withstand the pressure generated by extreme winds. The prototyping process includes the selection of an earthen mortar that is compatible with the compressed and stabilized earthen blocks (CSEBs) introduced in Chapter 2. The prototype SEM was load-tested to characterize relevant mechanical properties, and evaluate the applicability of existing masonry building codes, such as NZS 4297 (1998) in New Zealand, and CEN (2005) in Europe. Using the experimental strength results as inputs, a structural analysis of a single-story dwelling subjected to tornado wind effects is presented to demonstrated proof of concept.

3.1 INTRODUCTION

Recent tornado events that have had tragic consequences, such as Joplin 2011 and Moore 2013, have highlighted the need for safer construction systems that are available as well as affordable. Tornadoes routinely scourge the "Tornado Alley" causing human losses and property damage. This region often includes rural areas and farmlands where underrepresented and disadvantaged communities live. Here, affordable and tornado-resistant construction systems are needed to address the need for safe shelter.

Earth as a construction material has been widely used around the world. As a matter of fact, the majority of the world's rural population lives in earthen houses (Houben and Guillaud 1994). Earthen masonry is built with earthen blocks, which are formed through manual or mechanical compression, and mortar. Compelling features of earthen masonry include the local availability and affordability of suitable soils (including well dispersed clay-rich soil in the U.S.), thermal insulation properties, humidity control, and a relatively small carbon footprint (Morton 2008). In fact, earthen masonry is more often seen in the construction of sustainable buildings, ranging from modest to high-end houses in developing and developed countries. Matta et al. (2015) found that stabilized earthen masonry is a viable option to resist EF3 (Enhanced Fujita scale) tornado loads when using a conventional wall thickness of about 400 mm in one-story dwellings, provided that rigid floor or roof diaphragms are used, and compressed and stabilized earthen blocks (CSEB) masonry has a compressive strength in the range of 2-3 MPa, shear strength in the range of 0.1-0.15 MPa, and tensile strength in the range of 0.13-0.2 MPa. However, the non-engineered nature of earthen masonry, and the lack of a

suitable earthen masonry system with well-defined mechanical properties, have contributed to curtailing its implementation on load-bearing elements.

The mechanical properties of SEM depend on parameters such as block and mortar compressive strength, and masonry flexural bond and shear bond strength (Sarangapani et al. 2005; Venkatarama Reddy and Gupta 2006; Venu Madhava Rao et al. 1996; Walker 1999). Studies on the stabilization of earthen blocks suggest that block compressive strength and durability are improved by increasing the ordinary Portland cement (OPC) content (Morel et al. 2007; Walker and Stace 1997). The tendency is to use less than 10% of OPC content to limit costs and minimize the carbon footprint. The compressive strength of earthen blocks is also a function of other parameters, such as type of soil (clay content) and compaction pressure (Jiménez Delgado and Guerrero 2007; Muntohar 2011; Walker and Stace 1997). It is recommended to use soils with clay content in the range of 10% - 22% in addition to a plastic index and liquid limit ranging between 16-28 and 32-46, respectively.

As for any type of masonry, the mechanical properties of the mortar greatly contribute to the structural response of SEM. Earthen mortars tend to be more compatible with earthen block than conventional OPC mortars due to their water retention and flow properties, which lead to better block-mortar interfaces (Sarangapani et al. 2005; Venkatarama Reddy and Gupta 2006; Venu Madhava Rao et al. 1996; Walker 1999; Walker and Stace 1997). Sarangapani et al. (2005) concluded that the masonry compressive strength increases when both flexural bond and shear bond strength are improved. They suggested that the masonry compressive strength is more sensitive to the brick-mortar bond strength than the compressive strength of the mortar. Increasing the

mortar compressive strength does not always result in increased bond strength as much as other factors such as mortar type, clay content, and block moisture content (Venu Madhava Rao et al. 1996; Walker 1999).

The mechanical properties of the blocks and mortar have been the focus of different studies. In addition, some results of load tests on earth masonry subassemblages have been reported (Miccoli et al. 2014, Lima et al. 2012). To the best of the author's knowledge, there is still a significant gap in the archival literature (i.e., journal papers) in regard to the prototyping and comprehensive mechanical characterization of a high-performance earthen masonry. The research on the mechanical properties of earthen masonry systems that are capable of withstanding high-wind loads (and, in general, extreme loads due to natural hazards) is in its infancy. The main objective of the research presented in this chapter is to demonstrate a SEM system that can address the demand for an affordable and resilient dwelling in tornado-prone regions. The starting point is to assess if the target masonry compressive, shear, and flexural strength defined by Matta et al. (2015) can be achieved by a SEM that is made with a locally available soil in the tornado-prone areas. The SEM prototype introduced in this chapter was load-tested to characterize its salient mechanical properties, which are then used as input in the structural analysis and design of a realistic EF3 tornado-resistant dwelling structure, to demonstrate proof of concept.

3.2 MATERIALS AND METHODS

In this section, the materials and methods utilized in the prototype earthen masonry are described. A brief description of the locally available soil used to produce the earthen blocks is provided, along with the earthen blocks compressive strength

discussed in Chapter 2. This soil is also used in the production of earthen mortar, which was engineered to be compatible with the CSEBs while minimizing carbon footprint. After selecting a suitable combination of earthen blocks and mortar, relevant mechanical properties for the SEM are characterized experimentally.

3.2.1 Soil

The feasibility and affordability of earthen masonry strongly depends on the availability of suitable soils. Soil texture is the most common parameter used for the selection of the soil, which needs to provide a suitable proportion of gravel, sand, silt, and clay. However, the range for each component markedly varies with the location, resulting in a vast number of possible soils. In fact, based on the literature, the texture of suitable soils is associated with a range 0-40% (in weight) for gravels, 25-80% for sands, 10-55% for silts, and 5-50% for clays (Houben and Guillaud 1994; Jiménez Delgado and Guerrero 2007; Morton 2008; Rigassi 1985). Due to these relatively large possible ranges for each soil constituent, texture is an important indicator but is not sufficient for the selection of suitable soils. To this end, it is good practice to evaluate the soil texture, plasticity and compressibility. Nonetheless, basic parameters for soil with no organic material, a minimum clay content of 5% and a plasticity index between 16% – 28% (Jiménez Delgado and Guerrero 2007; Morton 2008), may be used as a benchmark reference for suitable soils.

The soil selected for the study presented in this chapter is located in Lexington, South Carolina. According to the soil particle size analysis, whose results are summarized in Figure 2.1 in Chapter 2, this soil has a silt, sand and clay content of 50%, 22% and 28%, respectively, with a plasticity index of 24%. It is classified as silty loam

in accordance with USDA (2008). Figure 3.1 shows the soil texture, and highlights the fact that similar soils are widely available in the US, in particular in tornado-prone areas. The soil is sun dried, crushed and sieved prior to the production of the earthen blocks, as described in Chapter 2.

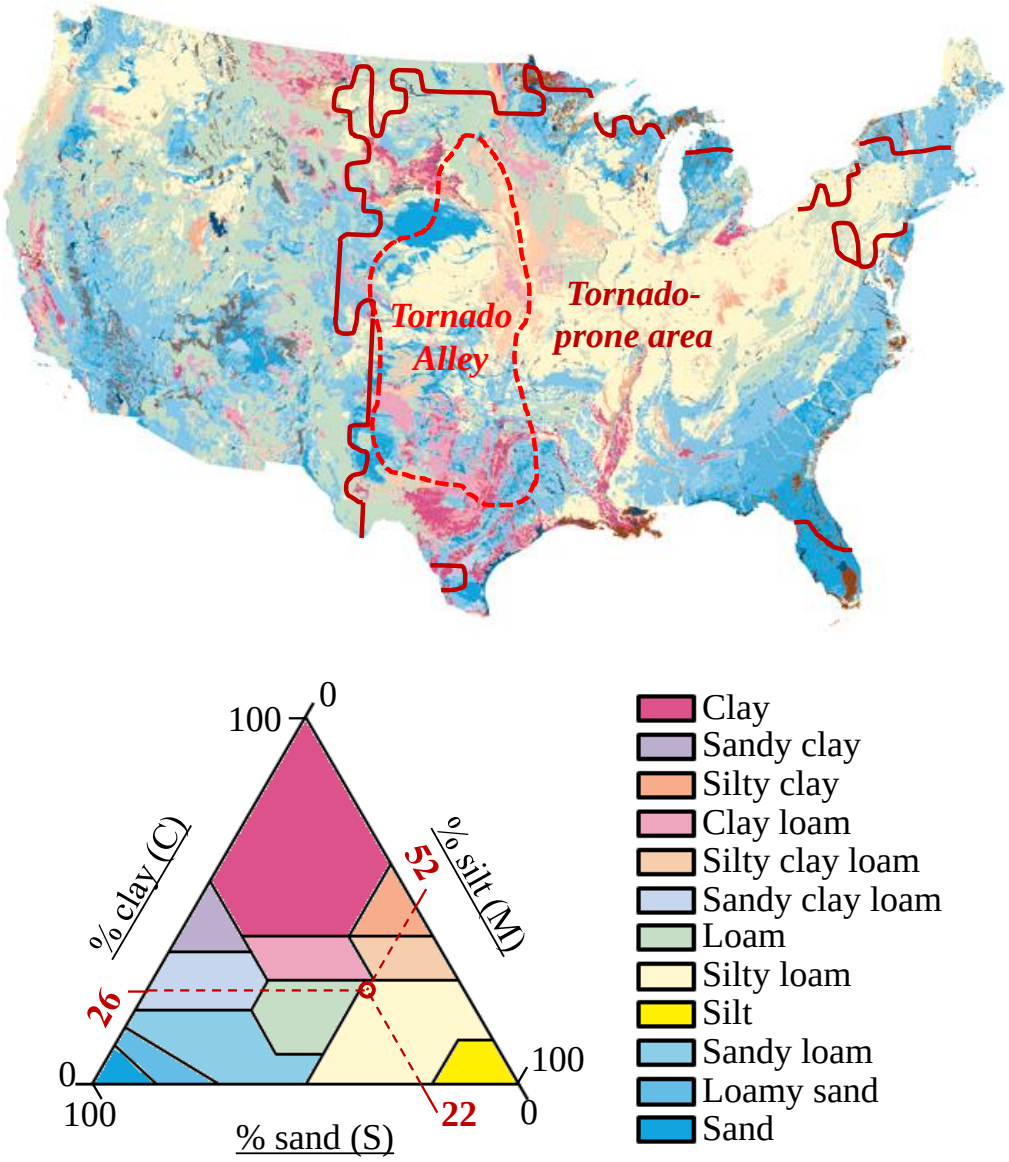

Figure 3.1 US Department of Agriculture soil textural classification and map (USDA 2008) showing tornado-prone areas, Tornado Alley and South Carolina silty loam soil used in prototype CSEB masonry

3.2.2 Earthen blocks

More detailed information on the material, production process and mechanical properties for the earthen blocks are presented in Chapter 2. The CSEBs were produced by compressing the moistened soil with OPC Type I in the amount of 0%, 6% and 9% in weight of soil (wt%). OPC is commonly used to mitigate the swelling of the soil mixture, improving its durability and compressive strength (Venny Riza et al. 2010). The blocks were compacted using a commercial hydraulic press (model EPH-2008, Fernco Metal Products, Capitan, NM) with a compaction pressure of 10 MPa. The average compressive strength of five specimens with dimensions of 127 mm x 127 mm x 89 mm for each type of block is presented in Table 3.1.

Table 3.1 Block compressive strength

Specimen series	OPC content [wt%]	Compressive strength [MPa]	
		Avg.	St. dev.
C	0	1.16	0.14
CS6	6	4.62	0.48
CS9	9	6.09	0.38

3.2.3 Earthen mortar

Two main criteria were followed for the selection of the soil mortar. First, the mortar compressive strength, which is taken as the average of five samples, is evaluated through the uniaxial compression testing of 28-days old 50 mm cubes (ASTM C109). The uniaxial compression load was applied with a displacement rate of 0.64 mm/min. The mortar compressive strength is a key parameter since masonry codes and standards,

such as MSJC (2013) and Eurocode 6 (CEN 2005), specify to estimate the masonry compressive strength as a function of the block and mortar compressive strength.

The mortar compressive strength is affected by the clay content of the soil. Clay minerals tend to weaken the bond between cement paste and inert soil matrix, reducing the strength of the mortar (Walker and Stace 1997). The clay content of the soil is usually modified by adding sand to the soil mixture to reduce the shrinkage cracking. Increasing the clay fraction of the soil mortar may reduce the tensile bond strength (Venkatarama Reddy and Gupta 2006), which is the second parameter for the selection of the soil mortar. Enhancing mortar-block bond strength can lead to an increase in the masonry compressive strength and modify the failure mode (Sarangapani et al. 2005).

The bond strength at the block mortar interface was assessed by testing five crossed-block couplet specimens (Figure 3.2) under uniaxial tensile loading (ASTM C952), with a displacement rate of 0.4 mm/min. The specimens were built with blocks having dimensions 178 mm × 254 mm × 89 mm, and mortar thickness of 13 mm. The block surfaces to be bonded were wetted prior to preparing the couplet specimens. The couplet specimens were covered with plastic sheets for curing and were tested after 28 days.

The mortar mixture SC10, which consists of soil with 10% OPC content by weight, was selected based on an analysis of compressive strength values reported in the literature (Walker and Stace 1997, Walker 1999, Venkatarama and Gupta 2006a). A mortar compressive strength of approximately 3 - 4 MPa using soil with a clay content of

25% - 30% could be tentatively achieved by adding 10% OPC in weight of soil (Figure 3.3).

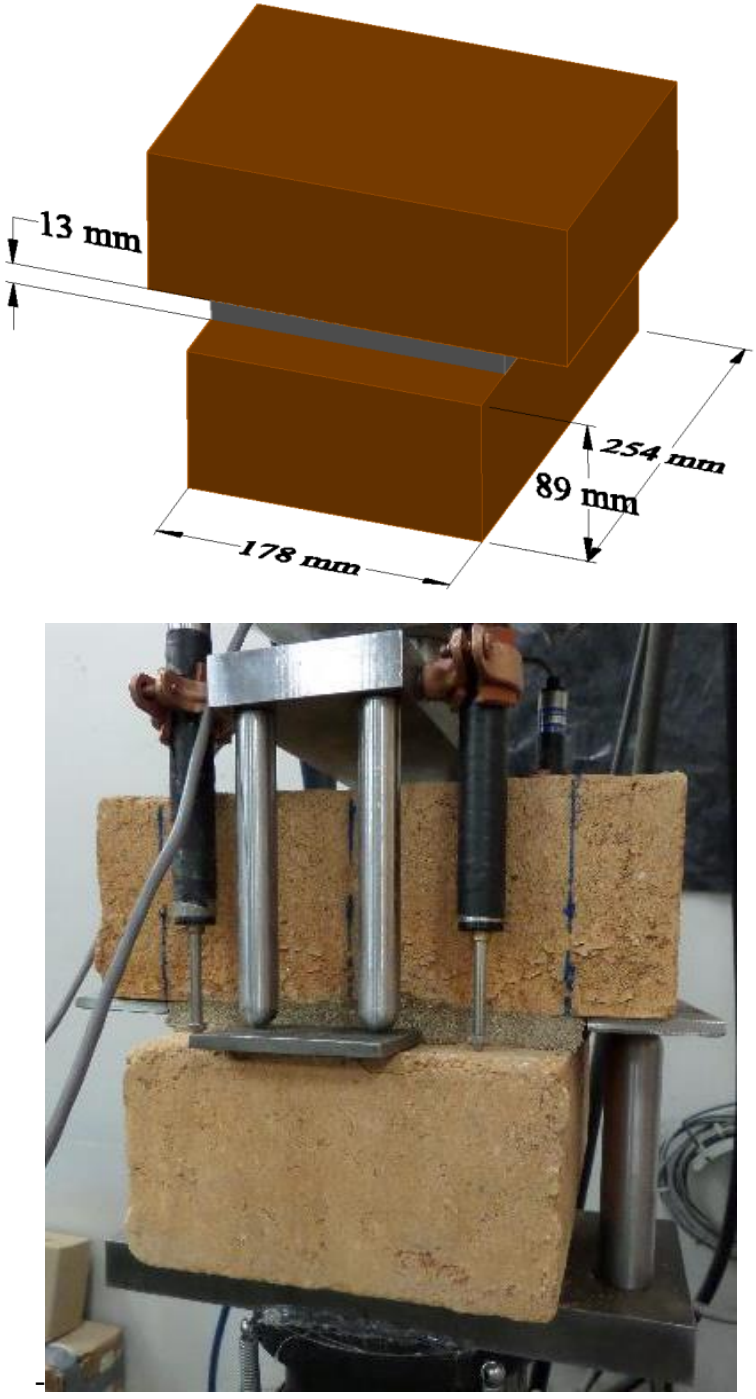

Figure 3.2 Couplet specimen subject to uniaxial tensile loading: evaluation of bond strength at block/mortar interface.

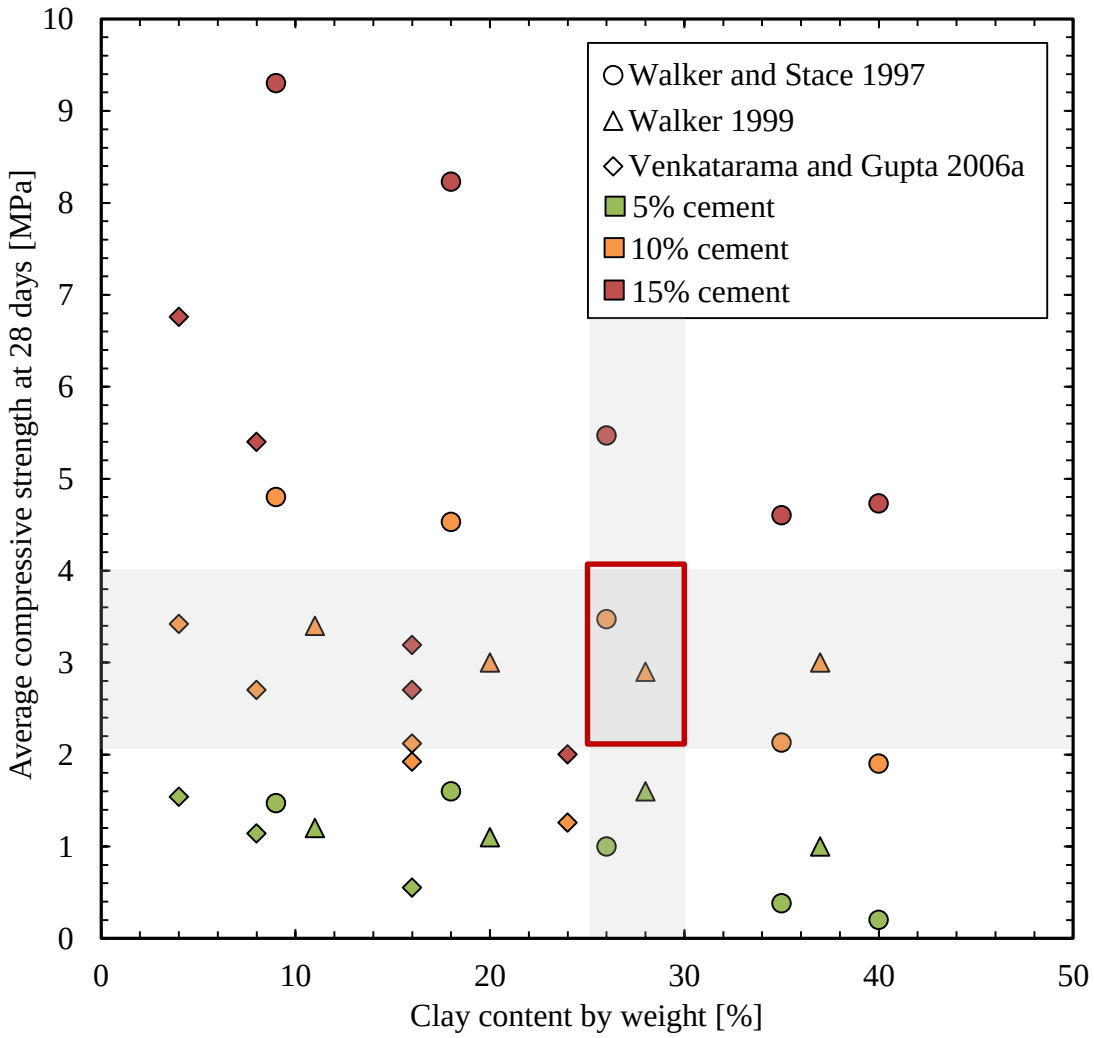

Figure 3.3 Literature evidence on soil cement mortars compressive strength.

In addition, two mortar mixtures with a reduced clay content were also tested. The soil was modified by adding sand. Soil mortars with lower clay content have been found to exhibit better bond strength than some OPC mortars (Venu Madhava Rao et al. 1996). First, the mortar mixture 1C:1So:6S (with cement:soil:sand proportions by weight) was considered. This mixture had been used in previous studies, resulting in a 28-day compressive strength of about 4.0 MPa (Sarangapani et al. 2005; Venu Madhava Rao et al. 1996). However, the OPC content is approximately 12.5 wt%, which is

relatively high with respect to the target maximum of 10 wt%. Therefore, another mortar having proportions 1C:2So:9S was also tested (OPC content equal to approximately 8.3 wt%). The water-to-cement ratio for mortars 1C:1So:6S and 1C:2So:9S was 1.32 and 2.4, respectively, to ensure sufficient workability during the mixing process.

3.2.4 Earthen masonry

Once the mortar is selected, the masonry compressive strength is evaluated for the three earthen blocks considered herein (C, CS6, and CS9 in Table 3.1). The expected outcome from the uniaxial compression test is a candidate combination of earthen blocks and mortar that provides a sufficiently strong masonry while minimizing the OPC content. Then, the shear and flexural strength of the prototype masonry were assessed.

3.2.4.1 Masonry compressive strength

Masonry compressive strength is the most important parameter for design purposes. Design standards such as MSJC (2013), CEN (2005), and NZS 4297 (1998) present the masonry tensile and shear strength as a function of the compressive strength. These standards also provide semi-empirical equations to estimate the masonry compressive strength as a function of the compressive strength of blocks and mortar. However, such relation between masonry, block and mortar compressive strength has not been established for earthen masonry.

The selected earthen mortar and blocks with three different cement contents (0 wt%, 6 wt% and 9 wt%) are used to produce five-block prisms and wallettes to test in uniaxial compression. The effect of block compressive strength on the masonry compressive strength is evaluated with prisms. These specimens were approximately 521

mm high, 178 mm width and 254 mm long (Figure 3.4a). Three specimens were tested after 28 days for each type of block (C, CS6 and CS9). In addition, uniaxial compression tests on wallettes having dimensions 622 mm × 178 mm × 521 mm were performed (Figure 3.4b). This test was designed to study the effect of the mortar head joint on the masonry compressive strength. For out-of-plane loads, it is typically required by masonry building codes to fill the vertical (head) joints (NZS 4297 1998). Three specimens were tested at 28 days for each type of block (C, CS6 and CS9).

Once the combination of earthen blocks and mortar is selected, the shear and flexural strength of the selected SEM prototype are evaluated. In addition to mechanically characterizing the SEM, the shear and flexural tests are also intended to provide information on the relation between shear and tensile strength, and masonry compressive strength, and whether or not traditional masonry design approaches may be considered for earthen masonry.

Shear strength is a key parameter for the design of masonry subjected to in-plane loads (i.e, lateral load such as those imparted by high winds and earthquakes). Shear forces may produce two different failures modes. When the vertical load and bond strength at the block-mortar interface are lower, *sliding shear failure* may take place. This failure mode depends on interface cohesion and friction, and is usually evaluated with a triplet test. The other shear failure mechanism is *diagonal cracking*, and is associated with the formation of diagonal cracks passing through mortar joints and/or blocks, and is usually evaluated with diagonal compression tests.

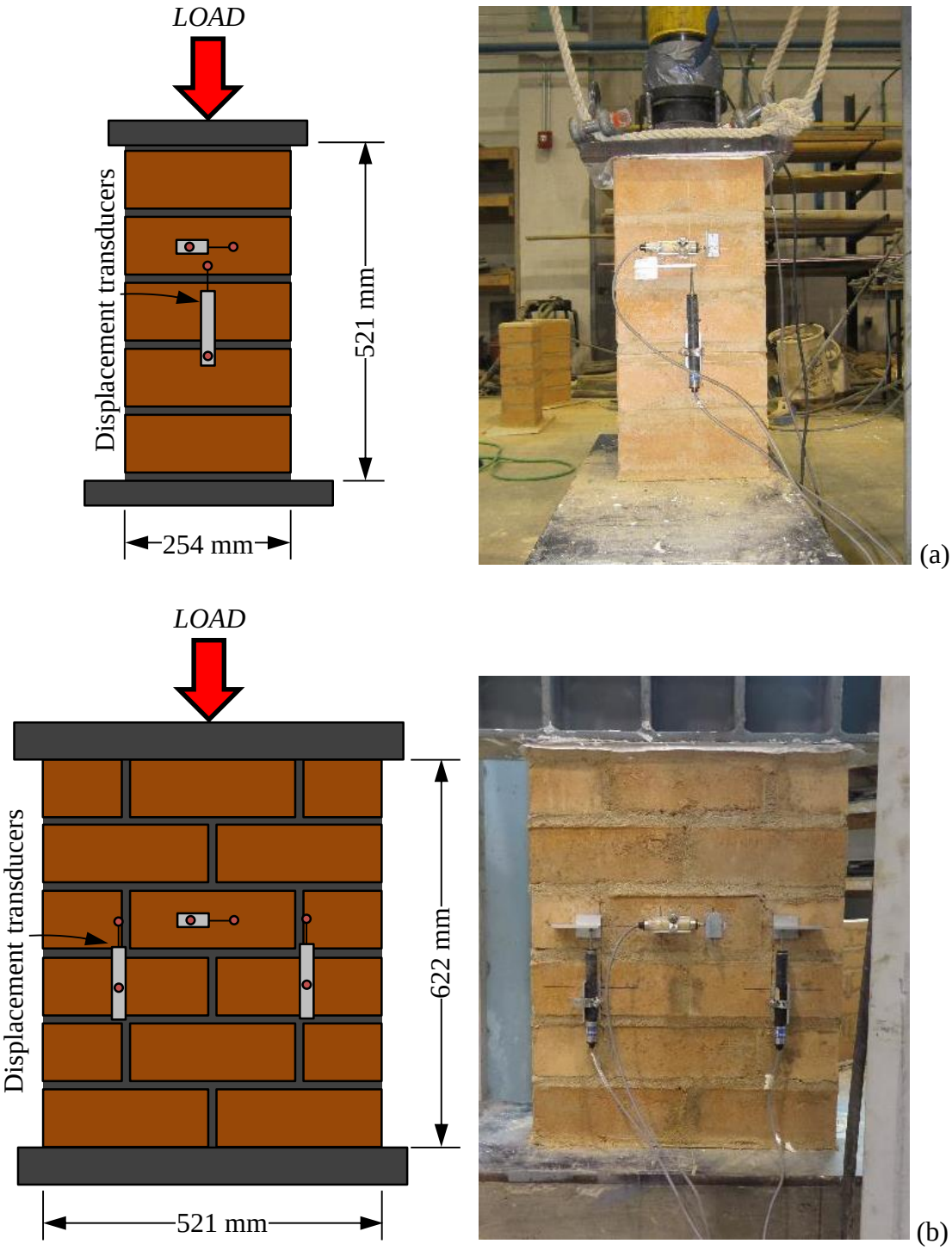

Figure 3.4 Compressive test specimens: (a) prims and (b) wallettes.

The question of which testing procedure should be used for the characterization of the masonry shear strength is common among structural engineers. The triplet test is preferred for masonry with mortar joints regularly arranged; otherwise the results would not be representative of the whole masonry. In addition, the triplet test allows obtaining local parameters of the masonry such as the cohesion and the friction coefficient. The diagonal compression test is applicable for new and existing structures. It is generally believed that the diagonal compression test is more suitable for masonry with homogeneous behavior and isotropic materials since this condition is assumed by the models for the test results interpretation. Alecci et al. (2013) intended to identify the most reasonable testing procedure by subjecting masonry specimens to triplet and diagonal compression testing using different types of mortars. This study concluded that the triplet test is the most suitable and convenient test procedure. This was concluded by the authors because the triplet test has a straightforward interpretation, whereas for the diagonal test two different methodologies are available and provide different results. One approach assumes that the diagonal compression test produces a uniform shear stress distribution (pure shear), as reflected in ASTM E519 (ASTM 2015). The other approach, which is used by RILEM TC 76-LUM (1998), assumes that the stress field in a panel subject to diagonal compression load is not uniform and the strength is found with an isotropic linear elastic model.

In the present work a triplet test and a diagonal compression test were carried out to characterize the shear behavior of the SEM.

3.2.4.2 Shear bond strength

Sliding shear is typically observed when the vertical (e.g., dead) loads are relatively low and the masonry has a poor mortar (Tomaževič 1999). This mechanism is typically observed in the upper part of a masonry wall and around openings, i.e., windows. A direct shear test on triplet specimens with pre-compression load perpendicular to the bed joint is used herein to study this failure mechanism. Besides the evaluation of the shear behavior, in many cases the triplet test has been also used as an indicator of interface bond strength (Olivier and El Gharbi 1995; Venkatarama Reddy et al. 2007). In this study, the pre-compression stress represents the level of compression caused by the self-weight at the top, middle and bottom of a 3 m high earthen masonry wall (0, 0.1, and 0.2 MPa, respectively). Three triplet specimens with dimensions 254 mm × 177 mm × 292 mm were tested at 28 days for each level of pre-compression stress (Figure 3.5). The pre-compression load and the shear load were applied manually with hydraulic cylinders with a 240 kN capacity. The shear strength load was recorded with a 90 kN load cell.

3.2.4.3 Diagonal tensile strength

Diagonal cracks are often observed in masonry walls subject to lateral forces. Diagonal cracking is attributed to the principal tensile stresses in the masonry subject to combined vertical and horizontal in-plane loading (Tomaževič 1999).

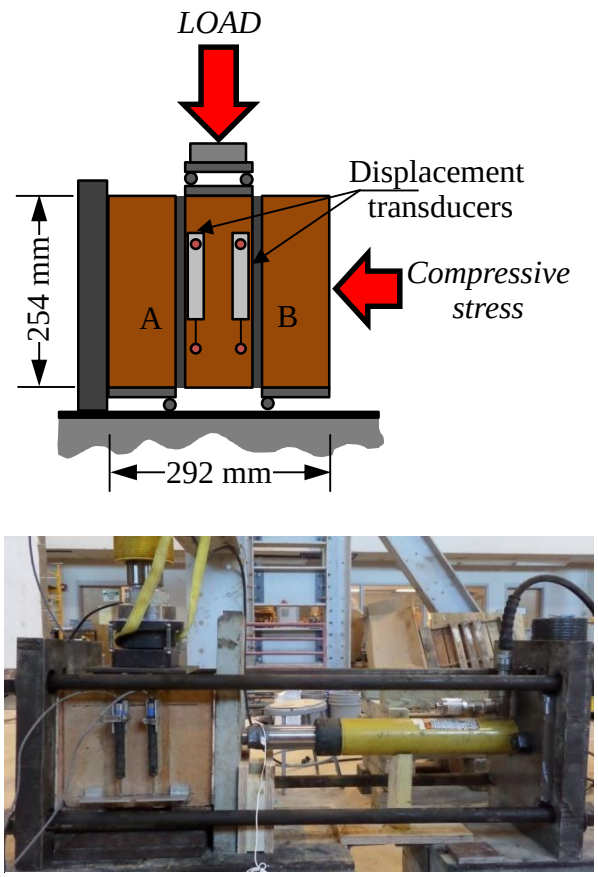

Figure 3.5 Triplet test specimens and setup.

A diagonal compression test was carried out on SEM assemblages to characterize this failure mechanism (Figure 3.6). This test has been used previously for earthen masonry to study the effect of different shear reinforcement systems (Lima et al. 2012; Sathiparan et al. 2006; Turanli and Saritas 2011). Miccoli et al. (2014) compared the shear behavior of earthen block masonry, rammed earth and cob. This study concluded that cob presents a better behavior in shear due to its monolithic construction process and the presence of fiber .reinforcement. However, it is noted that the earth masonry diagonal specimens failed along the bed joints, which is typically observed in masonries with weak block-mortar interface.

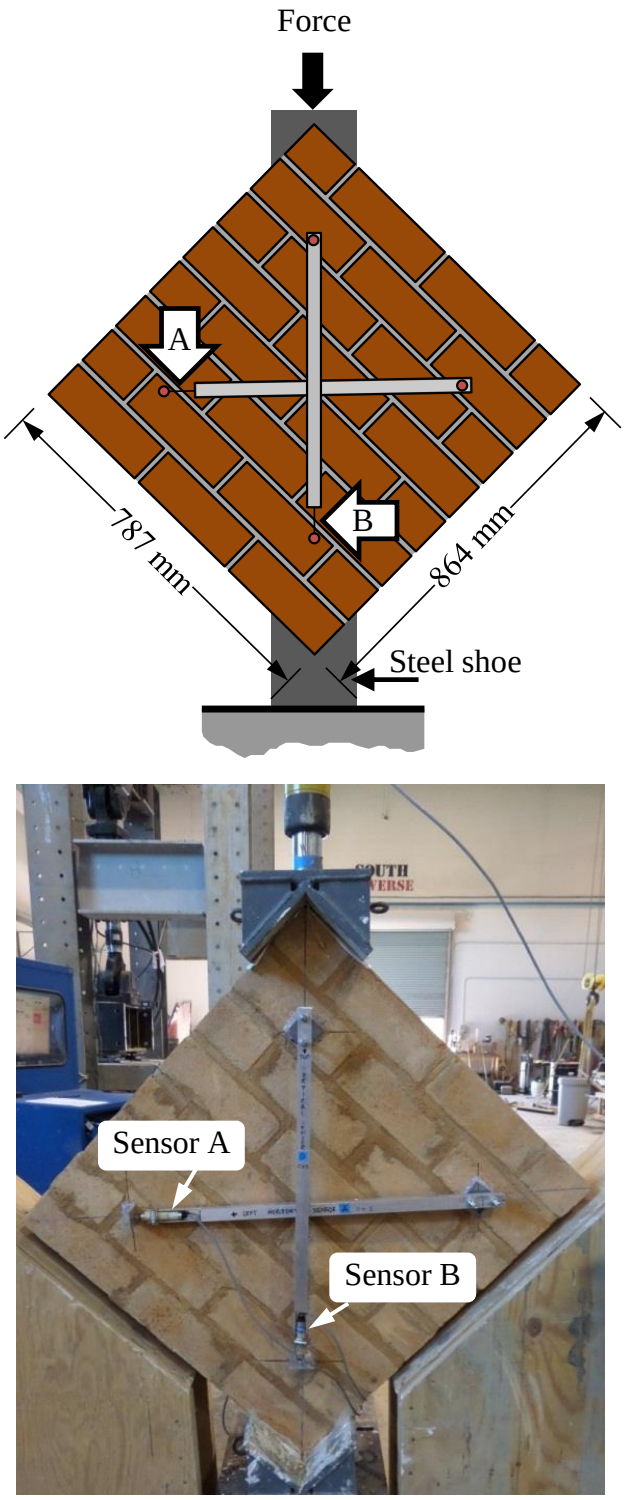

Figure 3.6 Diagonal compression test specimens and setup.

The specimens consisted of earth masonry wallettes having enough vertical and horizontal joints to be representative of earthen masonry systems. Three specimens with dimensions of 864 mm × 787 mm × 178 mm were tested at 28 days. Manual loading was applied with a hydraulic cylinder instrumented with a 40 kN pressure transducer. The vertical contraction and horizontal extension were recorded using displacement transducers located along the diagonal dimensions of the specimens. The gauge length was 711 mm for both directions. Two wood forms were placed on each side of the wallettes to act as bracing elements after failure (Figure 3.6).

3.2.4.4 Flexural strength

The structural response of the masonry when subject to out-of-plane (bending) loading is governed by the masonry flexural tensile strength. In general, flexural strength is recommended to be neglected due to its small value (often less than 0.1 MPa) and variability (Walker 1999). In fact, masonry building codes typically specify to neglect this value for design. However, it has been proposed to allow the use of experimental values for flexure (Tennant et al. 2013).

The masonry flexural strength with tension normal to the bed joints is investigated with a four point bending test. Five five-stacked block prisms, with 521 mm high, 178 mm width and 254 mm long (Figure 3.7), were tested at 28 days. This test aims to characterize the flexural strength and failure mode for the prototype earthen masonry. For flexural tension perpendicular to the bed joints, the expected failure is due to tensile cracking along the bed joints, which is a function of the boundary conditions provided to the specimen (Drysdale and Hamid 2008). The four point bending test represents the

worst condition for the evaluation of the flexural behavior of the masonry. It noted that a high variability, in the order of 20% - 30%, is expected for the interface flexural tensile bond strength (Walker 1999; Drysdale and Hamid 2008).

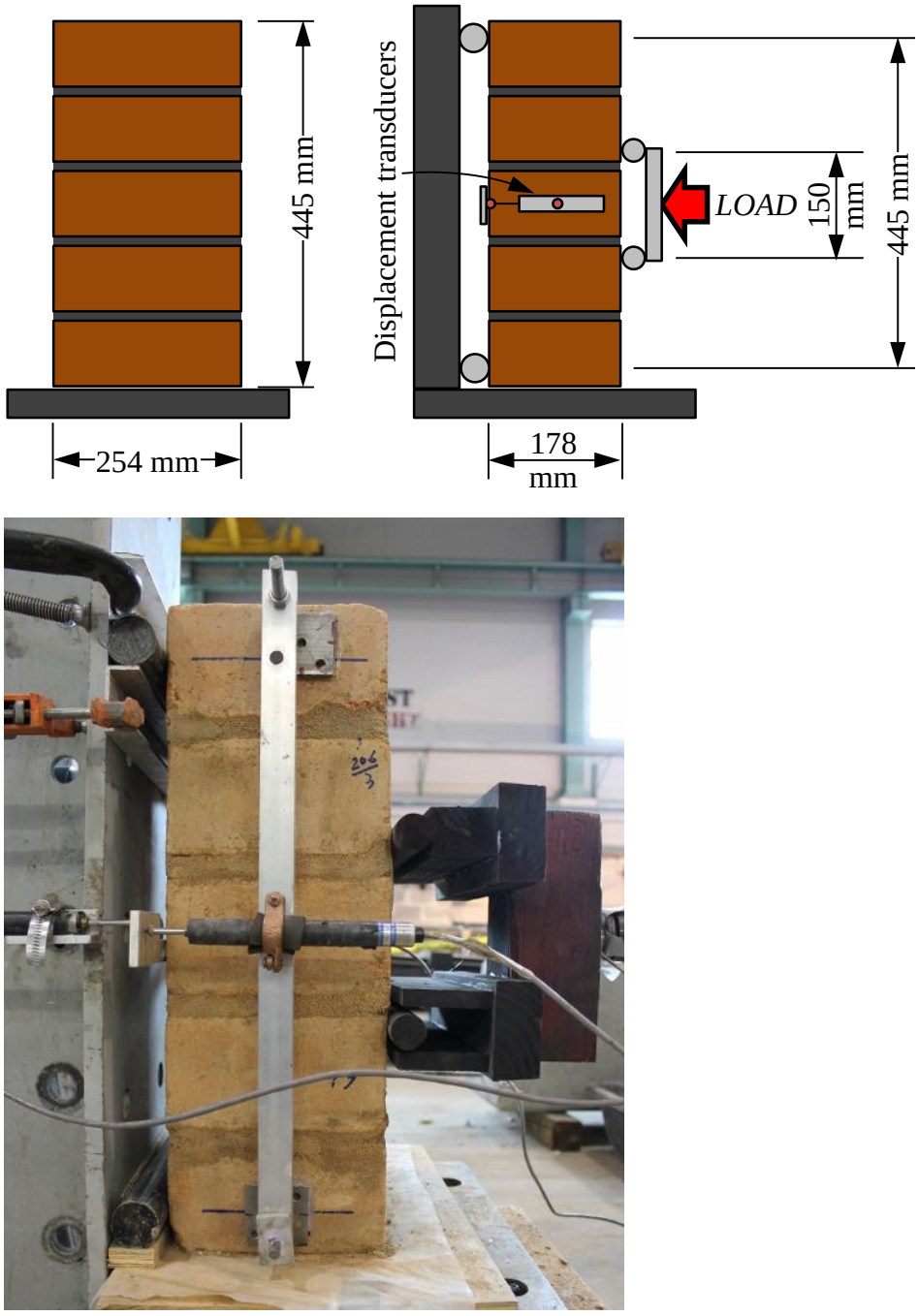

Figure 3.7 Flexural test specimens and set-up.

3.3 RESULTS AND DISCUSSION

The prototyping process starts with the selection of a suitable mortar, which enables the best combination of block and mortar. The following step is to select the earthen block that provides the most effective use of the material in terms of compressive strength. With the selected earthen block and mortar, the salient mechanical properties of the earth masonry prototype are then characterized.

3.3.1 Mortar selection

Table 3.2 summarizes the results for the mortar compressive and tensile bond strength. The SC10 mortar mixture had an average compressive strength of 2.79 MPa, which lies in the range of the required strength. However, with this mortar mixture negligible bond strength was attained at the interface based on couplet tests. This was attributed to the defects that were present in the mortar layer due to the shrinkage of the clayey soil, which negatively affects bond integrity (Figure 3.8). The self-weight of the lower block (6.8 kgf) was enough to separate the blocks. Therefore, it was decided to modify the high clay content of the soil is by adding sand to the mortar mixture.

Table 3.2 Mortar compressive strength and masonry tensile bond strength

Specimen / OPC content [wt%]	Compressive strength [MPa]			Tensile bond strength [MPa]	
	SC10	1C:1So:6S	1C:2So:9S	1C:1So:6S	1C:2So:9S
	10	12.5	8.3	12.5	8.3
1	2.62	7.95	2.57	0.02	0.11
2	2.92	7.85	2.64	0.02	0.03
3	2.73	7.79	2.76	0.12	0.04
4	2.84	8.90	2.63	0.02	0.04
5	2.85	8.33	2.94	0.11	0.07
Avg.	2.79	8.16	2.71	0.06	0.06
St. dev.	0.12	0.46	0.15	0.05	0.03

(a)

(b)

(c)

Figure 3.8 Shrinkage cracking at the block-mortar interface for SC10.

The compressive strength for the mixtures 1C:1So:6S and 1C:2So:9S were 8.16 MPa and 2.71 MPa, respectively (Table 3.2). 1C:1So:6S has a higher cement content and lower clay content resulting in larger compressive strength, which is consistent with the findings of previous studies (Walker and Stace 1997). Both mortar mixtures, 1C:1So:6S and 1C:2So:9S, presented similar tensile bond strengths. This indicated that the tensile bond strength does not necessarily improve by increasing the mortar compressive strength. This was also observed by Walker (1999) in the results of bond wrench tests on earthen masonry with different blocks and mortars.

The tensile bond strength data present high a standard deviation of 0.05 MPa and 0.03 MPa for the 1C:1So:6S and 1C:2So:9S mixture, respectively. High dispersion in couplet tests has been observed in other studies. The representative failure mode was cohesive mortar failure (Figure 3.9a). However, failure in the blocks was observed when higher bond strength was attained (Figure 3.9 b).


(a)
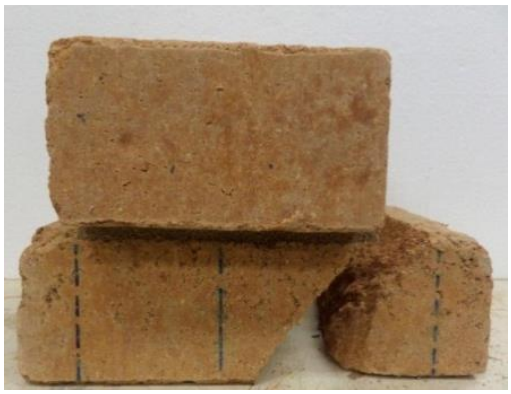
(b)

Figure 3.9 Couplet test failure: (a) cohesive mortar failure, and (b) failure in the block.

Based on the experimental evidence, 1C:2So:9S selected since it offers the best compromise between strength (compressive strength in the range selected for the mortar, and similar bond strength to 1C:1So:6S) and minimization of the OPC content.

3.3.2 Masonry compressive strength

Table 3.3 summarizes the average compressive strength and standard deviation for the uniaxial compression test on prism and wallette specimens. For the prism specimens, the value of masonry compressive strength increases linearly with the block compressive strength. This relationship resembles that proposed by the MSJC (2013) for solid clay units and Portland cement-lime mortar, and is consistent with evidence from prisms compression tests in the literature (Venkatarama Reddy and Gupta 2006; Walker 2004).

Table 3.3 Masonry compressive strength for prism and wallette specimens

OPC content [% wt]		Specimen	Compressive strength [MPa]	
			Prims	Wallettes
C	0	1	0.76	0.84
		2	0.82	0.90
		3	0.79	0.86
		Avg.	0.79	0.86
		St. dev	0.03	0.03
CS6	6	1	4.03	3.53
		2	3.94	4.08
		3	4.17	3.96
		Avg.	4.05	3.86
		St. dev	0.12	0.29
CS9	9	1	5.24	3.54
		2	5.10	4.42
		3	5.81	3.57
		Avg.	5.39	3.84
		St. dev	0.38	0.50

The compressive strength of the prisms is lower than that of the blocks, which is common for strong block-weak mortar combinations. In all cases, including the unstabilized specimens (C), at the same level of load, the vertical strain of the mortar is

slightly larger than the vertical strain of the blocks (Figure 3.10), which is a typical behavior when the mortar is weaker (and thus less stiff) than the blocks. Due to the triaxial confinement of the mortar generated by the axial load, the mortar does not reach its uniaxial compressive strength and failure initiates in the block.

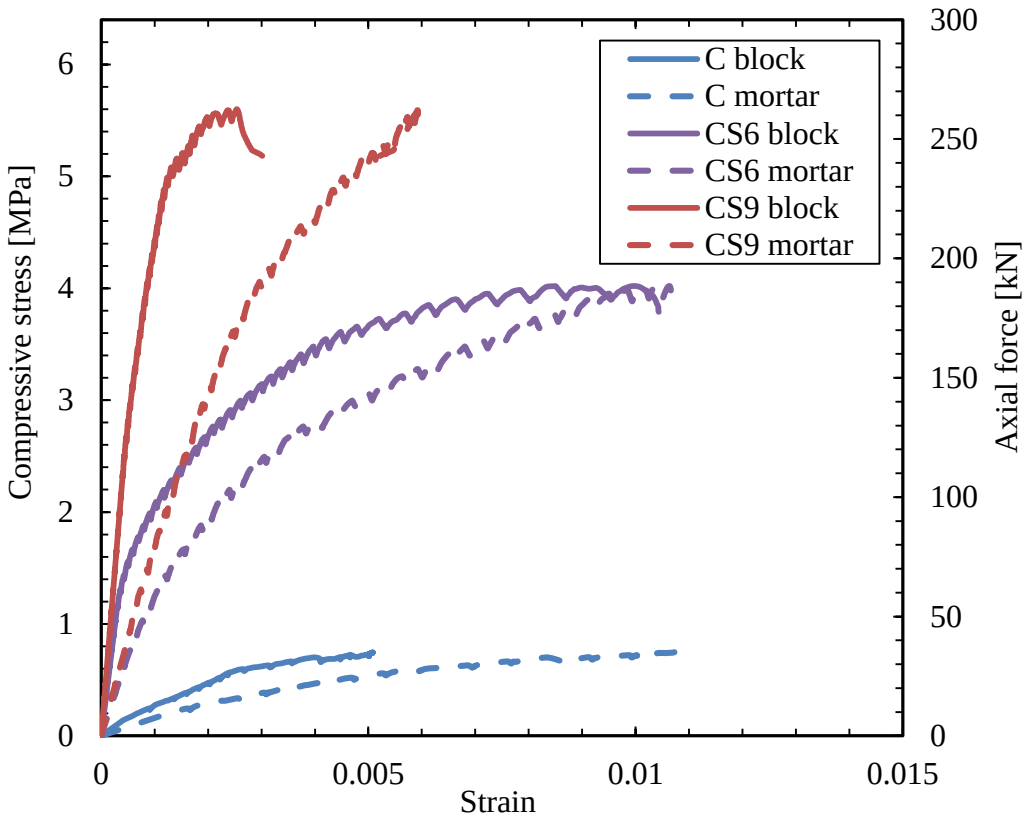

Figure 3.10 Representative stress-strain curve for block and mortar in prism specimens.

In general, a vertical crack through the earthen blocks and mortar was observed in prism specimens (Figure 3.11). This type of failure was also observed when a sufficiently strong bond at the mortar-block interface is provided. Otherwise, the controlling failure mode is bond (interface) separation (Gumaste et al. 2007; Sarangapani et al. 2005).


(a)


(b)


(c)

Figure 3.11 Representative failure mode of masonry prisms: (a) C, (b) CS6, and (c) CS9 specimens.

Figure 3.12 shows the masonry compressive strength (f_c) as a function of the block compressive strength (f_c) for a mortar compressive strength (f_m) equal to 2.5 MPa. Also, the masonry compressive, using CEN (2005) and NZS 4297 (1998) semi-empirical equations, is shown in Figure 3.12. NZS 4297 (1998) provides for two grade of masonry defined as standard grade and special grade (NZS 4297 1998). Standard grade masonry is for the construction of one and two stories buildings. SEM prototype is engineered for low-rise dwellings, thus is comparable with standard masonry. The special grade is for the construction of masonry buildings with higher load demands, and it is required to meet or exceed the requirements for standard grade masonry.

In the case of masonry wallettes, the masonry compressive strength increases with the strength of the blocks, up to 6 wt% in OPC content (CS6) (Figure 3.12). A similar masonry compressive strength was obtained when the cement content of the blocks is increased by 50% (CS9 blocks). This suggests that higher cement content in the blocks does not necessarily increase the masonry compressive strength. In fact, the controlling parameter shifted from the block compressive strength to the tensile strength of the mortar at the head joints. The effect of the head joints is reflected in both the masonry compressive strength values and the failure mode. The compressive load produces indirect lateral tensile stresses at the head joint causing local splitting cracks, which initiates the cracking passing through the earthen blocks, as is highlighted in Figure 3.13c. The load displacement curve of the vertical joint presented a plateau when the strain reached a value of approximately 0.0008, which is greater than the maximum lateral tensile strain associated with the tensile failure of the joint (approximately equal to 0.00063) (Figure 3.14). The plateau indicates the degradation of the vertical joint

interface and crack initiation. The maximum lateral strain was calculated assuming a Young's modulus (E) equal to 400 times the masonry compressive stress and a Poisson's ratio of 0.25. The resulting value of E is consistent with the theoretical range $200f_c \leq E \leq 2000f_c$ (Tomaževič 1999), where f_c is the masonry compressive strength. The cracking produced by splitting of the head joints has also been obtained in studies with similar testing (Gumaste et al. 2007; Miccoli et al. 2014; Walker 2004).

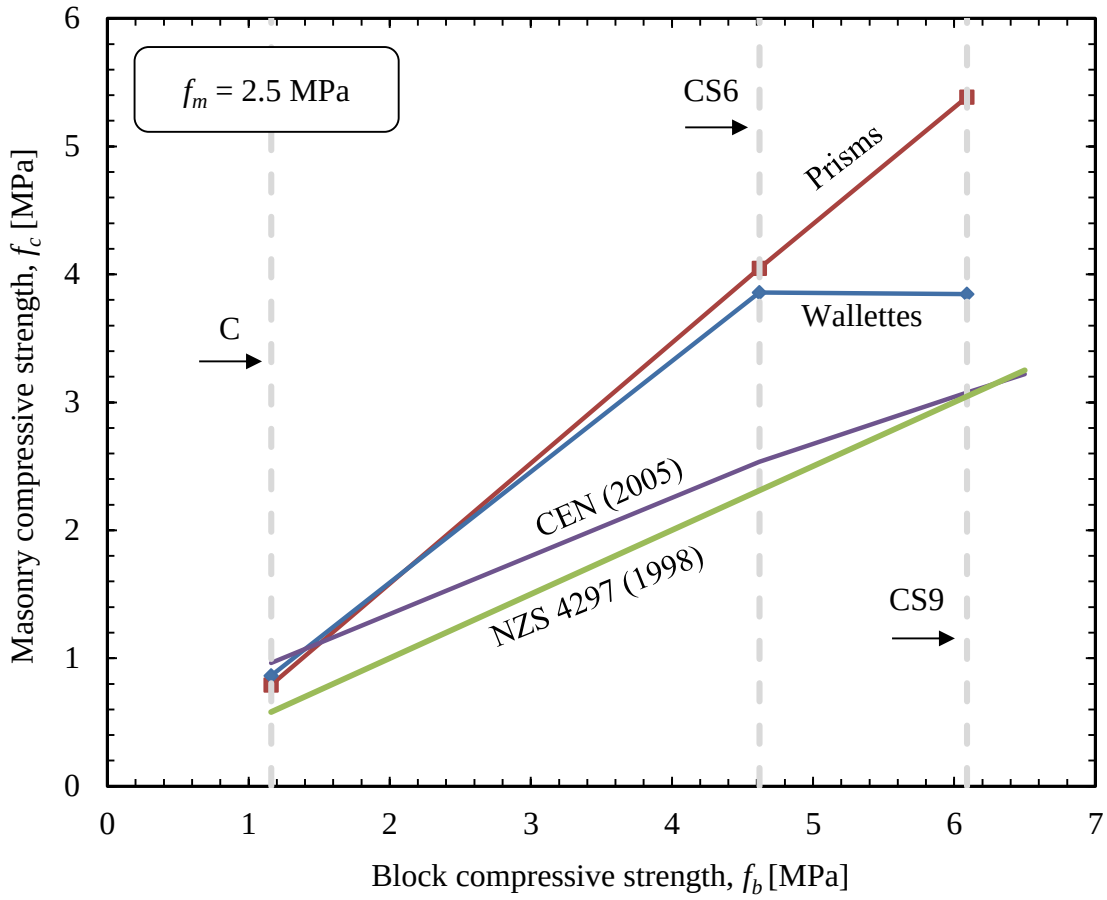

Figure 3.12 Experimental relation between masonry and block compressive strength for prisms and wallettes with a mortar compressive strength of 2.5 MPa. Comparison with theoretical relation per CEN (2005) and special grade construction from NZS 4297 (1998). Dashed, vertical lines indicate average block compressive strength.

(a)

(b)

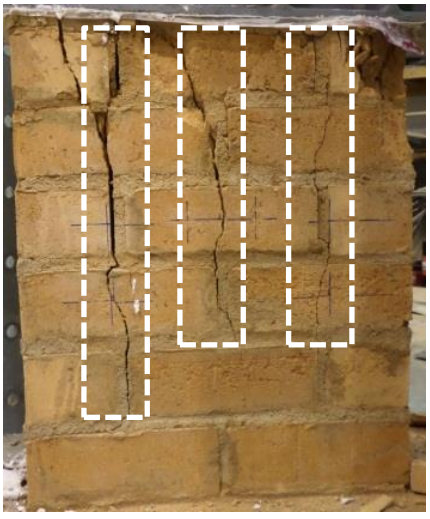

(c)

Figure 3.13 Representative failure mode for wallette specimens indicating head joint crack initiation in CS9 wallettes: (a) C, (b) CS6, and (c) CS9 specimens.

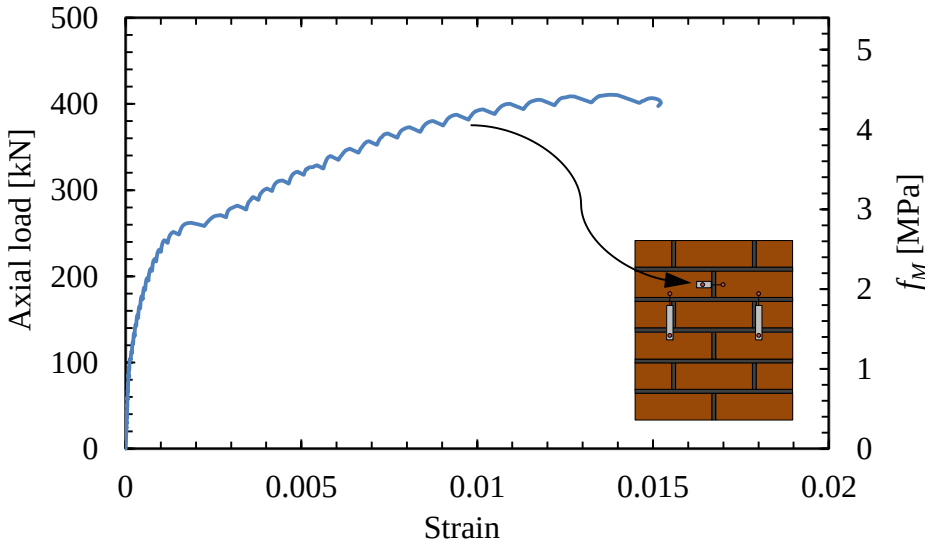

Figure 3.14 Representative load displacement curve at vertical joint for CS9 specimens.

The wallette specimens presented a higher variability than the masonry prisms. Since the head joint depends on the bond strength, which has large fluctuations, an increment in the standard deviation of the data is expected. Despite of this, it is suggested to use the results of compression tests on wallettes for the characterization of the masonry compressive strength. The wallettes are a closer representation of the actual masonry (block-mortar) system, whose behavior depends on that of the head joints.

In theory, the masonry compressive strength can be determined from the values of the block and mortar compressive strength. The MSJC (2013) code provides a linear equation where the masonry strength depends on the type of mortar and the block compressive strength. However, this equation was empirically determined based on tests on solid fired clay bricks and OPC-lime mortar, and is applicable for mortar units with a compressive strength higher than 8.6 MPa (ASTM C62). CEN (2005) provides an

equation that allows the estimation of the masonry compressive strength, including earthen masonry, for different values of block and mortar compressive strength.

$$f_c = K\, f_b^{0.7} f_m^{0.3}$$

In this equation the characteristic compressive strength of masonry, f_c, is a function of a constant K and the block and mortar compressive strength, f_b and f_m. For this case, the constant K is equal to 0.55, which corresponds to clay masonry for use with general purpose mortar. For comparison purposes with the experimental data, the theoretical values from the equation are multiplied by the correction factor 1.2, which is recommended by CEN (2005). Similarly, the NZS 4297 (1998) provides a linear equation to obtain the masonry compressive strength from the unconfined block compressive strength. For special grade earth construction, the masonry compressive strength is calculated as 50% of the block compressive strength. This relation does not include the strength of the mortar, and does not require the testing of prisms specimens. Figure 3.12 shows the graphical comparison between the compressive strength obtained with the equations from the two building codes discussed here (CEN 2005 and NZS 4297 1998) and the average experimental values. It is observed that both equations are overconservative in predicting the masonry compressive strength for the case of stabilized earthen masonry in prism as well as wallette specimens.

In addition, the masonry compression test results show that CS6 blocks and 1C:2So:1S mortar is the combination that offers the most appealing compromise between strength and minimization of OPC content. Therefore, this combination is selected for

the SEM prototype. For this block-mortar combination, relevant mechanical properties are discussed in the following sections.

3.3.3 Shear bond strength

Table 3.4 and Figure 3.15 show the resultant shear bond strength (f_{vk}) for each level of compressive stress applied. As expected, the earthen masonry shear strength follows the Coulomb friction theory, which has been observed in traditional masonry and on earthen masonry (Miccoli et al. 2014).

The continuous line in Figure 3.15 indicates the linear regression of the experimental data. The regression equation resembles the friction model adopted for the majority of masonry building codes, including the MSJC (2013), CEN (2005) and NZS 4297 (1998), to calculate the shear strength:

$$f_{vk} = f_{vo} + \mu_c \sigma_o$$

where σ_o is the compressive stress, μ_c is a constant associated with the contribution of the compression stress, or "friction coefficient", and f_{vo} is the shear strength under zero compressive stress, or "cohesion coefficient" (Tomaževič 1999). The friction coefficient and the cohesion coefficient for the prototype SEM are 0.14 MPa and 1.52, respectively.

Table 3.4 Shear strength results from triplet test.

Specimen / σ_o [MPa]	Shear strength [MPa]		
	0.0	0.1	0.2
1	0.05	0.34	0.41
2	0.28	0.24	0.45
3	0.12	0.17	0.42
Avg	0.15	0.25	0.43
St. dev	0.12	0.08	0.02

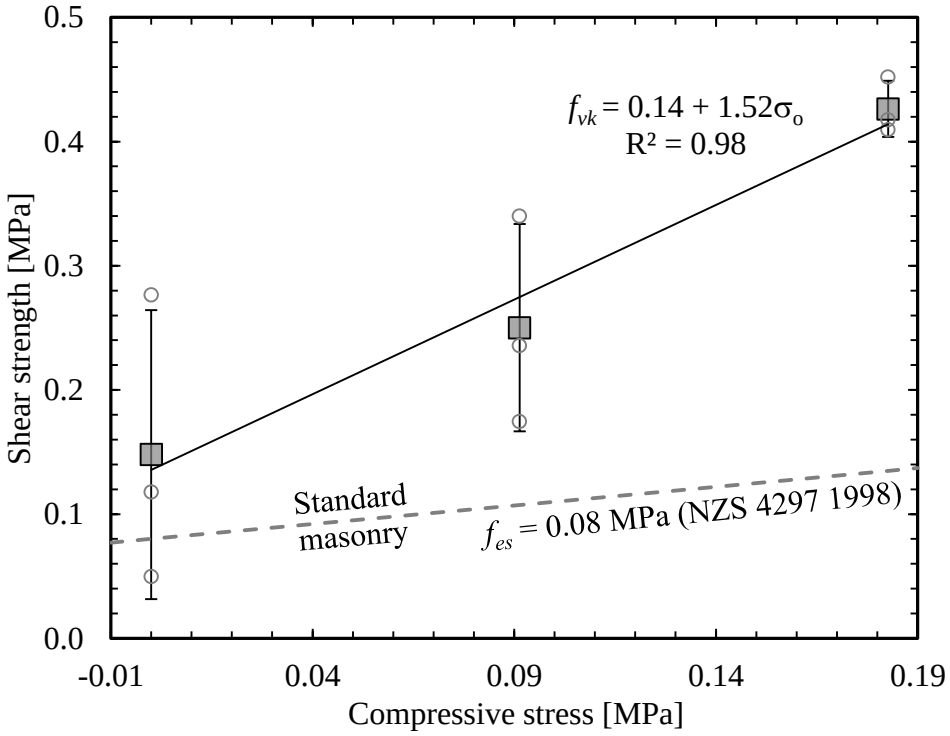

Figure 3.15 Shear strength vs. compressive stress curve. Filled squares represent the average strength and balls represent data points. The limit for standard earthen masonry in accordance with the NZS 4297 (1998) is indicated with dashed line.

In the NZS 4297 (1998), which applies to earthen masonry, the f_{vk} at zero pre-compression is equivalent to the shear strength of earth (f_{es}), and μ_c is defined as 0.30 at mortar bed joints. The value selected for f_{es} depends on the masonry grade and the type of load to which the masonry is subjected. For standard grade masonry subjected to wind loads this value is 0.08 MPa, which radically changes to 1/15 of the masonry compressive strength if the masonry is considered "special-grade". Those two cases are represented in Figure 3.15 with dashed lines. The prototype earthen masonry, for all levels of compressive stress, presents higher shear strength than the standard grade masonry for NZS 4297 (1998). It should be noted in this context that the NZS 4297 (1998) equation for standard masonry conservatively estimates the bond shear strength.

The presence of a pre-compression stress affects the resulting shear strength, its variability, and the failure mode of the triplet specimen. Figure 3.16 shows typical failures for triplet specimens.

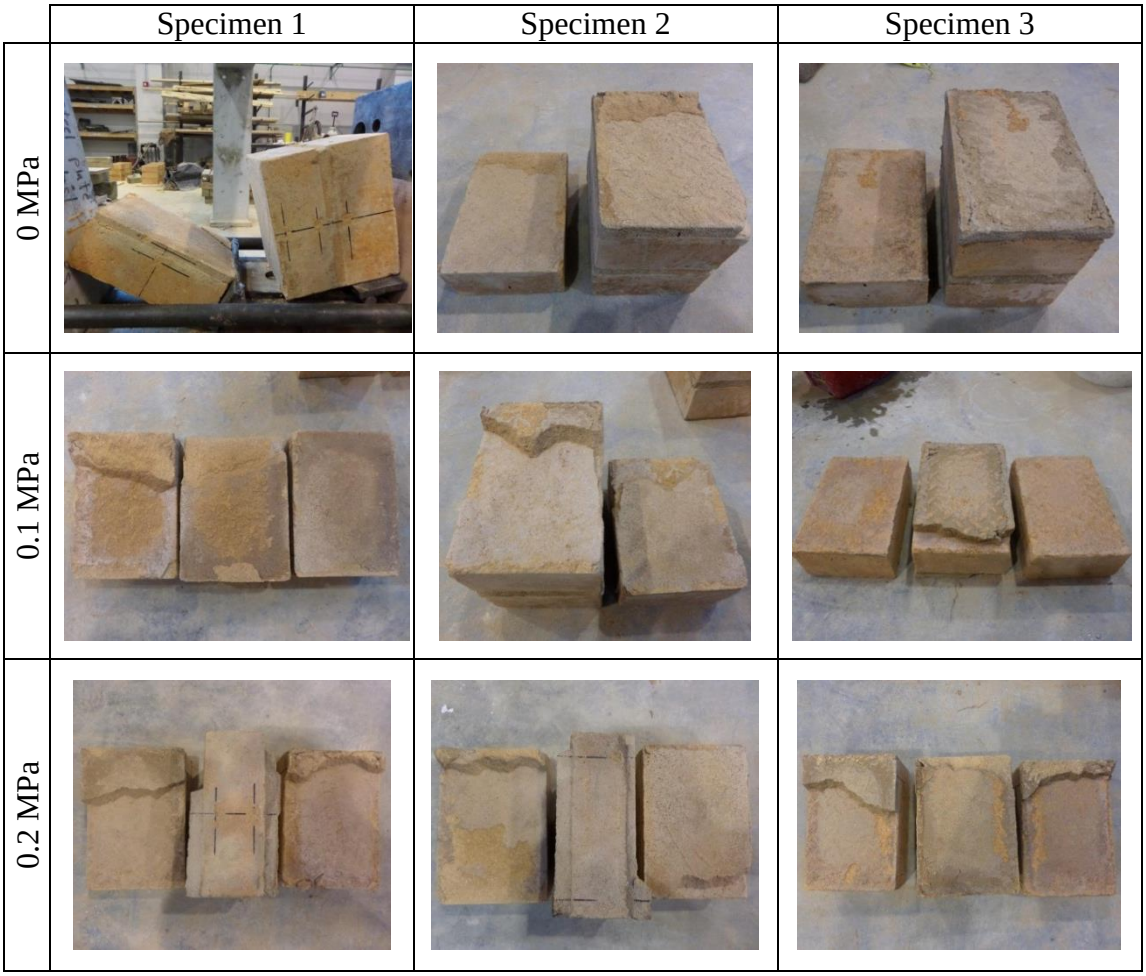

Figure 3.16 Failure mode of triplet specimens subjected to direct shear.

At zero pre-compression stress, the behavior of the specimen is controlled by the bond strength at the mortar-block interface. At zero pre-compression stress, a clean interface failure was typically observed at the weakest mortar joint. Increasing the pre-compression stress modifies the failure mode, including both mortar joints and dividing the failure between two faces (EN 1052-3 2003). In addition, it was observed that the standard deviation of the data is reduced at increasing pre-compression stresses.

3.3.4 Diagonal tensile strength, f_s

Due to its inherent brittle behavior, earthen masonry is susceptible to tensile cracking when subject to combined shear-compression forces. In these instances, the shear capacity can be characterized by means diagonal compression tests. Figure 3.17 shows the diagonal compression test instrumentation and the load – displacement curve for the three specimens tested (using CS6 blocks and 1C:2So:9S mortar). Two methodologies are available for the interpretation of the diagonal compression test. First, an elastic solution was proposed and theoretically demonstrated by Frocht (1931). Here, a comparison between results from the theory of elasticity and that of photoelasticity is carried out to define the elastic stress distribution in a square plate subject to diagonal compression. The results by Frocht (1931) present provide an effective procedure to estimate the principal stresses in masonry. This was confirmed by Yokel and Fattal (1976) with a finite element analysis, finding a difference between the two methods of less than 4%. In addition, Poisson's effects on the magnitude and distribution of the stress, which are assumed equal to zero by Frocht (1953), were found to be negligible. Later, Brignola et al. (2009), found through the use of finite element analysis that this approach is more accurate than the second common approach, which is based on the assumption of pure shear, to determine the stress distribution in regular masonry.

Therefore, the shear strength is calculated considering a not uniform stress distribution and assuming an isotropic linear elastic model (Frocht 1931). The stress state at the center of the panel, with an edge load equal to zero and loading direction of 45°, is calculated with the following equations:

$$\sigma_x = \sigma_y = -0.56\ P/A$$

$$\tau_{xy} = 1.05\ P/A$$

$$\sigma_I = -0.5\ P/A$$

$$\sigma_{II} = -1.62\ P/A$$

where: σ_x and σ_y are the axial compressive stresses in the x and y direction, respectively (Figure 3.19). σ_I and σ_{II} are the principal stresses. *P* is the (positive) compressive force, and A is the transverse area of the panel (herein the average *A* is 144,810 mm2 with a standard deviation of 2,211 mm2). The average fs is equal to 0.62 MPa, with a standard deviation of 0.05 MPa (Table 3.5). The SEM specimens presented a consistent behavior with a coefficient of variation of 8%. The relatively low dispersion of the data attests to the consistency of the materials and construction process. Similarly, the load-displacement curves in Figure 3.17 show comparable results as far as stiffness degradation. The SEM prototype behaves in a brittle fashion when subject to shear and shear-compression forces, and does not offer any residual strength after the maximum load is reached.

Table 3.5 Shear strength results from diagonal compression test.

Specimen	σ_x [MPa]	τ_{xy} [MPa]
1	0.31	0.58
2	0.32	0.60
3	0.36	0.68
Avg	0.33	0.62
St. dev.	0.03	0.05

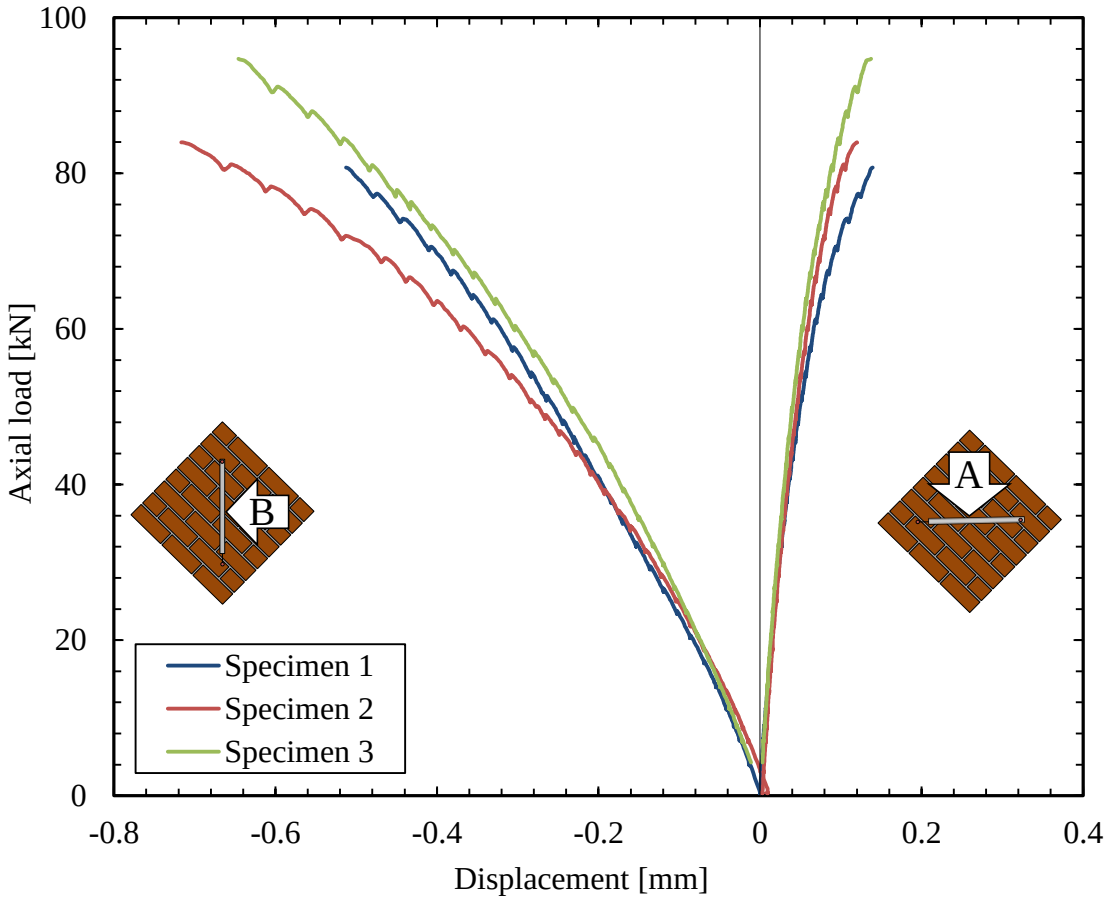

Figure 3.17 Axial load – vertical and horizontal displacement curve for diagonal compression test

The failure modes observed were also consistent for the three specimens tested. All specimens exhibited diagonal cracks parallel to direction of the load and oriented approximately 45° from the bed joints. Diagonal cracks were observed mainly through the blocks, and to a lesser extent along the head and bed joints (Figure 3.18). This showed that for the prototype masonry the weakest link is not the mortar or mortar block interface. Degradation of the interface initiated the failure until the tensile strength of the block is reached and cracks are formed. The failure along the joints was observed with the failure of the blocks, as is highlighted in Figure 3.18.

(a)

(b)

(c)

Figure 3.18 Diagonal compression test failure: (a) Specimen 1; (b) Specimen 2, with inset image showing cohesive bond failure, and (c) Specimen 3.

The resultant diagonal shear strength is approximately 1/7 of the masonry compressive strength. This indicates that the 1/15 recommended by the NZS 4297 (1998) for special grade construction is a conservative value. The diagonal tension strength has a similar value to the direct shear strength (triplet test) for the condition of maximum compressive stress provided.

In general, the building codes use the Mohr-Coulomb theory to represent the response of the masonry to shear forces. Since this theory includes the effect of the vertical (pre-compression) load, it is considered more conservative than the strength obtained from diagonal tension test. In fact, the shear strength obtained experimentally from the diagonal compression test may not be conservative for the cases of relatively low vertical loads (i.e., at the top of a wall and near openings).

3.3.5 Relationship between triplet and diagonal tensile strength

The question of which test is more suitable to characterize the shear behavior of the masonry is still debated. However, works such as the one by Calderini et al. (2010) have shown the similarity, and possibility the correlation between the results of triplet shear tests and diagonal compression tests. Calderini et al. (2010) used the linear elastic solution by Frocht (1931) to propose a diagonal compression test setup to identify shear parameters, such as cohesion and friction coefficients, conventionally found with a triplet test. The proposed diagonal test requires at least two samples with different edge loads, and is only applicable if failure is associated with cracking along the mortar joints.

Indeed, the experimental results presented herein show that by using the linear elastic solution (Frocht 1931) to interpret the results of the diagonal compression tests,

the two test procedures can be related. The stress state shown in Figure 3.19 is used for the comparison of the results from both tests.

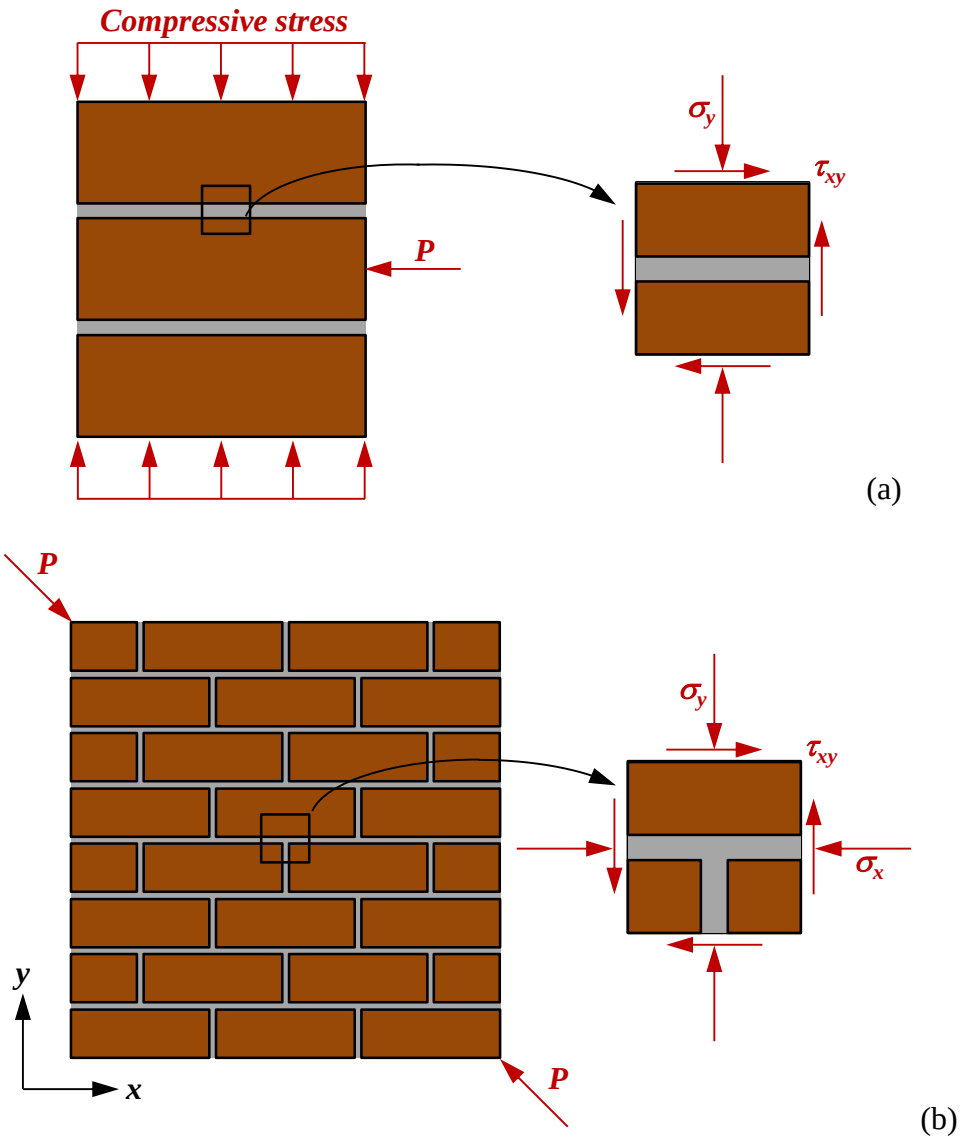

Figure 3.19 Stress state for shear testing: (a) triplet test, and (b) diagonal compression test.

Figure 3.20 shows the results from the triplet and diagonal compression test for the masonry prototype and for another earth masonry prototype assessed by Miccoli et al. (2014). It is clear that the diagonal compression test provides an additional data point to the set of data from triplet tests, for both cases reported.

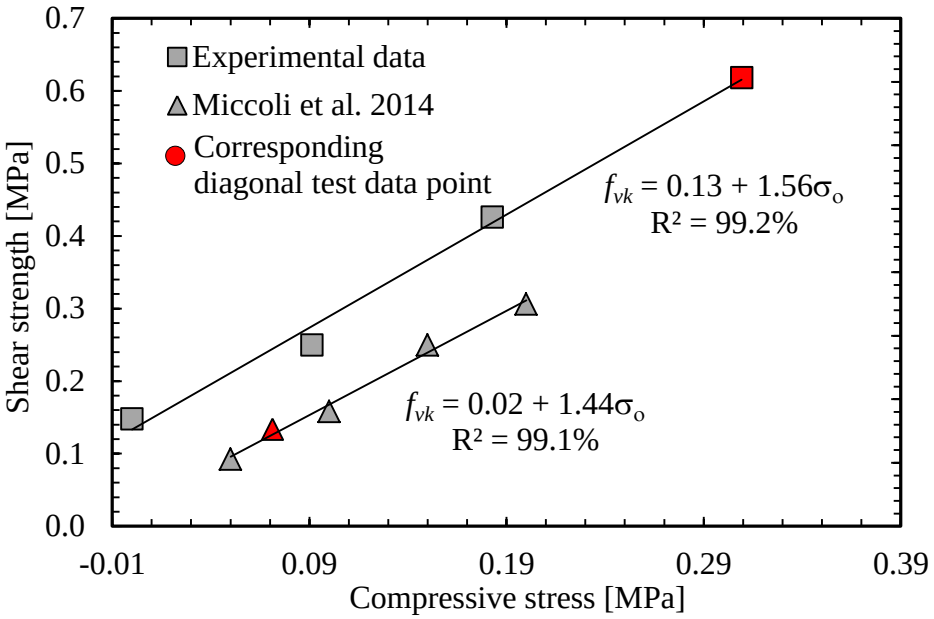

Figure 3.20 Comparison triplet test result with stress state from diagonal compression test

Both these earthen masonry systems presented different failure modes in diagonal compression. Miccoli et al. (2014) reported failure along the joints whereas the masonry prototype presented in this dissertation experienced failure primarily through the blocks. The failure mode of the diagonal panels may be explained by illustrating the failure modes of the triplet specimens, where bond failure affects either or both the adjacent blocks as the pre-compression stress increases. Figure 3.21 shows the different failure modes that can be observed in triplet specimens. Miccoli et al. (2014) reported failure along the joints for the triplet specimens and the diagonal compression test, whereas the SEM masonry prototype presented in this study exhibited different failure modes. For zero pre-compression stresses, the failure was a clean interface failure along the joints (type A1(a) in Figure 3.21). As the pre-compression stress increased, the failure mode transitioned to type A1(b). As the pre-compression stress increases, failure starts compromising the block until splitting crack through the blocks occur. This explains the

failure of the diagonal specimens, which are subject to higher compressive stress (σ_x in the range 0.31- 0.36 MPa in Table 3.5).

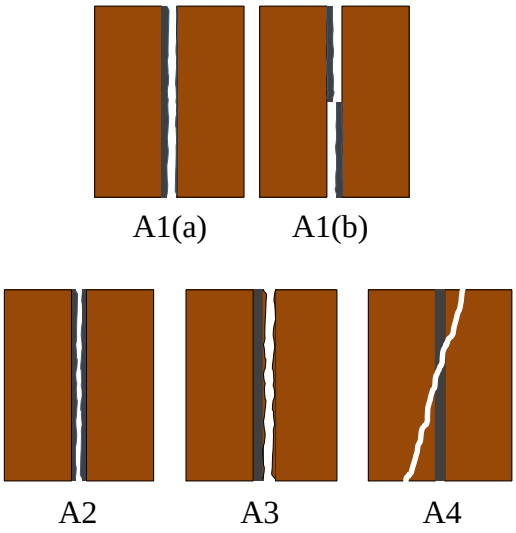

Figure 3.21 Triplet test failure modes: A1- joint failure on a face or divided between two faces, A2 – shear mortar failure, A3 – shear block failure, and A4 – crushing and/or splitting in blocks (UNI EN1052-3)

3.3.6 Flexural tensile strength, f_t

The average flexural strength of the masonry with tension normal to the bed joints is equal to 0.15 MPa with a standard deviation of 0.02 MPa (Table 3.6). The SEM flexural tensile strength lies in the range identified by Matta et al. (2015). Therefore, the masonry prototype is feasible for the resistance of out-of-plane load due to high-wind pressures. As it has been indicated by different authors and in previous sections, the flexural tensile bond strength is highly variable. However, a coefficient of variation of 15% is in the lower limit of the commonly observed range of 16-52% (Venu Madhava Rao et al. 1996; Walker 1999).

In general, the specimens presented a brittle failure mode, cracking along a bed joints with a mixed interface-cohesive failure (Figure 3.22). The failure observed, which involved the earthen blocks, reinforces the evidence of a good bond at the mortar block interface obtained from the couplet tests.

Table 3.6 Flexural tensile strength results.

Specimen	Flexural tensile strength [MPa]
1	0.16
2	0.12
3	0.17
4	0.16
5	0.13
Avg	0.15
St. dev	0.02
CV	15%

Due to the significant variability of the data and low values, the flexural strength is often neglected in masonry design. Since in the MSJC (2013) code this type of masonry is classified as "other" category, it is recommended to use a modulus of rupture equal to zero. However, more specialized building codes allow for the use of strength found experimentally, or provide equations or values from databases. NZS 4297 (1998) recommends a value for the flexural tensile strength that depends on the type of masonry. For standard masonry this values is equal to 0.1 MPa, which is conservative (33% less) in comparison with the strength obtained experimentally for the SEM prototype. CEN (2005) requires determining the flexural strength experimentally or from a database, although earthen masonry is not covered. This background highlights the need for

comprehensive experimental evidence to inform the integration or development of much needed codes of practice for stabilized earth masonry.

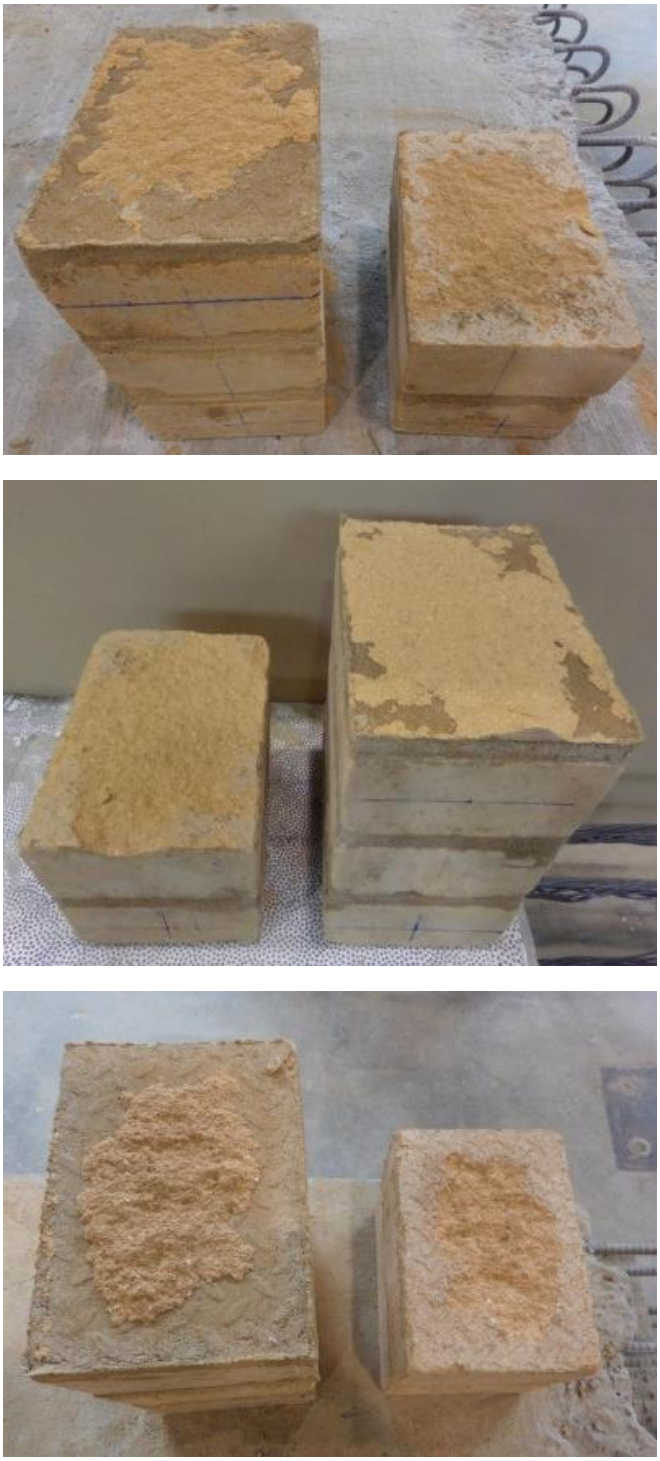

Figure 3.22 Representative failure mode of SEM specimens in flexure.

3.4 STRUCTURAL ANALYSIS

In this section, the experimental results for the prototype SEM are used as input data for the analysis of a typical single-story dwelling structure subject to tornado wind loads. The objective is to demonstrate feasibility with based on experimentally characterized strength properties. The structure has regular rectangular shape without recesses or protrusions, and a symmetric distribution of walls. A 15° gable roof is used. The analytical framework proposed by Matta et al. (2015) is used for the structural analysis of the main wind force resisting system (MWFRS) shown in Figure 3.23. The calculations were carried out assuming a rigid roof diaphragm and similar thickness for all walls.

A range of basic wind speeds of 50 – 90 m/s (180 – 324 km/h) was used for the analysis of the structure. The wind pressures for tornado effects were computed based on the recommendations by the ASCE 7 Subcommittee on Wind Loads for the revision of the ASCE/SEI 7-10 standard (Reinhold and Cope 2013), which draw from the findings by Haan (2010). The exposure category is taken as C because it is a representative scenario for tornado areas. The resultant wind forces were distributed to the walls based on their in-plane flexural and shear stiffness (Matta et al. 2015). For a specific basic wind speed, V, the nominal required wall thickness, t, is computed for the wall that fails first. The calculation assumes a strength reduction factors, ϕ, equal to 1. The uplift pressures applied to the roof, and the dead loads from the slab and self-weight of the wall, are also considered.

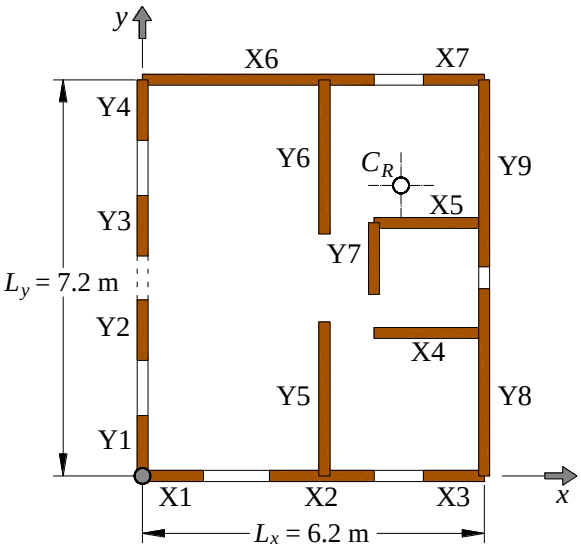

Figure 3.23 Sketch of MWFRS wall layout, dashed lines indicates main entrance and a continuous line indicates windows.

The distribution of vertical load for each wall is computed based on tributary areas. The axial stress for each wall, σ_i, is calculated as the sum of the compressive stress due to the masonry self-weight (σ_M), the weight of the diaphragm (σ_D) (herein taken equal to 337 kg/m^2), and the tensile stress produced by the wind uplift force (σ_W).

$$\sigma_i = \sigma_M + \sigma_D - \sigma_W$$

The required wall thickness is determined for three failure modes: flexural failure for out-of-plane wind pressures, in-plane flexural failure and in-plane shear failure. A simply supported unit length strip subjected to horizontal wind pressure is used for the out-of-plane analysis. The required wall thickness to withstand the wind pressure acting perpendicular to the face of the wall was computed based on the tensile strength at the section where the wall attained failure (Yttrup 1981). The out-of-plane tensile strength, $f_{t,of}$, and the contribution of the self-weight are as follows (Matta et al. 2015):

$$f_{t,of} = \frac{1}{\phi}\left(\frac{3H^2 p_s}{4t^2} - \frac{t^2\gamma^2}{12p_s} - \sigma_i\right)$$

$$\sigma_M = \frac{\gamma}{2}\left(H - \frac{\gamma t^2}{3p_s}\right)$$

Where, $f_{t,of}$ is the masonry tensile (flexural strength) obtained experimentally, H is the height of the walls in m, p_s is the net wind pressure, t is the required wall thickness, and γ is the specific weight of the masonry (herein taken as 1620 kg/m^3). In these equations, the design strength reduction factor, ϕ, is equal to one. A similar approach was used to determine the required wall thickness for in-plane flexure and shear failure. The required thickness for in-plane flexure was based on the masonry compressive force at the crushing toe. The masonry compressive strength for in-plane flexure, $f_{c,if}$, and the corresponding self-weight contribution for each wall of length, L_i, are computed using the following equations:

$$f_{c,if} = \frac{\sigma_i}{0.8\left(1 - \frac{2\tau_i H}{\phi\sigma_i L_i}\right)}$$

$$\sigma_M = \gamma H$$

$f_{c,if}$ is equal to the masonry compressive strength, f_c = 3.8 MPa, obtained experimentally. The required thickness for shear failure is computed in accordance with the shear bond strength equation, which is similar to the models adopted for NZS 4297 (1998), CEN (2005) and MSJC (2013). In the following equation, the shear factor indicating friction along the bed joints, k_v, is equal to 1.52 and the masonry strength for

in-plane shear, $f_{s,if}$, is taken as the masonry strength at zero pre-compression, f_{vo} = 0.14 MPa (as estimated from the experimental data in Figure 3.15**)**.

The contribution of the self-weight is taken at the mid-height of the wall section.

$$f_{s,if} = \frac{\tau_i}{\phi} - k_v \, \sigma_i$$

$$\sigma_M = \gamma \frac{H}{2}$$

A parametric curve that relates the basic wind speed with the thickness of the walls for the three failure modes is presented as a result of the structural analysis. In Figure 3.24 the shaded areas represent the tornado intensity in accordance to the Enhanced Fujita scale (from EF2 to EF5). The required wall thickness for out-of-plane and in-plane flexure follows a quadratic trend whereas for in-plane shear failure it varies in a linear fashion as a function of the wind speed. The failure mode controlling the nominal thickness of the walls is out-of-plane flexure for wind pressures associated with EF2 and EF3 tornadoes. When more severe winds are presented, more than 78 m/s (281 km/h), a rapid change in failure mode is observed. In this case, the failure mode controlling the nominal wall thickness is in-plane flexure. These results are consistent with those reported by Matta et al. (2015). The failure of wall X2 in Figure 3.23 controls the required wall thickness when the structure is subjected to in-plane flexure. For shear failure, walls Y8 and Y9 control the required wall thickness.

Based on the parametric analysis, a nominal wall thickness between 320 mm to 500 mm is required to nominally withstand the pressures imparted by 90% of the tornados recorded in the US, which are rated as EF3 or less (Coulbourne et al. 2002).

These wall thicknesses can be conveniently obtained using conventional double-wythe wall construction.

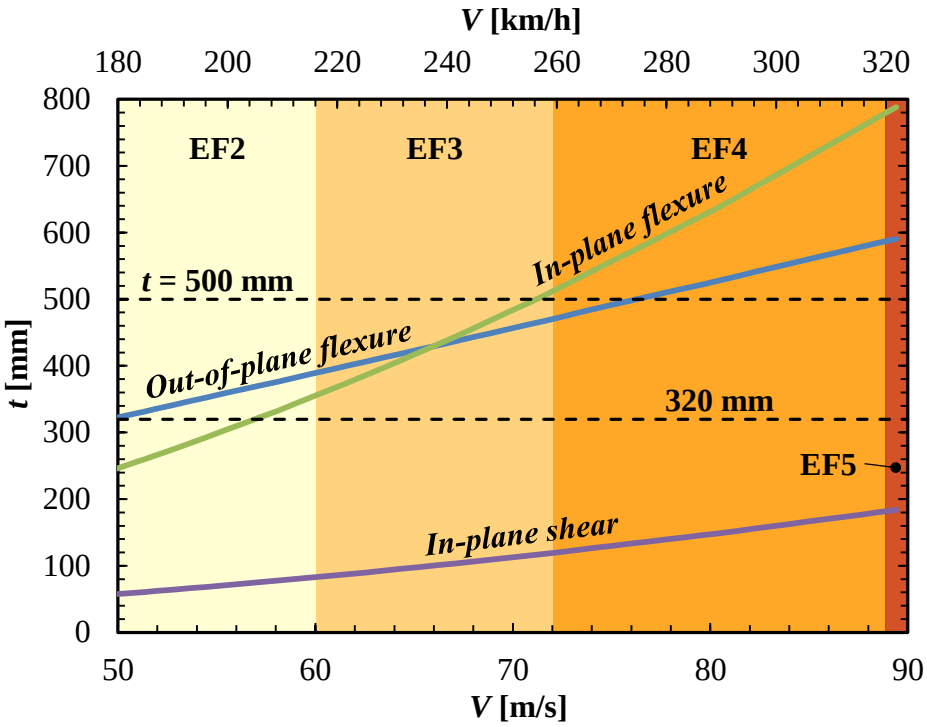

Figure 3.24 Nominal masonry wall thickness required for out-of-plane flexure, in-plane flexure and in-plane shear failure modes.

3.5 Conclusions

A stabilized earthen masonry has been prototyped and mechanically characterized. This masonry is intended for deployment in sustainable, locally appropriate and affordable low-rise family dwelling structures that are capable of withstanding tornado wind pressures. This prototype earthen masonry was analytically demonstrated for a single-story family dwelling structure. The following conclusions are drawn.

1. 1C:2So:9S (cement:soil:sand by weight) earthen mortar offers sufficient bond strength, with a relatively low cement content (8.3% by weight), allowing a suitable

combination with the prototype earthen blocks in terms of tensile strength and failure mode. Similar bond tensile strength was attained with 1C:1So:6S mixture, which has a higher compressive strength due to the bigger cement content (12.5% by weight). This indicates that increasing the mortar compressive strength and OPC content does not necessarily improve the bond at the interface. Earthen mortars with high clay content are not suitable for earthen masonry. The dimension instability of the soil mortar and susceptibility to shrinkage negatively affect the integrity of the mortar joints.

2. Based on the masonry compressive strength results, the combination of stabilized earthen blocks with 6 wt% OPC (CS6) and 1C:2So:9S mortar is selected for the earthen masonry prototype due to the suitable compromise between strength and amount of OPC. The prism specimens presented a linear relationship between compressive strength and block compressive strength, which resembles the equation provided by MSJC (2013) for solid clay masonry units and OPC-lime mortar, and NZS 4297 (1998) for earthen materials. Similar to traditional masonry, the prisms specimens presented splitting failure, which indicates a sufficiently strong block-mortar interface. The results of compression tests on wallette specimens showed the effect of the head joint on the masonry compressive strength. The compressive strength increased with the strength of the blocks up to a 6 wt% OPC content (CS6 blocks), whereas for CS9 blocks the masonry compressive strength is controlled by the tensile strength of the mortar in the head joint, resulting in a similar masonry compressive strength. Therefore, increasing the compressive strength of the blocks (and possibly the OPC content) does not necessarily improve the masonry compressive strength from certain levels of OPC content. For both prism and wallette specimens, existing standard building codes for masonry provide very

conservative estimates of stabilized earthen masonry compressive strength. Using NZS 4297 (1998) and CEN (2005), the experimental compressive strength values were underestimated by 18% to 43%, respectively.

3. The behavior of the prototype stabilized earthen masonry in direct shear follows the Coulomb friction theory, similar to traditional masonry. The Coulomb friction theory is used in the majority of building codes to estimate the masonry shear capacity. In general, the prototype masonry exceeded the shear requirements by the NZS 4297 (1998) for standard masonry. The presence of pre-compression stresses resulted in considerably higher shear strength values, and increasing differences between the required shear bond strength and that (higher) obtained experimentally. In fact, for higher pre-compression stresses (representative of masonry behavior at the base of a one-story wall), the prototype masonry had similar shear strength to the special grade masonry defined by the NZS 4297 (1998). The pre-compression stress also affects the variability of the data and the failure modes for triplet specimens. The variability reduces with the level of pre-compression. At zero pre-compression stress, the bond strength exclusively depends on the mortar joint strength, for which the data are more variable. The failure occurred when the bond strength at the weakest mortar joint was reached. Partial cohesive failure in the blocks, involving both mortar joints, was observed when the pre-compression stresses increased.

4. The SEM prototype presented a diagonal shear strength of 0.62 MPa with a standard deviation of 0.05 MPa. The small variability of the data attests to the consistency of the materials and the construction process. The cracks developed mainly

through the blocks, and less frequently along the mortar joints. NZS 4297 (1998) is conservative in the estimation of the shear capacity.

5. The shear strength obtained through diagonal compression tests can be representative of an additional data point in the shear strength-compressive stress line. It is shown that using a linear elastic solution to describe the stress state in a diagonal compression test specimen, the results of triplet and diagonal compression tests can be correlated. For the prototype masonry this additional set of data represents a stress condition with a higher compressive stress than that applied on the triplet specimens. This was confirmed by the failure mode observed in the diagonal specimens. Due to the higher compression stress, splitting cracks, mainly throughout the blocks, were observed.

6. The resultant flexural strength for the prototype masonry was 0.15 MPa with a standard deviation of 0.03 MPa. The specimens typically presented a mixed failure of interface (adhesive) and block (cohesive). Although the masonry flexural strength is often neglected due to its small value and high variability, more specialized earthen masonry building codes allow for the use of data obtained experimentally or from databases. The NZS 4297 (1998) code is conservative in the recommended value for flexural strength.

7. The experimental nominal compressive and shear strength exceeded the assumed value, and the flexural strength fell in the required range. Therefore, it can be concluded that the SEM prototype presented here in is feasible for the construction of high- wind resistant dwellings.

8. The prototype stabilized earthen masonry is theoretically suitable for tornado resistant single-story dwelling structures. Given a rigid diaphragm and proper

anchorage with the foundation and roof diaphragm, a nominal wall thickness between 320 mm to 500 mm is suitable for the resistance of loads representative of an EF3 tornado. The predominant failure mode is out-of-plane flexure. Therefore, the use of some internal reinforcement is recommended to increase the out-of-plane capacity and provide a robust connection with the foundation and roof diaphragm.

3.6 REFERENCES

Alecci, V., Fagone, M., Rotunno, T., and De Stefano, M. (2013). "Shear strength of brick masonry walls assembled with different types of mortar." *Construction and Building Materials*, 40, 1038-1045

ASCE 7 Standards Committee. Proposal to revise the 2010 edition of ASCE/SEI 7. Submitted by WL Coulbourne and TL Smith on January 7, 2013 for consideration by ASCE 7 Subcommittee on Wind Loads. Reston, VA: American Society of Civil Engineers; 2013.

ASTM (2012). "Standard Test Method for Bond Strength of Mortar to Masonry Units. ASTM C952 – 12." American Society for Testing and Materials, West Conshohocken, PA.

ASTM (2013a). "Standard Specification for Building Brick (Solid Masonry Units Made From Clay or Shale). ASTM C62 – 13a." American Society for Testing and Materials, West Conshohocken, PA.

ASTM (2013b). "Standard Test Method for Compressive Strength of Hydraulic Cement Mortars (Using 2-in. or [50-mm] Cube Specimens). ASTM C109 / C109M - 13." American Society for Testing and Materials, West Conshohocken, PA.

ASTM (2015). "Standard Test Method for Diagonal Tension (Shear) in Masonry Assemblages. ASTM E519 – 15." American Society for Testing and Materials, West Conshohocken, PA.

Brignola, A., Frumento, S., Lagomarsino, S., and Podestà, S. (2009). "Identification of shear parameters of masonry panels through the in-situ diagonal compression test." *International Journal of Architectural Heritage*: *Conservation, Analysis, and Restoration*, 3, 52-73.

CEN (2005). "European Committee for Standardization. Eurocode 6 – Design of masonry structures – Part 1-1: General rules for reinforced and unreinforced masonry structures." BS EN 1996-1-1:2005. Brussels, Belgium:

Calderini, C., CAttari, S., and Lagomarsino, S. (2010). "The use of the diagonal compression test to identify the shear mechanical parameters of masonry." *Construction and Building Materials*, 24, 677–685.

Coulbourne, W. L., Tezak, E. S., and McAllister, T. P. (2002). "Design guidelines for community shelters for extreme wind events." *Journal of Architectural Engineering*, 8(2), 69–77.

Drysdale, R. G., and Hamid, A. A. (2008). *Masonry structures: behavior and design*, Boulder, Colorado.

EN 1052-3 (2003). "Methods of test for masonry Determination of initial shear strength." Milano, Italy.

Frocht, M. M. (1931). "Recent advances in photoelasticity and an investigation of the stress distribution in square blocks subjected to diagonal compression." *Transaction ASME* 55, 135-153.

Gumaste, K. S., Nanjunda Rao, K. S., Venkatarama Reddy, B. V., and Jagadish, K. S. (2007). "Strength and elasticity of brick masonry prisms and wallettes under compression." *Materials and Structures*, 40, 241-253.

Haan Jr., F. L., Balaramudu, V. K., and Sarkar, P. P. (2010). "Tornado-induced wind loads on a low-rise building." *Journal of Structural Engineering*, 136(1), 106–116.

Houben, H., and Guillaud, H. (1994). *Earth construction: a comprehensive guide*, Intermediate Technology Publications, London, UK.

Jiménez Delgado, M. C., and Guerrero, I. C. (2007). "The selection of soils for unstabilised earth building: a normative review." *Construction and Building Materials*, 21(2), 237-251.

Lima, S. A., Varum, H., Sales, A., and Neto, V. F. (2012). "Analysis of the mechanical properties of compressed earth block masonry using the sugarcane bagasse ash." *Construction and Building Materials*, 35(0), 829-837.

MSJC (2013). "Building code requirements and specification for masonry structures (TMS 402-13 / ACI 530-13 / ASCE 5-13) and specification for masonry structures (TMS 602-13/ACI 530.1-13/ASCE 6-13) and companion commentaries." Farmington Hills, MI: American Concrete Institute; Reston, VA:

American Society of Civil Engineers; Longmont, CO: The Masonry Society; 2011.

Matta, F., Cuéllar-Azcárate, M. C., and Garbin, E. (2015). "earthen masonry dwelling structures for extreme wind loads." *Engineering Structures*, 83, 163-175.

Miccoli, L., Müller, U., and Fontana, P. (2014). "Mechanical behaviour of earthen materials: a comparison between earth block masonry, rammed earth and cob." *Construction and Building Materials*, 61, 327-339.

Morel, J. C., Pkla, A., and Walker, P. (2007). "Compressive strength testing of compressed earth blocks." *Construction and Building Materials*, 21(2), 303-309.

Morton, T. (2008). *Earth masonry design and construction guidelines*, IHS BRE Press, Garston, Watford.

Muntohar, A. S. (2011). "Engineering characteristics of the compressed-stabilized earth brick." *Construction and Building Materials*, 25(11), 4215-4220.

NZS 4297 (1998). "Standards New Zealand. Engineering design of earth buildings." Wellington, New Zealand.

NZS 4298 (1998). "Standards New Zealand (NZS). Materials and workmanship for earth buildings. " Wellington, New Zealand.

Olivier, M., and El Gharbi, Z. "Sisal fibre reinforced soil block masonry." *Proc., Fourth International Masonry Conference*, 55-58.

Reinhold, T. A, and Cope, A. D.(2013). Private communication; March 8, 2013.

Rigassi, V. (1985). "Compressed earth blocks: manual of production." CRATerre-EAG, Germany.

RILEM TC 76-LUM (1988). "General recommendations for methods of testing load-bearing masonry." *Materials and Structures*, 21(123), 227-231.

Sarangapani, G., Venkatarama Reddy, B., and Jagadish, K. (2005). "Brick-mortar bond and masonry compressive strength." *Journal of Materials in Civil Engineering*., 17(2), 229–237.

Sathiparan, N., Mayorca, P., Nasrollahzadeh Neshali, K., Guragain, R., and Meguro, K. (2006). "Experimental study on unburned brick masonry wallettes retrofitted by pp-band meshes." *Monthly Journal of the Institute of Industrial Science*, 58(3), 121-124.

Tennant, A. G., Foster, C. D., and Venkatarama Reddy, B. V. (2013). "Verification of masonry building code to flexural behavior of cement-stabilized soil block." *Journal of Materials in Civil Engineering*, 25(3), 303-307.

Tomaževič, M. (1999). *Earthquake-resistant design of masonry buildings*, Daryaganj, New Deli.

Turanli, L., and Saritas, A. (2011). "Strengthening the structural behavior of adobe walls through the use of plaster reinforcement mesh." *Construction and Building Materials*, 25(4), 1747-1752.

UNI EN1052-3 (2003). " Methods of test for masonry - Determination of initial shear strength." Norma Europea, Milano, Italia.

US Department of Agriculture (USDA) (2008). US soil textural map, USDA, <http://www.soilinfo.psu.edu/index.cgi> (Dec. 16, 2013).

Venkatarama Reddy, B. V., and Gupta, A. (2006). "Strength and elastic properties of stabilized mud block masonry using cement-soil mortars." *Journal of Materials in Civil Engineering*, 18(3), 472-476.

Venkatarama Reddy, B. V., and Gupta, A. (2006). "Tensile bond strength of soil-cement block masonry couplets using cement-soil mortars." J *Journal of Materials in Civil Engineering*, 18(1), 36-45.

Venkatarama Reddy, B. V., Lal, R., and Nanjunda Rao, K. S. (2007). "Enhancing bond strength and characteristics of soil-cement block masonry." *Journal of Materials in Civil Engineering*, 19(2), 164-172.

Venny Riza, F., Rahman, I. A., and Zaidi, A. M. A. (2010). "A brief review of compressed stabilized earth brick (CSEB)." *Science and Social Research (CSSR), 2010 International Conference*, IEEE Xplore, Kuala Lumpur, Malaysia, 999 - 1004.

Venu Madhava Rao, K., Venkatarama Reddy, B. V., and Jagadish, K. S. (1996). "Flexural bond strength of masonry using various blocks and mortars." *Materials and Structures*, 29, 119-124.

Walker, P. (1999). "Bond characteristics of earth block masonry." *Journal of Materials in Civil Engineering*, 11(3), 249-256.

Walker, P., and Stace, T. (1997). "Properties of some cement stabilised compressed earth blocks and mortars." *Materials and Structures*, 30(203), 545-551.

Walker, P. J. (2004). "Strength and erosion characteristics of earth blocks and earth block masonry." *Journal of Materials in Civil Engineering*, 16(5), 497-506.

Yokel, F. Y., and Fattal, S. G. (1976). "Failure hypothesis for masonry shear walls." *Journal of the Structural Division*, 102, 515-532.

Yttrup, P. J. (1981). "Strength of earth walls subjected to lateral wind forces." *First National Local Government Engineering Conference*, Adelaide, Australia, 24-27

CHAPTER 4

RECYCLABLE PLASTIC FIBER REINFORCEMENT FOR DAMAGE TOLERANCE TRANSFORMATION OF STABILIZED EARTHEN MASONRY

ABSTRACT. This chapter introduces a compressed, stabilized and reinforced earthen masonry (SREM), which is manufactured using soil that is widely available throughout the US, and incorporates non-biodegradable and recyclable plastic fiber reinforcement. The fiber-reinforced system aims to radically enhance the mechanical behavior of the prototype stabilized masonry system (SEM) discussed in the previous chapter, with an emphasis on damage tolerance against local penetration of wind-borne debris. The prototype SREM is engineered to enhance the residual strength and energy absorption of the earthen masonry system for in-plane and out-of-plane loads. The objective is to prototype and characterize a SREM system that pairs the well-known "green" features and affordability of earthen construction materials with the structural strength and deformability needed to engineer safe hazard resilient dwellings.

The prototype SREM blocks are stabilized with a small amount of ordinary Portland cement (OPC, 6% in weight or wt%) to enhance strength and durability. In addition, recycled and non-biodegradable polyethylene terephthalate (PET) plastic fibers are incorporated in the blocks, and are shown to transform the damage tolerance of the earthen blocks. This outcome is particularly important for the masonry resistance against flying debris in extreme wind events. The fiber reinforced system was constructed with a compatible mortar made with the same soil, sand, and small amount of OPC (8 wt%), and

reinforced with low-cost synthetic microfibers. The fiber reinforcement radically enhanced the dimensional stability of the mortar and, in turn, the integrity of the block mortar interface. First, the selection of the fiber volume fraction (V_f) for the reinforced mortar, and its mechanical characterization, are presented. Then, the strength and deformability properties that are relevant for the in-plane and out-of-plane behavior of the masonry system were comprehensively characterized through physical experiments. The experimental evidence from uniaxial tension, out-of-plane flexure, bond and diagonal shear tests, is presented and discussed. In addition, proof of concept for the resistance of the prototype earthen masonry against the impact of wind-borne debris impact is demonstrated through preliminary results from high-velocity impact experiments.

4.1 INTRODUCTION

Earth construction systems have been used widely around the world. Their uses vary greatly due to the numerous benefits; among them are natural thermal and acoustic insulation, humidity control, relatively low carbon footprint, and local availability of soil (Morton 2008). Compressed earthen masonry consists of compressed earthen blocks (CEBs) and mortar. The mechanical properties and durability (e.g., erosion resistance) of CEBs can be enhanced by using binders and, in some instances, reinforcing fibers (Rafalko et al. 2007).

Different materials have been used to reinforce earthen blocks. The choice for these materials usually depends on the local availability, and sometimes on the need to recycle and reuse a particular by-product or waste. The main purpose of the fibers is to mechanically stabilize the soil matrix (Hejazi et al. 2012). It has been found that the incorporation of fibers contributes to mitigating shrinkage effects, and in general to

enhance dimensional stability (Ghavami et al. 1999, Bouhicha et al. 2005). Mechanical stabilization by means of fibers often has a beneficial effect on compressive strength (Ghavami et al. 1999, Taallah et al. 2014, Mustapha et al. 2015), flexural strength and post-cracking strength and deformability of the soil (Bouhicha et al. 2005, Millogo et al. 2014, Mustapha et al. 2015). Here, toughening effects are particularly important to radically change the damage tolerance of earthen masonry. Organic fibers from plants and animals are the most common form of fiber reinforcement. In particular, straw and sisal fibers are often used in earthen block matrices (Ghavami et al. 1999, Bouhicha et al. 2005, Binici et al. 2007, Clementi et al. 2008, Yetgin et al. 2008, Quagliarini and Lenci 2010, Lenci et al. 2011, Piattoni et al. 2011, Mesbah et al. 2014). However, it has been pointed out that natural fibers are susceptible to excessive water absorption in the mixture process, reducing workability and increasing the amount of water to be added in the mixture. Then, part of the absorbed water is released after the drying process, facilitating the formation of voids that contribute to weakening the fiber-matrix interface and the durability of earthen blocks (Ghavami et al. 1999, Taallah et al. 2014). The tendency is to use fibers that provide satisfactory results in other cement composites, such as concrete and mortar. For example, polypropylene, nylon and poly vinyl alcohol (PVA) fibers have been used to reinforce soil matrices. It has been reported that plastic fibers contribute to enhancing soil matrices by increasing the compressive strength, tensile strength, toughness (Maher and Ho 1994, Rafalko et al. 2007), and elastic stiffness of the soil matrix (Plé and Le 2012). The reinforcing effect of the plastic fibers is due to the bond (friction) strength at the fiber-cement matrix interface (Tang et al. 2007), which contributes to offsetting crack growth (Senol 2012). In addition, the presence of plastic

fibers reduce the susceptibility to swelling due to moisture effects (Cai et al. 2006). However, it is recommended to limit the amount of fiber reinforcement to 0.8% in weight of soil to avoid negatively affecting the fiber dispersion and the workability of the mixture (Miller and Rifai 2004).

Lately, fibers obtained from recycled plastic materials have been investigated with promising results. Azeko et al. (2015) found that, by incorporating polyethylene fibers in blocks made of laterite and OPC, the compressive strength, flexural strength and toughness are increased for a V_f up to 20% in volume. In fact, further increasing the V_f negatively affected the mechanical properties of the blocks, due to the introduction of stress raisers from entangled polyethylene particles. Similarly, Subramaniaprasad et al. (2015) used recycled fibers from grocery bags and PET bottles in stabilized blocks in amounts of 0.1% and 0.2% by weight of soil. The fibers were chopped to obtain a width and length between 1 mm - 2 mm and 10 and 20 mm, respectively. They found that the incorporation of fibers resulted in increasing the tensile strength. The reinforced specimens displayed a tensile strength up to 4.5 times higher than the obtained for the unreinforced specimens. In Chapter 2, the PET fibers were successfully used to radically change the post-cracking behavior of the earthen blocks. This was attributed to the crack-bridging effect of the PET fibers, as a result of their length and the interface friction between the fibers and the surrounding stabilized soil.

Although many studies have focused on the physical and mechanical characterization of reinforced earthen blocks, the literature is far more limited for the case of (chemically) stabilized and (fiber) reinforced earthen masonry (Turanli and Saritas 2011, Lima et al. 2012, Wu et al. 2013).

The in-plane and out-of-plane behavior of masonry are key factors for the resistance against lateral loads, such as those imparted by hurricane and tornado winds. The in-plane and out-of-plane behavior depend on the shear and flexural strength and deformability of the masonry. Although numerous building codes recommend to neglect the flexural strength of unreinforced masonry, it has been suggested to allow the use of experimental data (Tennant et al. 2013). On the other hand, the resistance against in-plane shear forces such as those produced by earthquakes, depends on the in-plane shear capacity and deformability of the walls.

The aim of this chapter is to study if the presence of fiber reinforcement results in a transformed strength and deformability when the masonry is subject to in-plane and out-of-plane loads. Here, it is hypothesized that such transformation is enabled by stabilization with OPC for strength and durability, and reinforcement using low-cost, recyclable plastic fibers for deformability. To this end, local ductility is particularly important to withstand the impact of wind-borne debris in extreme wind events, and provide residual strength to prevent post-event collapses.

This chapter reports on the prototyping and mechanical characterization of a stabilized and reinforced earthen masonry (SREM), which is engineered by modifying the prototype suitable for resisting extreme wind pressures presented in Chapter 3. SREM is manufactured using earthen blocks that are stabilized with 6% OPC content in weight of soil (wt%), and reinforced with 0.5 wt% (or 0.6% in volume) recycled polyethylene terephthalate (PET) fibers. The mechanical properties of these blocks are discussed in detail in Chapter 2. In combination with PET fiber-reinforced earthen blocks, a polyvinyl alcohol (PVA) fiber-reinforced earthen mortar is used to build the

masonry specimens. The selection process of the PVA volume fraction for the earthen mortar, including the mortar compression, flexural and bond tensile tests, is described. SREM prototype subassemblies are load-tested in flexure and shear to describe their out-of-plane and in-plane behavior, respectively. The main objective is to evaluate the toughening effect of plastic fiber reinforcement on the earthen masonry system, with an emphasis on local ductility to provide resistance against the impact of wind-borne debris. Preliminary evidence from high-velocity impact tests, in accordance with the requirements for residential safety rooms (ICC 2014, FEMA 2015), are presented to demonstrate proof of concept of the transformed damage tolerance of the earthen masonry system by means of the plastic reinforcement.

4.2 MATERIALS AND METHODS

In Chapter 3 the prototyping of the earthen masonry is discussed in detail, including the selection of the block OPC content and the earthen mortar mixture. In this chapter, the compressed and stabilized earthen block with 6% cement by weight (CS6) and the mortar mixture 1C:2So:9S (cement:soil:sand by weight) are modified to prototype a non-biodegradable plastic fiber-reinforced earthen masonry. The methodology is summarized in Figure 4.1. This section starts with a brief summary of the mechanical properties of the plastic fiber-reinforced CS6 blocks, and presents the methods followed for the engineering and selection of the fiber-reinforced mortar. Then, the test methods used to assess the effect of plastic fiber reinforcement on the mechanical properties of the SREM are presented.

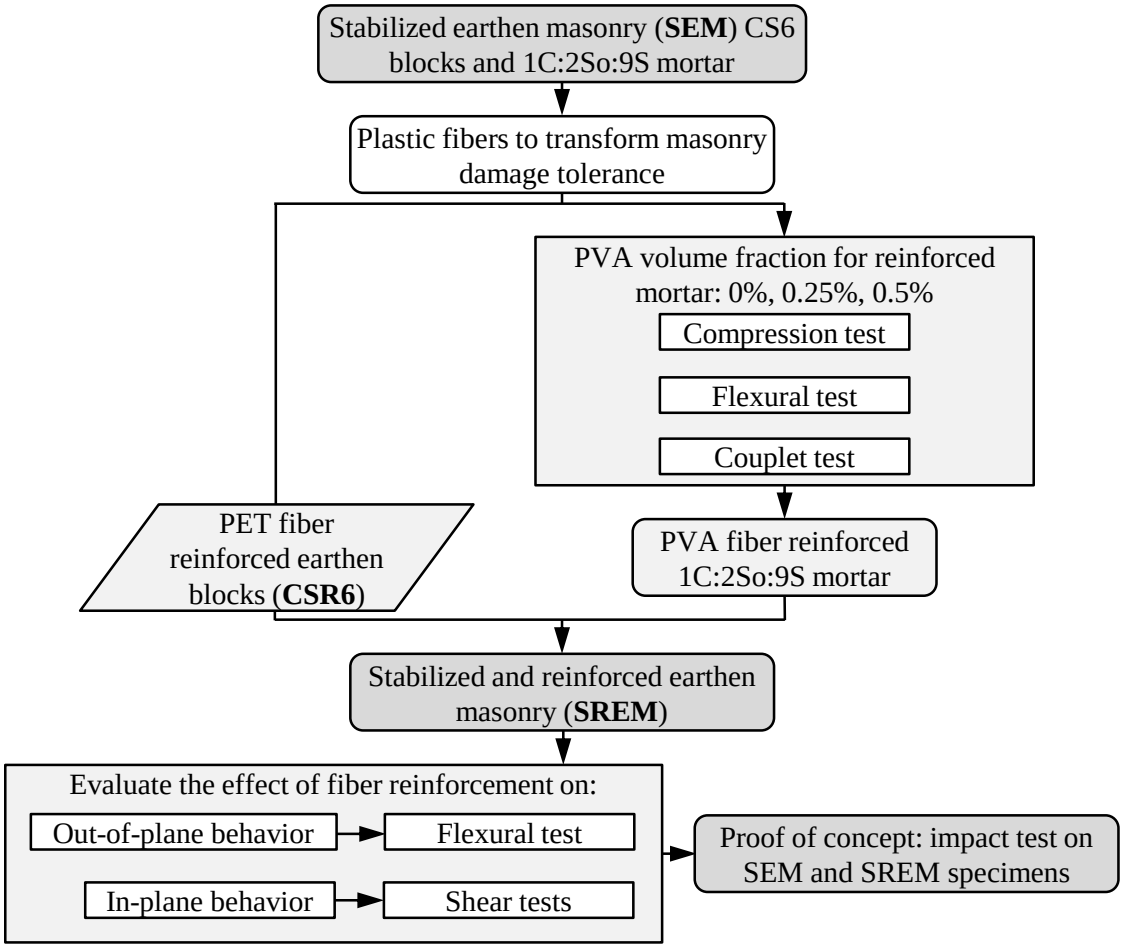

Figure 4.1 Procedure for selection and mechanical characterization of prototype stabilized and plastic fiber-reinforced earthen masonry.

4.2.1 PET reinforced earthen blocks

The results from the PET fiber reinforced earthen blocks are discussed with more detail in Chapter 2, section 2.3. Table 4.1 summarized the results for flexural and compressive strength for the unreinforced and fiber-reinforced earthen blocks. The presence of PET fibers marginally affects the strength of the stabilized and compressed soil mixture as it inevitably introduces some discontinuities. In fact, the reduction in the compressive and flexural strength was on average 4% and 21%, respectively.

Table 4.1 Material and mechanical properties of compressed and stabilized earthen blocks with and without plastic fiber reinforcement

Specimen series	OPC content [%wt]	PET fiber content [%wt]	Flexural strength		Compressive strength	
			Avg [MPa]	St. dev [MPa]	Avg [MPa]	St. dev [MPa]
CS6	6	-	0.67	0.12	4.62	0.48
CSR6	6	0.5	0.53	0.08	4.80	0.41

The higher difference for the flexural strength was attributed to the higher sensitivity of the soil matrix to the discontinuities introduced by the fibers. Similarly, the presence of plastic fibers moderately reduced the stiffness of the soil matrix (Figure 4.2). However, the fiber reinforcement radically changes the post-cracking behavior of the earthen blocks, which exhibit considerable post-cracking (residual) strength and deformability.

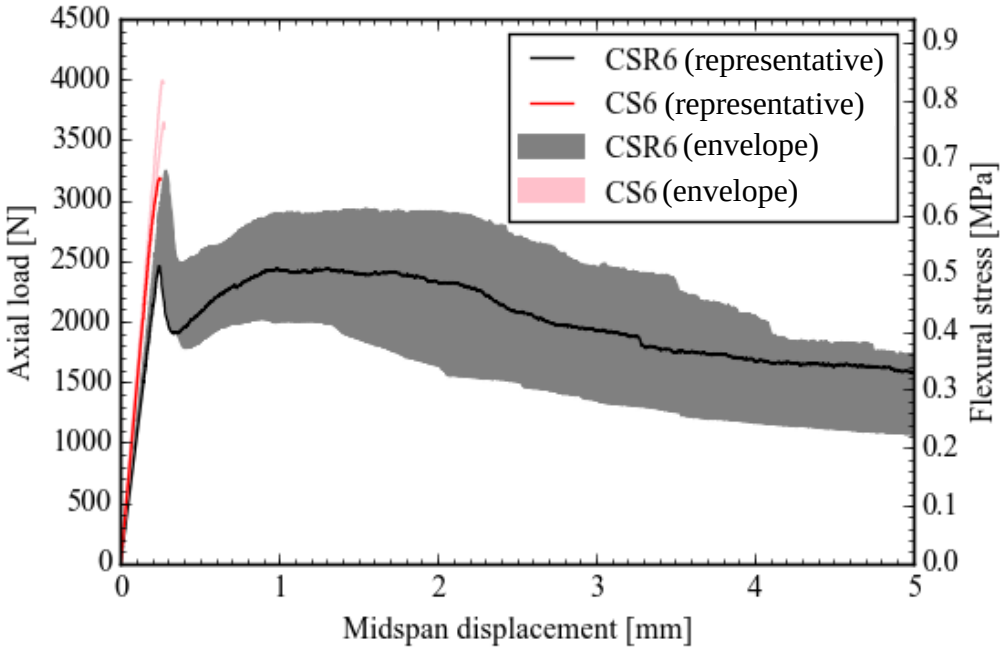

Figure 4.2 Representative load – displacement curve with corresponding envelope for unreinforced and fiber-reinforced earthen blocks tested in three-point bending.

In accordance with the experimental evidence from Chapter 2, CSR6 is selected for the blocks to be used in the plastic fiber-reinforced masonry.

4.2.2 Fiber-reinforced earthen mortar

In Chapter 3, the selection of the mortar mixture 1C:2So:9S was presented. In this section, the selection process of the fiber volume fraction for the modified plastic fiber-reinforced mortar is described. First, the plastic fibers used are described, followed by the selection of the fiber volume fraction, V_f.

4.2.2.1 Plastic fibers for earthen mortar

Reinforcing fibers in mortar mixtures are used to improve shrinkage resistance and toughness (Sanjuán and Moragues 1996, Tolêdo Filho and Sanjuán 1999). Studies on the effect of different types of fiber in cement mortars generally reported that the incorporation of fibers enhances post-cracking strength and deformability, with marginal effects on the compressive strength (Fanella and Naaman 1985, Skourup and Erdogmus 2010). PVA fibers in cementitious mortars have been shown to be effective in enhancing the post-cracking behavior (Skourup and Erdogmus 2010, Armwood et al 2011). In fact, Betterman et al. (1995) used pull-out tests to show that PVA fibers have a significantly higher specific bond energy at failure than steel fibers. The improvement of the mortar properties is directly related with an increase in *Vf* (Betterman et al. 1995, Lange et al. 1996). However, it has been found that the mortar properties begin to deteriorate past an optimum value of *Vf* (Fanella and Naaman 1985). In general, the amount and dimensions of fibers are controlled by workability and aesthetics considerations. For PVA fibers, different volume fractions with similarly successful results have been reported (Betterman et al. 1995, Skourup and Erdogmus 2010, Armwood et al 2011).

summarizes the physical properties of the PVA fibers selected for the earthen mortar reinforcement. These fibers are commercially known as RECS-15 (Figure 4.3).

The improvement of the mortar properties is directly related with an increase in V_f (Betterman et al. 1995, Lange et al. 1996). However, it has been found that the mortar properties begin to deteriorate past an optimum value of V_f (Fanella and Naaman 1985). In general, the amount and dimensions of fibers are controlled by workability and aesthetics considerations. For PVA fibers, different volume fractions with similarly successful results have been reported (Betterman et al. 1995, Skourup and Erdogmus 2010, Armwood et al 2011).

In the present chapter, 0%, 0.25% and 0.5% PVA volume fraction are tested for the 1C:2So:9S mortar mixture presented in Chapter 3. The volume fraction selected allowed for adequate workability and a good dispersion of the fibers (Figure 4.3b). A water cement ration of 2.4 was used for the mortar mixture.

Table 4.2 PVA RECS-15 physical properties.

Filament diameter	38 mμ
Fiber length	8 mm
Tensile strength	1600 MPa
Flexural strength	40 GPa
Melting point	225°C
Water absorption	<1% in weight

4.2.2.2 Selection of PVA fibers volume fraction

To determine a suitable fiber volume fraction, 1C:2So:9S mortar samples were load-tested in uniaxial compression, flexure, and uniaxial tension (couplet test) (Figure 4.4). Six 500 mm cubes were used for compression testing. The load was applied with a

displacement rate of 0.64 mm/ min. The cubes were cured in saturated lime water and tested at 28-days (ASTM C109). For the flexural test, three 28-day beams with dimensions of 45 mm × 45 mm × 162 mm were subjected to three-point bending with a clear span of 127 mm. The displacement rate for the flexural test was 0.1 mm/min. The quality of the block-mortar interface was evaluated using six 28-day crossed-block couplet specimens under uniaxial tensile loading (ASTM C952), with a displacement rate of 0.4 mm/min (see detailed information in Appendix C).

In addition to the determination of the volume fraction, the tests were used to identify the effect of the PVA fibers on the mechanical behavior of the earthen mortar and, in particular, to evaluate if the presence of fibers results in better post-cracking behavior, and whether the fibers affect the strength of the mortar.

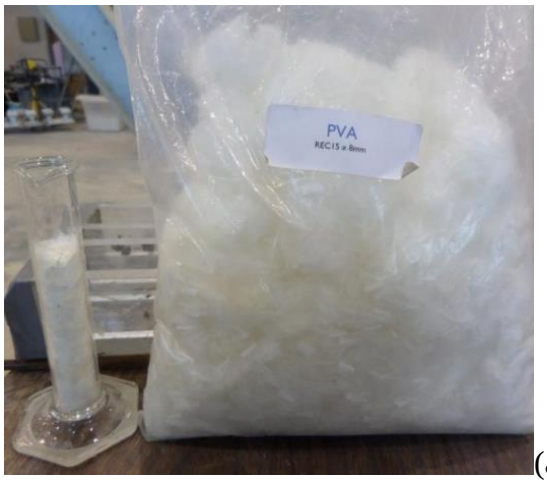

(a)
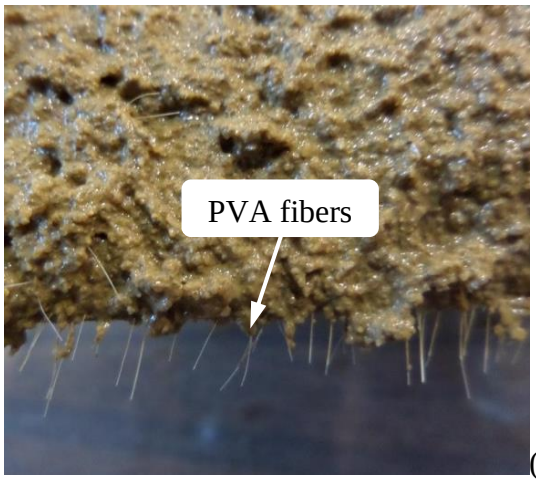

(b)

Figure 4.3 Fiber-reinforced mortar: (a) PVA fibers RECS-15, and (b) PVA fiber in mortar mixture.

(a)

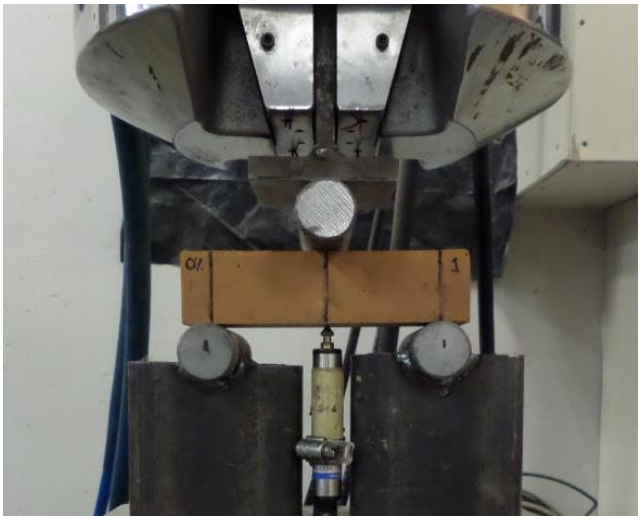

(b)

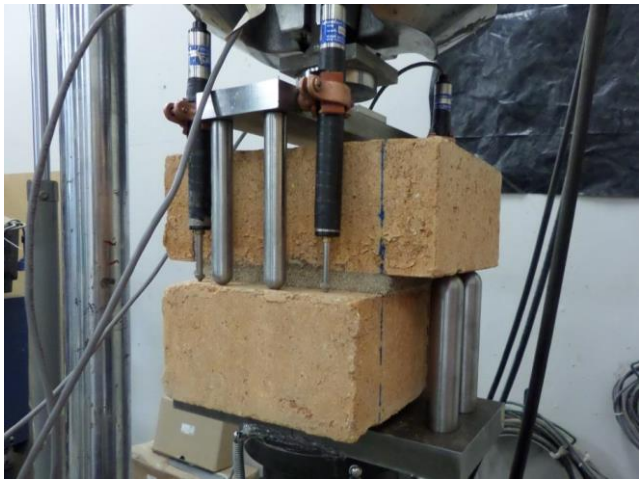

(c)

Figure 4.4 Mechanical characterization of fiber-reinforced mortar: (a) compression, (b) flexural, and (c) direct-tension (couplet) testing.

4.2.3 SREM mechanical characterization

This section presents the mechanical characterization of the SREM for out-of-plane (flexural) and in-plane (shear) behavior.

4.2.3.1 Flexural strength

The couplet tests (Figure 4.4) were performed to evaluate the effect of fiber reinforcement on the bond strength and failure mode. However, this test is not representative of the out-of-plane flexural strength of the masonry. In flexure, the mortar region opposite to that of load application is subjected to a maximum tensile stress whereas in couplet specimens the entire joint surface is subject to nearly uniform maximum tensile stresses (Figure 4.5), thus providing a lesser ability to redistribute stress and resist tensile forces.

The flexural tensile strength governs failure when the masonry is subject to out-of-plane forces (i.e., acting perpendicular to the face of a wall). Matta et al. (2015) found that the predominant failure mode when for walls subject to high wind loads is out-of-plane flexure. In addition, in high wind regions, buildings are required to resist the out-of-plane impact from wind-borne debris.

Here, first, PET fibers are incorporated in the earthen blocks to increase the local ductility of the system. As presented in Chapter 2, the incorporation of PET fibers radically changed the energy absorption capability of the blocks subject to tensile stresses. PVA-reinforced mortar was used for the construction of the flexural specimens.

Four Five-block stack prisms with dimension of 495 mm × 254 mm × 178 mm were used to assess the masonry behavior under to out-of-plane loading. Each specimen

was load tested using a four-point bending setup with a clear span of 445 mm (Figure 4.6). The load was manually applied with a hydraulic cylinder and measured with a 40-kN load cell. The midspan displacement was recorded using two displacement transducers (one on either side of the specimen).

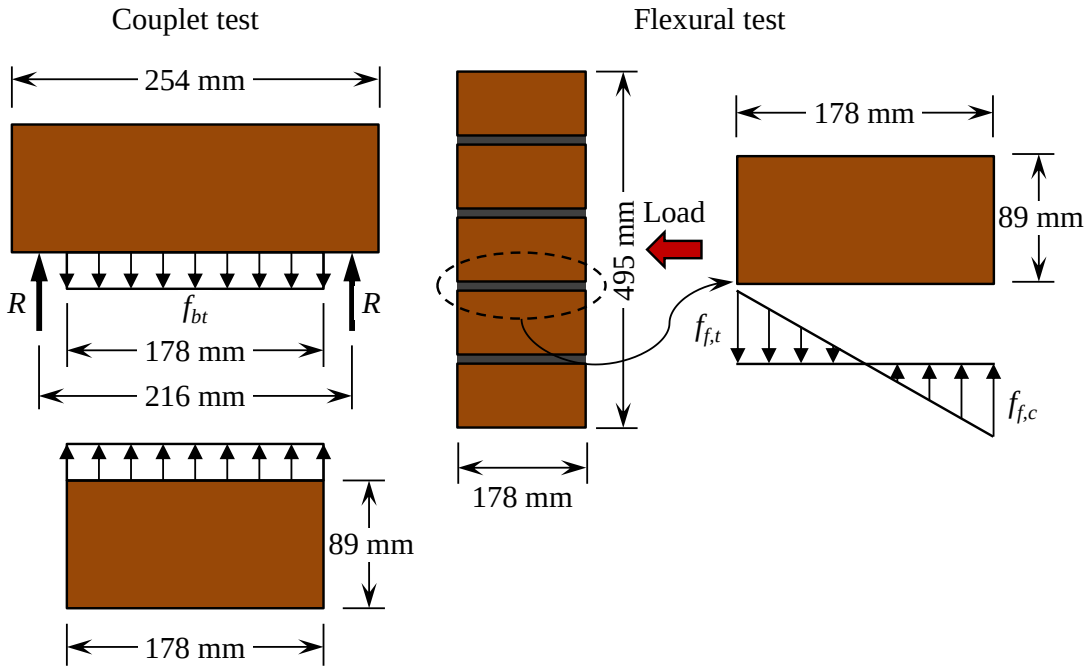

Figure 4.5 Stress distribution for couplet and flexural test.

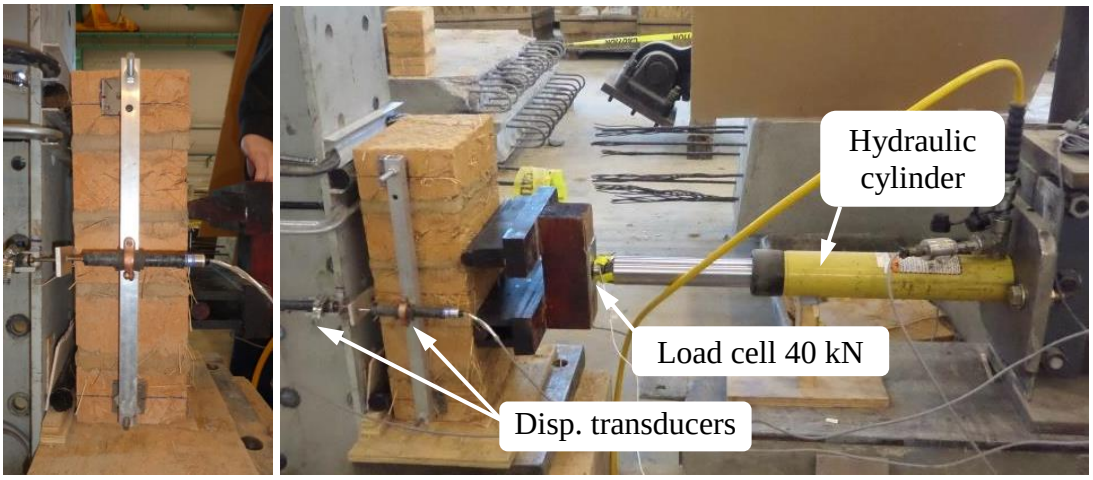

Figure 4.6 Out-of-plane flexural test setup for SREM prototype.

The objective of the instrumentation of the flexural test was to obtain the nominal flexural strength and representative load-displacement curves. The flexural test results were then compared with those obtained from the unreinforced masonry system (Chapter 3) to evaluate the influence of the plastic fibers.

4.2.3.2 Shear strength

The in-plane behavior is assessed through shear tests. In particular, the aim of the shear characterization is to identify the effect of the plastic fiber reinforcement on the local and global response of the prototype earthen masonry. Shear response is particularly important when the structure is subjected to in-plane loads such as those caused by extreme winds (Matta et al. 2015) and earthquakes. Triplet and diagonal compression tests were carried out to characterize the shear behavior of the earthen masonry. The shear test on the triplet specimens, which characterizes sliding shear behavior along the mortar bed joint, focuses on interface behavior. In addition, the triplet test allows to quantify cohesion and friction coefficients. On the other hand, diagonal compression tests are used to simulate a more representative behavior of the earthen masonry system. This test is typically used to characterize diagonal cracking failure mechanisms (Drysdale and Hamid 2008). The shear specimens and instrumentation are described in the following sections.

The behavior of the masonry bed joints subject to shear forces is characterized by means of triplet tests. Three levels of compressive stress representative of the weight of a unit-length masonry wall at the top, middle and bottom section were considered. Three specimens per pre-compression stress level were tested. This constant pre-compression

stress was applied with a hydraulic cylinder and measured with 40-kN load cell (Figure 4.7). The triplet specimens with dimensions of 254 mm high, 292 mm long and 178 mm wide were tested 28 days after casting.

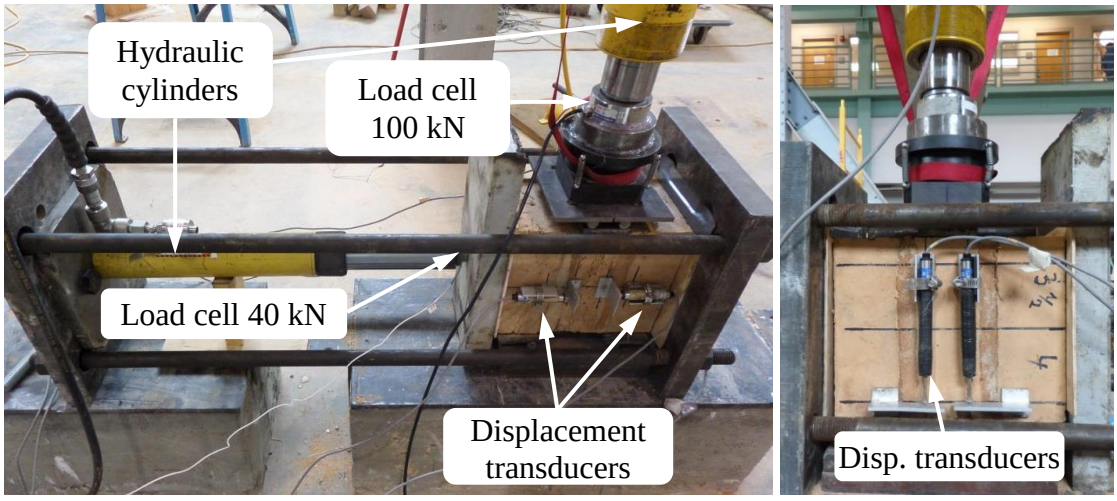

Figure 4.7 Triplet test setup.

Four displacement transducers were used to measure vertical (slip) and horizontal (joint opening) displacements (Figure 4.7). The load was imparted on two steel cylinders through a steel plate that was connected to a swivel joint (see detailed information in Appendix C), and was measured with a 100-kN load cell (Figure 4.7).

To complete the shear characterization of the masonry system, diagonal compression tests were performed. This type of test aims to characterize a more representative behavior of the masonry when subject to in-plane shear loads. Three masonry subassemblages with dimensions of 800 mm × 787 mm × 178 mm were tested 28 days after casting. Each specimen was supported using two steel toes (Figure 4.8). A fast curing plaster layer was applied between the steel toe and the masonry surface to provide a uniform contact area.

Figure 4.8 Diagonal compression test setup.

A hydraulic cylinder (capacity of 240 kN) instrumented with a 70-MPa pressure transducer was used to apply the vertical load in a manual fashion. The vertical and horizontal displacement, along the wall diagonals were measured with displacement transducers having a 5-mm stroke.

4.3 Results and Discussion

4.3.1 Mechanical characterization of PVA fiber-reinforced earthen mortar

In this section, the effect of the PVA fibers in the mortar is discussed based on the compression, flexure and couplet test results, which are summarized in Table 4.3. In addition, representative load – displacement curves for the compression and flexural tests are shown in Figure 4.9a and Figure 4.9b, respectively.

From the average compressive strength values, it can be seen that the presence of fiber reinforcement does not significantly affect the compressive strength and deformability of the 1C:2So:9S mortar.

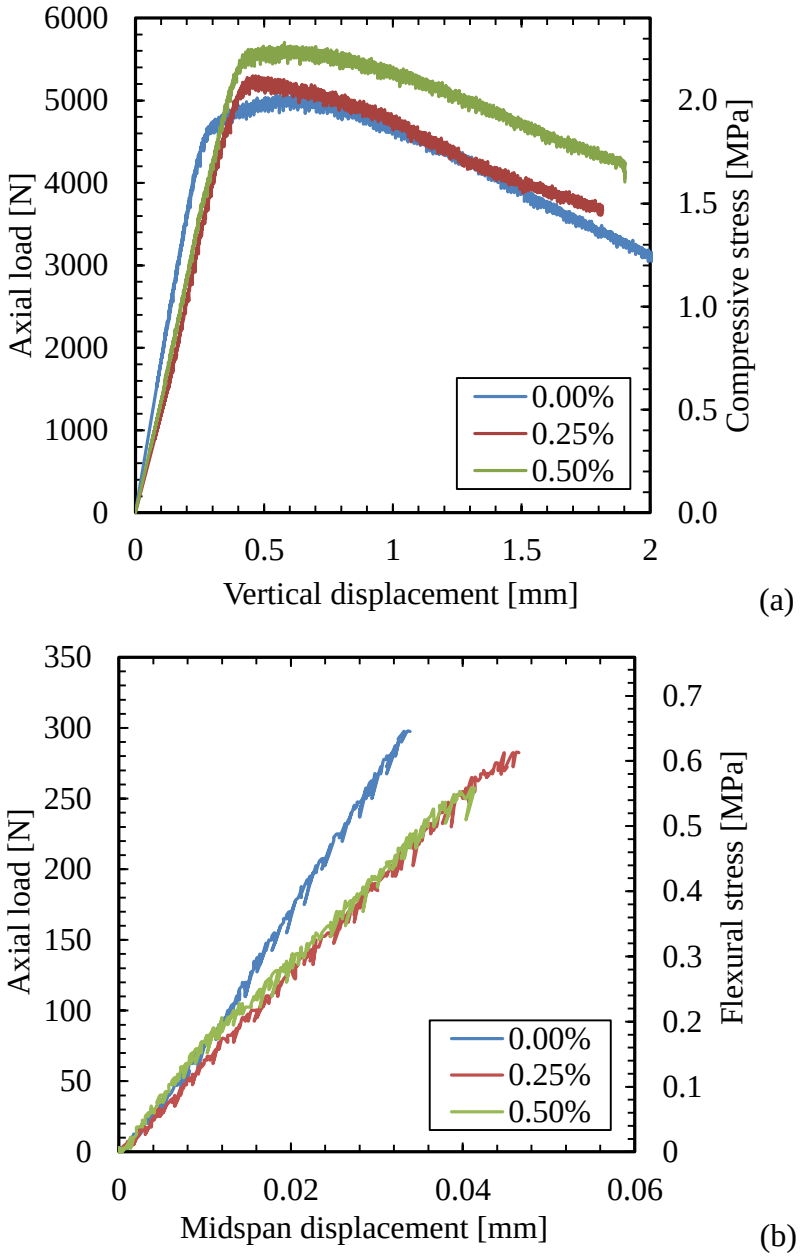

Figure 4.9 Representative load – displacement curves for PVA fiber-reinforced mortar: (a) compression test, and (b) flexural test.

The mortar with V_f = 0.5% presented a reduction in the average flexural strength of 24.6% compared to the unreinforced counterpart, which is attributed to the effect of the physical discontinuities introduced by reinforcement in this amount. These results show that the flexural strength is more sensitive to discontinuities in the matrix as introduced by the PVA fibers. The representative load-displacement curves shown in Figure 4.9b reveal that there was no enhancement in post-cracking strength and deformability with the addition of PVA fibers. Apparently, the length of the fibers (8 mm) was not sufficient to effectively bridge cracks in the mortar matrix.

Table 4.3 Mechanical properties of 1C:2So:9S earthen mortar fiber reinforced with different volume fractions.

Sample	Compressive strength [MPa]			Flexural strength [MPa]			Tensile bond strength [MPa]		
PVA Vf [%]	0%	0.25%	0.50%	0%	0.25%	0.50%	0%	0.25%	0.50%
1	2.2	2.1	2.3	0.6	0.6	0.6	0.11	0.13	0.17
2	2.4	1.8	2.3				0.03	0.13	0.11
3	2.1	2.0	2.3	0.6	0.6	0.5	0.04	0.15	0.13
4	2.0	2.1	2.3				0.04	0.14	0.09
5	2.3	2.0	2.3	-	0.7	0.4	0.07	0.13	0.17
6	2.4	2.0	2.2					0.16	0.16
Avg	2.23	2.00	2.27	0.65	0.63	0.49	0.06	0.14	0.14
St. dev	0.15	0.12	0.04	0.00	0.05	0.09	0.03	0.01	0.04

However, the key advantage of adding PVA fibers was noted in the couplet test results. The bond strength increased on average by 233% for both volume fractions tested (0.25% and 0.50%). Therefore, a fiber volume fraction of 0.25% is sufficient to radically and consistently enhance the tensile bond strength.

Figure 4.10 shows the representative failure modes for the three fiber volume fractions evaluated. The unreinforced specimen presented a mixed adhesive-cohesive

failure mode, with partial failure within the blocks. For both V_f, 0.25% and 0.50%, failure of the block was noted. This result indicates that the bond strength is sufficient to offset failure until flexural failure of the block occurs.

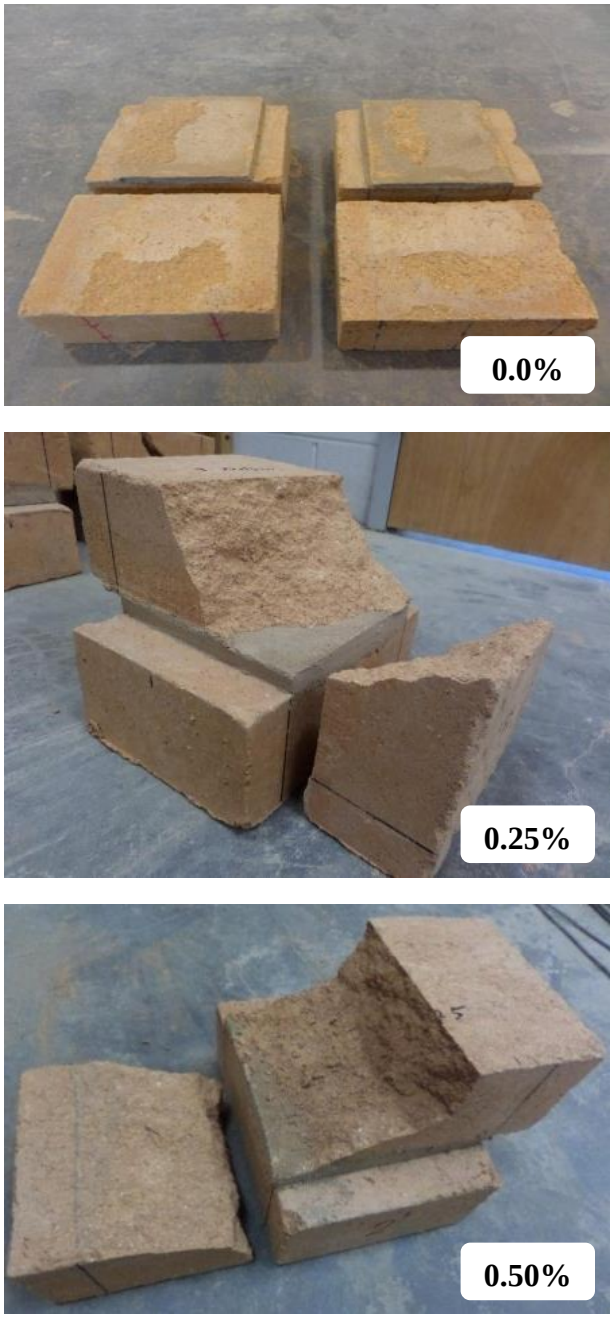

Figure 4.10 Representative failure mode for couplets with V_f = 0.0%, 025% and 0.5%.

The transformation in the tensile bond strength and failure mode was attributed to the integrity of the block mortar interface enabled by the PVA fibers, which mitigates shrinkage during curing. Therefore, a 0.25% PVA volume fraction was selected for the SREM system.

4.3.2 SREM mechanical characterization

The out-of-plane and in-plane response of the SREM system, which is made of CSR6 blocks and 1C:2So:9S mortar reinforced with PVA fibers (V_f = 0.25%), were assessed by means of load tests. In this section, the results for the SREM system are also compared to those obtained for the unreinforced prototype masonry (SEM) to evaluate the influence of plastic fiber reinforcement on the earthen masonry strength and deformability.

4.3.2.1 Flexural strength

Table 4.4 summarizes the flexural strength results for SREM. The average flexural strength was 0.16 MPa with a standard deviation of 0.06 MPa. This value is similar to that of the SEM average strength, which indicates that the presence of plastic fiber reinforcement, PET and PVA, does not negatively affect the flexural strength of the earthen masonry. In flexure, the PVA fibers do not have a significant effect on the strength as for the case of uniaxial tension. In the latter case, the entire mortar area resists the applied load, allowing for a more effective redistribution of tensile stresses, and the effect of the fiber reinforcement becomes more relevant.

Table 4.4 SREM flexural strength.

Specimen	Flexural strength[MPa]
1	0.12
2	0.13
3	0.24
4	0.15
Avg	0.16
St. dev	0.06

Although the PVA fibers did not contribute to increasing the flexural strength, the PET fibers protruding from the blocks into the bed joint somewhat contribute to the post-cracking (residual) strength (Figure 4.11).

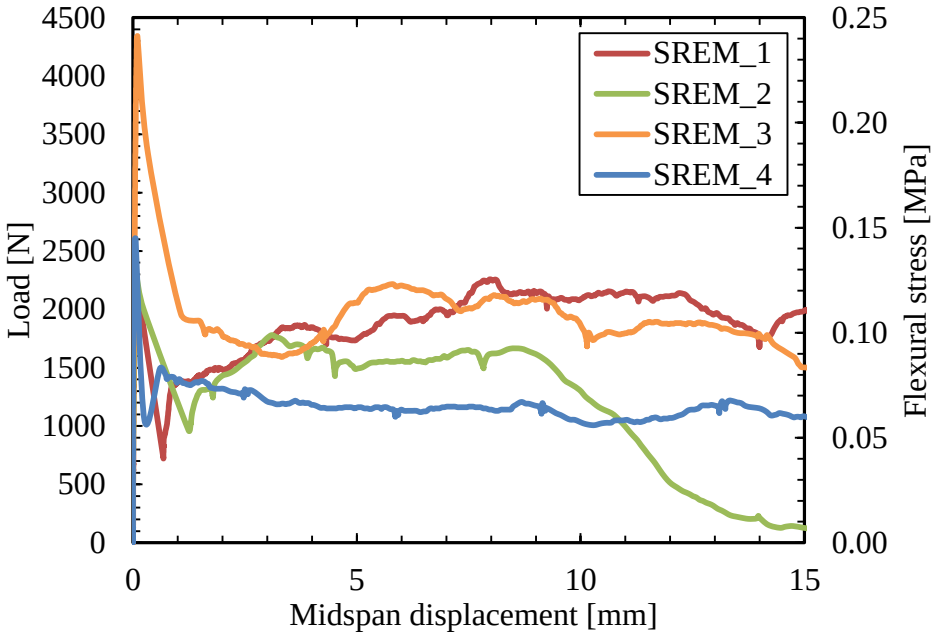

Figure 4.11 Load – displacement curves for SREM specimens tested in out-of-plane flexure.

Figure 4.12 shows the representative failure mode. Similarly to the SEM, the specimens presented failure at the interface in the second or third joint. In Figure 4.12, it is possible to see the PET fibers that pulled out from the mortar joints.

Figure 4.12 Representative failure mode for SREM specimens subject to out-of-plane loading.

4.3.2.2 Shear strength

The results from the triplet test are summarized in Figures 4.13 and Table 4.5. Figure 4.13 shows the shear strength (f_{vk}) as a function of the pre-compression stress (σ_o) applied to the SREM triplet specimens. Similar to traditional masonry and SEM, the shear strength varies in a linear fashion with the compression load. At zero pre-compression strength, the shear strength was higher than the required by NZS 4297 (1998) for standard masonry.

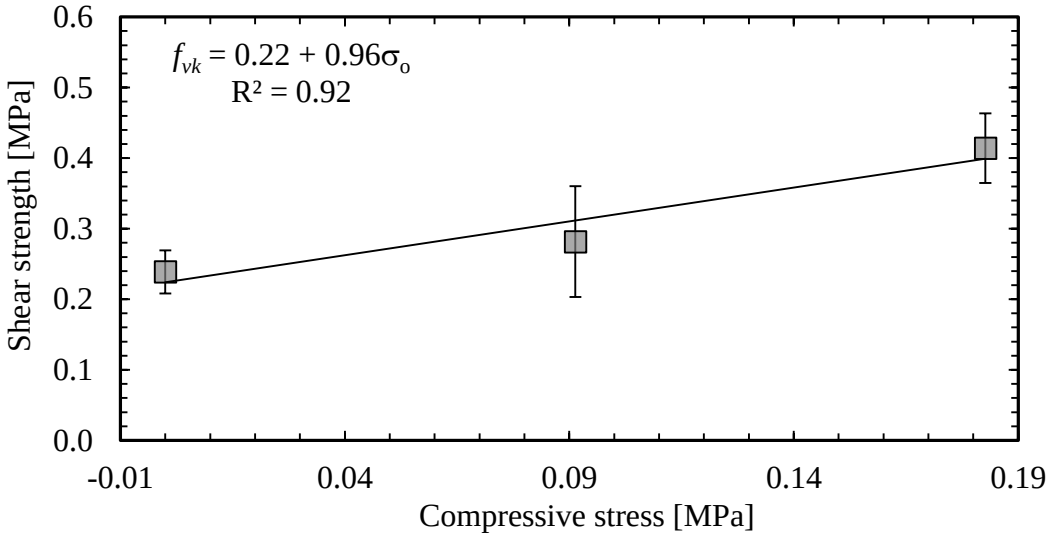

Figure 4.13 Shear strength vs. compressive stress curve. Filled squares represent average strength and continued curve represents adjusted linear equation.

Table 4.5 Shear strength results from triplet test.

Specimen	Shear strength [MPa]		
	0.0 MPa	0.1 MPa	0.2 MPa
1	-	0.26	0.47
2	0.26	0.22	0.37
3	0.22	0.37	0.41
Avg	0.24	0.28	0.41
St. dev	0.03	0.08	0.05

A graphical comparison of the triplet test results for both masonry prototypes are shown in Figure 4.14. The filled markets and continuous lines represent the average data and the shaded areas represent the envelopes. At zero pre-compression stress, the SREM shear strength was 60% higher than SEM. At zero pre-compression stress, where shear strength is controlled by the integrity of the interface, the fiber reinforcement contribute to increasing the shear strength. The PVA fibers produce better integrity (because of dimensional stability) of the mortar joint.

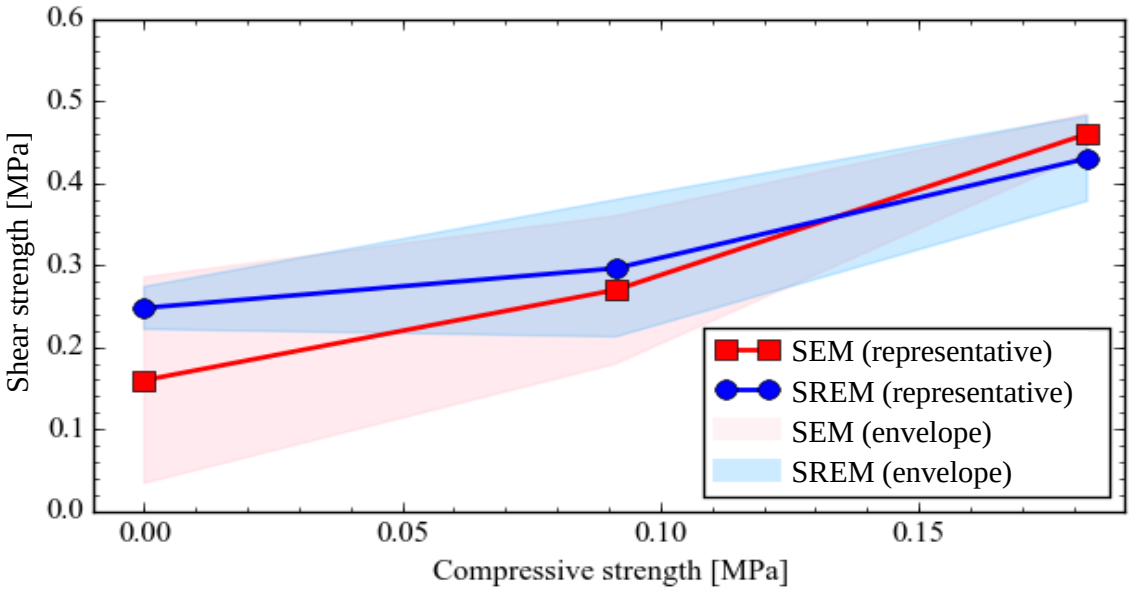

Figure 4.14 Comparison between shear strength vs. compressive stress curves for SEM and SREM specimens.

The failure modes exhibited by the triplet specimens are shown in Figure 4.15. Mixed adhesive-cohesive failure (with partial block damage) was observed in specimens with and without pre-compression stress, indicating good adhesion. In fact, in some instances, block failure occurred. Cohesive failure of the mortar is also seen in some specimens, especially when pre-compression stresses are applied.

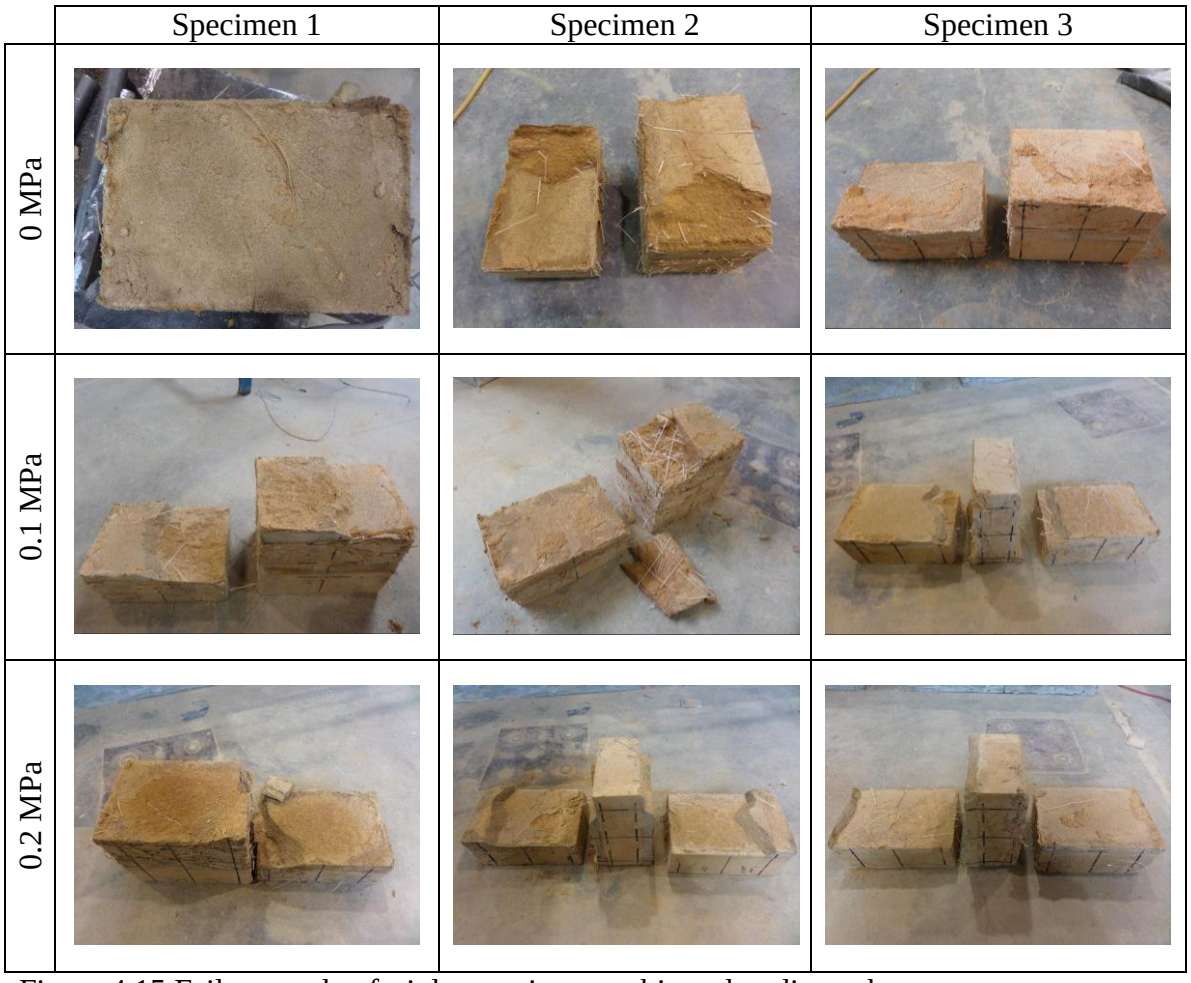

Figure 4.15 Failure mode of triplet specimens subjected to direct shear.

The strength and deformability of the SREM system subject to shear loads were assessed through diagonal compression tests. The shear strength obtained with the diagonal compression test was interpreted based on the stress states described through the linear elastic solution proposed by Frocht (1931). This approach has been shown to be more accurate than a more simplistic pure-shear solution (Yokel and Fattal 1976, Brignola et al. 2009). Therefore, the shear strength is calculated as $\tau_{xy} = 1.05\ P/A$. Here, A is the transverse area and P is the compression load. The shear strength yields an average strength of 1.34 MPa with a standard deviation equal to 0.33 MPa. The shear strength increased more than twice with respect to the unreinforced specimen as a result

of the addition of plastic fiber reinforcement (the strength for prototyped SEM was 0.62 MPa with standard deviation of 0.05 MPa, as summarized in Table 3.5 in Chapter 3). Representative load-displacement curves, and their envelopes, for both masonry prototypes are shown in Figure 4.16. The plastic fiber reinforcement radically transforms the strength and deformability of the earthen masonry. In addition to the strength enhancement, changes in the stiffness, stiffness degradation, and residual (post-peak) strength were observed.

Table 4.6 Shear strength results from diagonal compression test.

Specimen	τ_{xy} [MPa]
1	0.98
2	1.11
3	1.58
Avg	1.34
St. dev.	0.33

The representative failure mode presented by the specimens is shown in Figure 4.17. Diagonal tension cracks mainly through the blocks were observed. In general, this failure mode is observed when a sufficient bond interface is attained. When the load is applied, the block mortar interface starts degrading until the strength of the CSR6 blocks is reached and cracks are formed. This enhancement of the interface is attributed to the volume stability that the PVA fibers provide to the mortar. Similarly, the higher stiffness and reduced stiffness degradation that the SREM specimens presented is associated with the better integrity of the mortar-block interface. However, it is note that the crack path may also be affected by relatively weaker (preferential) planes produced by the PET fiber in the blocks.

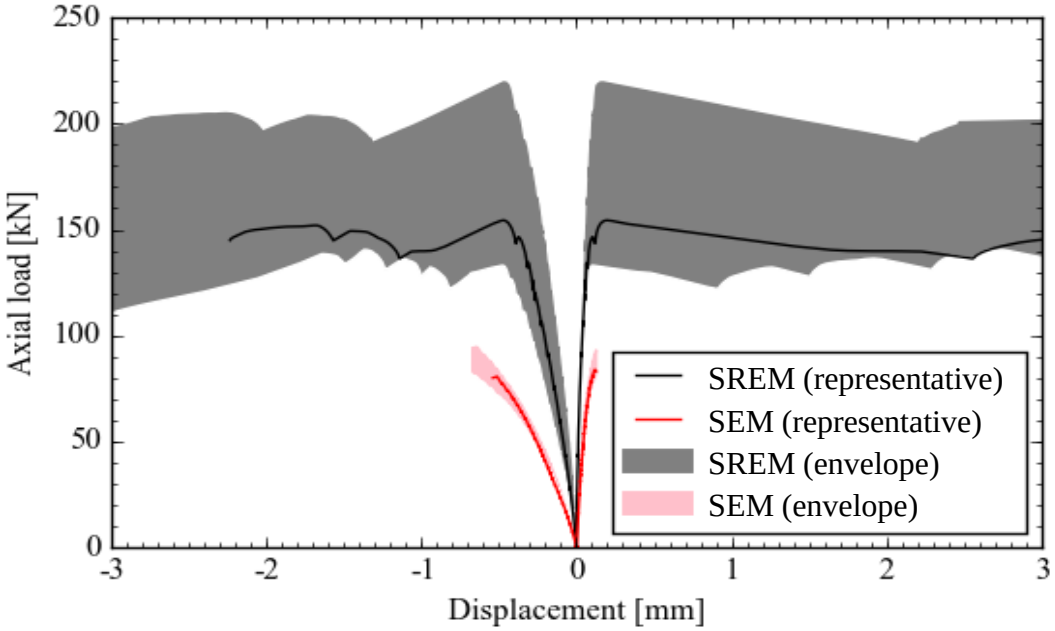

Figure 4.16 Load – displacement response of SEM and SREM panels tested in diagonal compression.

Figure 4.17 Representative failure mode for SREM specimens with close-up photograph of PET fibers bridging cracks.

The PET fibers are responsible for the residual strength noted in the load displacement curves, which is comparable to the peak load (Figure 4.16). Remarkably,

the specimens did not collapse even after extensive damage was produced, as a result of the crack-bridging action exerted by the PET fibers (Figure 4.17). This feature is important for post-hazard safety of the occupants.

In summary, the plastic fiber reinfocement radically transforms the behavior of the earh masonry subjected to in-plane shear loads. The PVA fibers enhanced the integrity of the mortar joints, allowing to attain a higher shear strength at zero pre-compression stress (in triplet specimens) and in diagonal compression. In addition, the PVA fibers increased the shear stiffness and reduced stiffness degradation in the diagonal compression specimens. The PET fiber reinforcement is primarily responsible for the post-cracking strength and deformability of the masonry.

4.4 FLYING DEBRIS IMPACT EXPERIMENT

Results from high-velocity impact experiments are presented to demonstrate the SREM damage tolerance. Wind-borne debris is considered one of the biggest threats to occupant safety during high-wind events. The most common debris threats are medium-weight missiles, such as lumber from failed structures. For impact testing, the Department of Energy (DOE) standardized a “15lb 2 by 4” (6.8 kg, 50 mm x 100 mm) stud as a representative tornado-generated missile. This missile has been adopted by the ICC-500 (2014) standard and the FEMA P 361(2015) as the representative missile for the debris impact test for all the components of a residential safe room (walls, doors, windows, etc.). The speed of the missile impacting the wall varies between 129 km/h and 161 km/h (80 mph to 100 mph), which is representative of wind speeds between 210 km/h and 402 km/h (130 mph to 250 mph) (EF2-EF5 Enhanced Fujita Scale), respectively (ICC 2014).

4.4.1 Impact test setup

One specimen for each series, SEM and SREM, with dimensions of 1308 mm × 1195 mm × 178 mm, was tested (Figure 4.18).

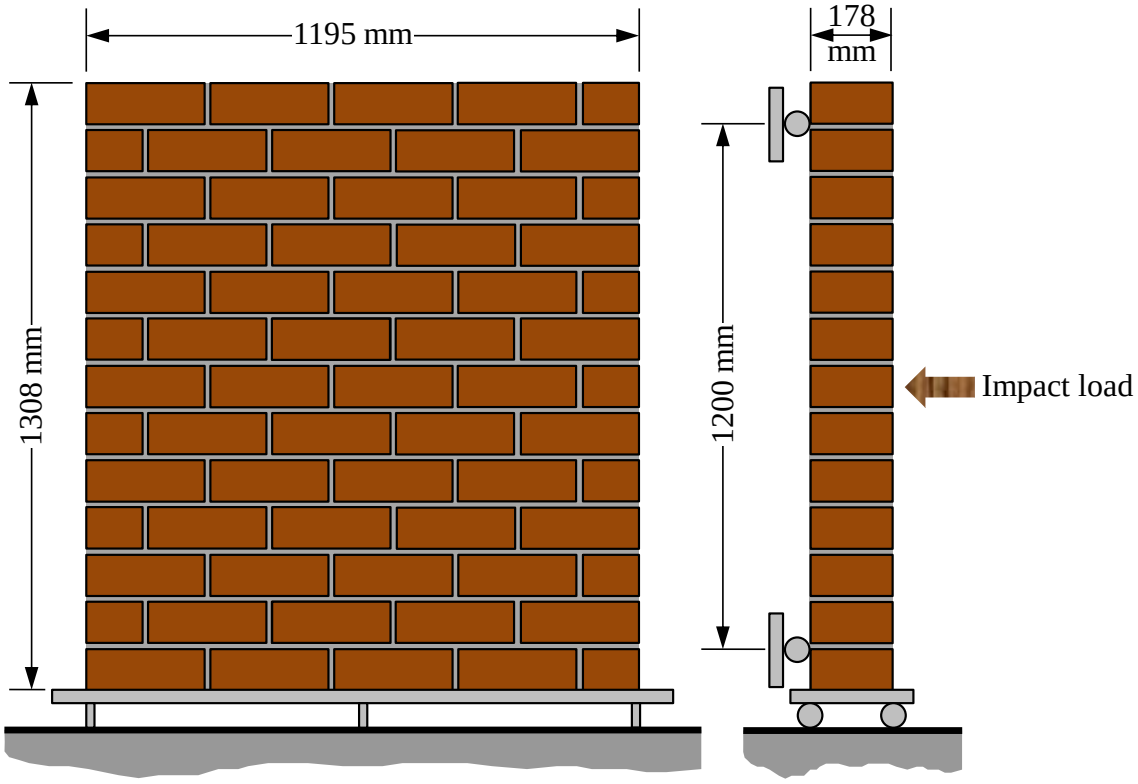

Figure 4.18 Schematic of SEM and SREM impact specimens.

Each specimen was simply supported at the top and bottom using a steel frame connected to the laboratory strong floor. The top and bottom simple supports were simulated using steel pipes serving as rollers. To secure the specimen to the frame, a steel pipe at the front of the specimen and a threaded rod connected to a support roller were used as a clamping system. PTFE sheets were inserted between the specimen and the rollers to minimize friction (Figure 4.19).

Figure 4.19 Support frame with close-up photograph of simple support connection.

The missile was launched using compressed air. The air cannon was built using a commercial air cannon manufactured by Martin Engineering® with an operational capacity of 1 MPa (150 psi). A steel pipe of 100 mm (4 in) diameter was attached to the air cannon to serve as barrel. The distance from the specimen to the end of the barrel was around 6.4 m, which complies with the minimum distance of 1.5 times the length of the

missile required by ICC-500 (2014) (Figure 4.20). An electronic triggering system opens the valve to release the pressure inside the tank and launch the missile.

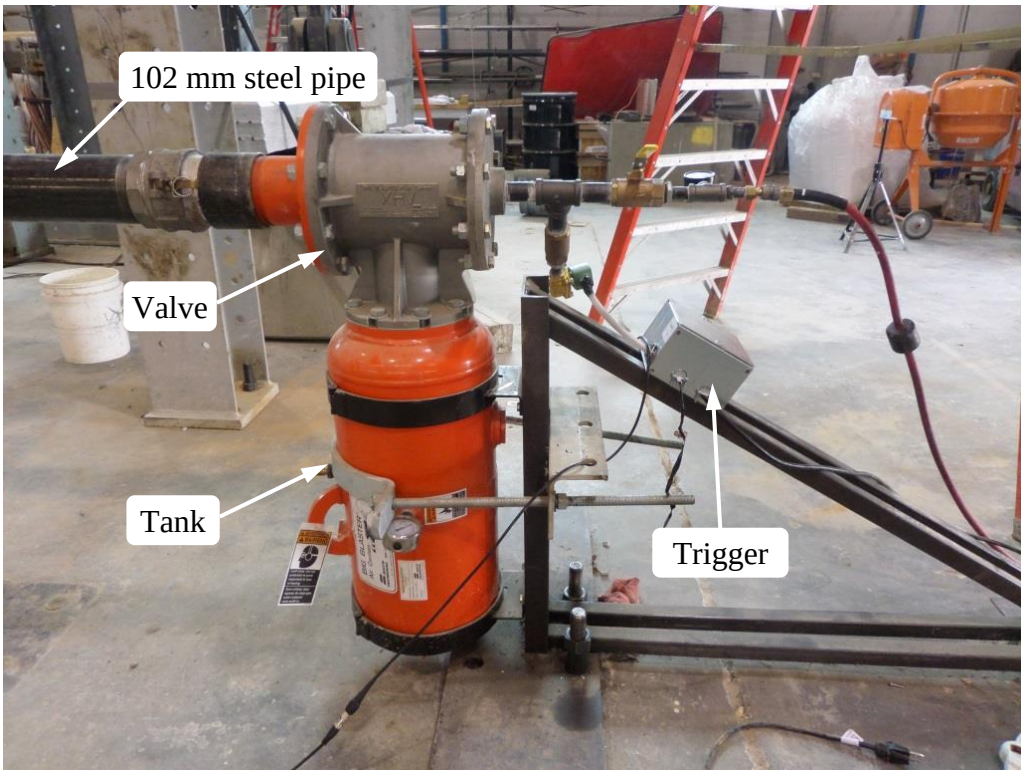

(a)

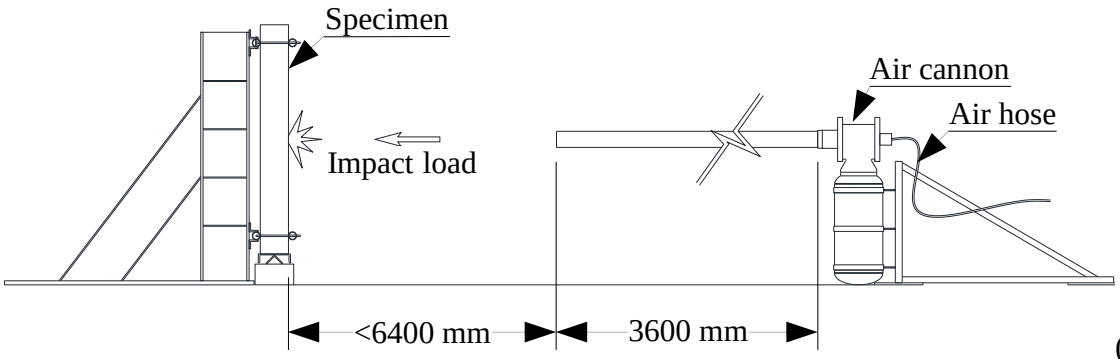

(b)

Figure 4.20 Impact test setup: (a) air cannon details and (b) cannon position with respect to masonry specimen.

The walls were tested for an impact representative of an EF3 tornado, which covers around 90% of the recorded tornados in the U.S (wind speed of 250 km/h). A 6.8 kg stud with nominal cross sectional area of 50 mm × 100 mm and traveling at an

approximate speed of 134 km/h was used to impact the wall specimen at the center of its surface. The speed of the missile was mesured with a radar gun. The kinetic energy of the missile traveling at this velocity is 3029 J.

4.4.2 Impact test results

The impact seuence for SEM and SREM specimens is shown in Figure 4.21 and Figure 4.22, respectively. The photographs were taken with a video camera that records 30 frames per second (fps).

The SEM specimen was fully penetrated by the missile. The failure was localized as it involved a single block that was sheared off by the impacting stud. This failure was the result of block-mortar interface failure along the bed and head joints around the block that was sheared off. Figure 4.23a shows a close-up of the impact location, highlighting a clear interface failure along the block-mortar interface.

The SREM specimen was capable of resisting a full (through-and-through) penetration of the missile (Figure 4.23b), which broke as a result of the stress wave produced upon impacting the wall. There was a noticeable participation of the blocks surrounding the impact location due to the presence of plastic fibers. The missile was stopped immediately after penetrating the specimen. This shows that the plastic fiber reinforcement transforms the damage tolerance of the stabilized masonry system.

In additon, a better behavior of the block mortar interface was observed for the SREM specimens (Figure 4.23b). The reinforced specimen exhibited a better distribution of the damage, involving the material surrounding the impact location.

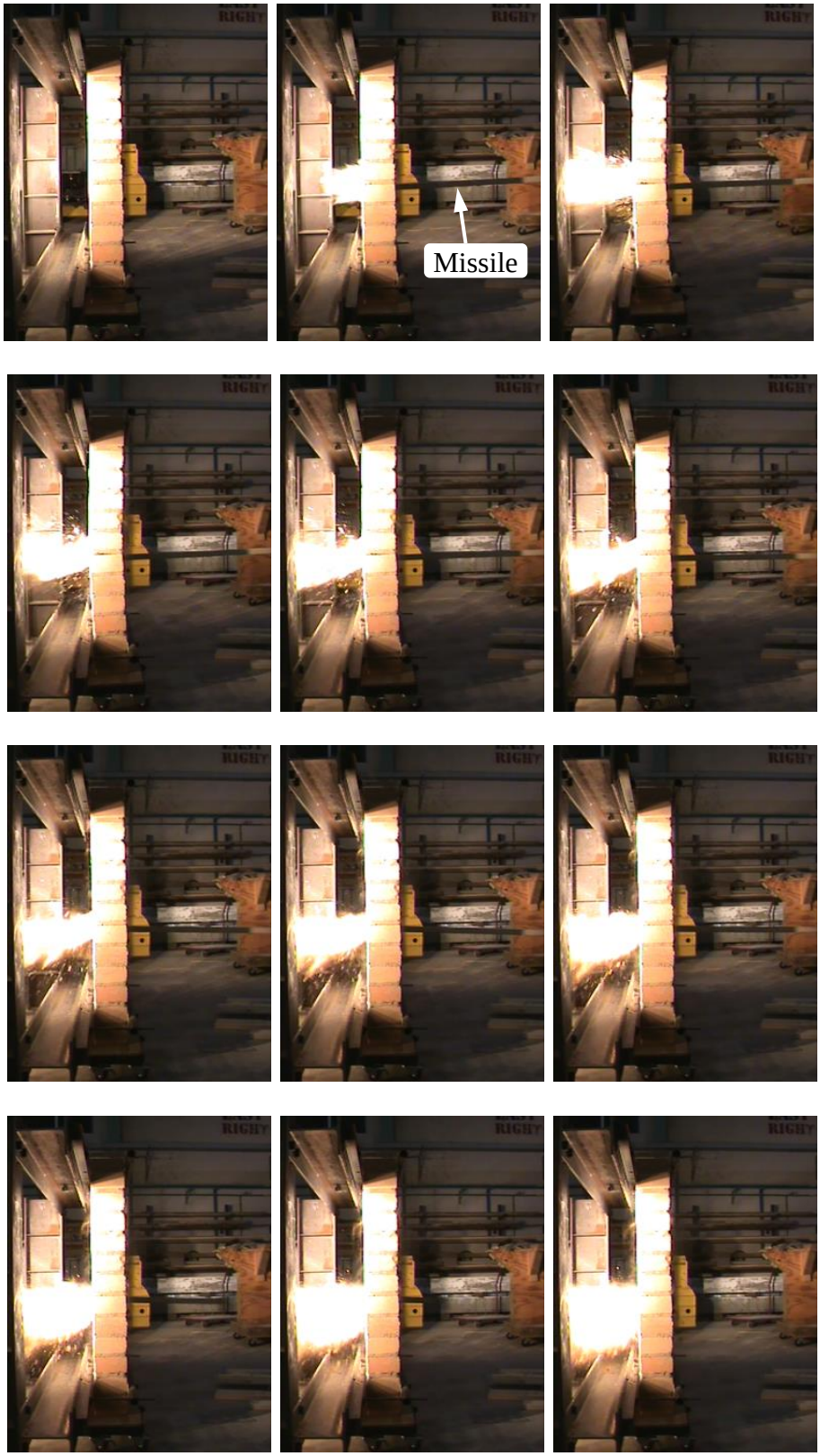

Figure 4.21 Impact sequence for SEM specimen showing full penetration of wall (images every 33 ms).

Figure 4.22 Impact sequence for SREM specimen showing missile stopped after partial penetration, (images every 33 ms).

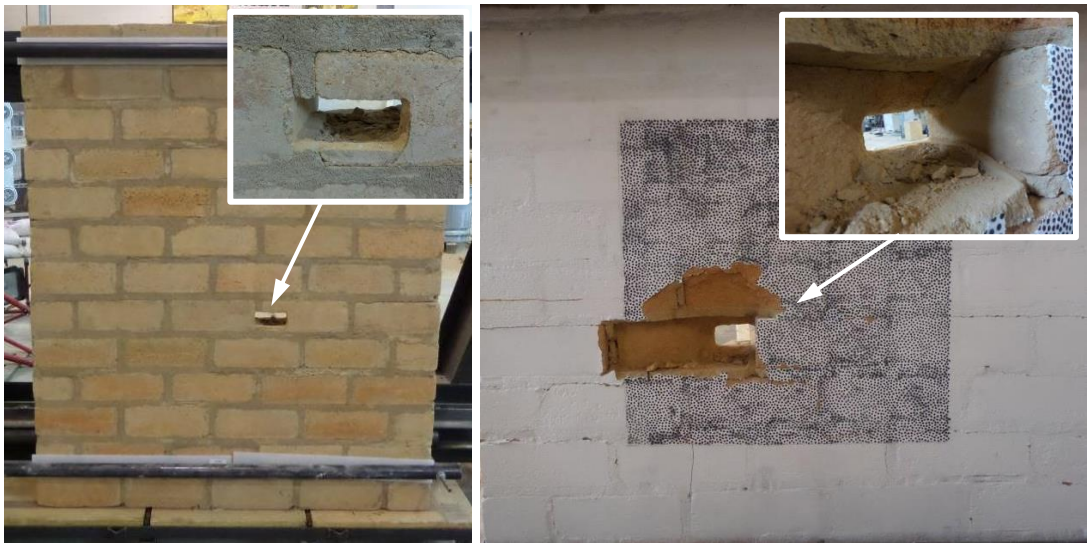

(a)

(b)

Figure 4.23 Photographs of post-impact damage from front and back face: (a) SEM specimen with localized (one-block) damage, and (b) SREM specimen with partial penetration and distributed damage.

The post-impact photographs are evidence of higher energy absorption in the SREM specimen. The better performance of the SREM specimen against the impact of flying debris was attributed to: (a) a better integrity of the block mortar interface, as provided by the PVA fibers in the mortar matrix; and (b) the crack bridging action of the PET fibers in the earthen blocks. The evidence of the work of the PET fibers against the missile penetration is presented by ruptured fibers on the failure surface (Figure 4.24).

Figure 4.24 Photograph of post-impact damage showing broken PET fiber on SREM specimen.

In summary, the plastic fiber reinforcement radically enhanced the energy absorption capacity of the prototype earthen masonry system, making it suitable for the construction of thicker walls (for safety shelters) that must provide resistance against flying debris.

4.5 CONCLUSIONS

This chapter discusses the effect of incorporating recyclable plastic fiber reinforcement on the out-of-plane and in-plane behavior of prototype earthen masonry. The following conclusions are drawn:

1. The compression strength of the 1C:2So:9S mortar is not negatively affected by the presence of PVA fiber reinforcement. The flexural strength was not affected by the PVA fibers for V_f = 0.25%.

2. The addition of PVA fibers to the mortar matrix can result in increased tensile bond strength. It was shown that 0.25% and 0.5% PVA fiber volume fractions are equally effective in improving the bond strength at the mortar-block interface. This is attributed to the better integrity of the interface, which is a result of the dimensional stability (e.g., shrinkage resistance) enabled by the fiber reinforcement.

3. A PVA volume fraction of 0.25% was selected for the reinforcement of the 1C:2So:9S mortar used in the SREM system. It was shown that a 0.25% volume fraction does not affect the compressive and flexural strength and provides higher bond strength compared to the unreinforced masonry. In addition, a 0.25% volume fraction has similar bond strength to the mixture containing twice the amount of fibers.

4. The out-of-plane flexural behavior is modified by the PET fibers, which provided some post-cracking strength and deformability in flexure.

5. The in-plane shear behavior of the earthen masonry was transformed through the incorporation of plastic fiber reinforcement. Each plastic fiber had a different role in the enhancement of the earthen masonry. The interface integrity provided by the PVA fibers resulted in remarkably higher the shear strength in both the zero pre-compression triplet specimens and the diagonal compression panels. Similarly, the integrity of the interface resulted in higher stiffness and lower stiffness degradation under in-plane shear forces. In addition, the PET fibers transformed the post cracking behavior of the earthen masonry by bridging the cracks. The PET fibers were able to hold the

weight of the specimen after cracking, avoiding sudden collapse. Such residual strength is particularly important for occupant safety after a destructive hazard.

6. The addition of plastic fiber reinforcement to the SEM resulted in the transformation of the damage tolerance of the system, increasing its resistance against wind-borne debris. Full (through-and –through) penetration of the impacting missile was observed for the SEM specimen, which presented a failure due to weak block-mortar interface. On the other hand, the reinforced specimen did not allow the through-and-through penetration of the missile. Here, the PVA fibers in the mortar enhance the integrity of the interface, helping in the distribution of the impact damage to the adjacent blocks. Furthermore, the crack-bridging action exerted by PET fibers contributed to damage redistribution and thus energy absorption, thereby contributing to stop the impacting missile. The evidence gathered from the impact tests suggests that missile penetration can be entirely prevented by using more practical structural wall thicknesses (250 mm to 350 mm).

4.6 REFERENCES

Armwood, C. K., Erdogmus, E., and Haider, H. (2011). "Effect of fibers on the flexural strength of masonry mortars." *The Masonry Society Journal*, 29(1), 18–32.

ASTM (2012). "Standard Test Method for Bond Strength of Mortar to Masonry Units. ASTM C952 – 12." American Society for Testing and Materials, West Conshohocken, PA.

ASTM (2013). "Standard Test Method for Compressive Strength of Hydraulic Cement Mortars (Using 2-in. or [50-mm] Cube Specimens). ASTM C109 / C109M - 13." American Society for Testing and Materials, West Conshohocken, PA.

Azeko, S. T., Mustapha, K., Annan, E., Odusanya, O. S., and Soboyejo, W. O. (2015). "Recycling of polyethylene into strong and tough earth-based composite building materials." *Journal of Materials in Civil Engineering*, 04015104-1- 04015104-10.

Betterman, L. R., Ouyang, C., and Shah, S. P. (1995). "Fiber-matrix interaction in microfiber-reinforced mortar." *Advanced Cement based Materials*, 2(2), 53–61.

Binici, H., Aksoganb, O., Bodurc, M. N., Akcad, E., and Kapur, S. (2007). "Thermal isolation and mechanical properties of fibre reinforced mud bricks as wall materials." *Construction and Building Materials,* 21, 901–906.

Bouhicha, M., Aouissi, F., and Kenai, S. (2005). "Performance of composite soil reinforced with barley straw." *Cement and Concrete Composites*, 27, 617–621.

Brignola, A., Frumento, S., Lagomarsino, S., and Podestà, S. (2009). "Identification of shear parameters of masonry panels through the in-situ diagonal compression test." *International Journal of Architectural Heritage*: *Conservation, Analysis, and Restoration*, 3, 52-73.

Cai, Y., Shia, B., Ng, C. W.W., and Tang, C. (2006). "Effect of polypropylene fibre and lime admixture on engineering properties of clayey soil." *Engineering Geology*, 87, 230–240.

Clementi, F., Stefano Lenci, S., and Sadowski, T. (2008). "Fracture characteristics of unfired earth." *International Journal of Fracture*, 149, 193–198.

Danso, H., Martinson, B., Ali, M., and Mant, C. (2014). "Performance characteristics of enhanced soil blocks: a quantitative review." *Building Research and Information*, 43(2), 253–262.

Donkor, P., and Obonyo, E. (2015). "Earthen construction materials: assessing the feasibility of improving strength and deformability of compressed earth blocks using polypropylene fibers." *Materials and Design*, 83, 813–819.

Drysdale, R. G., and Hamid, A. A. (2008). *Masonry structures: behavior and design*, Boulder, Colorado.

Fanella, D. A., and Naaman, A. E. (1985). "Stress-strain properties of fiber reinforced mortar in compression." *ACI Journal*, 82(4), 475–483.

Frocht, M. M. (1931). "Recent advances in photoelasticity and an investigation of the stress distribution in square blocks subjected to diagonal compression." *Transaction ASME* 55, 135-153.

Ghavami, K., Toledo Filho, R. D., and Barbosa, N. P. (1999). "Behaviour of composite soil reinforced with natural fibres." *Cement and Concrete Composites*, 21, 39–48.

Hejazi, S. M., Sheikhzadeh, M., Abtahi, S. M., and Zadhoush, A. (2012). "A simple review of soil reinforcement by using natural and synthetic fibers." *Construction and Building Materials*, 30, 100–116.

ICC 500 (2014). "ICC/NSSA Standard for the design and construction of storm shelters." International Code Council. Washington, D.C., USA.

FEMA P-361 (2015). "Safe rooms for tornadoes and hurricanes – Guidance for community and residential safe rooms." Federal Emergency Management. Washington, D.C., USA.

Lange, D. A., Ouyang, C., and Shah, S. P. (1996). "Behavior of cement based matrices reinforced by randomly dispersed microfibers." *Advanced Cement Based Materials*, 3, 20–30.

Lenci, S., Piattoni, Q., Clementi, F., and Sadowski, T. (2011). "An experimental study on damage evolution of unfired dry earth under compression." *International Journal of Fracture*, 172, 193–200.

Lima, S. A., Varum, H., Sales, A., and Neto, V. F. (2012). "Analysis of the mechanical properties of compressed earth block masonry using the sugarcane bagasse ash." *Construction and Building Materials*, 35, 829–837.

Maher, M. H., and Ho, Y. C. (1994). "Mechanical properties of kaolinite/fiber soil composite." *Journal of Geotechnical Engineering*, 120(8), 1381–1393.

Matta, F., Cuéllar-Azcárate, M. C., and Garbin, E. (2015). "Earthen masonry dwelling structures for extreme wind loads." *Engineering Structures*, 83, 163-175.

Mesbah, A., Morel, J. C., Walker, P., and Ghavami, K. (2004). "Development of a direct tensile test for compacted earth blocks reinforced with natural fibers." *Journal of Materials in Civil Engineering*, 16, 95–98.

Miller, C. J., and Rifai, S. (2004). "Fiber reinforcement for waste containment soil liners." *Journal of Environmental Engineering*, 130(8), 891–895.

Millogo, Y., Morel, J. C., Aubert, J. E., and Ghavami, K. (2014). "Experimental analysis of pressed adobe blocks reinforced with hibiscus cannabinus fibers." *Construction and Building Materials*, 52, 71–78.

Morton, T. (2008). Earth Masonry Design and Construction Guidelines, IHS BRE Press, Garston, Watford.

Mustapha, K., Annan, E., Azeko, S. T., Kana, M. G. Z., and Soboyejo, W. O. (2015). "Strength and fracture toughness of earth-based natural fiber-reinforced composites." *Journal of Composite Materials*, 0(0), 1–16.

NYCON (2016). "Nycon-PVA RECS15," http://nycon.com/nycon-pva-recs15/ (accessed March 18, 2016).

NZS 4297 (1998). "Standards New Zealand. Engineering design of earth buildings." Wellington, New Zealand.

Piattoni, Q., Quagliarini, E., and Lenci, S. (2011). "Experimental analysis and modelling of the mechanical behaviour of earthen bricks." *Construction and Building Materials*, 25, 2067–2075.

Pé, O., and Le, T. N. H. (2012). "Effect of polypropylene fiber-reinforcement on the mechanical behavior of silty clay." *Geotextiles and Geomembranes*, 32, 111–116.

Quagliarini, E., and Lenci, S. (2010). "The influence of natural stabilizers and natural fibres on the mechanical properties of ancient roman adobe bricks." *Journal of Cultural Heritage*, 11, 309–314.

Rafalko, S. D., Brandon, T. L., Filz, G. M., and Mitchell, J. K. (2007). "Fiber reinforcement for rapid stabilization of soft clay soils." *Journal of the Transportation Research Board*, 21–29.

Sanjuán, M. A., and Moragues, A. (1996). "Polypropylene-fibre-reinforced mortar mixes: optimization to control plastic shrinkage." *Composites Science and Technology*, 57, 655–660.

Senol, A. (2012). "Effect of fly ash and polypropylene fibres content on the soft soils." *Bulletin of Engineering Geology and the Environment*, 71(2), 379–387.

Skourup, B. N., and Erdogmus, E. (2010). "Polyvinyl alcohol fiber-reinforced mortars for masonry applications." *ACI Materials Journal*, 107(1), 57–64.

Subramaniaprasad, C. K., Benny Mathews Abraham, and Kunhanandan Nambiar, E. K. (2015). "Influence of embedded waste-plastic fibers on the improvement of the tensile strength of stabilized mud masonry blocks." *Journal of Materials in Civil Engineering*, 27(7), 1–7.

Taallah, B., Guettala, S., Guettala, S., and Kriker, A. (2014). "Mechanical properties and hygroscopicity behavior of compressed earth block filled by date palm fibers." *Construction and Building Materials*, 59, 161–168.

Tang, C., Shi, B., Gao, W., Chen, F., and Cai, Y. (2007). "Strength and mechanical behavior of short polypropylene fiber reinforced and cement stabilized clayey soil." *Geotextiles and Geomembranes*, 25, 194–202.

Tennant, A. G., Foster, C. D., and Venkatarama Reddy, B. V. (2013). "Verification of masonry building code to flexural behavior of cement-stabilized soil block." *Journal of Materials in Civil Engineering*, 25(3), 303-307.

Tolêdo Filho, and Sanjuán, M. A. (1999). "Effect of low modulus sisal and polypropylene fibre on the free and restrained shrinkage of mortars at early age." *Cement and Concrete Research*, 29, 1597–1604.

Turanli, L., and Saritas, A. (2011). "Strengthening the structural behavior of adobe walls through the use of plaster reinforcement mesh." *Construction and Building Materials*, 25, 1747–1752.

Wu, F., Li, G., Li, H. N., and Jia, J. Q. (2013). "Strength and stress–strain characteristics of traditional adobe block and masonry." *Materials and Structures*, 46, 1449–1457.

Yetgin, S., Cavdar, O., and Cavdar, A. (2008). "The effects of the fiber contents on the mechanic properties of the adobes." *Construction and Building Materials*, 22, 222–227.

Yokel, F. Y., and Fattal, S. G. (1976). "Failure hypothesis for masonry shear walls." *Journal of the Structural Division*, 102, 515-532.

CHAPTER 5
CONCLUSIONS AND RECOMMENDATIONS FOR FUTURE WORK

In this chapter, the main conclusions drawn from the studies in Chapter 2 through Chapter 4 are summarized, and recommendations for future work are offered.

In Chapter 2, the physical and mechanical characterization of earthen blocks that are produced with a South Carolina (silty loam) soil that is also widely available in tornado-prone regions of the United States. The main contributions from this research are summarized as follows.

1. Relatively strong but brittle compressed and stabilized earthen blocks are transformed into radically more damage tolerant blocks by incorporating recyclable and non-biodegradable plastic fibers as reinforcement. In fact, the plastic fibers change the post-cracking deformability and residual load-carrying capacity of the blocks when subject to tensile stresses. The dimensions of the plastic fibers were suitable for ensuring sufficient embedment and anchorage within the stabilized soil matrix, as revealed by the presence of ruptured fibers along the fracture surfaces.

2. For the soil used, increasing the amount of ordinary Portland cement (OPC) from 6% in weight of soil (wt%) to 9 wt% does not result in an enhancement of the interface strength between the fibers and the surrounding soil, and thus the post-cracking behavior in flexure does not appreciably change.

More research is needed to optimize the dimensions of the PET fibers, and perhaps further investigate the influence of fiber slenderness and surface finish on themechanical behavior of earthen blocks. Previous experimental evidence pointed out the importance of selecting the fiber dimensions. For example, Subramaniaprasad et al. (2015) used PET chopped fibers from beverage bottles in stabilized earthen blocks, and reported that the mechanical properties of the blocks were negatively affected.

Chapter 3 presents the prototyping of stabilized earthen masonry for tornado-resistant low-rise dwelling structures. The main conclusions from this research are summarized as follows.

1. 1C:2So:9S (cement:soil:sand proportions by weight) earthen mortar offers sufficient bond strength, with a relatively low cement content (8.3% by weight), allowing a suitable combination with the prototype earthen blocks. A similar bond tensile strength was attained with 1C:1So:6S mixture, which has a higher compressive strength due to the larger OPC content (12.5 wt%). This indicates that increasing the mortar compressive strength and OPC content does not necessarily improve the quality of the interface bond. Earthen mortars with high clay content are not suitable for earthen masonry as the susceptibility to shrinkage negatively affects the integrity of the mortar joints.

2. Based on the masonry compressive strength results, the combination of stabilized earthen blocks with 6 wt% OPC (CS6) and 1C:2So:9S mortar is selected for the earthen masonry prototype due to the suitable compromise between strength and amount of OPC. The prism specimens presented a linear relation between compressive strength and block compressive strength, which resembles the equation provided by MSJC (2013) for solid clay masonry units and OPC-lime mortar, and NZS 4297 (1998)

for earthen materials. Similar to traditional masonry, the prism specimens presented splitting failure, which indicates a sufficiently strong block-mortar interface. The results of compression tests on wallette specimens showed the effect of the head joint on the masonry compressive strength. The compressive strength increased with the strength of the blocks up to a 6 wt% OPC content (CS6 blocks), whereas for CS9 blocks the masonry compressive strength is controlled by the tensile strength of the mortar in the head joint, resulting in a similar masonry compressive strength. Therefore, increasing the compressive strength of the blocks does not necessarily improve the masonry compressive strength from certain levels of OPC content (here, from 6 wt% to 9 wt%). For both prism and wallette specimens, existing standard building codes for masonry provide conservative estimates of stabilized earthen masonry compressive strength. Using NZS 4297 (1998) and CEN (2005), the experimental compressive strength values were underestimated on average by 18% to 43%, respectively.

3. The behavior of the prototype stabilized earthen masonry in direct shear follows the Mohr-Coulomb friction law, similar to traditional masonry. This theory is used in the majority of building codes to estimate the masonry shear capacity. In general, the prototype masonry exceeded the shear requirements set forth in NZS 4297 (1998) for standard masonry. The presence of pre-compression stresses resulted in considerably higher shear strength values, and increasing differences between the required shear bond strength and that (higher) obtained experimentally. In fact, for higher pre-compression stresses (representative of masonry behavior at the base of a one-story wall), the prototype masonry had similar shear strength to the special grade masonry defined in NZS 4297 (1998). The pre-compression stress also affects the variability of the data and

the failure modes for triplet specimens. The variability reduces with the level of pre-compression. At zero pre-compression stress, the bond strength exclusively depends on the mortar joint strength, for which the data are more variable. The failure occurred when the bond strength at the weakest mortar joint was reached. Partial cohesive failure in the blocks, involving both mortar joints, was observed at increasing pre-compression stresses.

4. Based on the results of diagonal compression tests on masonry panels, the SEM prototype presented an average shear strength of 0.62 MPa with a standard deviation of 0.05 MPa (combined with an average compressive stress of 0.33 MPa and standard deviation of 0.03 MPa). The small variability of the data attests to the consistency of the materials and the construction process. The cracks developed primarily through the blocks, and to a lesser extent along the mortar joints. NZS 4297 (1998) is conservative in the estimation of the shear capacity.

5. The shear strength obtained through diagonal compression tests can be representative of an additional data point in the shear strength-compressive stress Mohr-Coulomb failure envelope. It is shown that using a linear elastic solution to describe the stress state in a diagonal compression test specimen, the results of triplet and diagonal compression tests can be correlated. For the prototype masonry, this additional set of data represents a stress condition with a higher compressive stress than that applied on the triplet specimens. This was confirmed by the failure mode observed in the diagonal specimens, which highlight a nearly isotropic material behavior. Due to the higher compression stress, splitting cracks, mainly throughout the blocks, were observed.

6. Based on the results of out-of-plane flexural tests on masonry prisms, the flexural strength for the prototype masonry was on average 0.15 MPa with a standard deviation of 0.03 MPa. The specimens typically presented a mixed failure of interface (adhesive) and block (cohesive). Although the masonry flexural strength is often neglected due to its small value and high variability, more specialized earthen masonry building codes allow for the use of data obtained experimentally or from databases. The NZS 4297 (1998) code is conservative in the recommended value of 0.1 MPa for flexural strength.

7. All target compression, shear and flexural strength ranges determined based on the analytical framework demonstrated by Matta et al. (2015) were met by the SEM prototype. Therefore, it can be concluded that the SEM prototype presented herein is suitable for high-wind resistant dwellings.

8. For tornado-resistant single-story dwelling structures made with the SEM prototype, and given a rigid diaphragm and proper anchorage with the foundation and roof diaphragm, a nominal wall thickness between 320 mm and 500 mm is suitable for the resistance of loads representative of an EF3 tornado. The predominant failure mode is out-of-plane flexure. Therefore, the use of some internal reinforcement is recommended to increase the out-of-plane capacity and provide a robust connection with the foundation and roof diaphragm.

Further research is needed to study the effect of head joints on the earthen masonry compressive strength. At increasing compressive strength values for the blocks with respect to the mortar, the opening of head joints may control the failure of wallette specimens subject to compression. This effect may also be noted by further examining

experimental results from previous work (Walker 2004). Thus, characterizing the masonry compressive strength using prisms (ASTM 2014) could lead to unconservative values. In addition, research with larger sample populations to evaluate the applicability of the existing nominal strength algorithms used for conventional masonry is recommended. The applicability provided herein is limited to the specific case of the earthen masonry prototype presented. Including additional parameters in the analysis, such as type of soil and earthen mortar, more comprehensive results could be drawn. Similarly, studies on the strength reduction factors for the limit state design of earthen masonry structures are required.

Chapter 4 introduced the transformation of the SEM damage tolerance by means of recyclable plastic fiber reinforcement. The main conclusions from this research are summarized as follows.

1. The compression strength of the 1C:2So:9S mortar is not negatively affected by the presence of short-length (8-mm) PVA fiber reinforcement. The flexural strength was not affected by the PVA fibers for a volume fraction $V_f = 0.25\%$.

2. The addition of PVA fibers to the mortar matrix can result in increased tensile bond strength. It was shown that 0.25% and 0.5% PVA fiber volume fractions are equally effective in improving the bond strength at the mortar-block interface. This is attributed to the better integrity of the interface, which is a result of the dimensional stability (e.g., shrinkage resistance) enabled by the fiber reinforcement.

3. A PVA volume fraction of 0.25% was selected for the reinforcement of the 1C:2So:9S mortar used in the SREM system. It was shown that a 0.25% volume fraction does not affect the compressive and flexural strength and provides higher bond

strength compared to the unreinforced masonry. In addition, a 0.25% volume fraction has similar bond strength to the mixture containing twice the amount of fibers.

4. The out-of-plane flexural behavior is modified by the PET fibers, which provided some post-cracking strength and deformability in flexure.

5. The in-plane shear behavior of the earthen masonry was transformed through the incorporation of plastic fiber reinforcement. Each plastic fiber had a different role in the enhancement of the earthen masonry. The interface integrity provided by the PVA fibers resulted in remarkably higher the shear strength in both the zero pre-compression triplet specimens and the diagonal compression panels. Similarly, the integrity of the interface resulted in higher stiffness and lower stiffness degradation under in-plane shear forces. In addition, the PET fibers transformed the post cracking behavior of the earthen masonry by bridging the cracks. The PET fibers were able to hold the weight of the specimen after cracking, avoiding sudden collapse. Such residual strength is particularly important for occupant safety after a destructive hazard.

6. The addition of plastic fiber reinforcement to the SEM resulted in the transformation of the damage tolerance of the system, increasing its resistance against wind-borne debris. Full (through-and-through) penetration of the impacting missile was observed for the SEM specimen, which presented a failure due to weak block-mortar interface. On the other hand, the reinforced specimen did not allow the through-and-through penetration of the missile. Here, the PVA fibers in the mortar enhance the integrity of the interface, helping in the distribution of the impact damage to the adjacent blocks. Furthermore, the crack-bridging action exerted by PET fibers contributed to damage redistribution and thus energy absorption, thereby contributing to stop the

impacting missile. The evidence gathered from the impact tests suggests that missile penetration can be entirely prevented by using more practical structural wall thicknesses (250 mm to 350 mm).

More research is needed to understand the mechanisms involved in the effect of the plastic fiber reinforcement on the behavior of the block-mortar interface, which greatly affects the mechanical behavior of the masonry. Based on the experimental results presented herein, the dimensional stability (e.g., shrinkage resistance) of the interface is a critical factor for the strength of the masonry when it is subject to static and dynamic shear and tensile forces (e.g., in-plane diagonal compression and out-of-plane impact of flying debris). Research on the parameters and mechanisms that influence the interface strength between PET fibers and soil matrix in earthen blocks is also needed (including an in-depth analysis of the results presented here) to understand the toughening effects on the proposed plastic fiber-reinforced earthen masonry.

Further research is recommended to evaluate the failure mechanisms of the earthen masonry subject to impact loads. Based on the preliminary results presented herein, the reinforced prototype masonry may be considered for the construction of safety shelters with structural wall thickness of 250-350 mm. In addition, the use of internal reinforcement (e.g., steel bars) is recommended to provide adequate anchorage with diaphragms and foundation.

5.1 References

ASTM (2014). "Standard Test Method for Compressive Strength of Masonry Prisms. ASTM C1314 – 14." American Society for Testing and Materials, West Conshohocken, PA.

Subramaniaprasad, C. K., Benny Mathews Abraham, and Kunhanandan Nambiar, E. K. (2015). "Influence of embedded waste-plastic fibers on the improvement of the tensile strength of stabilized mud masonry blocks." *Journal of Materials in Civil Engineering*, 27(7), 1–7.

Walker, P. J. (2004). "Strength and erosion characteristics of earth blocks and earth block masonry." *Journal of Materials in Civil Engineering*, 16(5), 497-506.

APPENDIX A – REVIEW OF SUITABLE SOIL FOR STABILIZED EARTHEN MASONRY IN NATURAL HAZARD-PRONE HAZARD REGIONS IN THE U.S.

The feasibility of stabilized earthen masonry (SEM) depends on the local availability of a suitable soil. For the selection of the soil, most recommendations are based on the texture (i.e., granularity distribution, with adequate proportions of gravels, sand, silts and clays). The properties and behavior of the soil are defined by the proportion of each material (Rigassi 1985, Houben et al. 1996). However, the ranges for each soil component vary, resulting in a number of possible types of soil. For suitable soils reported in the literature, the proportion (weight) ranges are 0-40% for gravels, 25-80% for sands, 10-55% for silts, and 5-50% for clays (Jiménez Delgado and Guerrero 2007, Morton 2008, Rigassi 1985, Waitakere City Council 2008). However, soils with different texture may be successfully used to produce compressed and stabilized earthen blocks (CSEB), as reported in Chapter 2. Therefore, the ranges noted above are to be considered indicative and not mandatory.

Soil characterization is a key task (Rigassi 1985). A soil with a plasticity index in the range 16-28 and a liquid limit in the range 32-46 is suggested for earthen construction (Jiménez Delgado and Guerrero 2007). Most of these soils are classified ad as inorganic clays of medium plasticity in accordance with Casagrande's plasticity chart. However, low-plasticity inorganic clays as well as inorganic silts of low and medium compressibility are also suitable for CSEBs (Jiménez Delgado and Guerrero 2007). In addition, the soil must not contain organic matter, which generally excludes topsoils

(Morton 2008). Clay is an important component of the soil because it provides cohesion and waterproofing (Waitakere City Council. 2008). To this end, it is recommended to use a minimum clay content of 5%. However, clays are susceptible to swelling and shrinkage, and thus more than 50% is considered unsuitable (Waitakere City Council 2008). Moreover, it has been shown that stabilized earthen blocks reach their optimum strength when the clay content is in the range 14-16% (Venkatarama Reddy et al. 2007). It noted that soils in their raw state are often not ideal, and the proportions can be adjusted by adding sand or clay, and by removing large stones (Minke 2006).

In the US, the availability of suitable soils makes SEM attractive for hazard-resistant construction. This dissertation presents a study of earthen masonry for high wind (e.g., tornado) regions. However, suitable soils are also found in earthquake-prone regions. Figure A.1 shows the US soil textural map and chart (USGS 2014), confirming that suitable soils are available in tornado- and earthquake-prone regions. For example, silty loams are available in the New Madrid seismic zone. Loam is widely available in the west coast. Loam, having clay, sand and silt contents in the range 10-25%, 25-50% and 30-50%, respectively, falls well within the boundaries for recommended soil textures for earthen construction (Figure A.1).

Stabilization is of the soil is recommended for earthen masonry to be directly exposed to water (i.e., without exterior plaster). In addition, a key objective of this process is to provide dimensional stability (e.g., minimize swelling), and enhance strength and durability (Venny Riza et al. 2010). Stabilization may be mechanical (e.g., using fibers) or chemical. This review focuses on the latter. The type of stabilizer to be used depends on the soil characteristics. There are numerous products that have been

used as stabilizers but the most common are cement and lime, either stand-alone or combined (Houben et al. 1996).

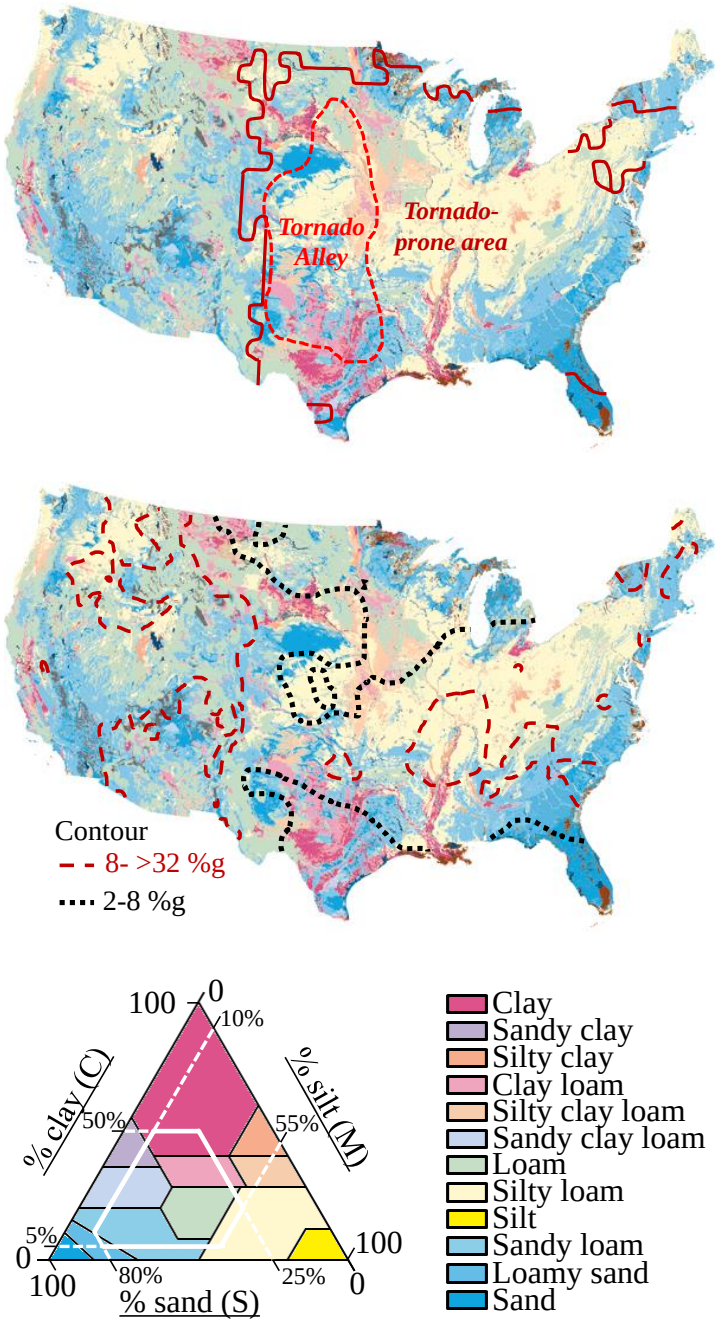

Figure A.1 US Department of Agriculture soil texture classification (USGS 2014) with contours for tornado- and earthquake-prone areas. The boundaries highlighted in the texture chart include recommended sand, silt and clay content for earthen blocks.

Lime is typically recommended for soils having a high clay content (30-40% and up to 70%) and plasticity index above 15 (Venny Riza et al. 2010, Houben et al. 1996). The optimum lime content for the soil varies and needs to be evaluated in each case (Minke 2006). Lime binds primarily with the clay particles and hardly with sand. The manufacturing of earthen blocks requires soils with low moisture content and relatively high sand content, therefore lime may not be recommended for CSEBs (Rigassi 1985). Instead, ordinary Portland cement (OPC) is widely recommended as the most suitable stabilizer for compressed earthen blocks (Rigassi 1985, Houben et al. 1996). The amount of OPC may vary between 4 and 10% to provide satisfactory strength while minimizing costs and embodied energy (Rigassi 1985, Venny Riza et al. 2010). Hydrating OPC mainly reacts with the sandy fraction of the soil, while some secondary reactions may be observed with the clay particles (Rigassi 1985). The type and amount of clay affects the effectiveness of the OPC to enhance the physical and mechanical properties of the stabilized soil. In general, stabilization using OPC is not recommended for soils with a high clay content (>30%) and high plasticity index (Rigassi 1985; Houben et al. 1996; Minke 2006). However, it has been found that OPC is as effective as lime in the stabilization of clayey soils with moderate to high plasticity (Prusinski and Bhattacharja 1999).

REFERENCES

Houben, H., Rigassi, V., and Garnier, P. (1996). "Compressed Earth Blocks: Production Equipment." CDI and CRATerre-EAG, Brussels, Belgium.

Jiménez Delgado, M. C., and Guerrero, I. C. (2007). "The Selection of Soils for Unstabilised Earth Building: A Normative Review." *Construction and Building Materials*, 21(2), 237-251.

Minke, G. (2006), "Building with Earth: Design and Technology of Suitable Architecture." Birkhäuser – Publishers for Architecture, Basel, Switzerland.

Morton, T. (2008). Earth masonry design and construction guidelines, IHS BRE Press, Garston, Watford.

Prusinski, J. R., and Bhattacharja, S. (1999). "Effectiveness of Portland Cement and Lime in Stabilizing Clay Soils." Seventh International Conference on Low-Volume Roads 1999, Vol 1: Planning, Administration, and Environment; Design; Materials, Construction, and Maintenance; Operations and Safety(1652), 215-227.

Rigassi, V. (1985). "Compressed Earth Blocks: Manual of Production." CRATerre-EAG, ed., Deutsches Zentrum für Entwicklungstechnologien, Germany, 143.

Venkatarama Reddy, B. V., Lal, R., and Nanjunda Rao, K. S. (2007). "Optimum Soil Grading for the Soil-Cement Blocks." Journal of Materials in Civil Engineering, 19(2), 139-148.

Venny Riza, F., Rahman, I. A., and Zaidi, A. M. A. (2010). "A Brief Review of Compressed Stabilized Earth Brick (CSEB)." Science and Social Research (CSSR), 2010 International Conference, IEEE Xplore, Kuala Lumpur, Malaysia, 999 - 1004.

Waitakere City Council (2008), "Waitakere City Council's Sustainable Home Guidelines: Earth buildings." Waitakere City Council, Henderson, New Zealand

APPENDIX B – SOIL CHARACTERIZATION

This appendix covers the characterization of the soil based on particle sized distribution analysis of samples of the soil used to manufacture the earthen masonry prototypes.

Three different soil samples from the same site were collected and analyzed. This site is located in Lexington, SC, with coordinates 34.07, -81.06. The natural soil was air dried, crushed and sieved (No. 8 sieve) to obtain the particle size desired for the production of the earthen masonry (Figure B.1). For the crushing, the soil was placed in a mechanical mixer with 12 steel balls with a diameter of 48 mm. The steel balls used had the standard size and weight required for standard abrasion testing of aggregates.

Figure B.1 Photographs of undergraduate research assistants working on the soil selection for crushing and sieving.

A soil sample of approximately 100 g was used to perform the particle sized distribution analysis. Fist, a hydrometer analysis was performed to determine the size distribution for fine soil particles. Sodium hexametaphosphate (SHMP, in a

concentration of 40 g per one liter of water) was used to flocculate the clay particles. The water was heated up to 80°C, and then mixed with the SHMP. The solution was mixed with the soil mechanically (Figure B.2). After the hydrometer analysis was completed, the soil sample was washed using sieve No. 200, and air dried. The sample retained in sieve No. 200 was dried to perform the dry sieve analysis. The soil particle size distribution data are summarized in Figure B.3.

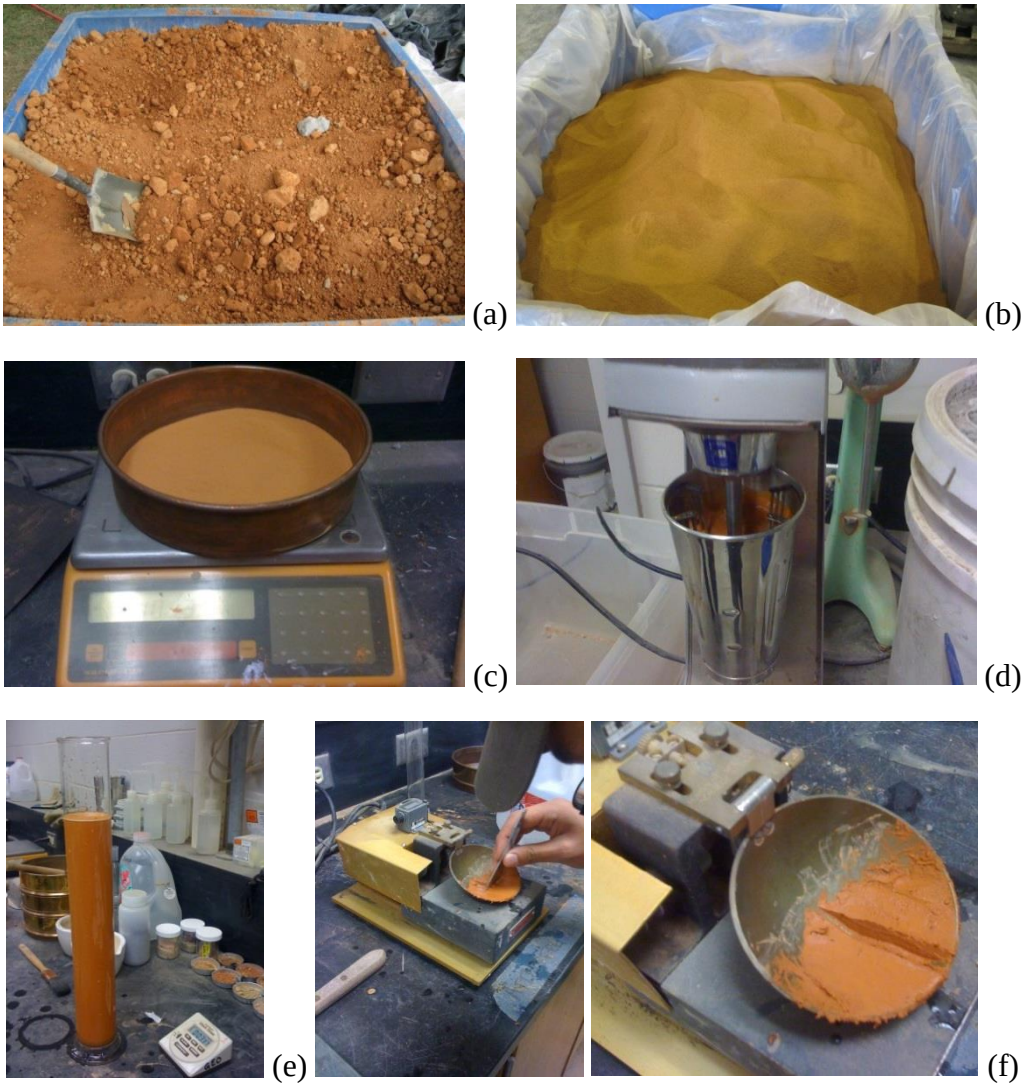

Figure B.2 Photographs of soil characterization process: (a) raw soil, (b) soil dried, crushed and sieved, (c) soil sample for particle size distribution test, (d) mechanical mixing of soil with SHMP solution, (e) hydrometer analysis, and (f) Atterberg Limits test (liquid limit).

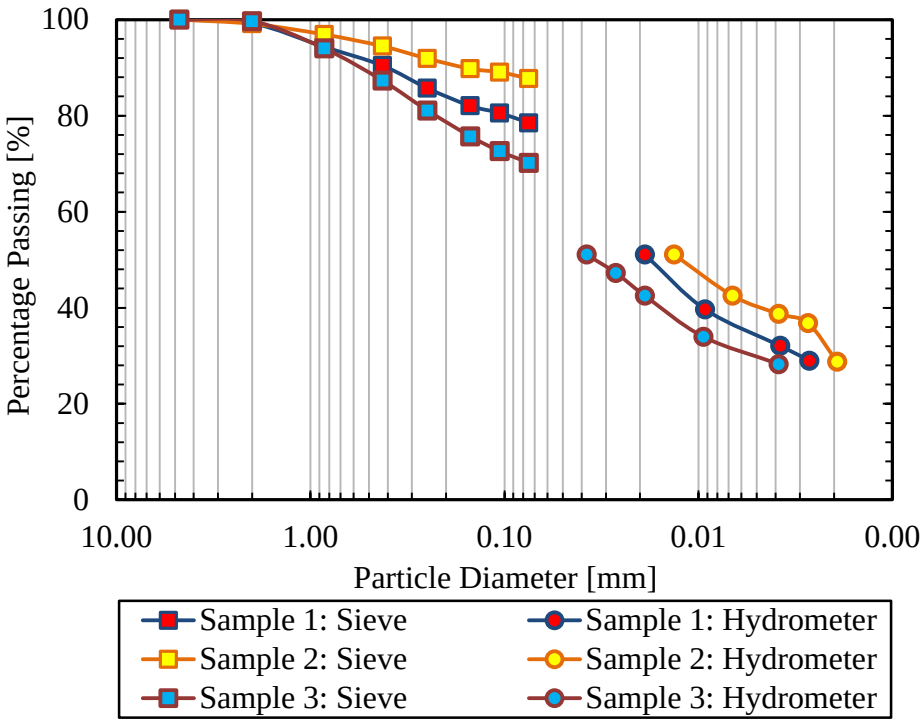

Figure B.3 Particle size distribution for soil samples.

APPENDIX C – TESTING APPARATUS

This appendix presents the test setups used for the material and mechanical characterization of the earthen blocks and masonry.

Linear displacement transducers (LDT) were used to record displacements. The LDTs used had a displacement range of 5 mm and 50 mm. For the earthen blocks and mortar characterization tests, the load was applied with a servo-hydraulic load frame with a capacity of 220 kN. Manually-operated hydraulic cylinders with a capacity of 250 and 500 kN were also used for the masonry characterization in compression, flexure and shear.

C.1. EARTHEN BLOCK COMPRESSION AND FLEXURAL STRENGTH CHARACTERIZATION

The displacements in the flexure and compression test setups were recorded with 50-mm LDTs. In addition to the load cell from the universal machine, a 40-kN load cell was used to measure the vertical load in the flexure test (Figure C.1). A comparison between the loads measured with the two load cells is shown in Figure C.2. The load was applied under displacement control with a rate of 1.2 mm/min and 1.8 mm/min for the flexural and compression tests, respectively. Five specimens per series were tested.

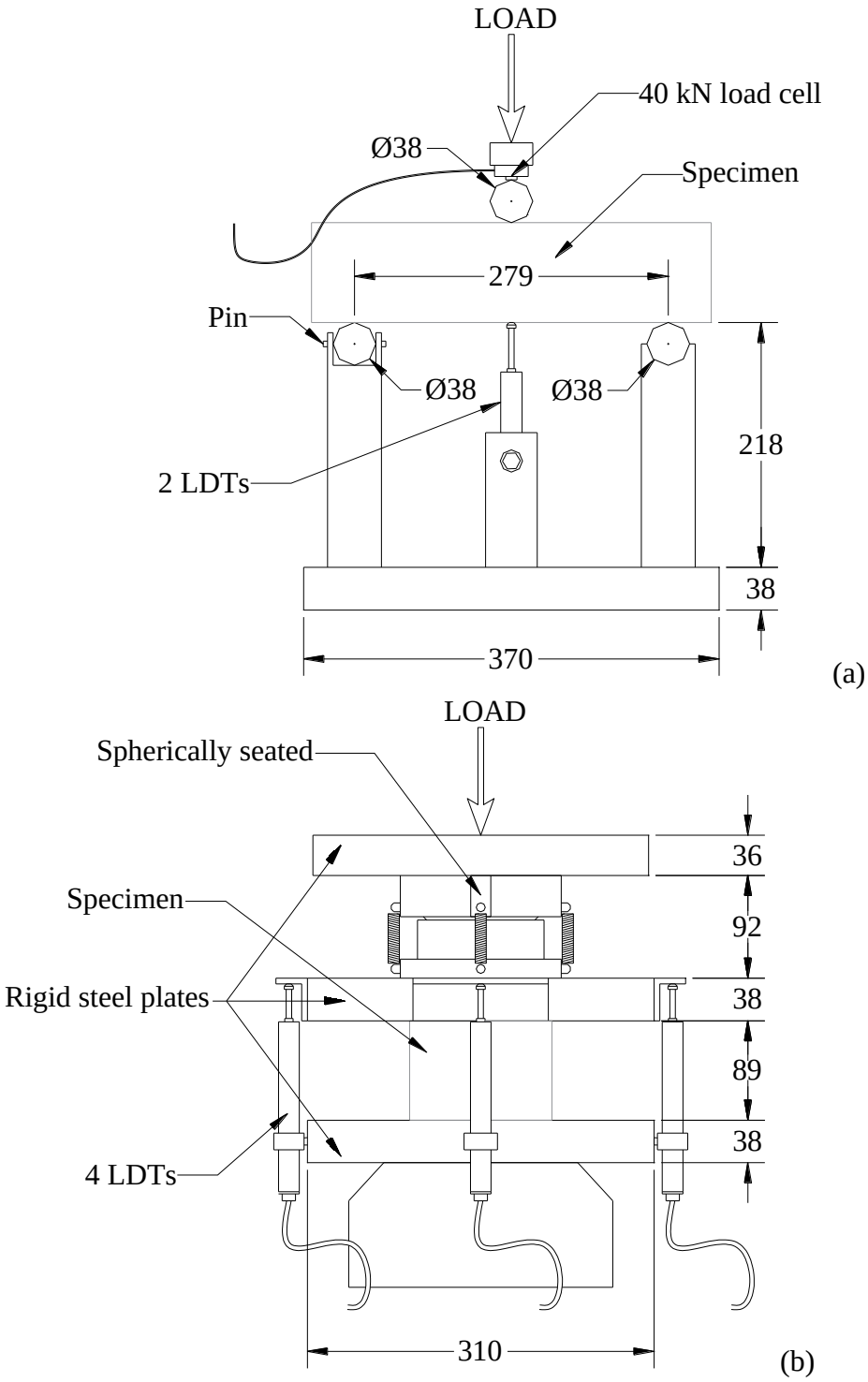

Figure C.1 Test setup for (a) flexural and (b) compression test on earthen block. Dimensions in mm.

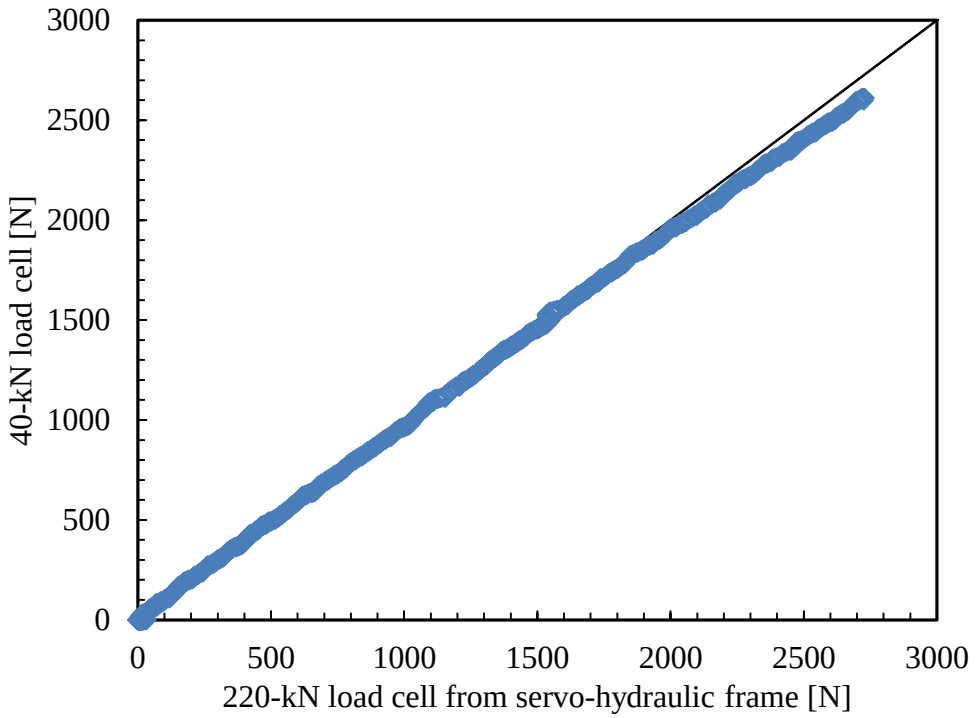

(a)

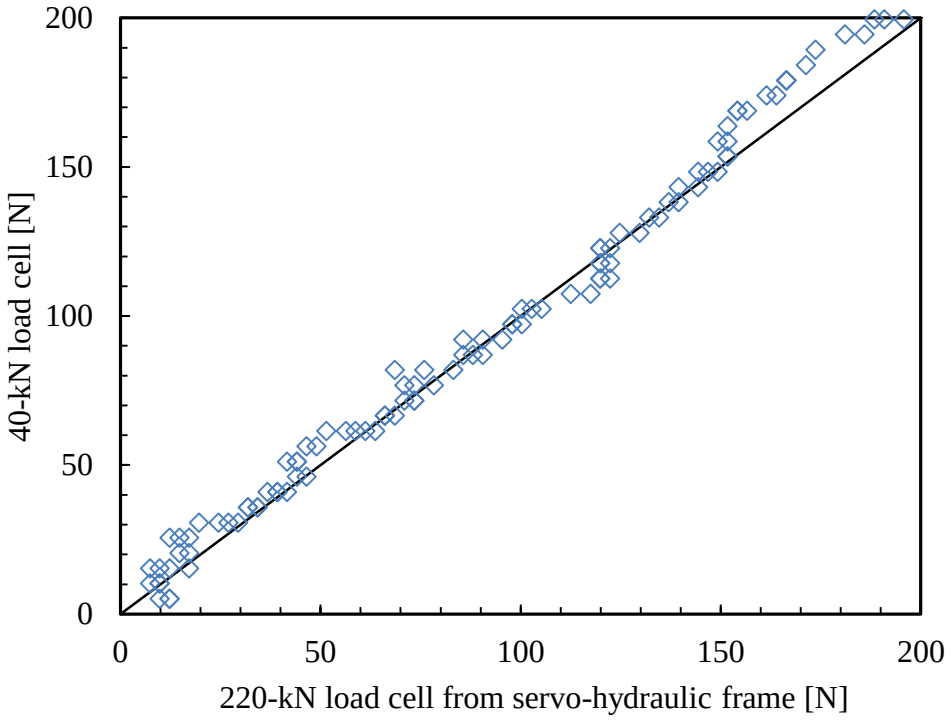

(b)

Figure C.2 Comparison between load cell from hydraulic universal machine and 40 kN load cell: (a) range of 0 to 3000 N, and (b) range of 0 to 200 N.

C.2. EARTHEN MORTAR TENSILE BOND STRENGTH CHARACTERIZATION

The tensile bond strength of the earthen masonry was characterized through couplet tests (ASTM C952). The load was applied under displacement control with a rate of 0.4 mm/min. The opening of the mortar joint was recorded with four 50 mm LDTs (Figure C.3). Six specimens for each series were tested.

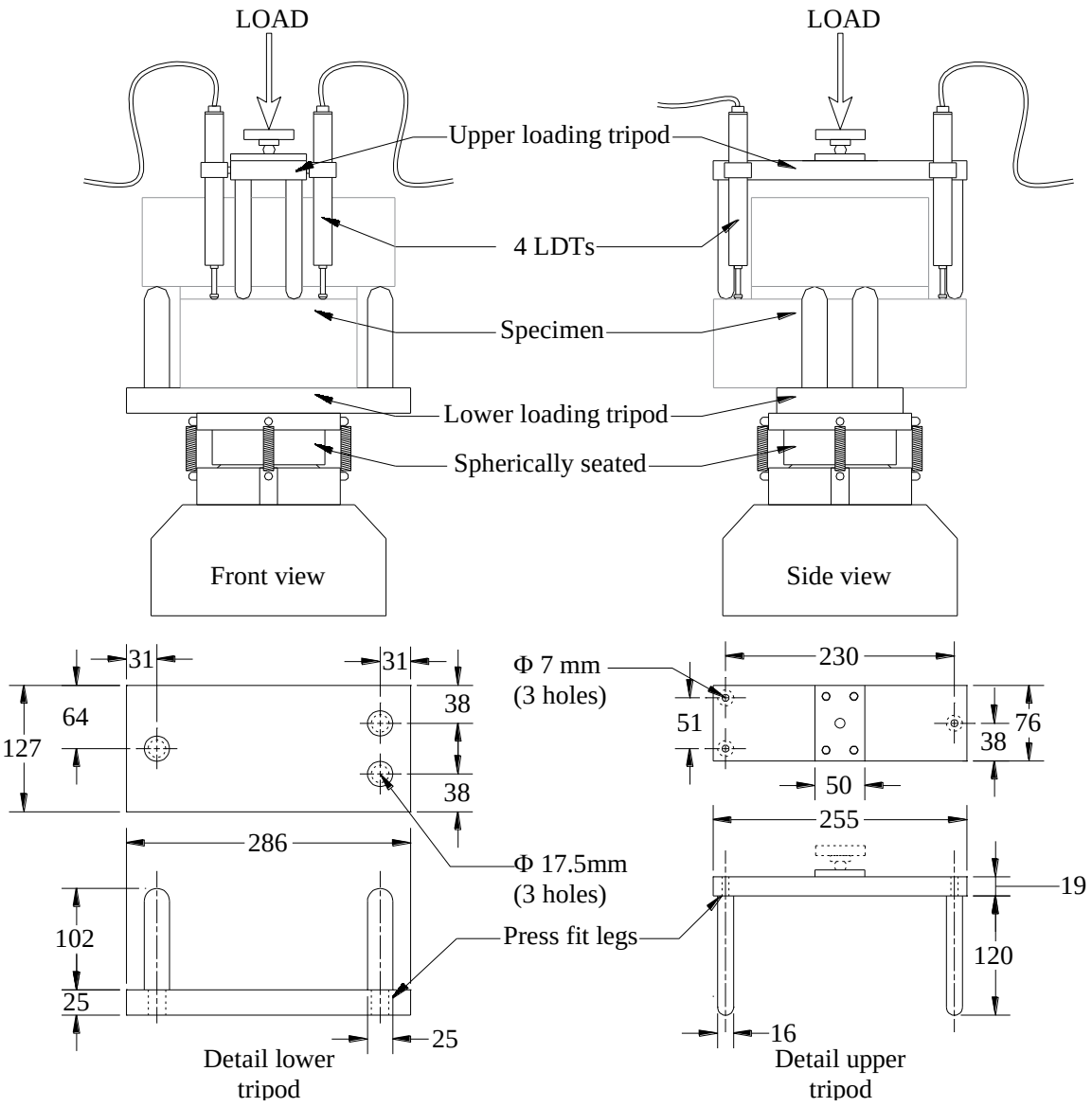

Figure C.3 Test setup for couplet test. Dimensions in mm.

C.3. EARTHEN MASONRY COMPRESSION STRENGTH CHARACTERIZATION

The compression load was applied manually using a 500 kN hydraulic cylinder. Three specimens for each series were tested. For the prisms, the front face was instrumented with a 5-mm and a 50-mm LDT to measure the horizontal displacement of the block and the vertical displacement of the block and joints, respectively. The displacements along a single joint and block were recorded with two 5-mm LDTs mounted on the back face of the prism (Figure C.4).

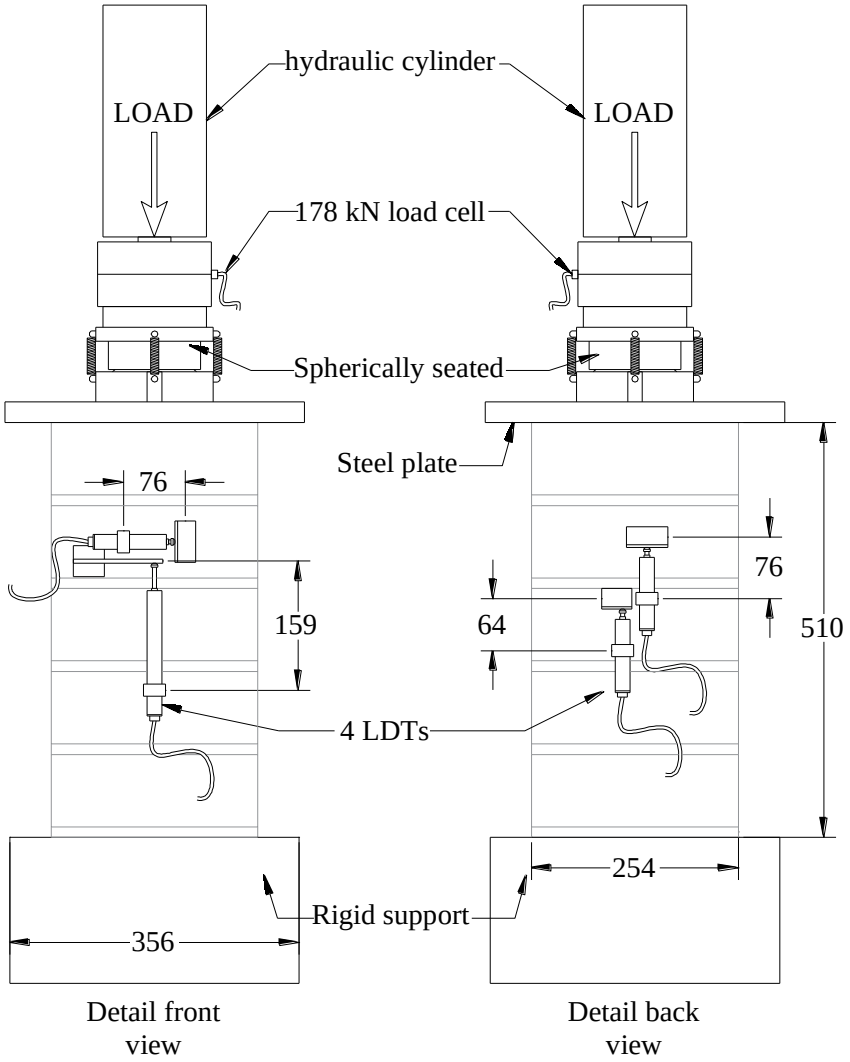

Figure C.4 Test setup for compression test on earthen masonry prisms. Dimensions in mm.

The wallettes specimens were instrumented with six LDTs placed on the front and back face. On the front face, the horizontal deformation of the center block was recorded with a 5-mm LDT. The vertical displacement of representative mortar joints was measured with two symmetrically placed 50-mm LDTs (Figure C.5).

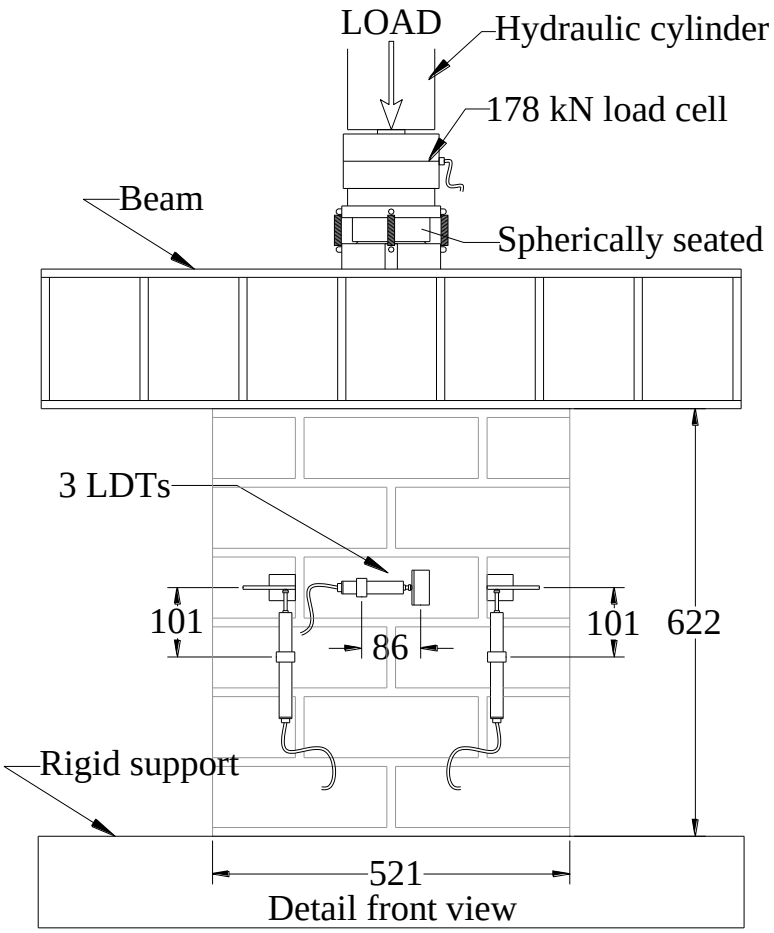

Figure C.5 Test setup for compression test on earthen masonry wallettes, front face. Dimensions in mm.

The opening of a representative head joint was recorded with a 5-mm LDT that was mounted on the back face of each wallette. In addition, the displacement of two bed joints was measured with two 50-mm LDTs (Figure C.6).

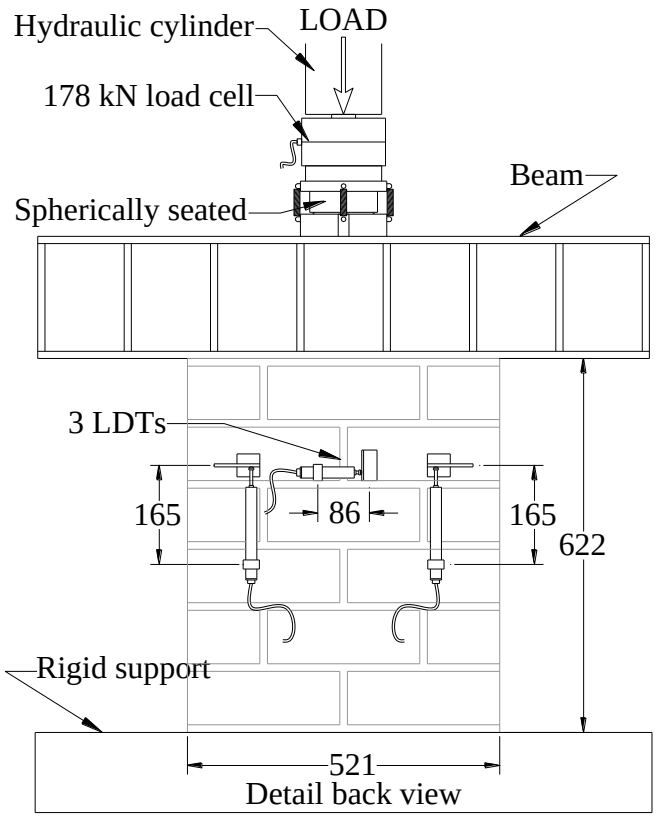

Figure C.6 Test setup for compression test on earthen masonry wallettes, back face. Dimensions in mm.

C.4. EARTHEN MASONRY SHEAR STRENGTH CHARACTERIZATION

For the shear strength characterization by means of diagonal compression tests, the load on the wallette specimens was applied manually with a 250-kN hydraulic cylinder, and measured with a 70-MPa pressure transducer (Figure C.7).

The vertical and horizontal displacement along the wallette diagonals were measured with displacement transducers having a 5-mm stroke. Three specimens were tested for each series.

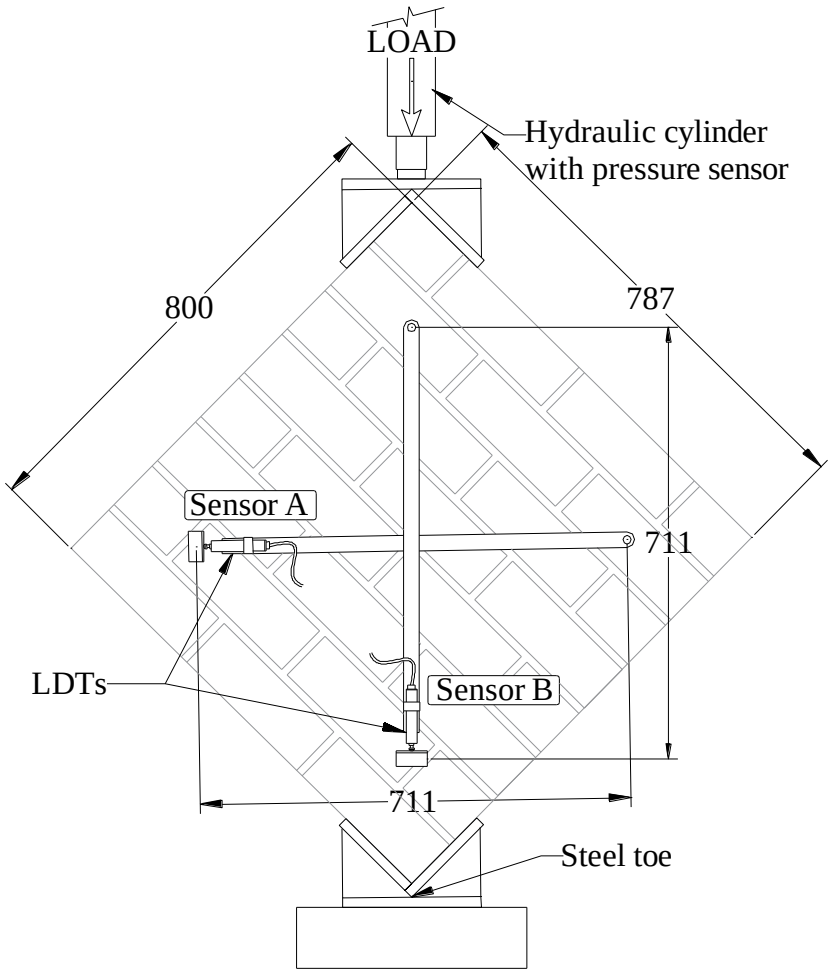

Figure C.7 Diagonal compression test setup for shear characterization of earthen masonry wallettes. Dimensions in mm.

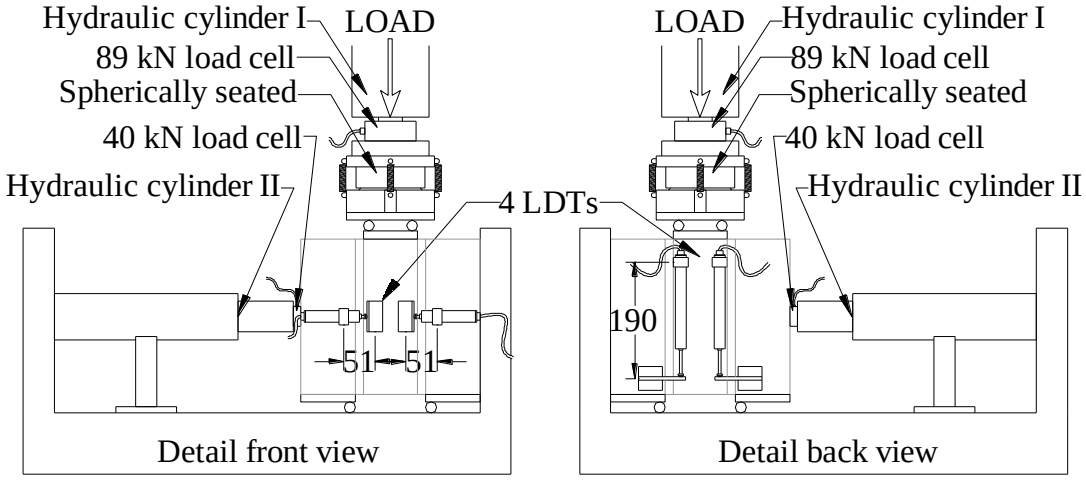

Figure C.8 Shear test setup for earthen masonry triplets. Dimensions in mm.

For the shear strength characterization by means of triplet tests, three specimens for each level of pre-compression stress were tested. The pre-compression load was imparted with a 250-kN hydraulic cylinder that was operated with an electrical pump, and measured with a 40-kN load cell (Figure C.8). Four LDTs were used, two recording the horizontal displacement (opening) of the mortar joints and two recording the relative vertical displacement (slip) of the earthen blocks (Figure C.8).

C.5. EARTHEN MASONRY FLEXURAL STRENGTH CHARACTERIZATION

The load was imparted manually with a 250-kN hydraulic cylinder, and was recorded with a 40-kN load cell (Figure C.9). The midspan displacement was recorded with two 50-mm LDTs (one on each side of the specimen). One of the LDTs was mounted on the specimen using a pinned frame (attached to the specimen) to minimize the contribution of rigid displacements. The other LDT was attached to the rigid reaction frame. For the analysis, the data from the LDT attached on the specimen were used.

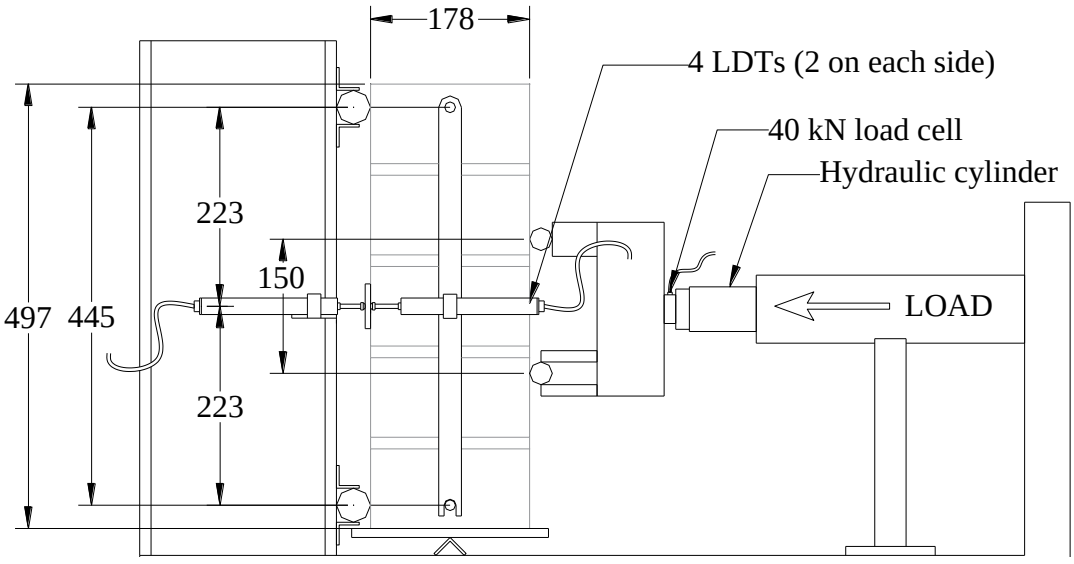

Figure C.9 Out-of-plane flexural test setup for earthen masonry prisms. Dimensions in mm.

APPENDIX D – EARTHEN BLOCKS CHARACTERIZATION

This appendix presents the results for all the specimens used for the characterization of the earthen blocks, including: flexural and uniaxial compression response, and SEM micrograph and EDX analysis of block samples.

D.1. EARTHEN BLOCK FLEXURAL TEST RESULTS

The results from flexural tests are presented in the following table and figures. Table D.1 summarizes the flexural strength data, and Figure D.1 and Figure D.2 show the load-displacement curves for all specimens.

Table D.1 Earthen blocks flexural strength

Specimen	Flexural strength [MPa]				
	C	CS6	CSR6	CS9	CSR9
1	0.32	0.80	0.59	0.91	0.85
2	0.30	0.52	0.43	0.99	0.98
3	0.32	0.71	0.45	1.01	0.76
4	0.29	0.64	0.61	1.14	0.95
5	0.32	-	0.56	-	0.96
Avg.	0.31	0.67	0.53	1.01	0.90
St. dev.	0.01	0.12	0.08	0.10	0.10

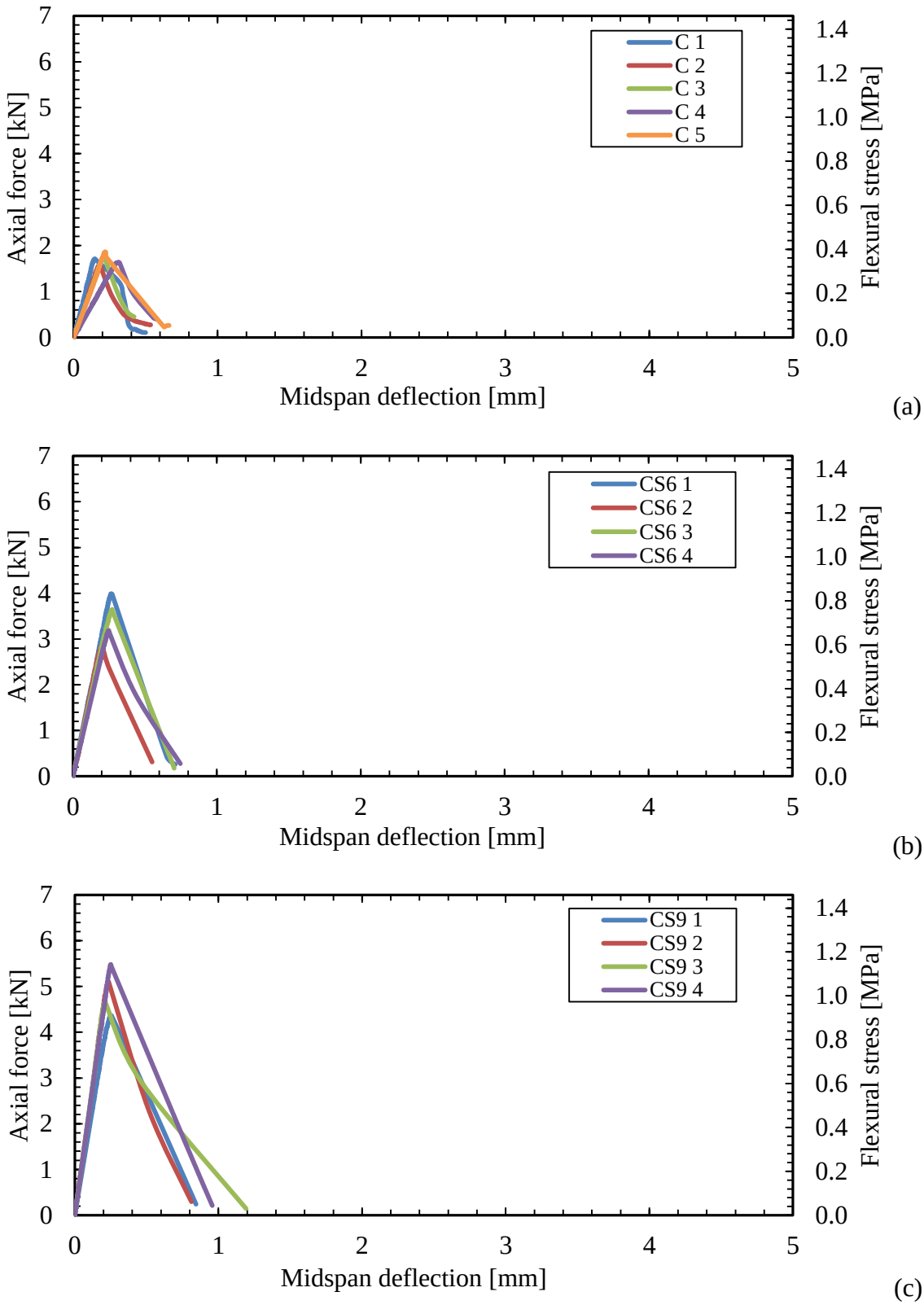

Figure D.1 Load-displacement curves in flexure for unreinforced block specimens: (a) C, (b) CS6, and (c) CS9 (representative LDTs).

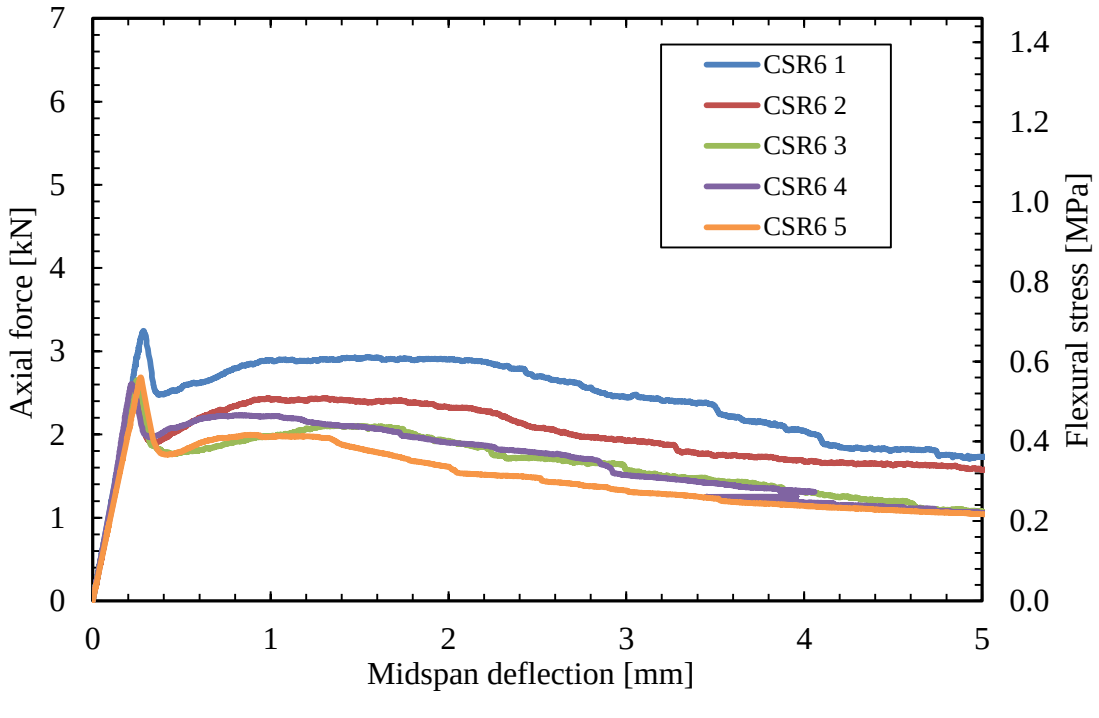

(a)

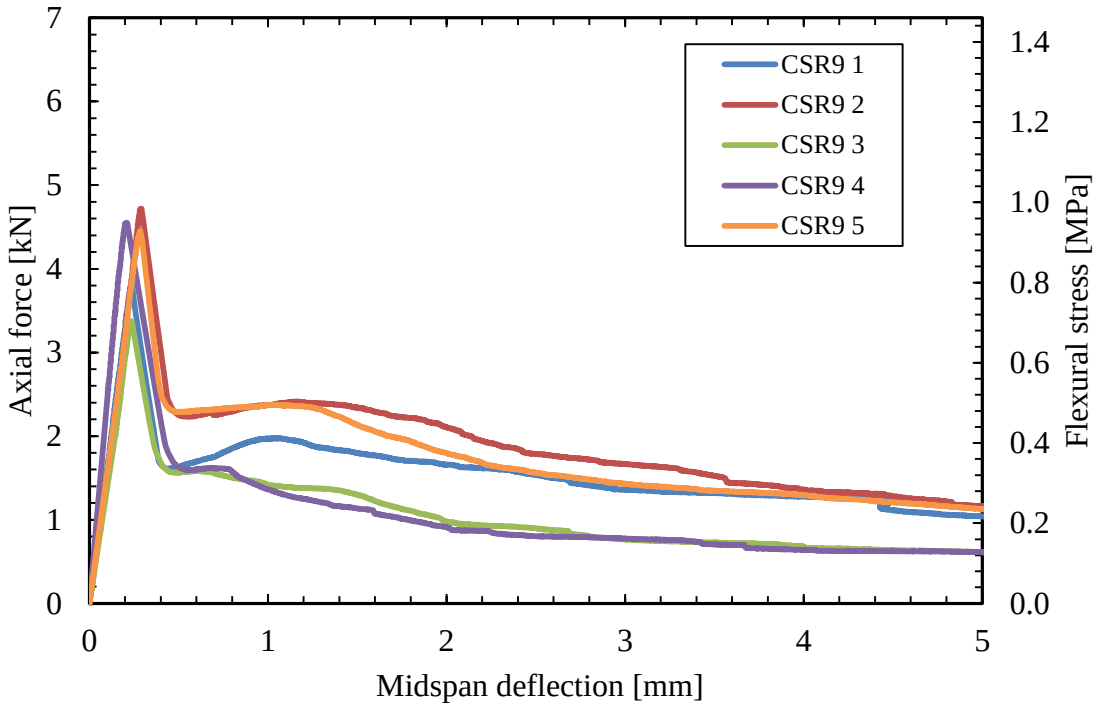

(b)

Figure D.2 Load-displacement curves in flexure for fiber-reinforced block specimens: (a) CSR6, and (b) CSR9 (representative LDTs)

D.2. EARTHEN BLOCK COMPRESSION TEST RESULTS

The block compressive strength results are summarized in Table D.2. In addition, the load-displacement curves for all specimens (based on representative LDTs) are presented in Figure D.3 through Figure D.5.

Table D.2 Earthen blocks compressive strength

Specimen	Compressive strength [MPa]				
	C	CS6	CSR6	CS9	CSR9
1	1.11	5.35	4.80	6.45	6.16
2	1.40	4.53	5.43	5.84	6.07
3	1.13	4.33	4.63	5.56	6.38
4	1.09	4.10	4.85	6.39	5.42
5	1.07	4.80	4.30	6.21	5.49
Avg.	1.16	4.62	4.80	6.09	5.90
St. dev.	0.14	0.48	0.41	0.38	0.43

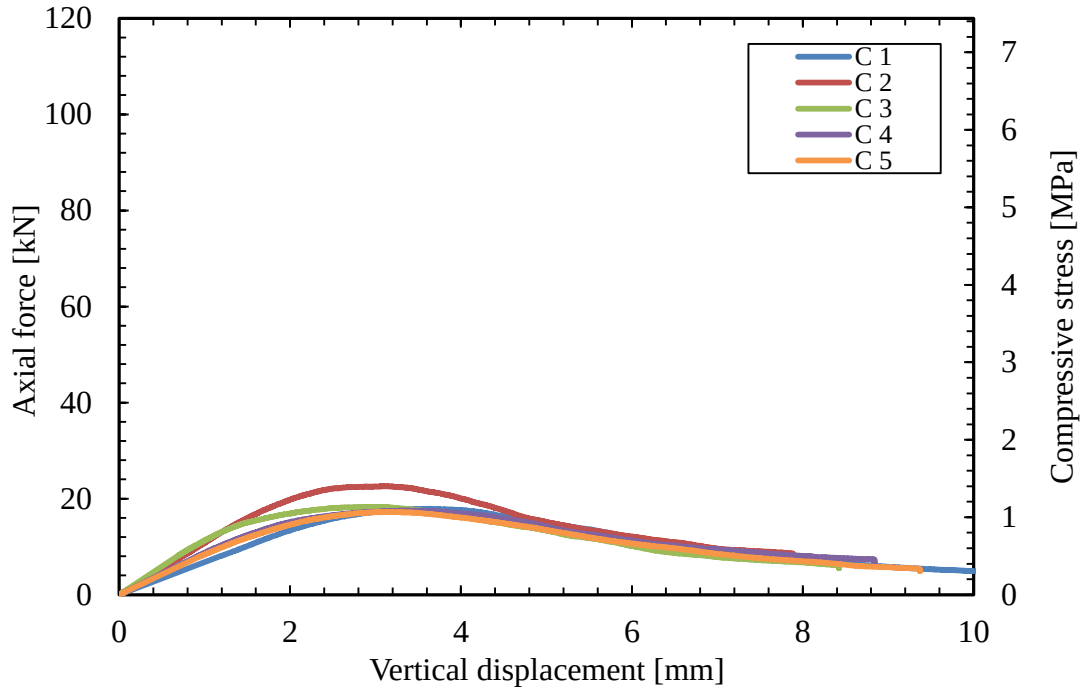

Figure D.3 Load-displacement curves in compression for C specimens.

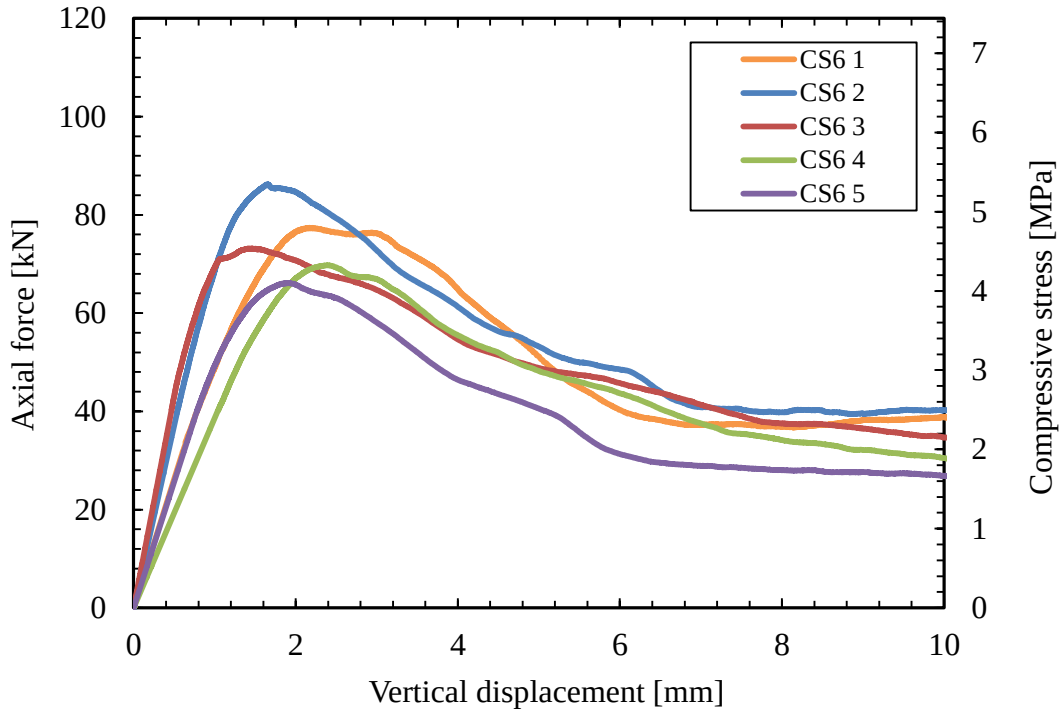

(a)

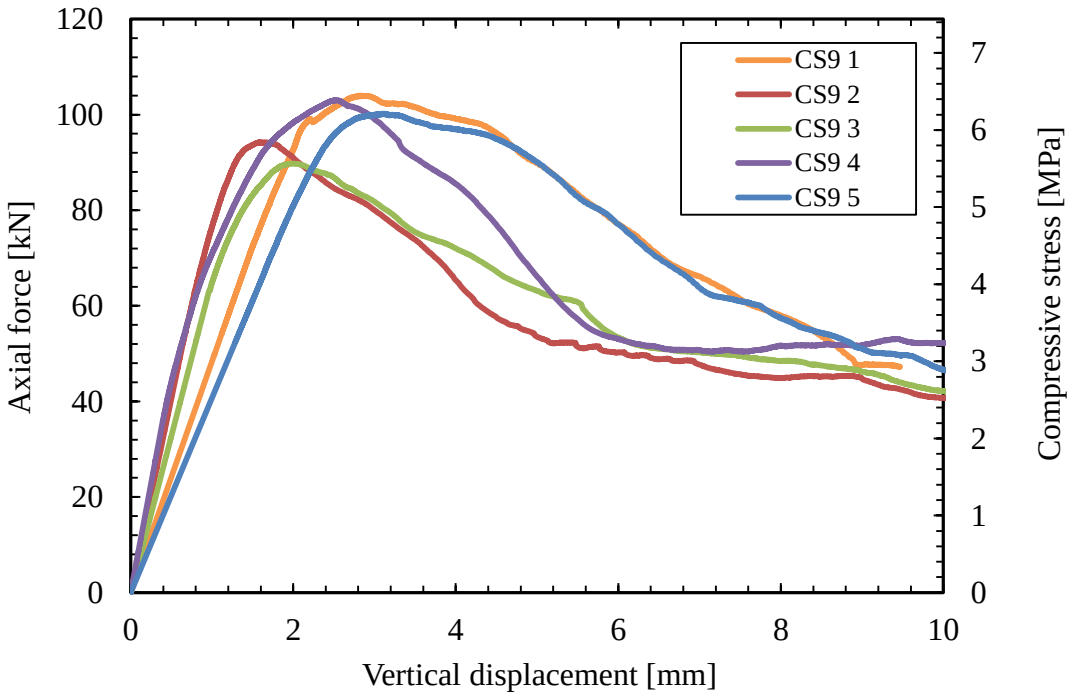

(b)

Figure D.4 Load-displacement curves in compression for OPC stabilized blocks: (a) CS6, and (b) CS9 (representative LDTs)

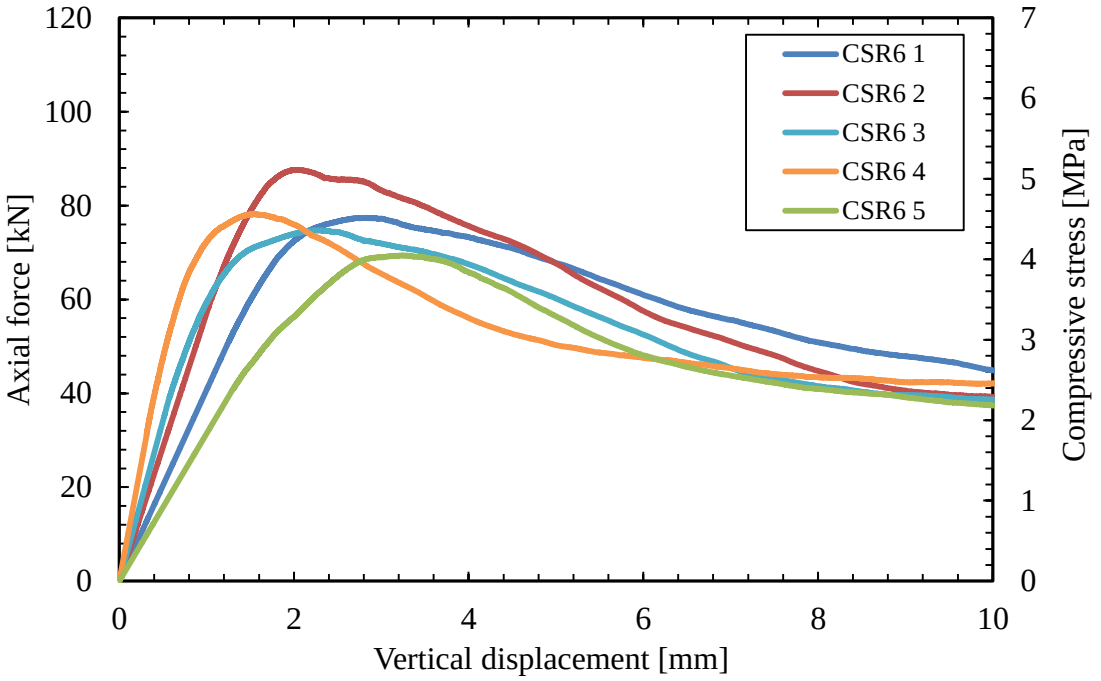

(a)

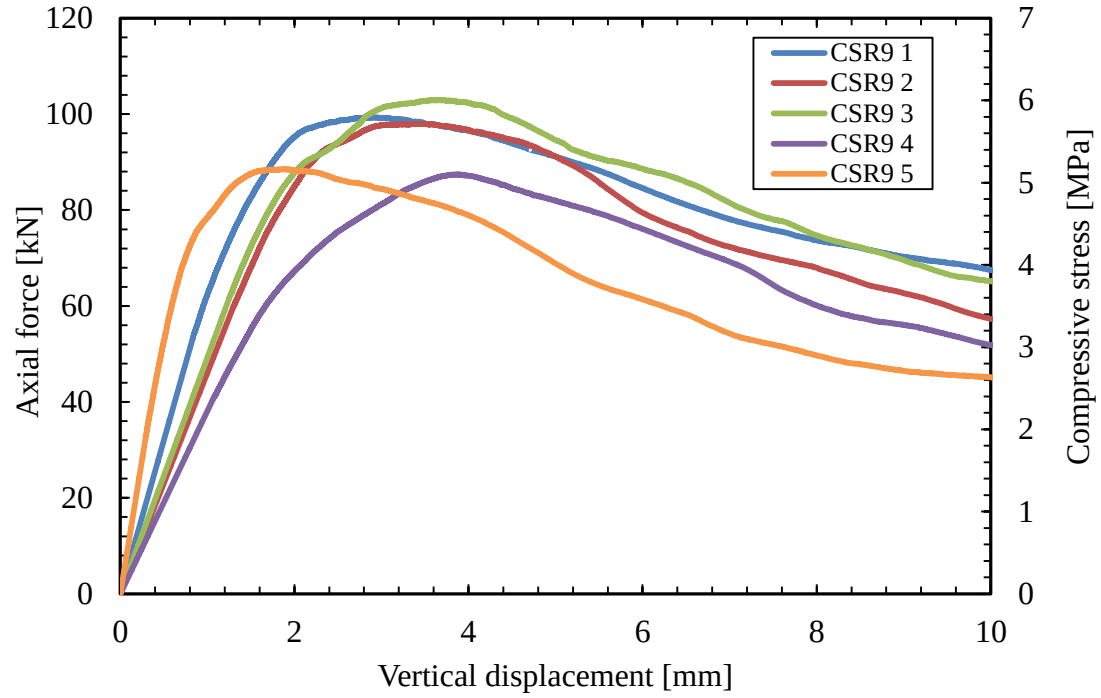

(b)

Figure D.5 Load-displacement curves in compression for stabilized and reinforced blocks: (a) CSR6, and (b) CSR9 (representative LDTs)

D.3. EARTHEN BLOCK SEM MICROGRAPHS AND EDX ANALYSIS

Samples from the surface fracture of the failed blocks were used to obtain scanning electron microscopy (SEM) micrographs and for the EDX analysis. The samples, having dimensions of 8 mm × 10 mm × 10 mm, were gold-sputtered to create a conductive layer. The images were taken from five randomly-selected points with four different magnifications. Then, one or two of the points were used for the EDX analysis, as illustrated in Figure D.6.

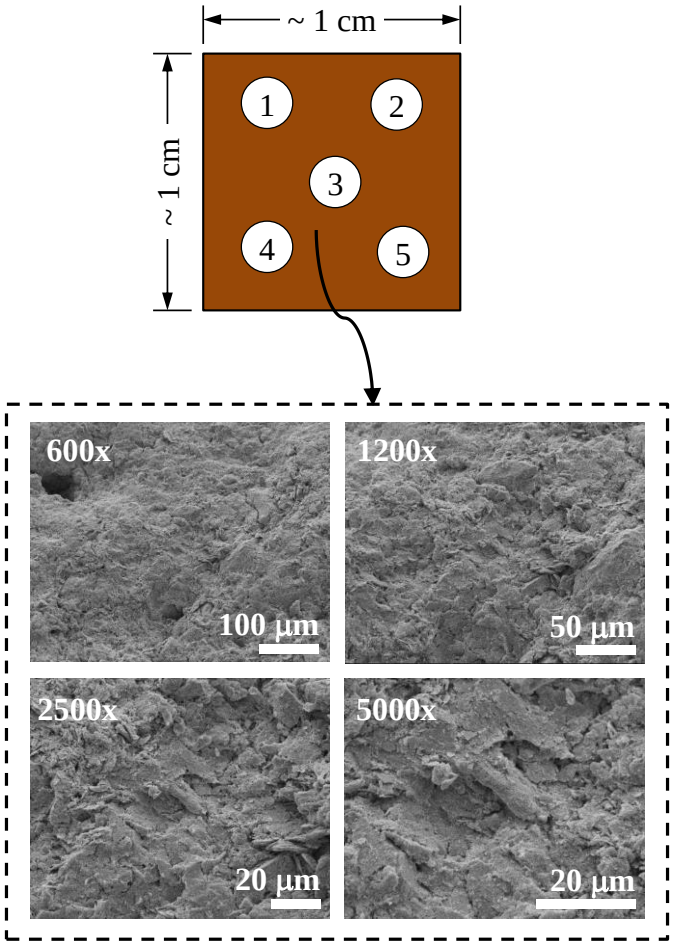

Figure D.6 Sketch for methodology followed to select locations to acquire SEM micrographs from earthen block samples.

C specimen 1 – Point 1			
600x	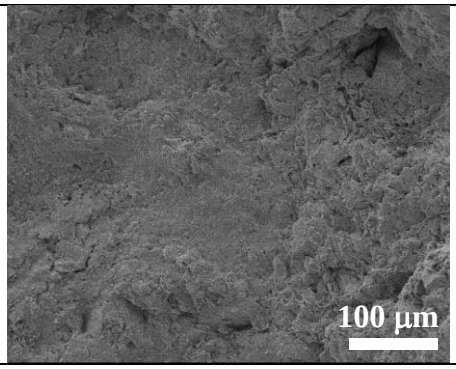	1200x	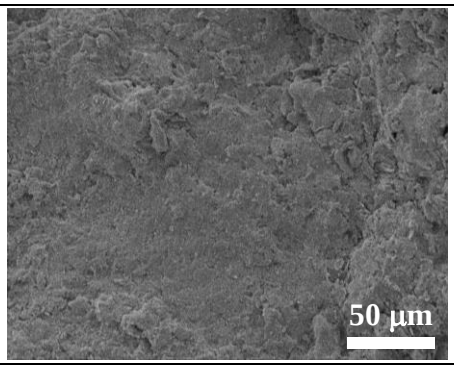
2500x	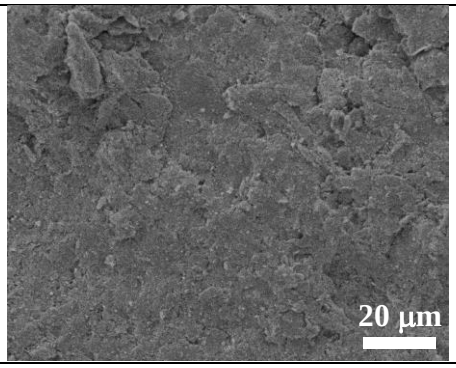	5000x	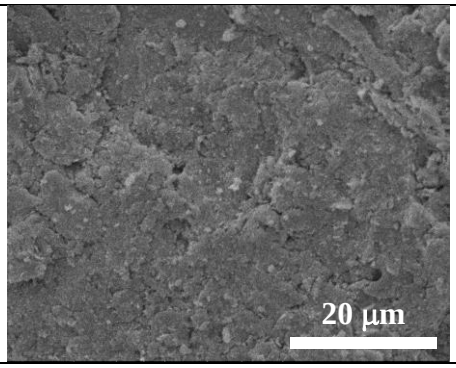

C specimen 1 – Point 2			
600x	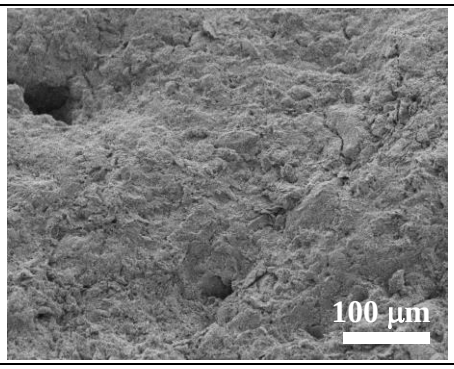	1200x	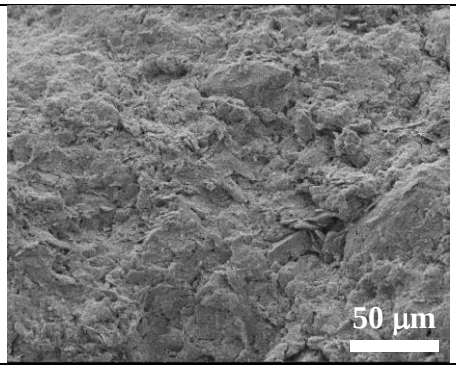
2500x	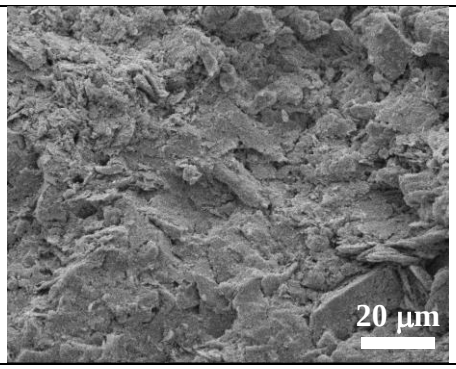	5000x	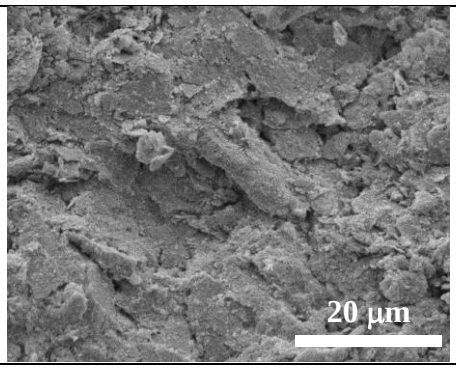

C specimen 1 – Point 3

600x

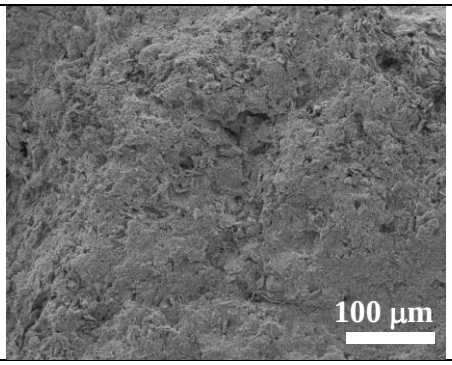

1200x

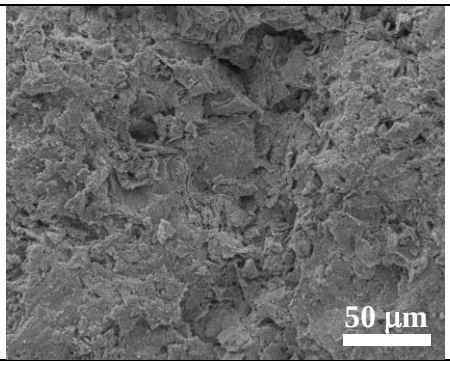

2500x

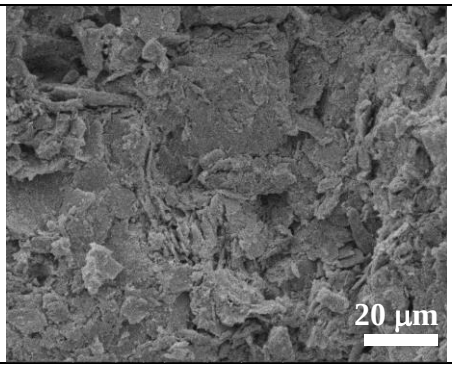

5000x

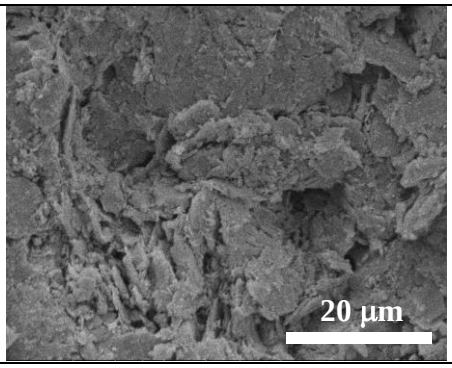

C specimen 1 – Point 4

600x

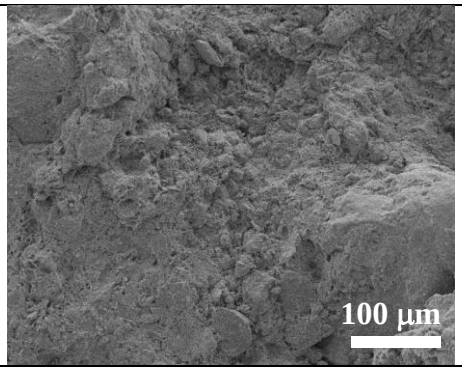

1200x

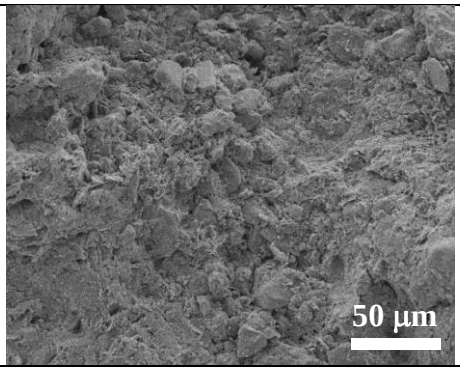

2500x

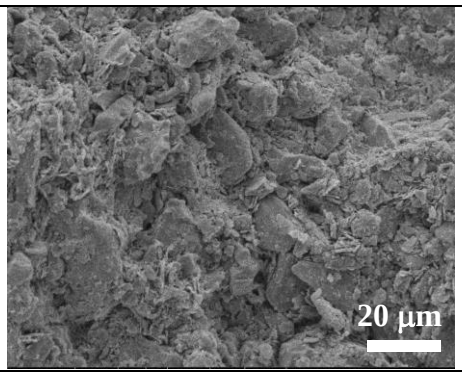

5000x

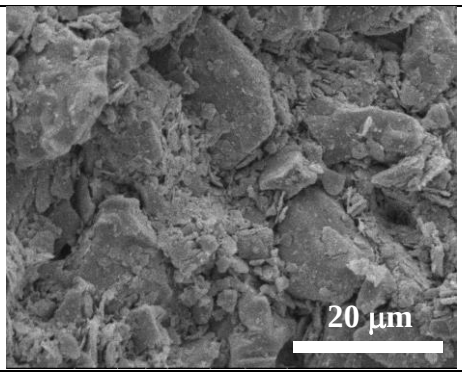

C specimen 1 – Point 5

600x

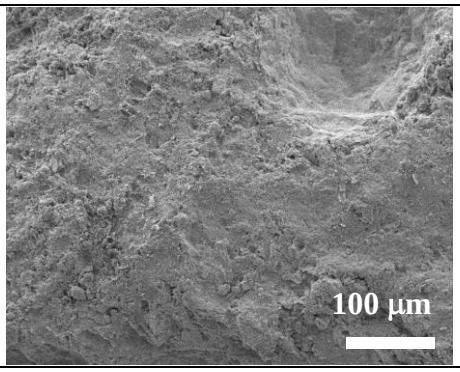

1200x

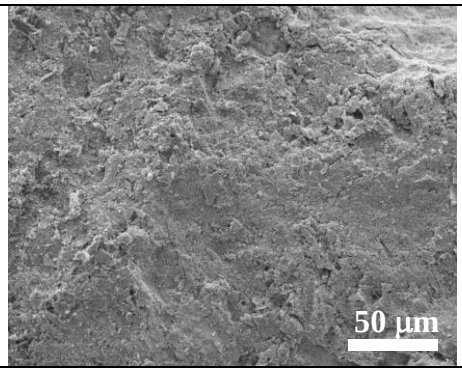

2500x

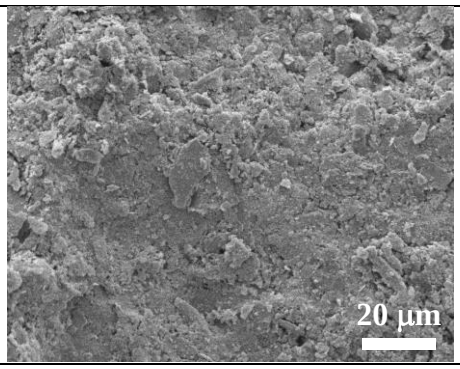

5000x

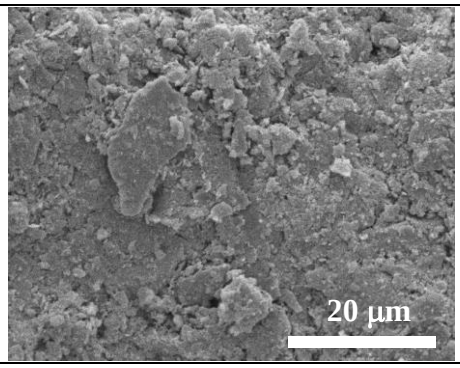

C specimen 2 – Point 1

600x

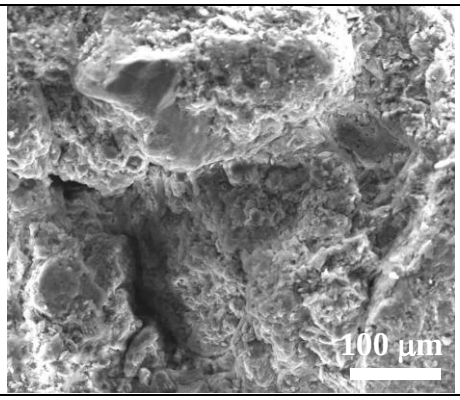

1200x

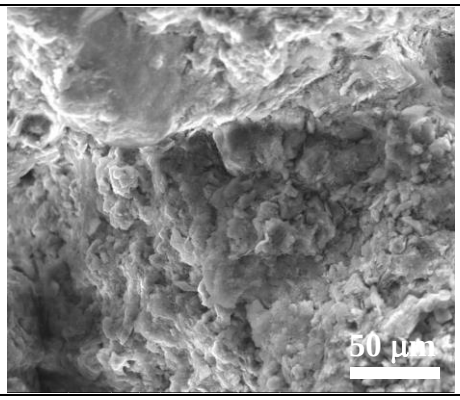

2500x

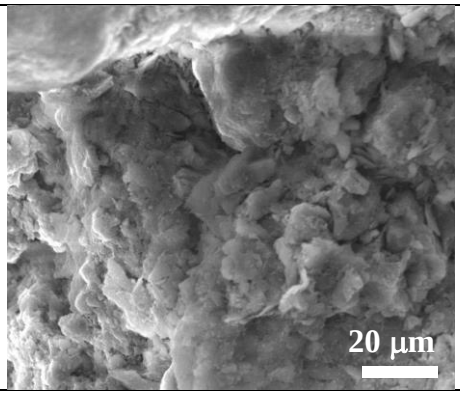

5000x

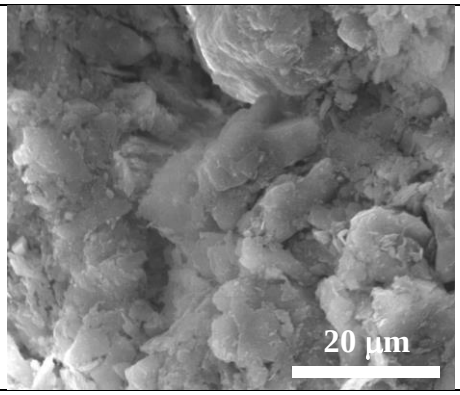

C specimen 2 – Point 2

600x

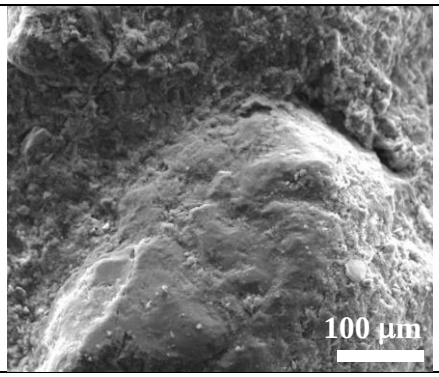

1200x

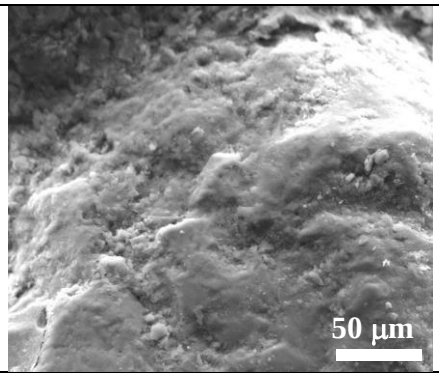

2500x

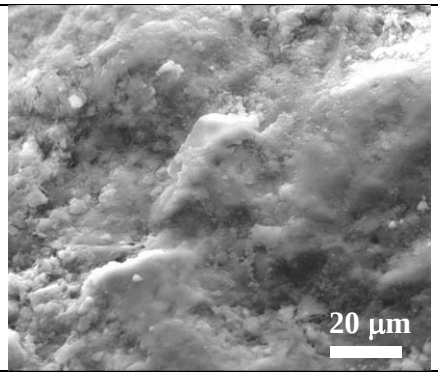

5000x

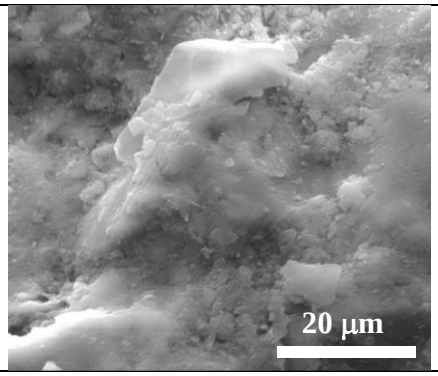

C specimen 2 – Point 3

600x

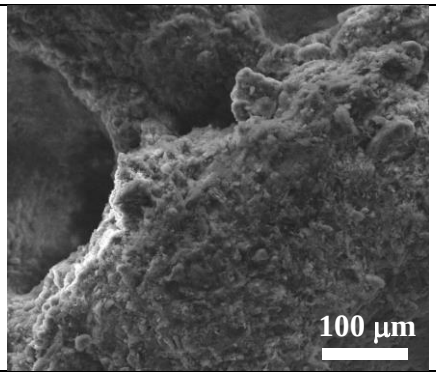

1200x

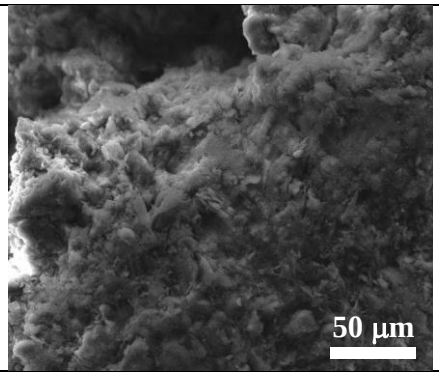

2500x

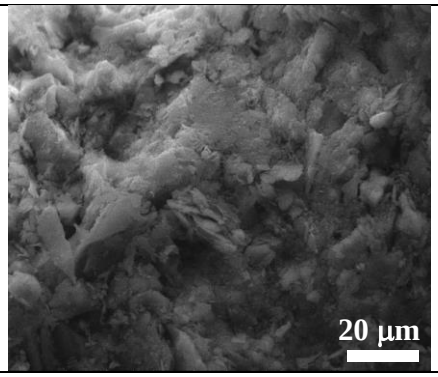

5000x

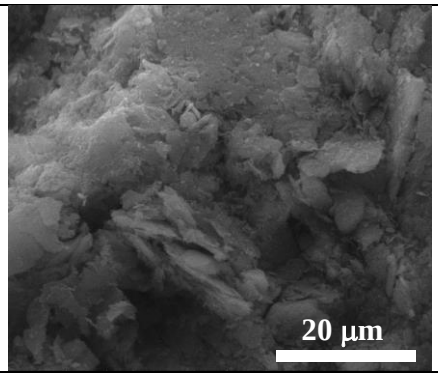

C specimen 2 – Point 4			
600x	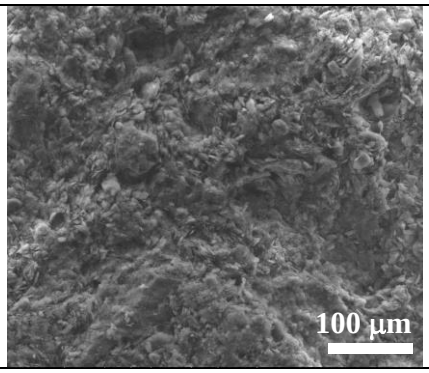	1200x	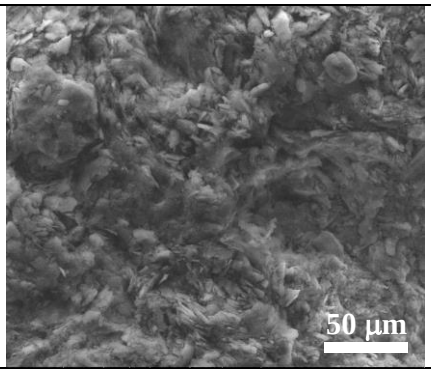
2500x	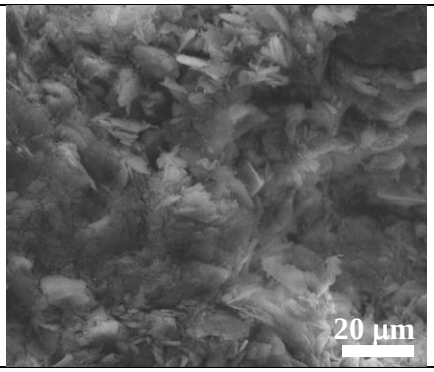	5000x	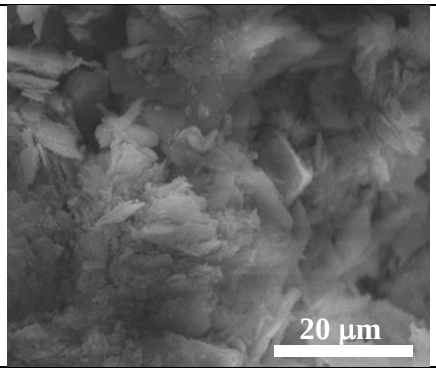

C specimen 2 – Point 5			
600x	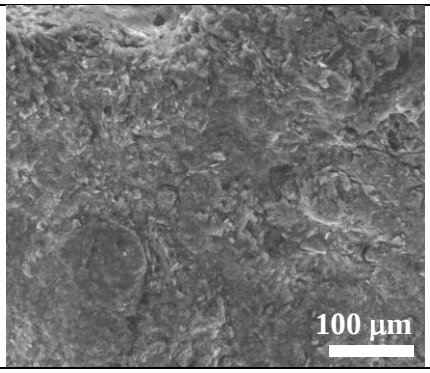	1200x	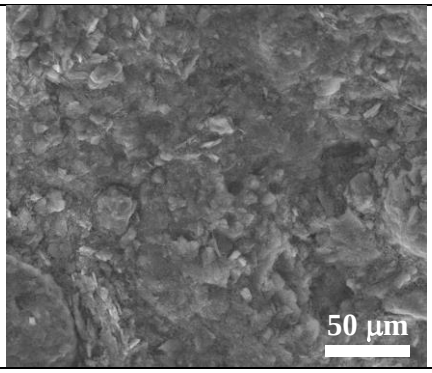
2500x	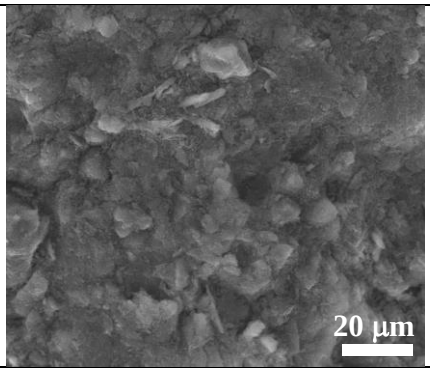	5000x	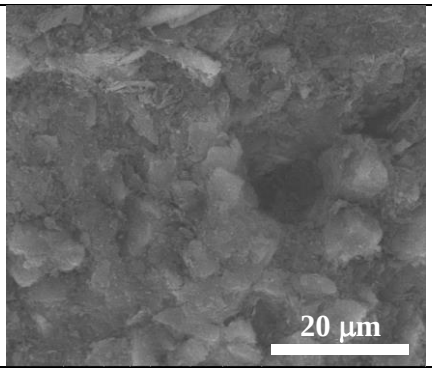

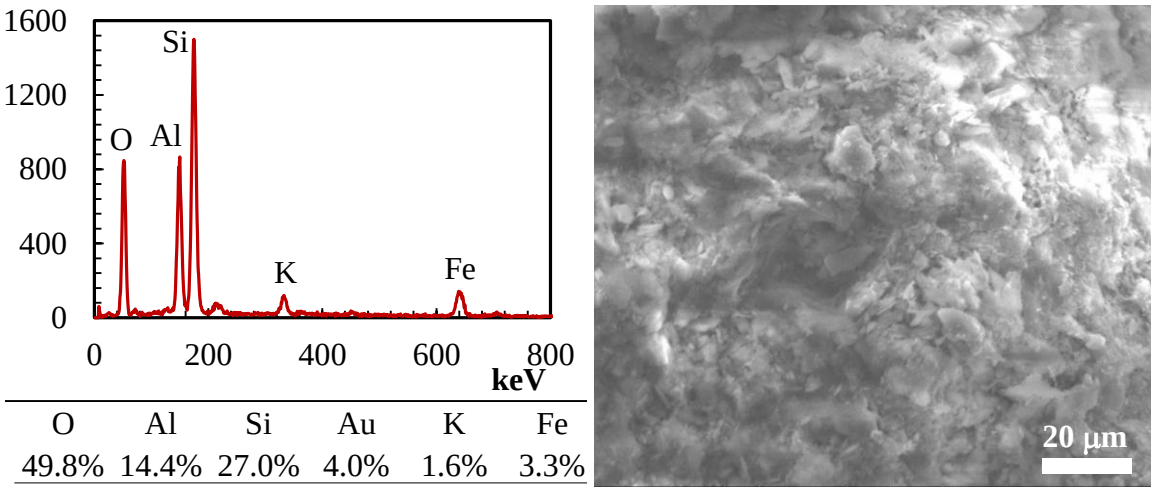

O	Al	Si	Au	K	Fe
49.8%	14.4%	27.0%	4.0%	1.6%	3.3%

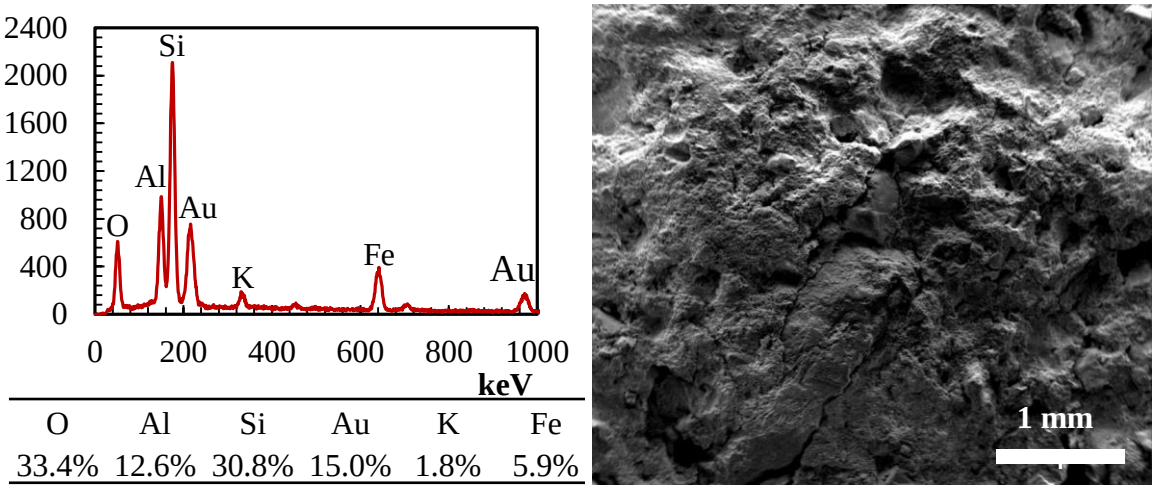

O	Al	Si	Au	K	Fe
33.4%	12.6%	30.8%	15.0%	1.8%	5.9%

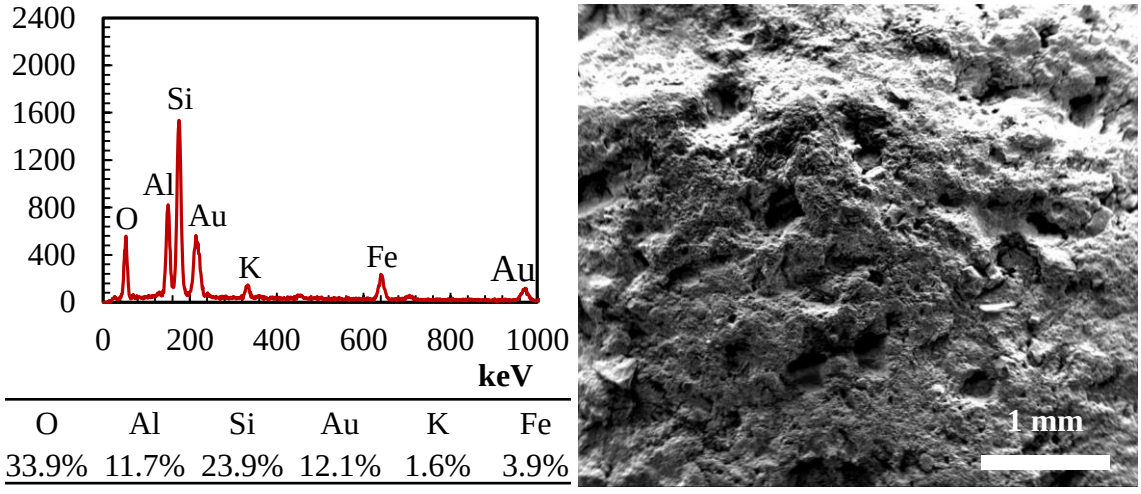

O	Al	Si	Au	K	Fe
33.9%	11.7%	23.9%	12.1%	1.6%	3.9%

Figure D.7 EDX analysis and SEM micrographs for C specimen.

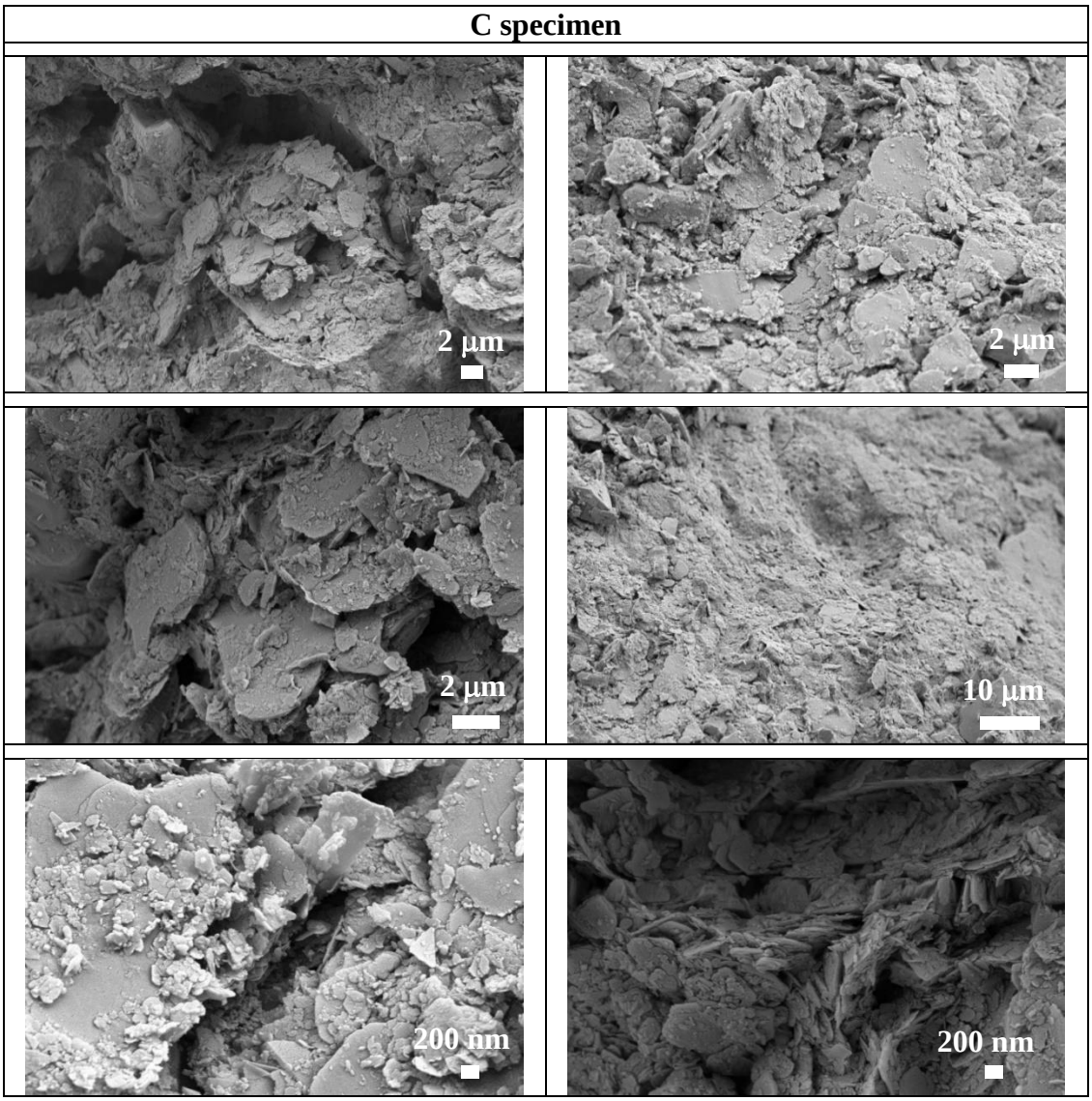

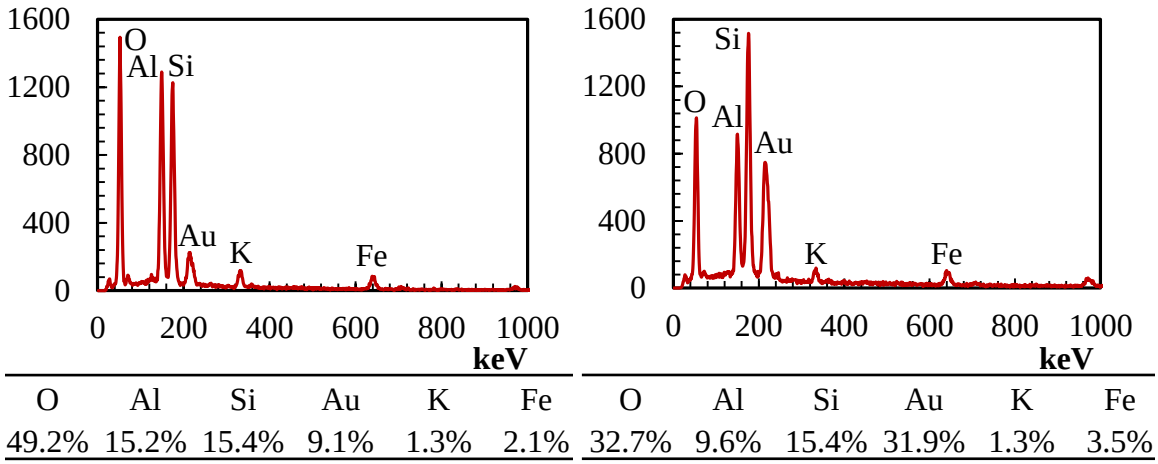

O	Al	Si	Au	K	Fe
49.2%	15.2%	15.4%	9.1%	1.3%	2.1%

O	Al	Si	Au	K	Fe
32.7%	9.6%	15.4%	31.9%	1.3%	3.5%

Figure D.8 EDX analysis for C specimen.

CS6 specimen 1 – Point 1

600x

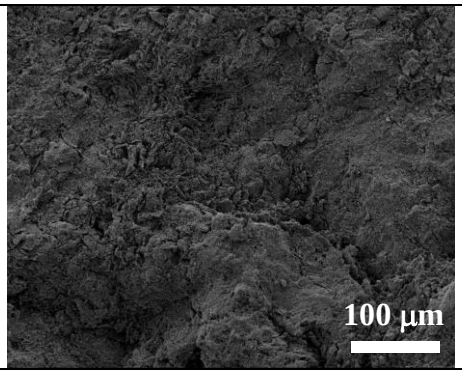

1200x

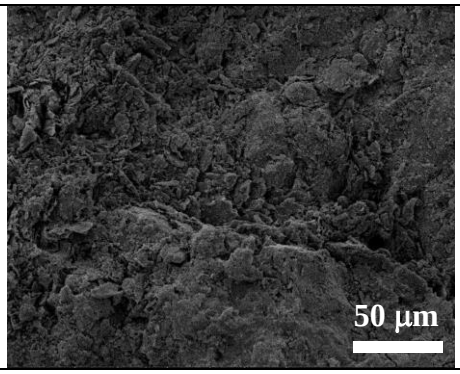

2500x

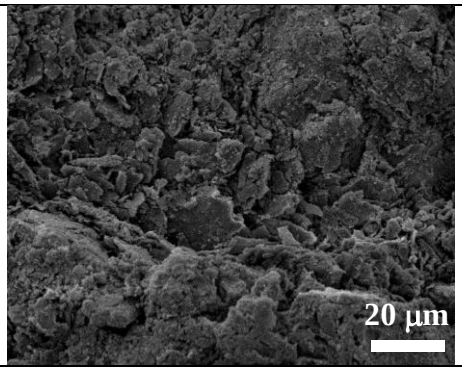

5000x

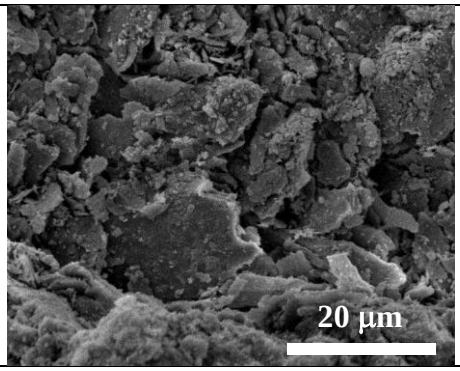

CS6 specimen 1 – Point 2

600x

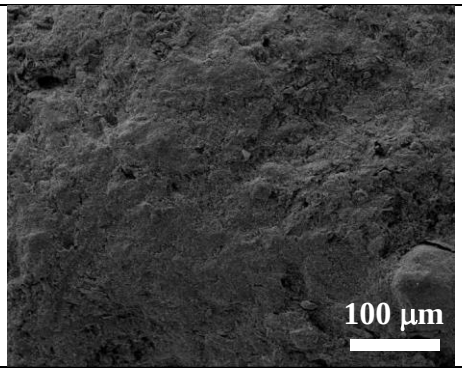

1200x

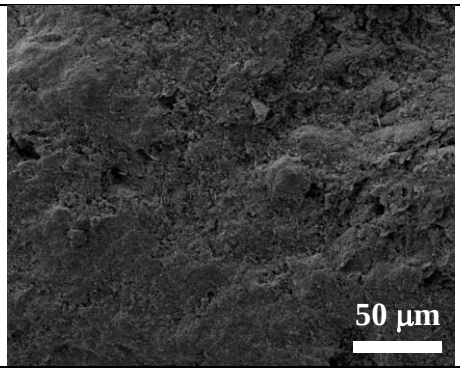

2500x

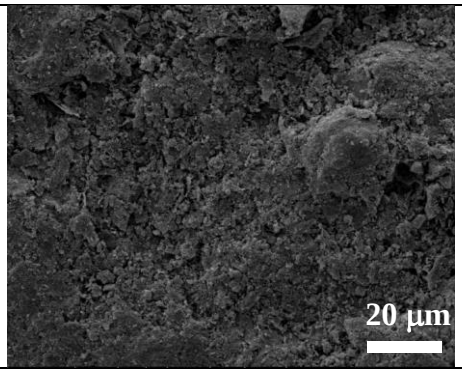

5000x

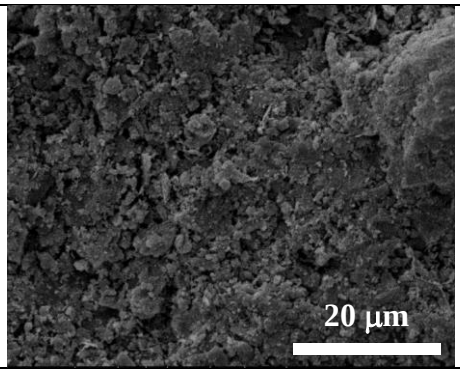

CS6 specimen 1 – Point 3

600x

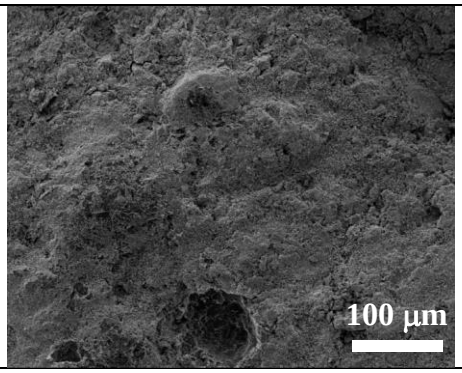

1200x

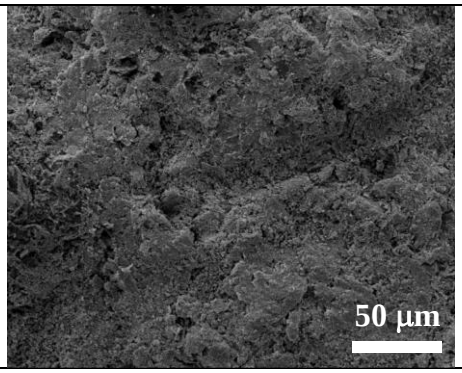

2500x

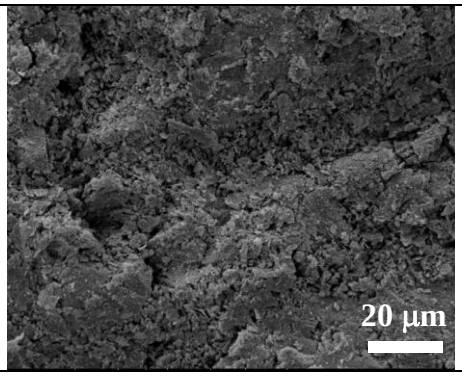

5000x

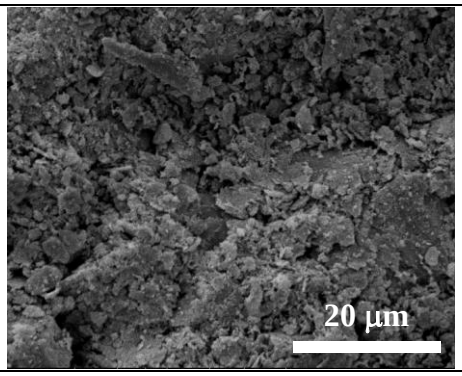

CS6 specimen 1 – Point 4

600x

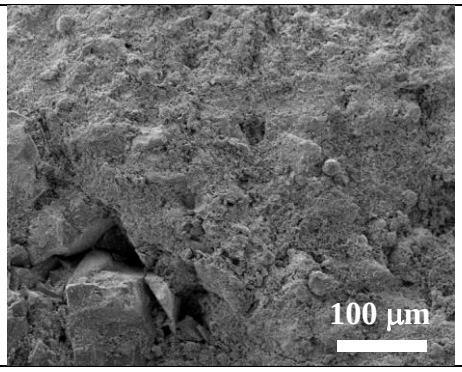

1200x

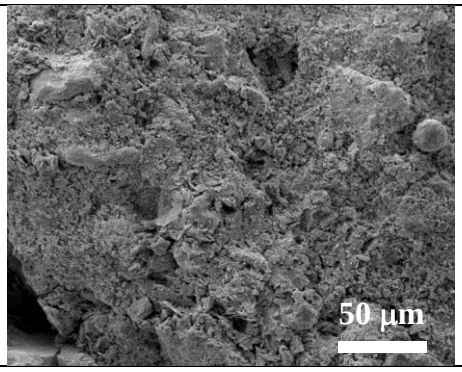

2500x

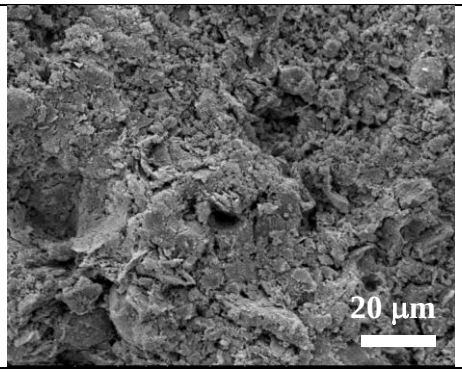

5000x

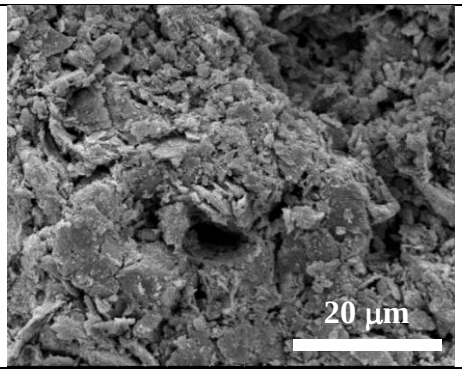

CS6 specimen 1 – Point 5

600x

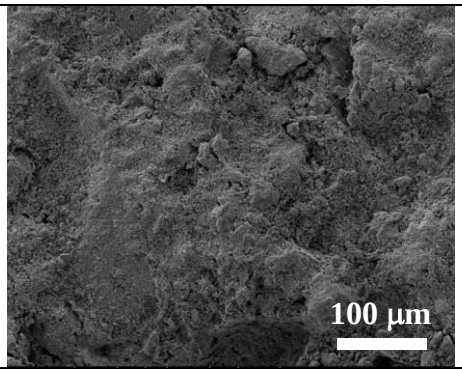

1200x

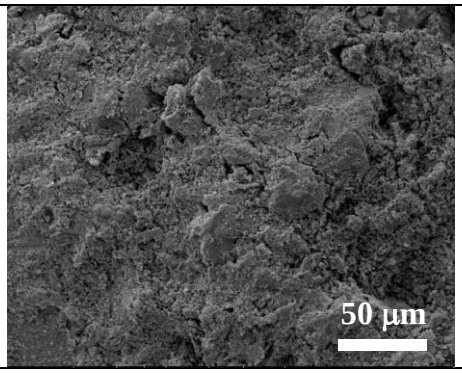

2500x

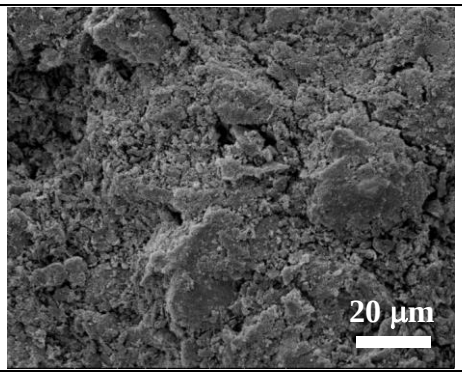

5000x

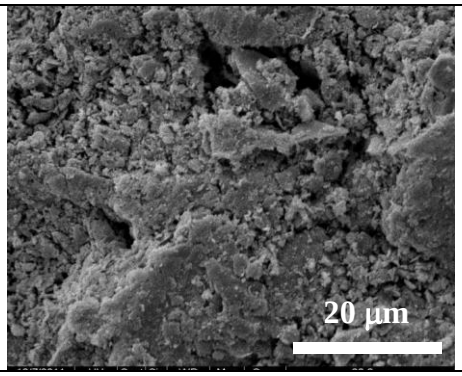

CS6 specimen 2 – Point 1

600x

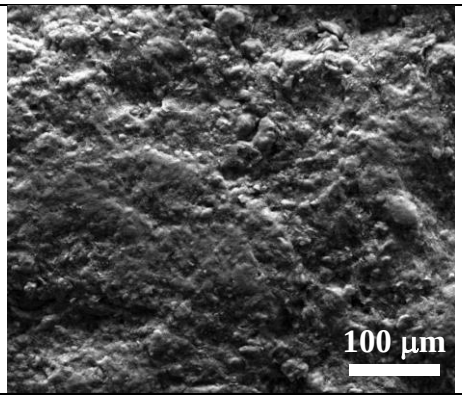

1200x

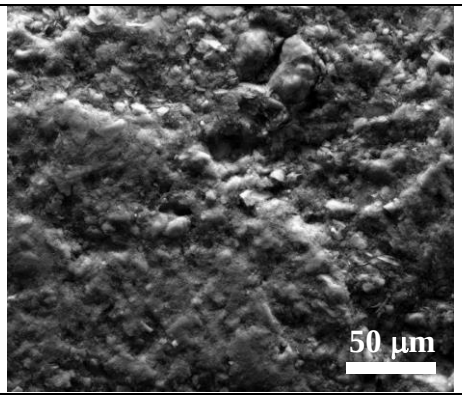

2500x

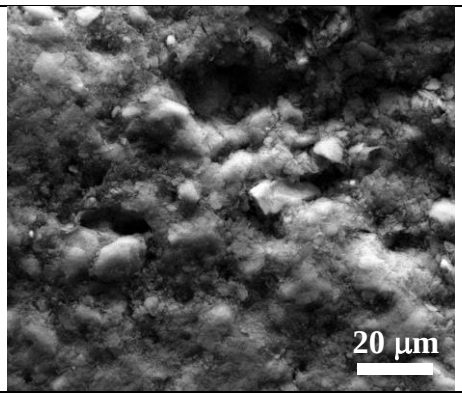

5000x

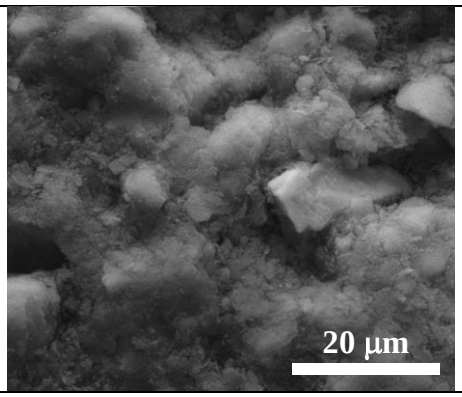

CS6 specimen 2 – Point 2

600x

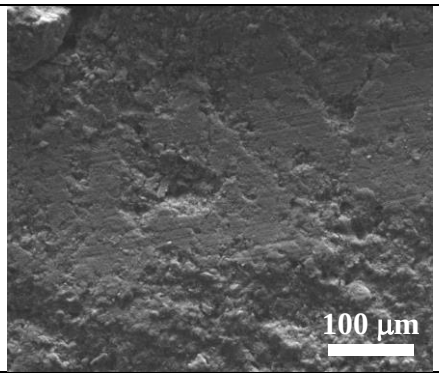

1200x

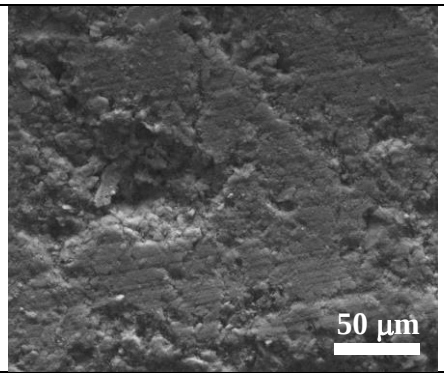

2500x

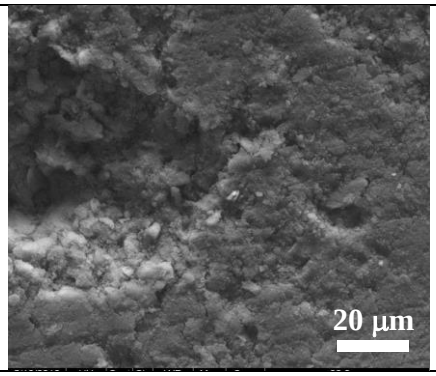

5000x

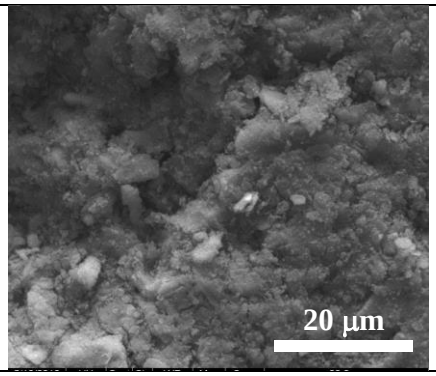

CS6 specimen 2 – Point 3

600x

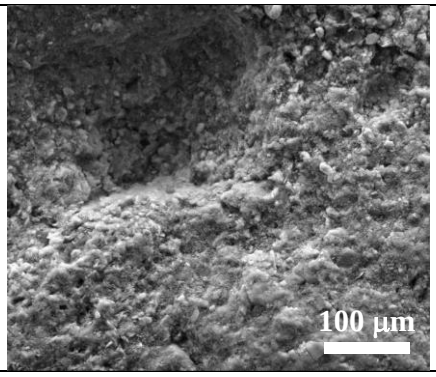

1200x

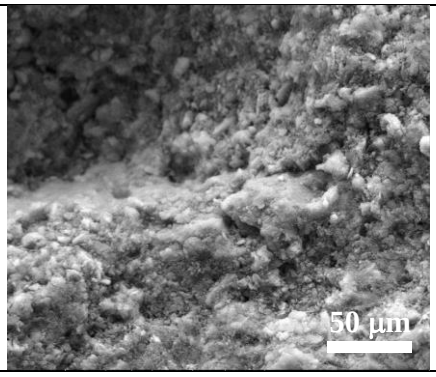

2500x

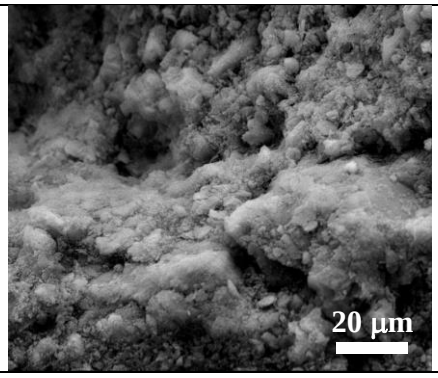

5000x

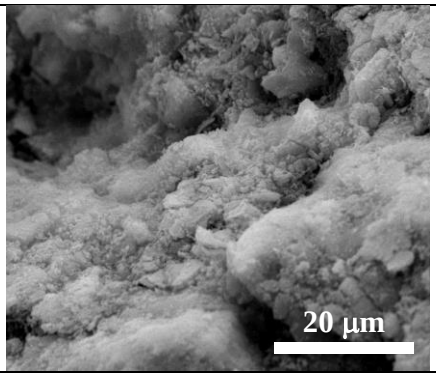

CS6 specimen 2 – Point 4

600x

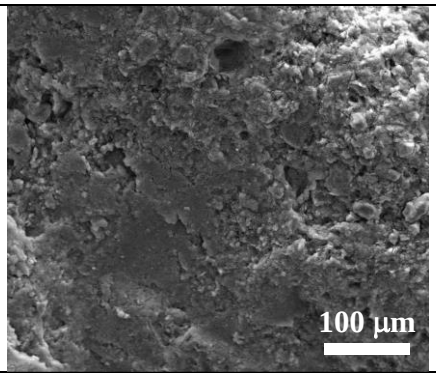

1200x

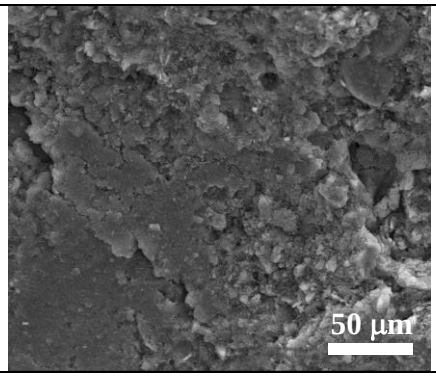

2500x

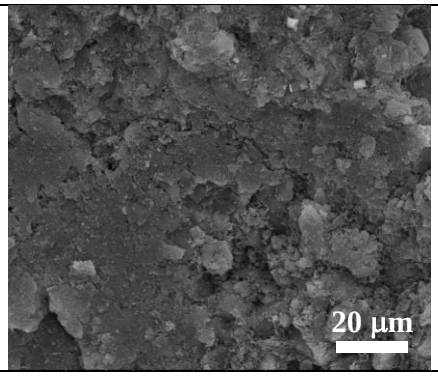

5000x

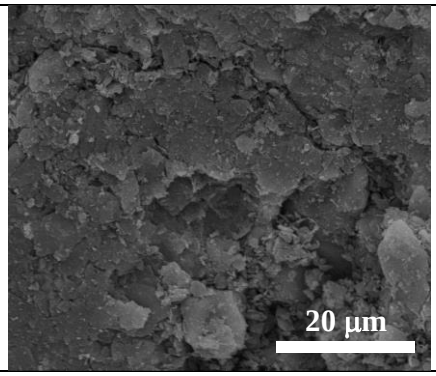

CS6 specimen 3 – Point 1

600x

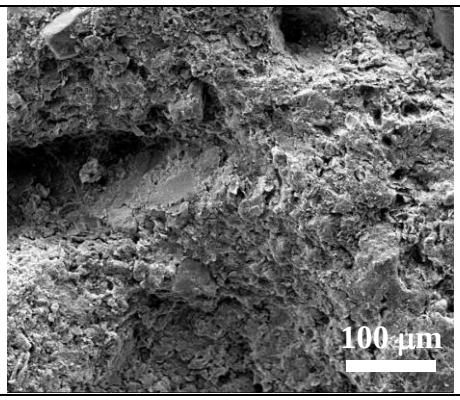

1200x

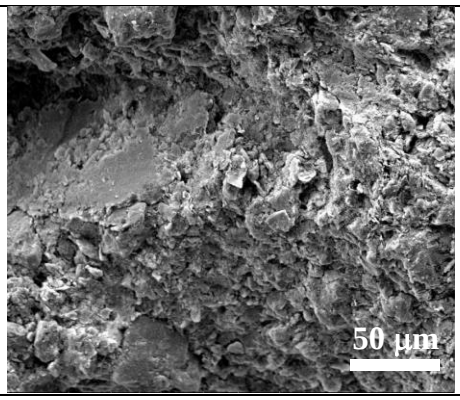

2500x

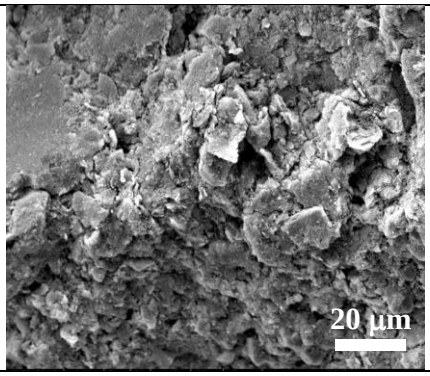

5000x

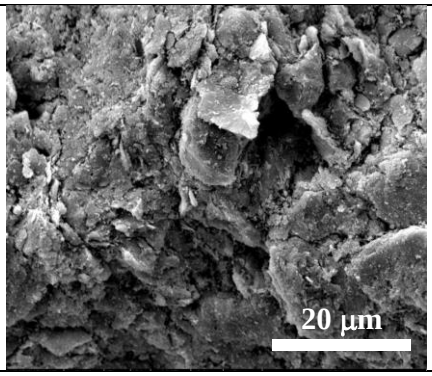

CS6 specimen 3 – Point 2			
600x	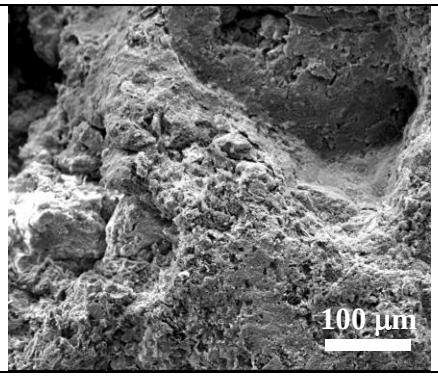	1200x	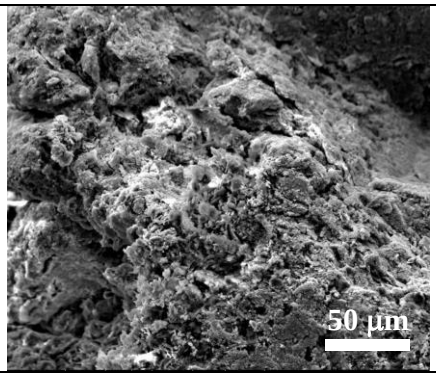
2500x	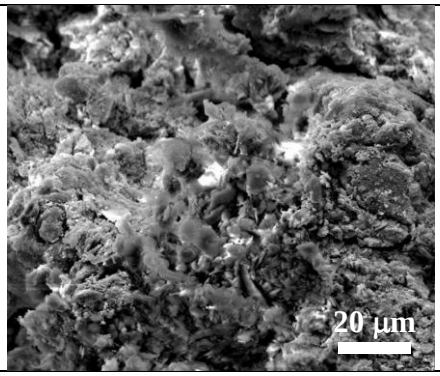	5000x	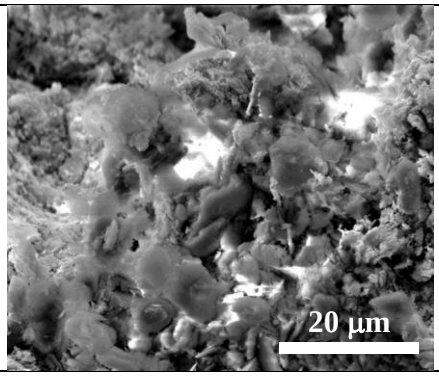

CS6 specimen 3 – Point 3			
600x	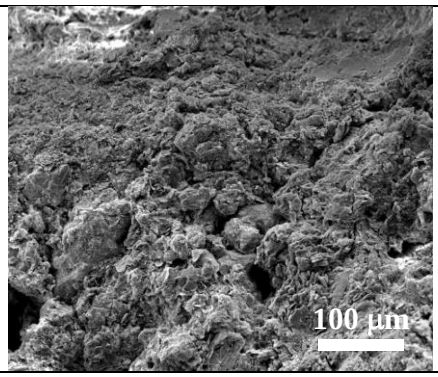	1200x	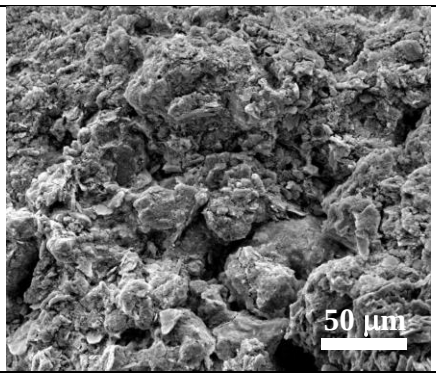
2500x	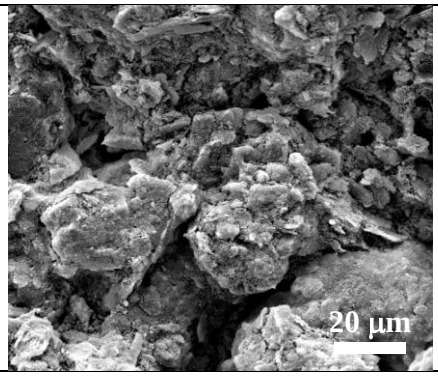	5000x	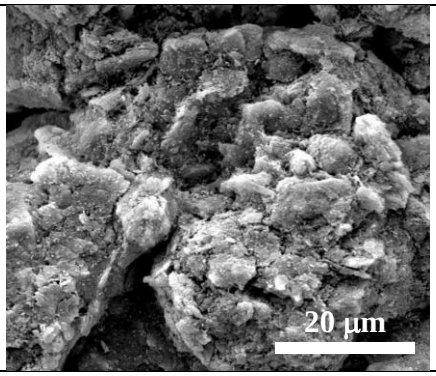

CS6 specimen 3 – Point 4			
600x	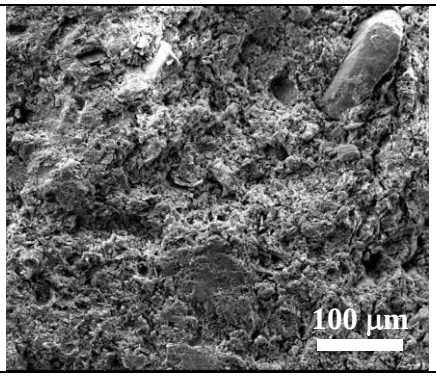	1200x	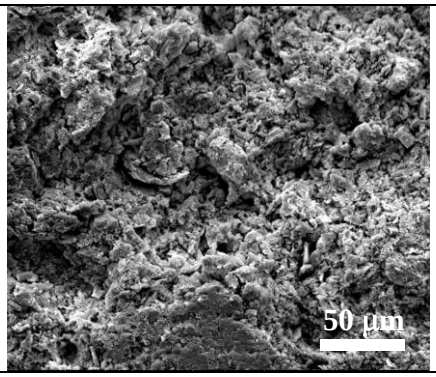
2500x	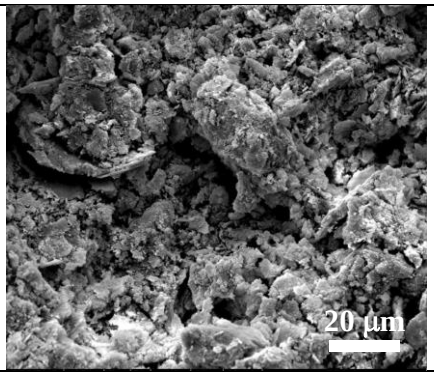	5000x	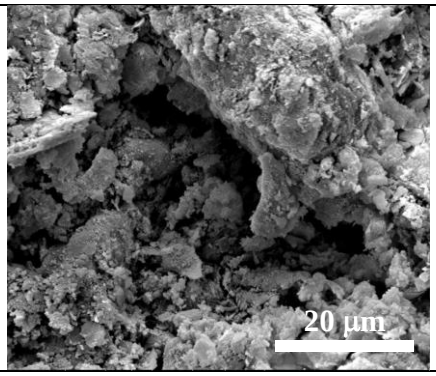

CS6 specimen 3 – Point 5			
600x	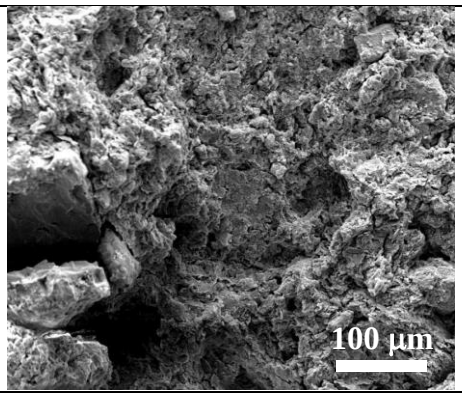	1200x	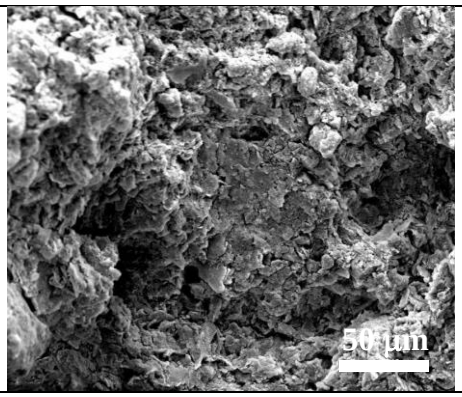
2500x	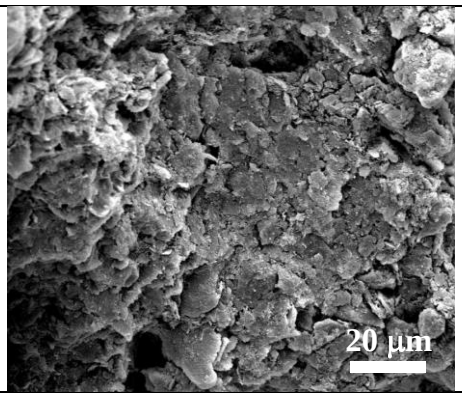	5000x	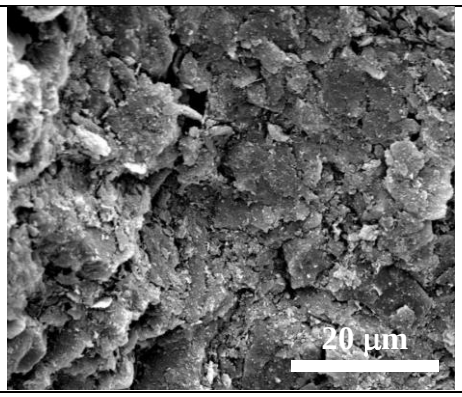

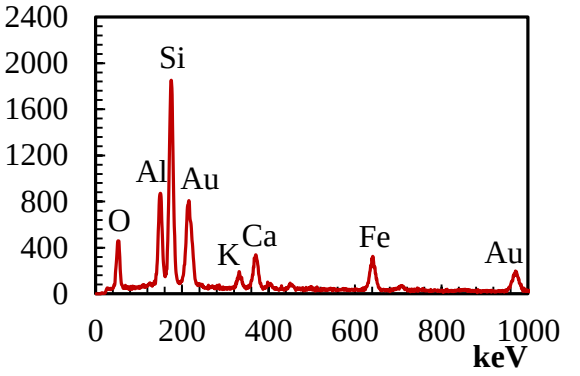

O	Al	Si	Ca	K	Fe
37.5%	14.9%	34.6%	4.2%	2.0%	5.7%

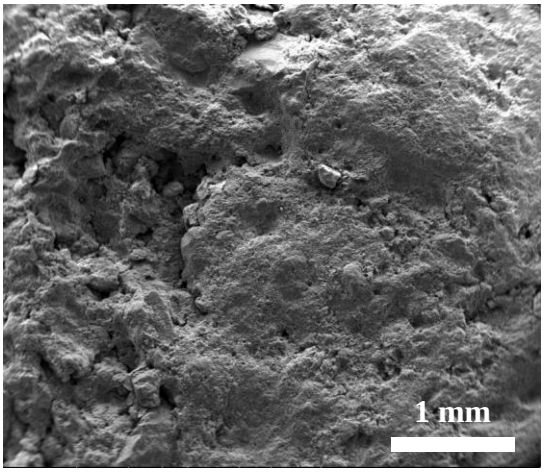

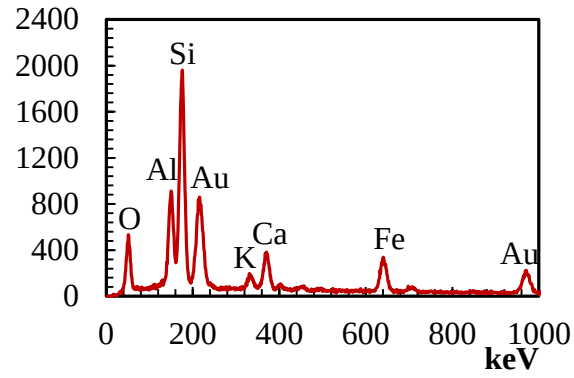

O	Al	Si	Ca	K	Fe
39.7%	13.8%	35.0%	4.1%	1.8%	5.6%

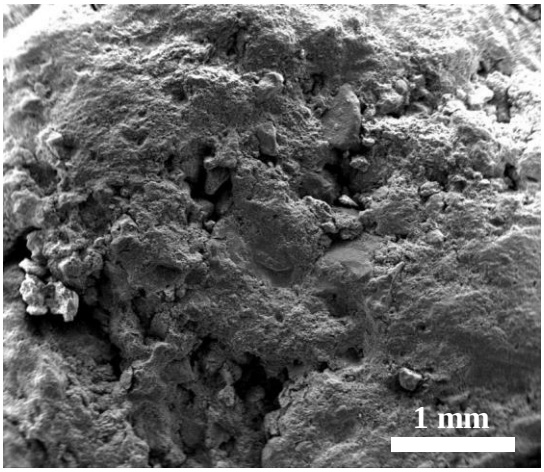

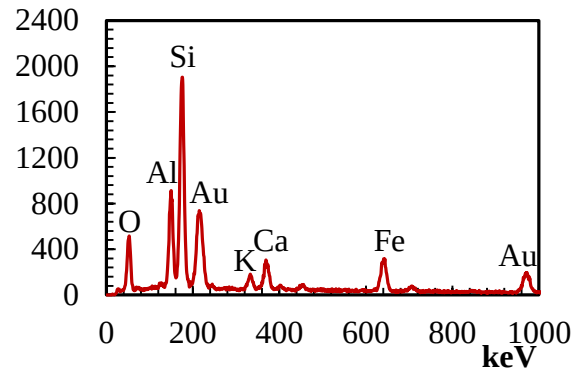

O	Al	Si	Ca	K	Fe
37.0%	12.3%	28.2%	2.7%	1.5%	4.9%

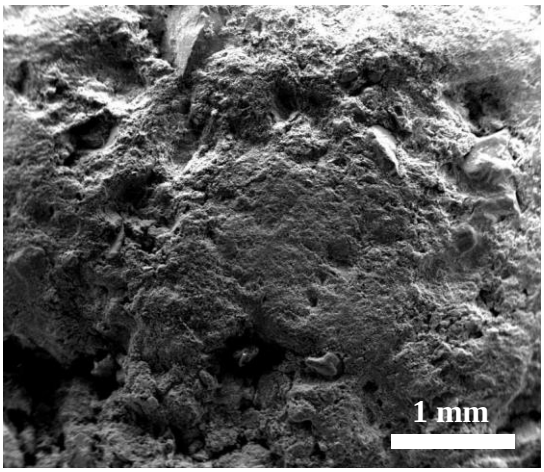

Figure D.9 EDX analysis and SEM micrographs for CS6 specimens.

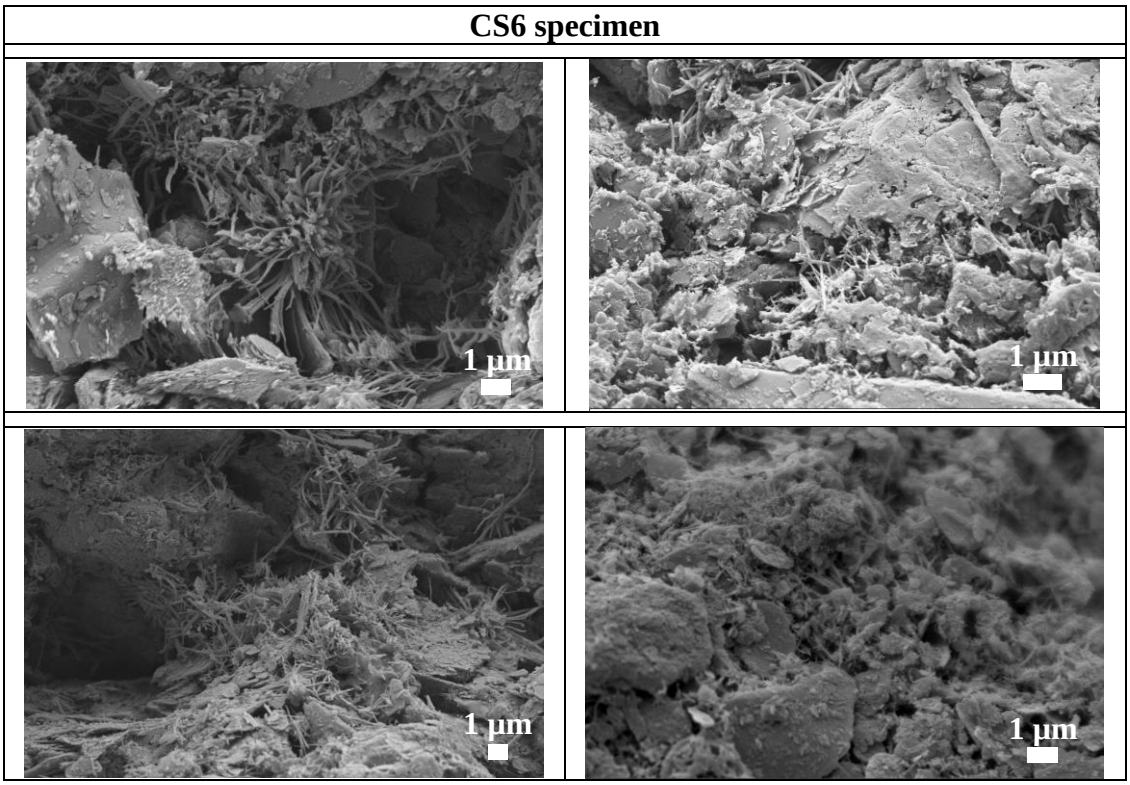

Figure D.10 SEM micrographs for CS6 specimens.

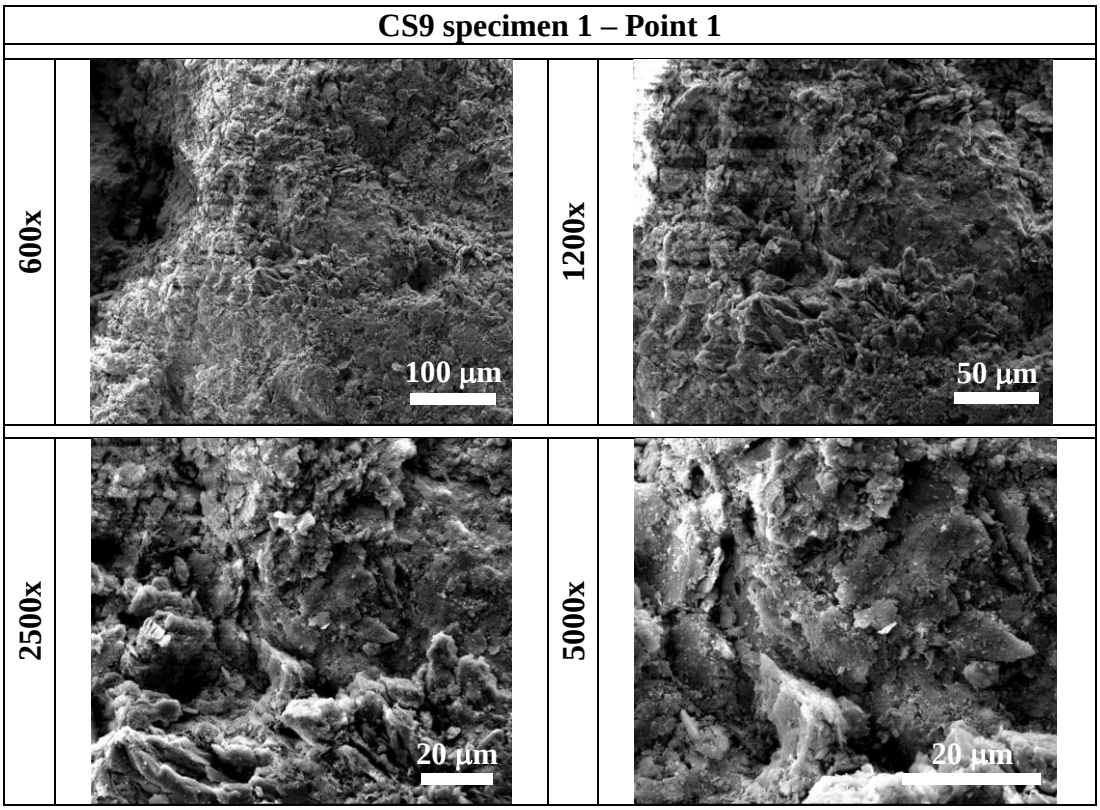

CS9 specimen 1 – Point 2			
600x	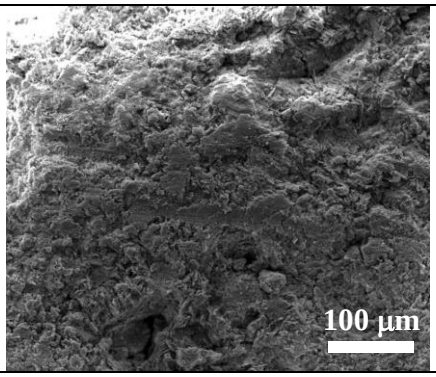	1200x	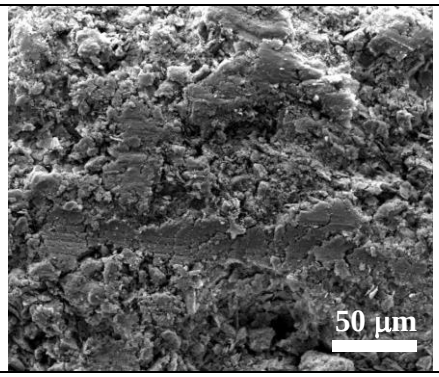
2500x	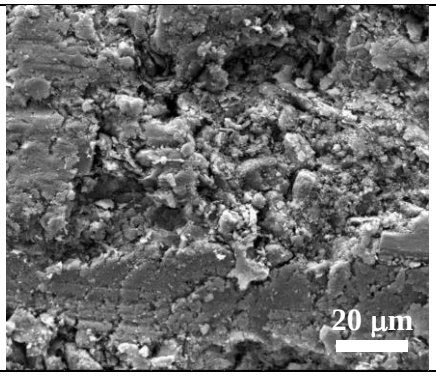	5000x	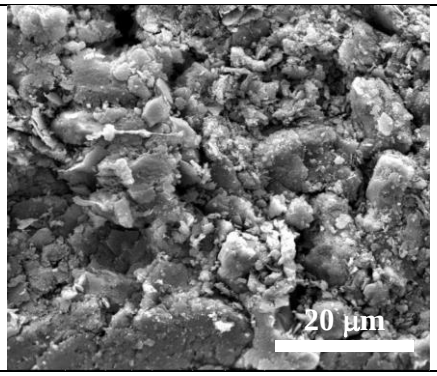

CS9 specimen 1 – Point 3			
600x	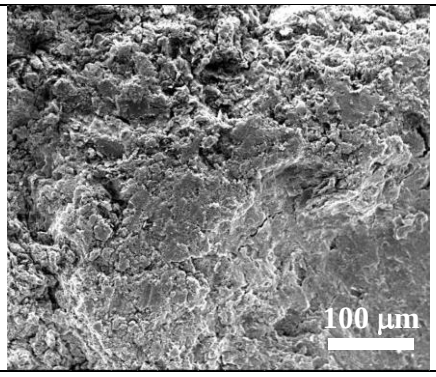	1200x	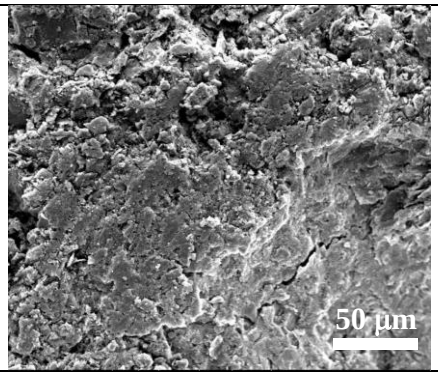
2500x	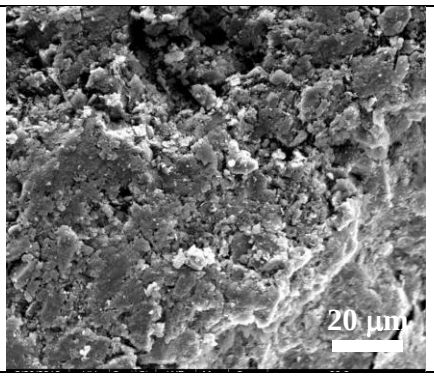	5000x	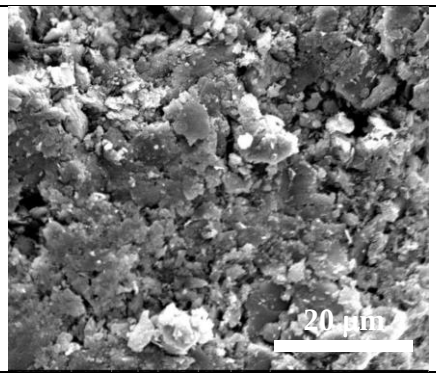

CS9 specimen 1 – Point 4			
600x	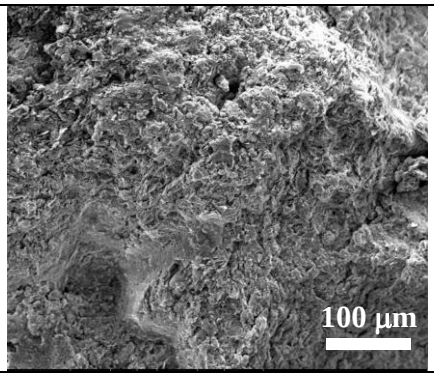	1200x	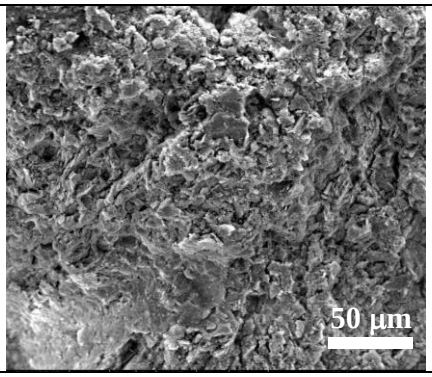
2500x	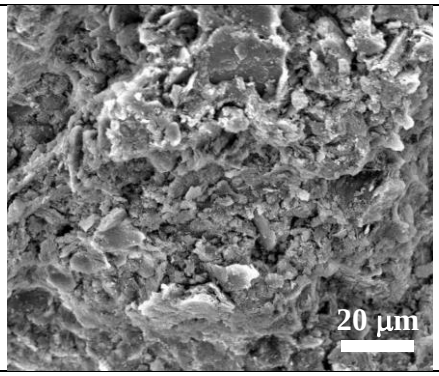	5000x	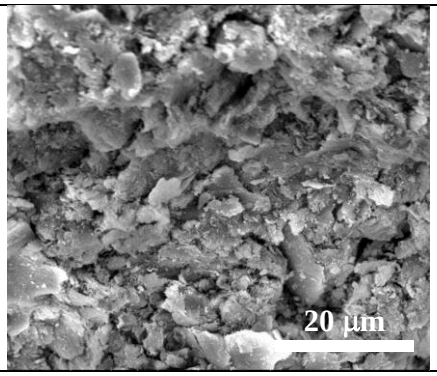

CS9 specimen 1 – Point 5			
600x	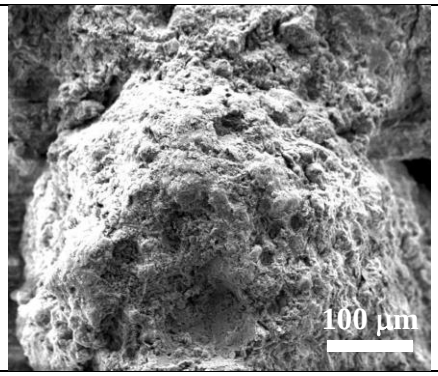	1200x	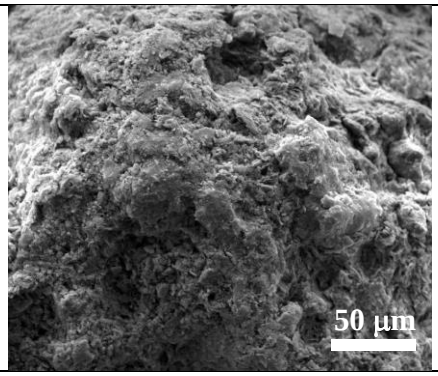
2500x	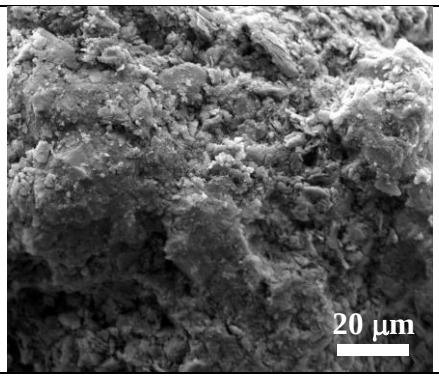	5000x	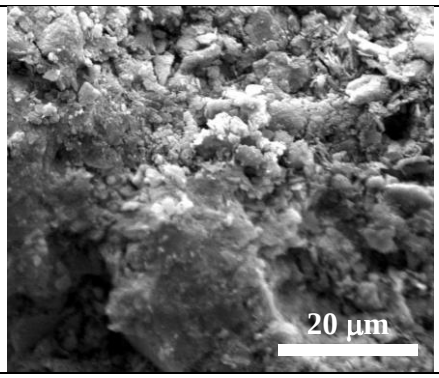

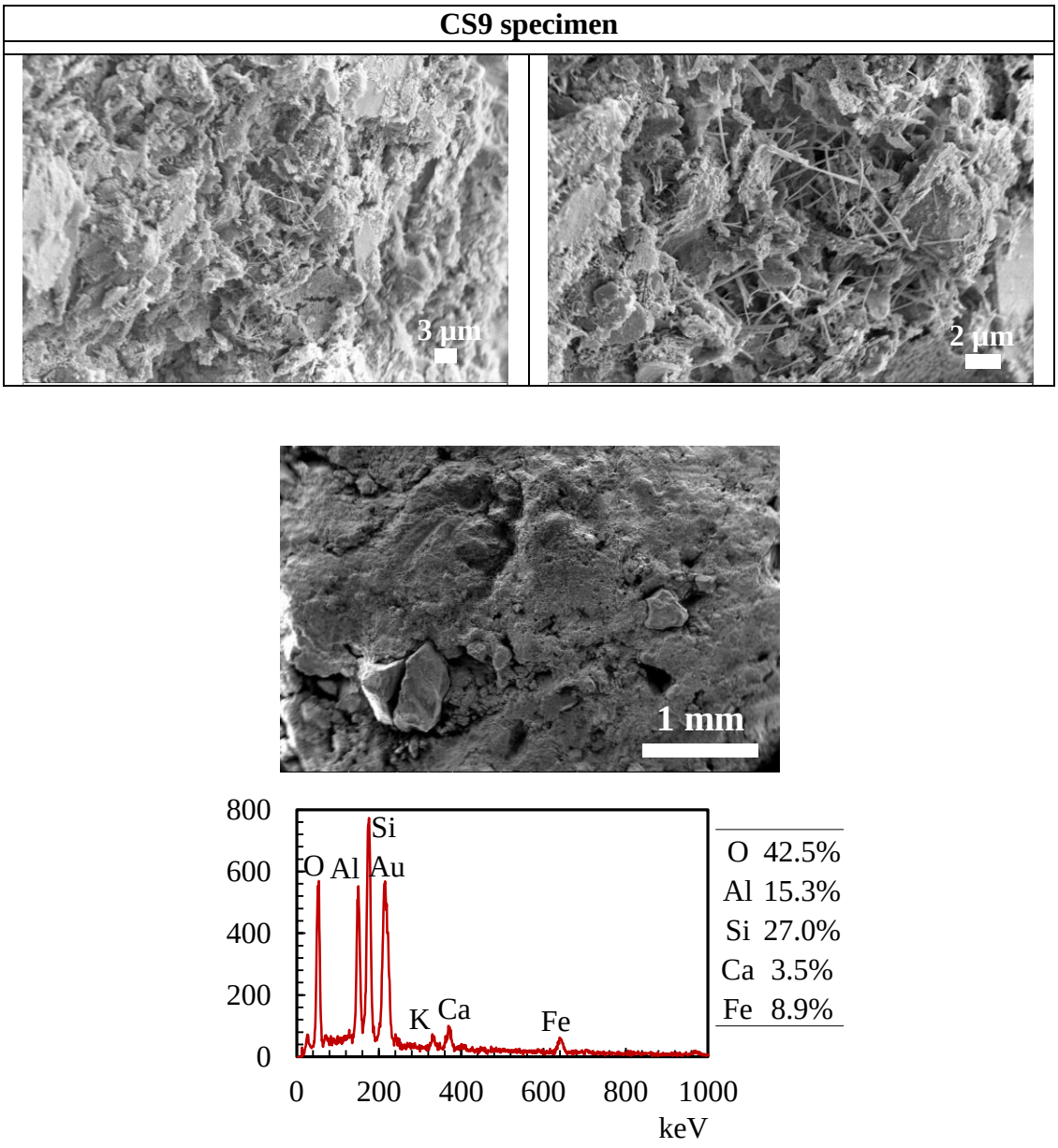

Figure D.11 EDX analysis and SEM micrographs for CS9 specimens.

APPENDIX E – SEM COMPRESSIVE STRENGTH CHARACTERIZATION

This appendix presents the load-displacement curves for the prims and wallettes that were characterized in uniaxial compression. Figure E.1 shows the nomenclature used for the LDTs that were mounted on prisms and wallette specimens.

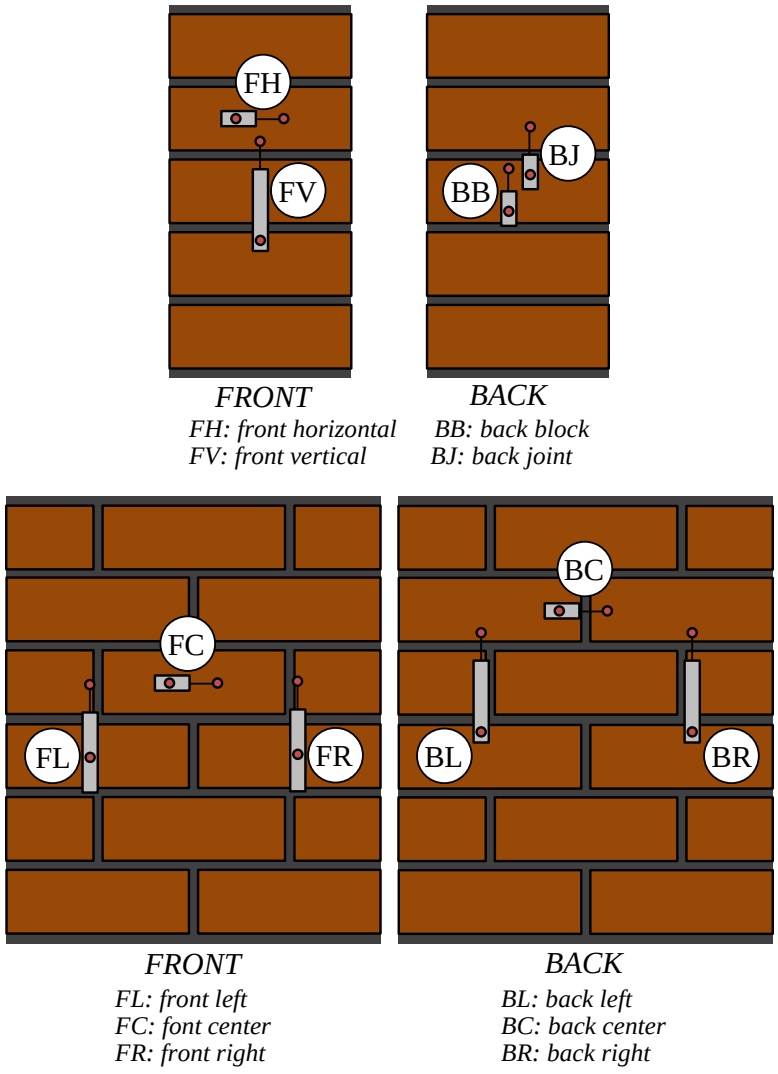

Figure E.1 Sensor location and nomenclature for prism and wallette specimens.

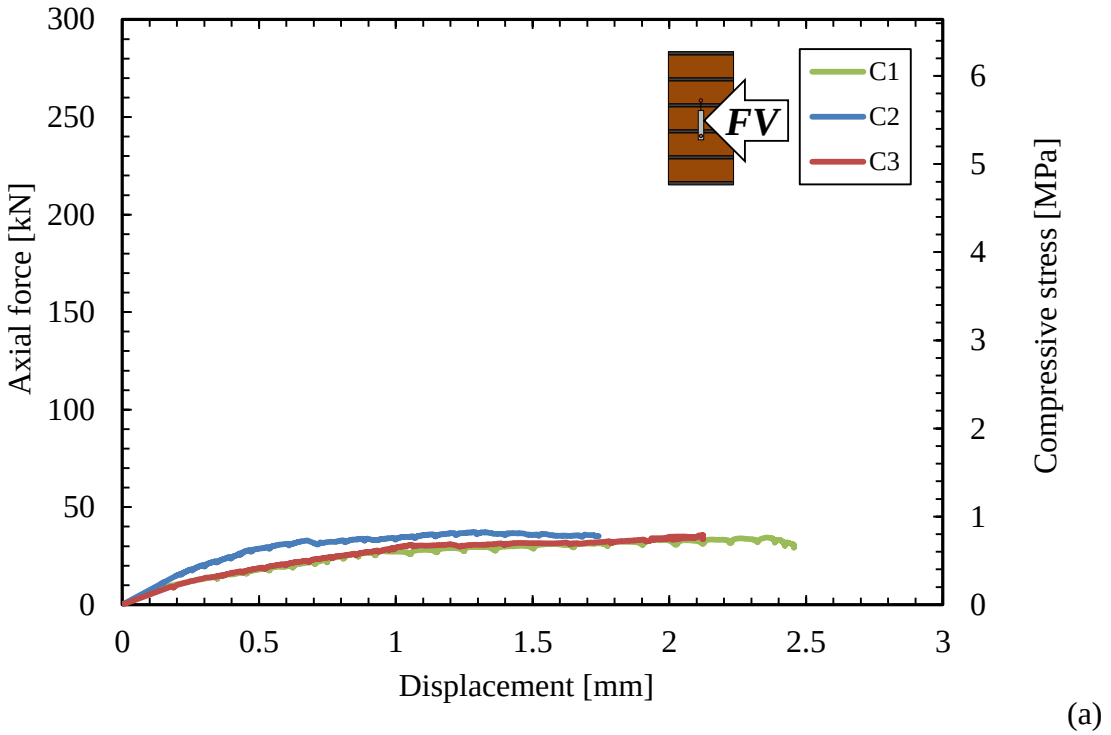

(a)

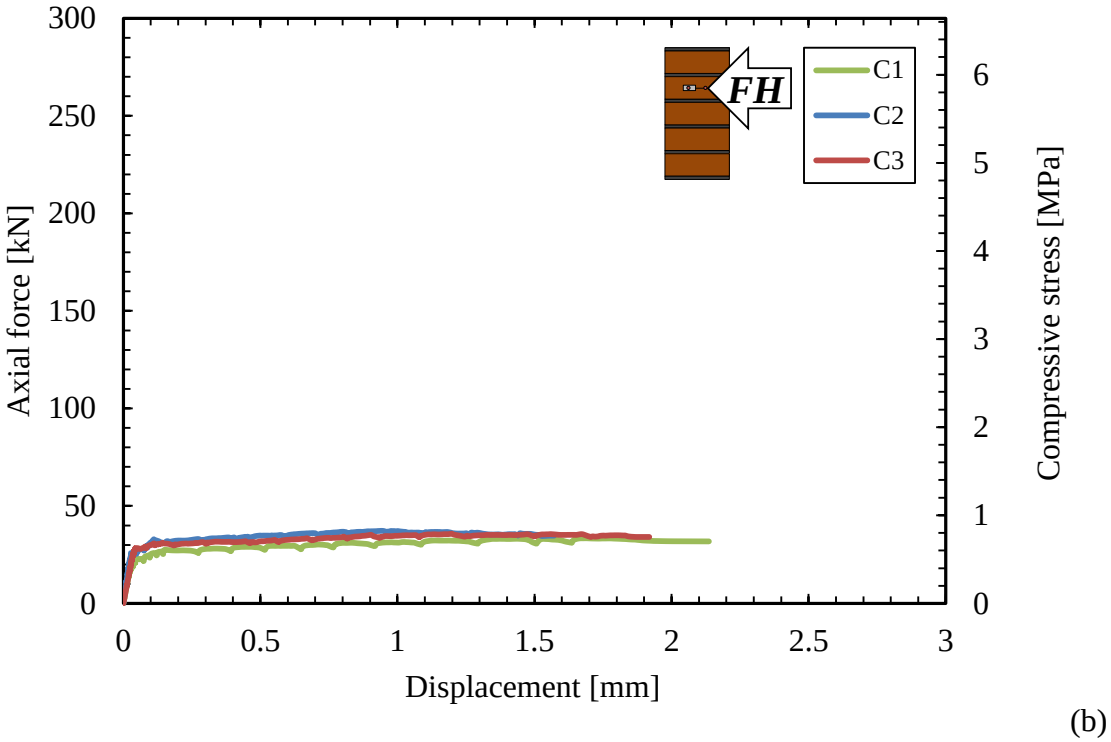

(b)

Figure E.2 Load-displacement curves from compression tests on prisms made with C blocks, front face sensors: (a) vertical, and (b) horizontal.

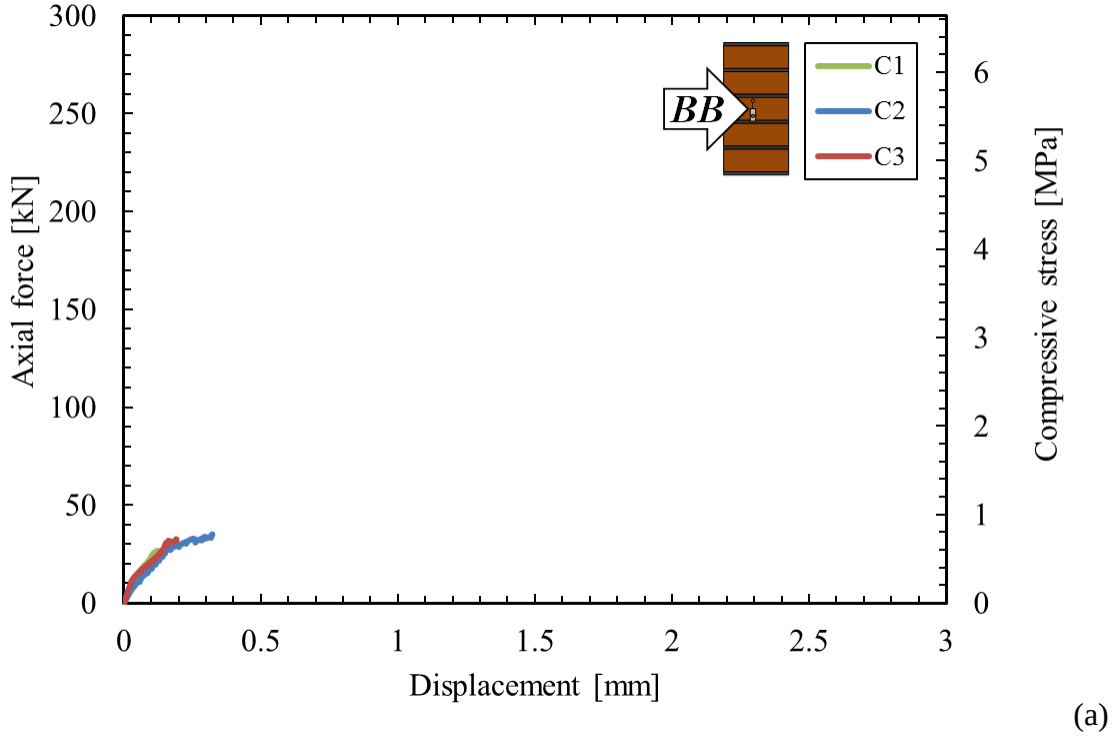

(a)

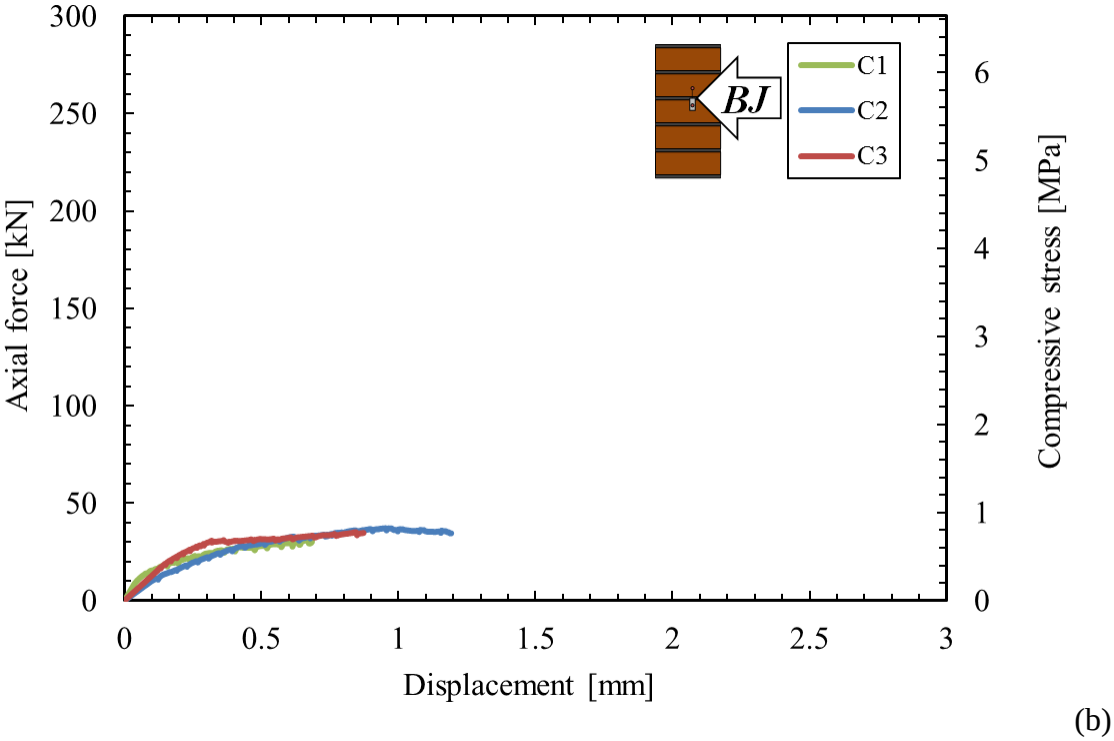

(b)

Figure E.3 Load-displacement curves from compression tests on prisms made with C blocks, back face sensors: (a) block, and (b) joint.

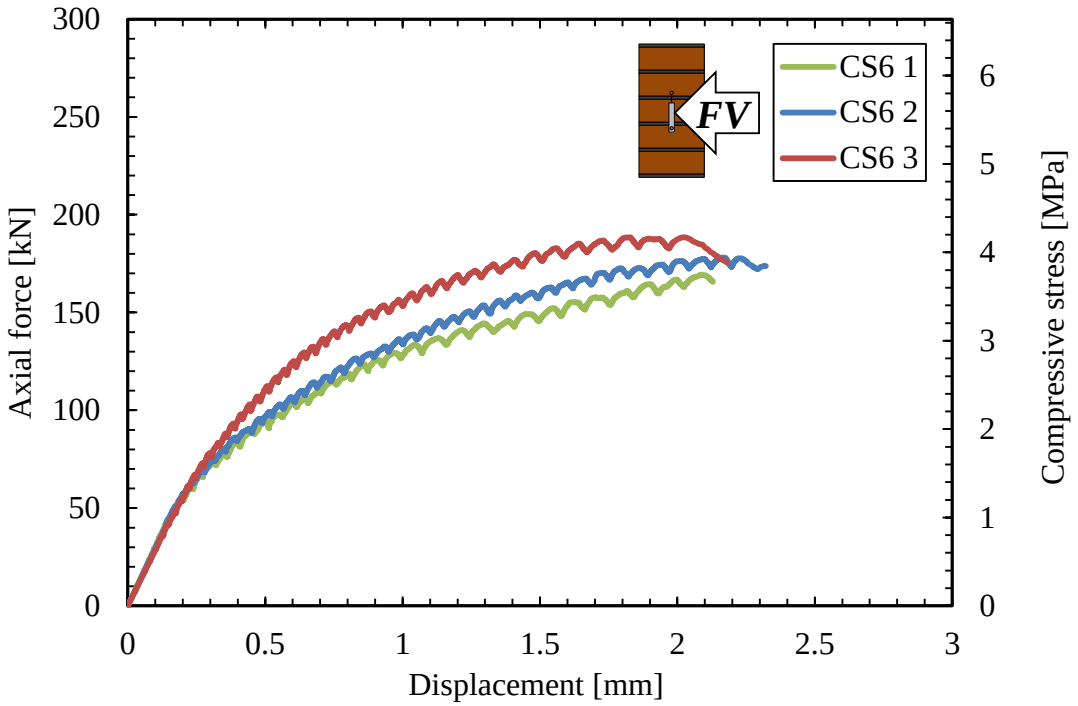

(a)

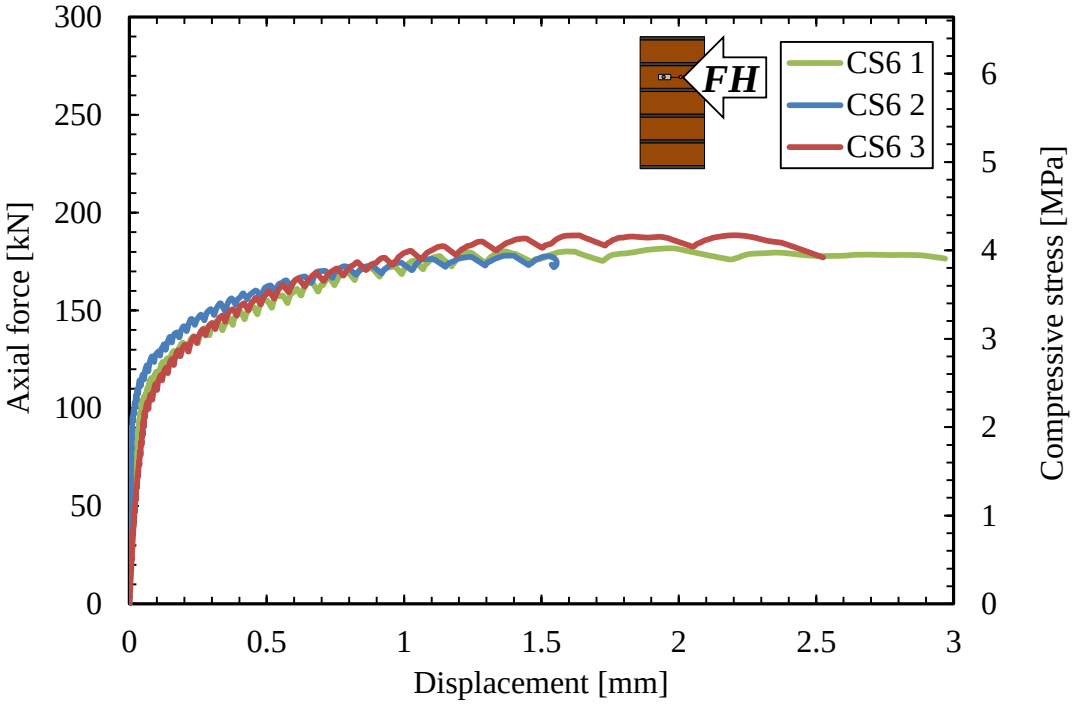

(b)

Figure E.4 Load-displacement curves from compression tests on prisms made with CS6 blocks, front face sensors: (a) vertical, and (b) horizontal.

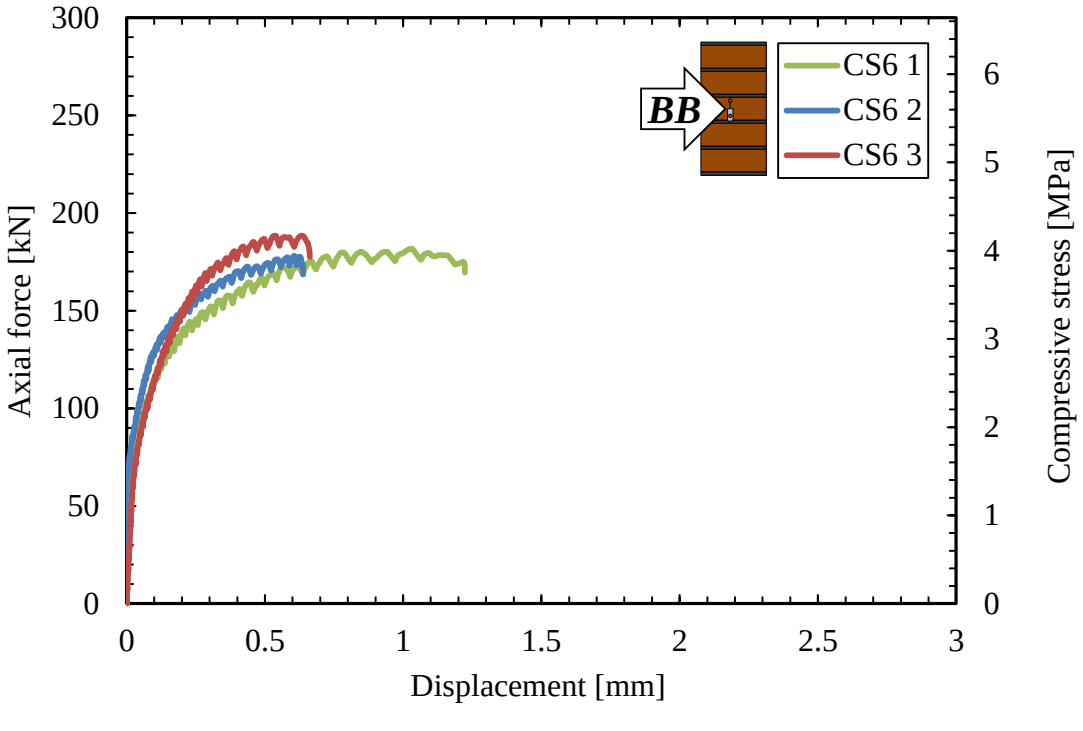

(a)

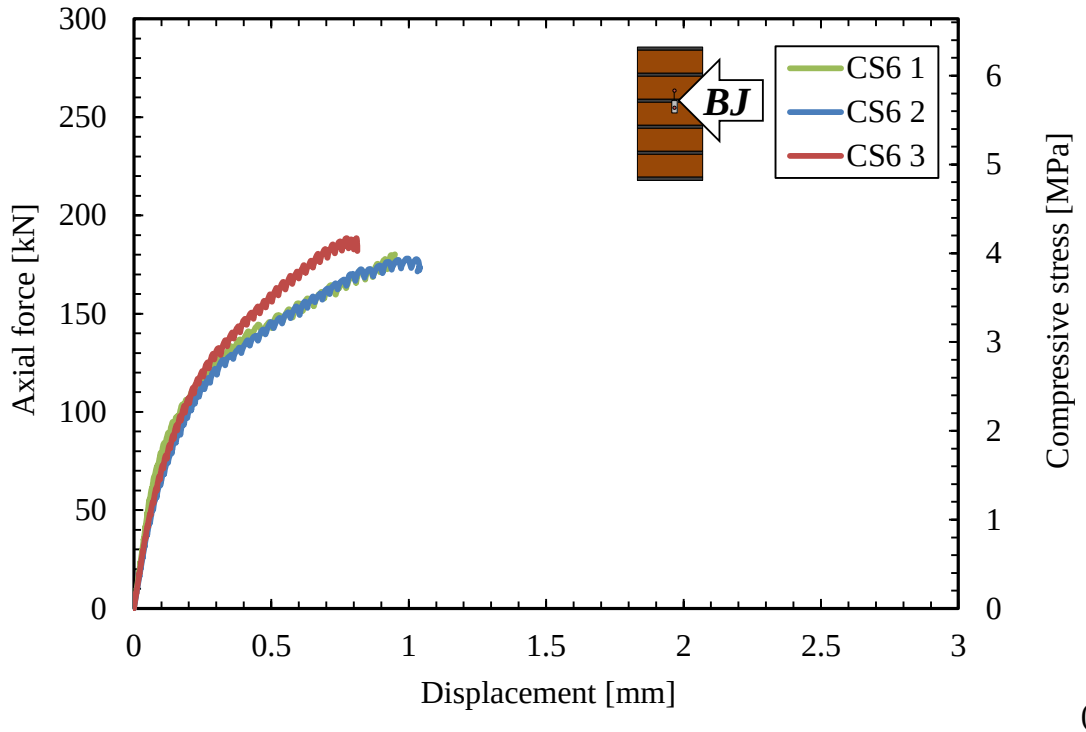

(b)

Figure E.5 Load-displacement curves from compression tests on prisms made with CS6 blocks, back face sensors: (a) block, and (b) joint.

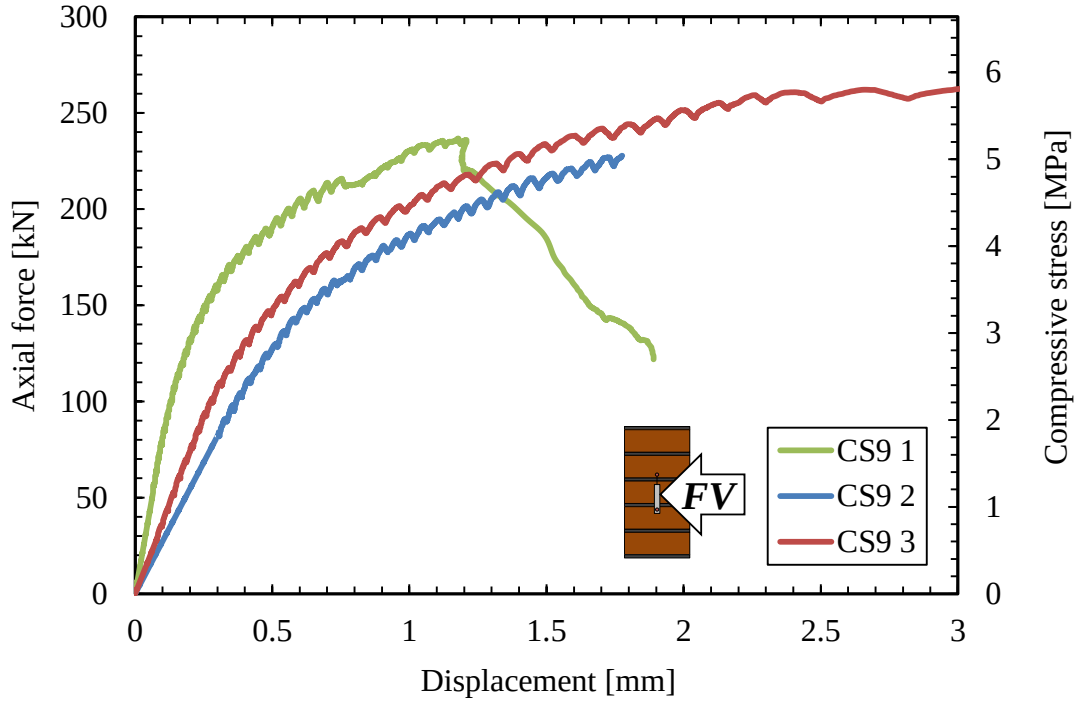

(a)

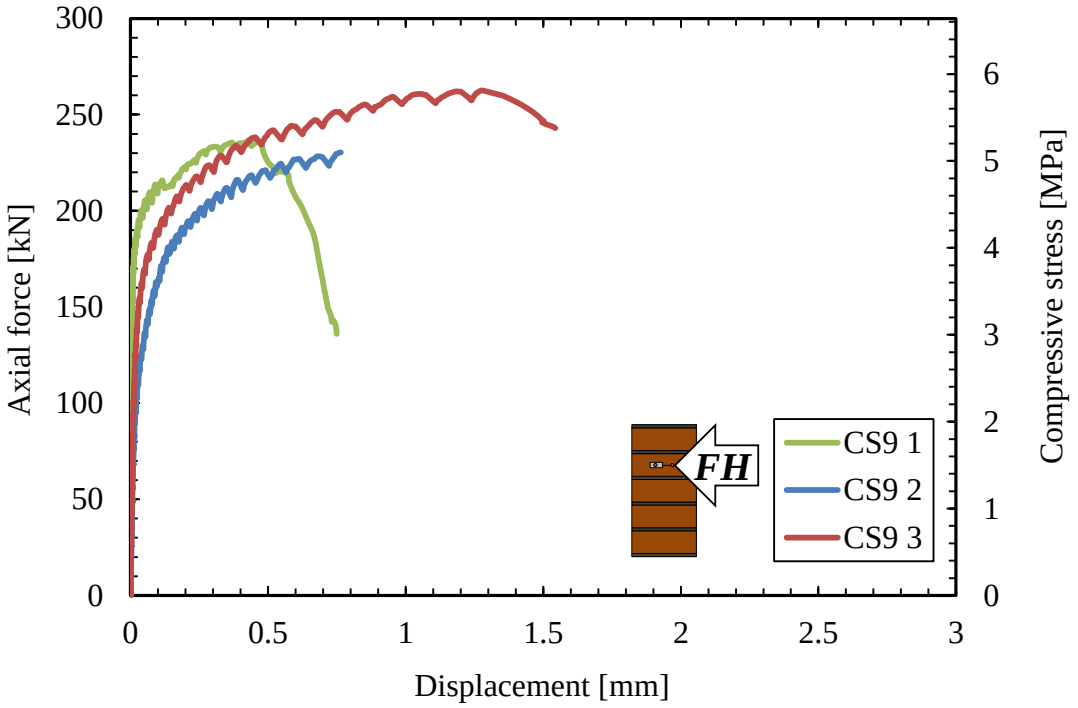

(b)

Figure E.6 Load-displacement curves from compression tests on prisms made with CS9 blocks, front face sensors: (a) vertical, and (b) horizontal.

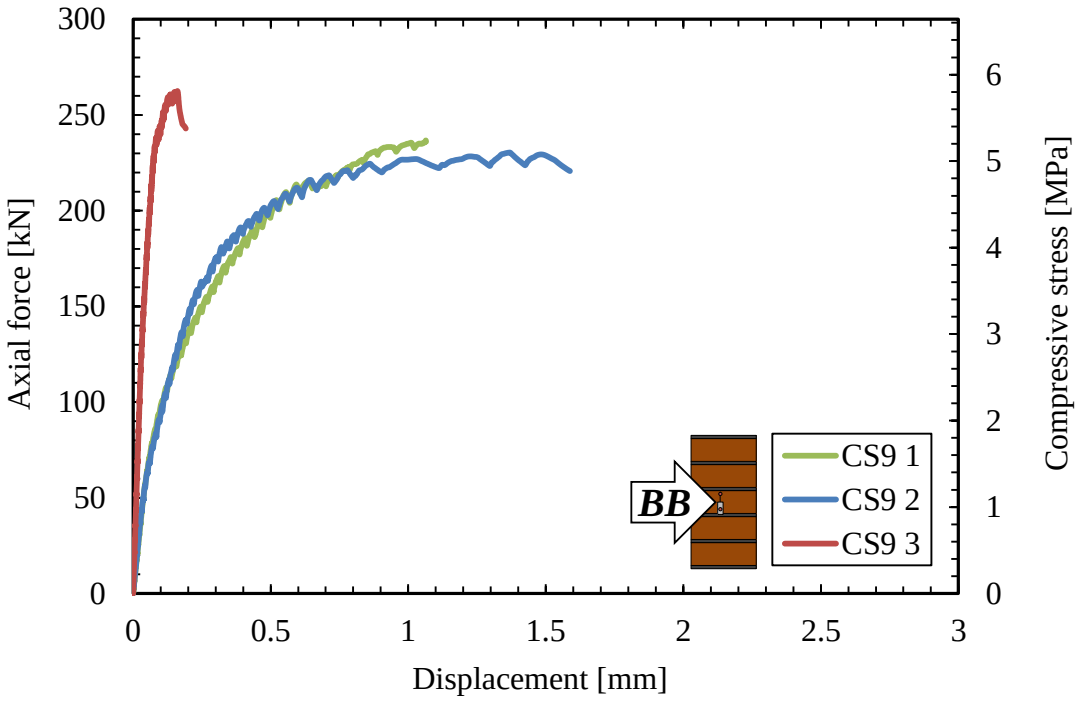

(a)

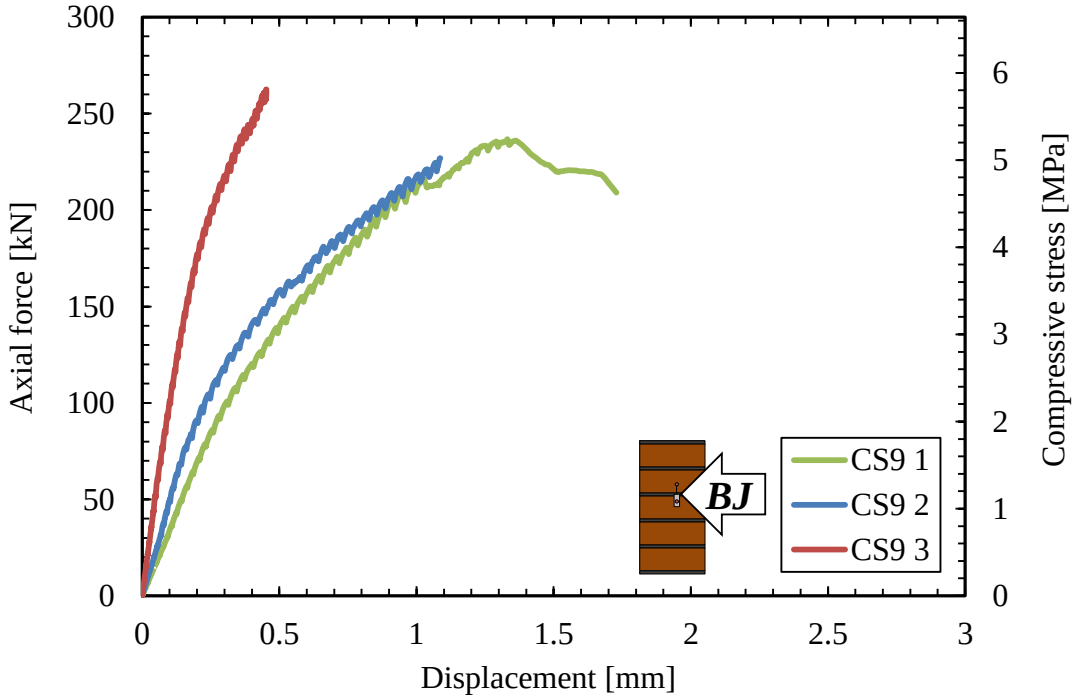

(b)

Figure E.7 Load-displacement curves from compression tests on prisms made with CS9 blocks, back face sensors: (a) block, and (b) joint.

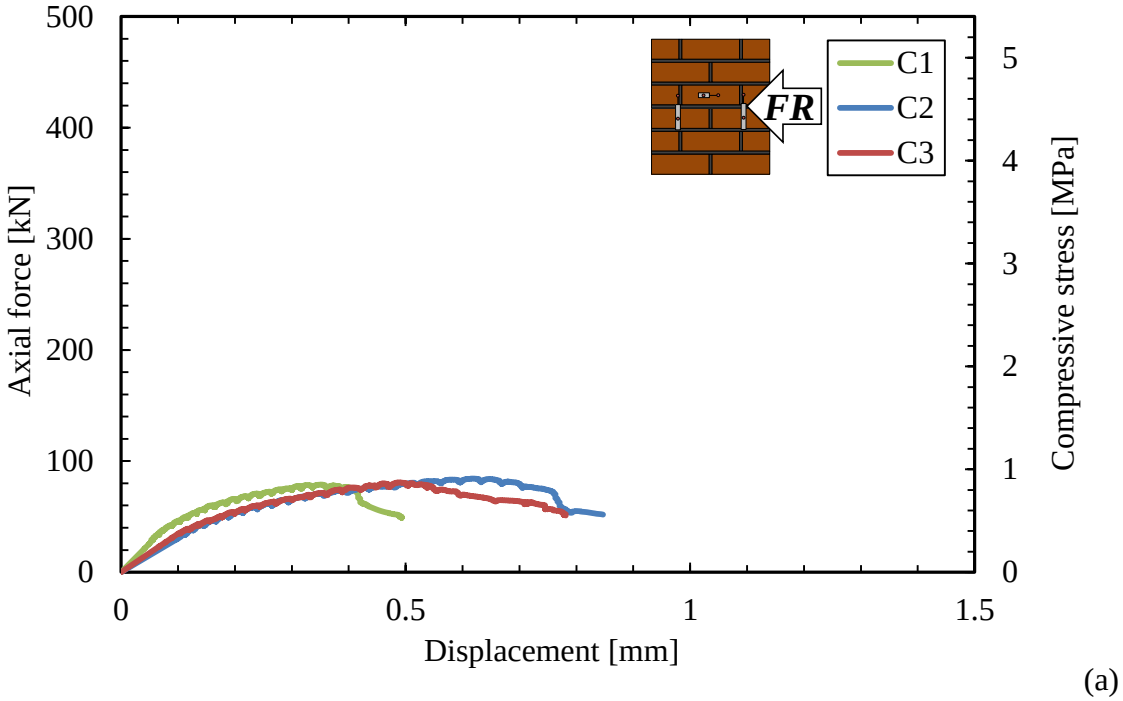

(a)

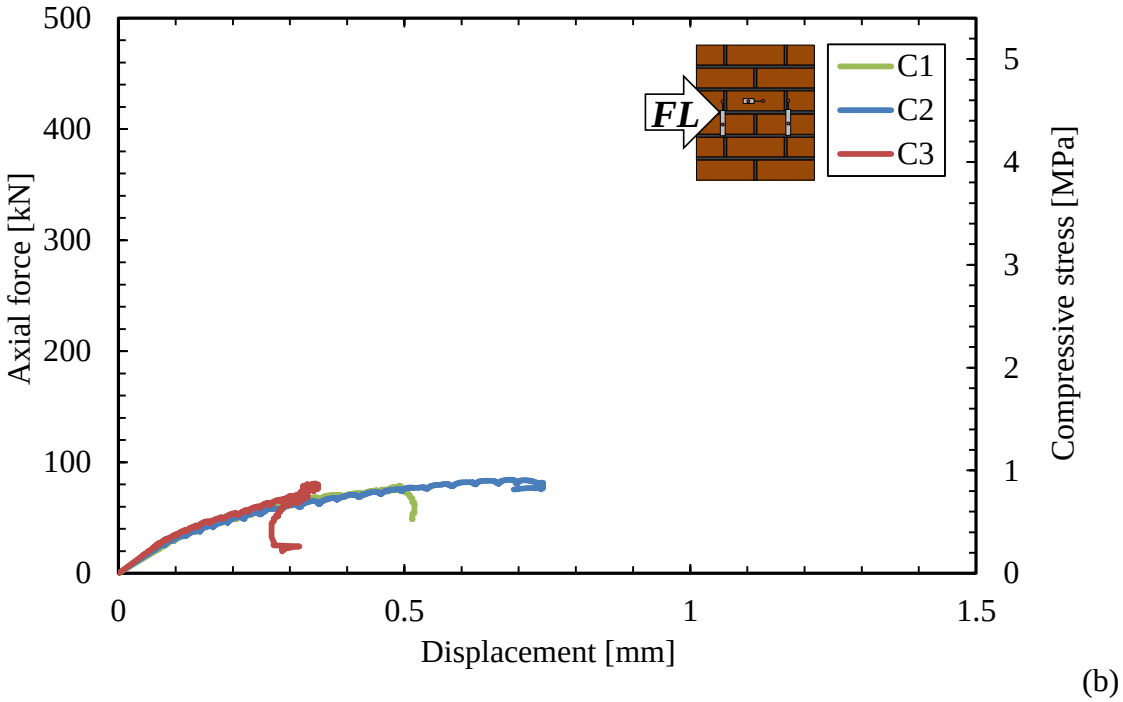

(b)

Figure E.8 Load-displacement curves from compression tests on wallettes made with C blocks, front face sensors: (a) right, and (b) left.

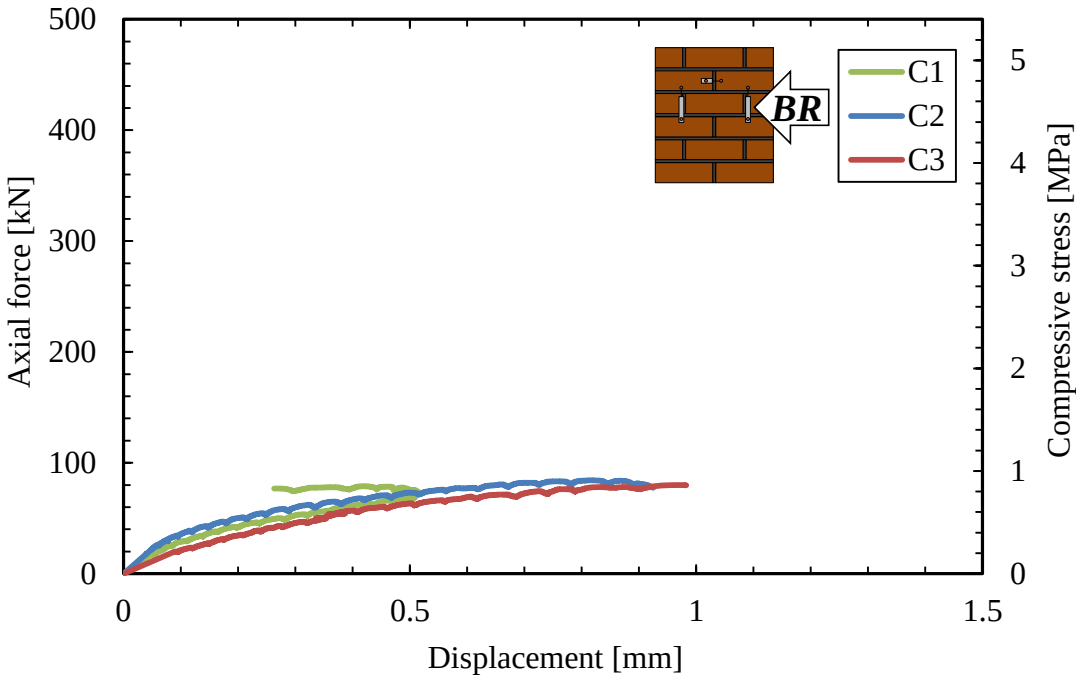

(a)

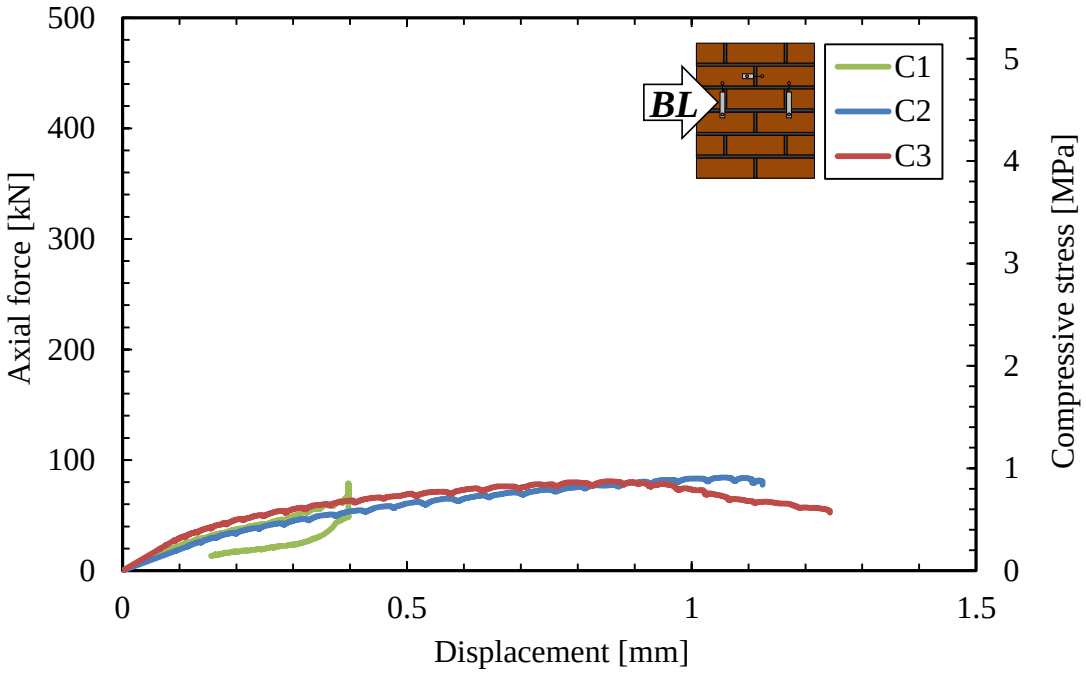

(b)

Figure E.9 Load-displacement curves from compression on wallettes made with C blocks, back face sensors: (a) right, and (b) left.

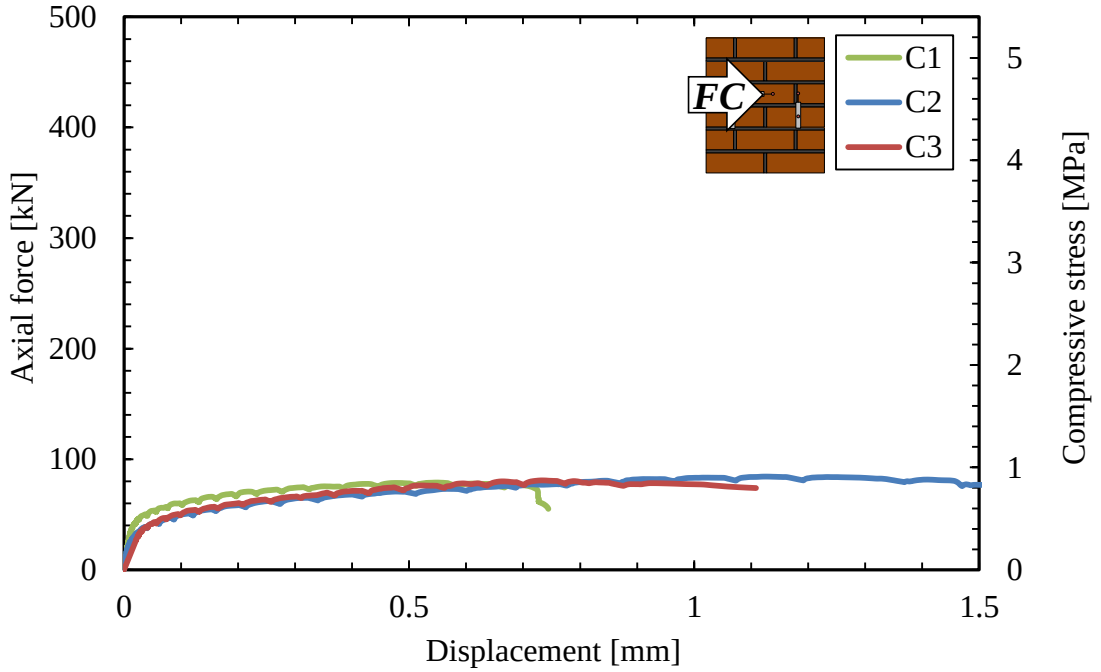

(a)

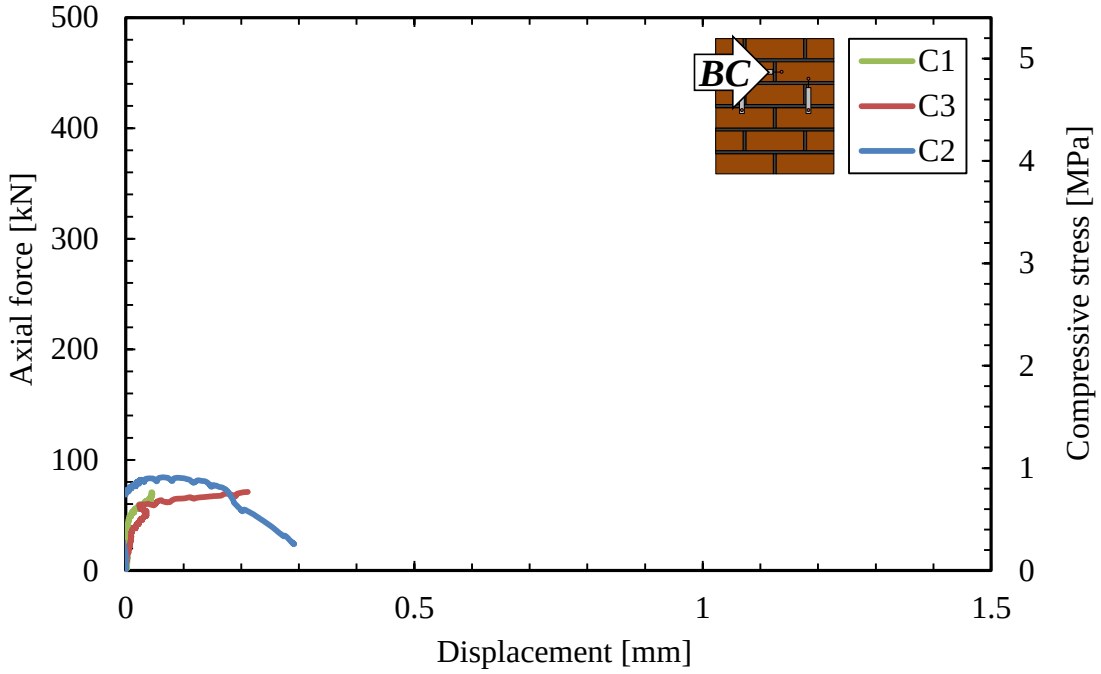

(b)

Figure E.10 Load-displacement curves from compression tests on wallettes made with C blocks: (a) front face center, and (b) back face center.

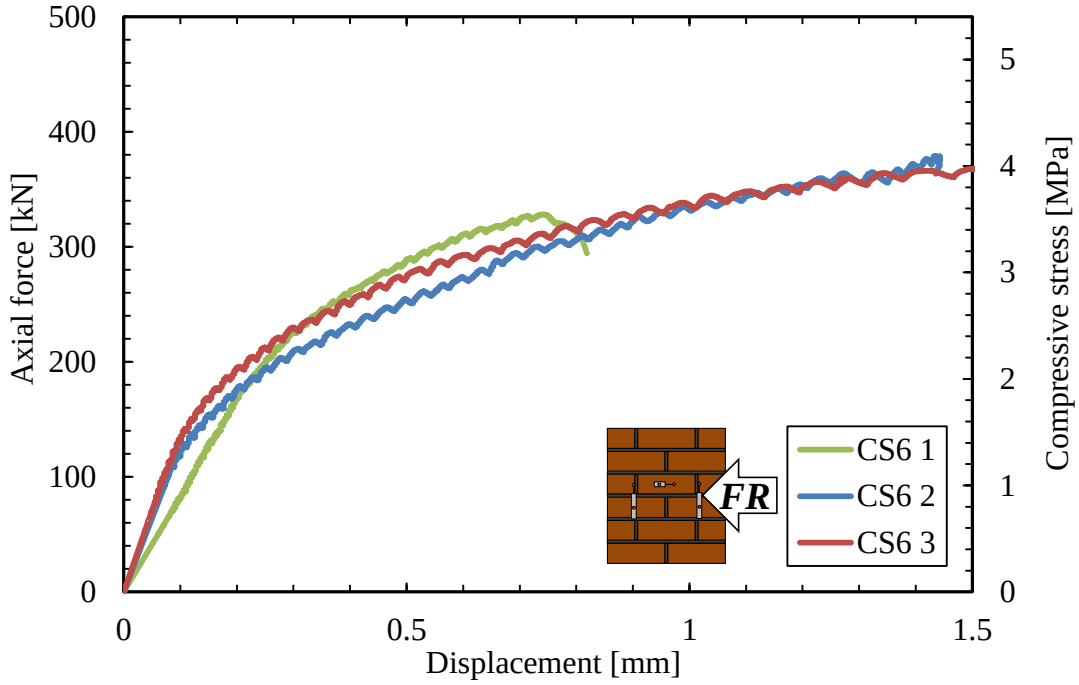

(a)

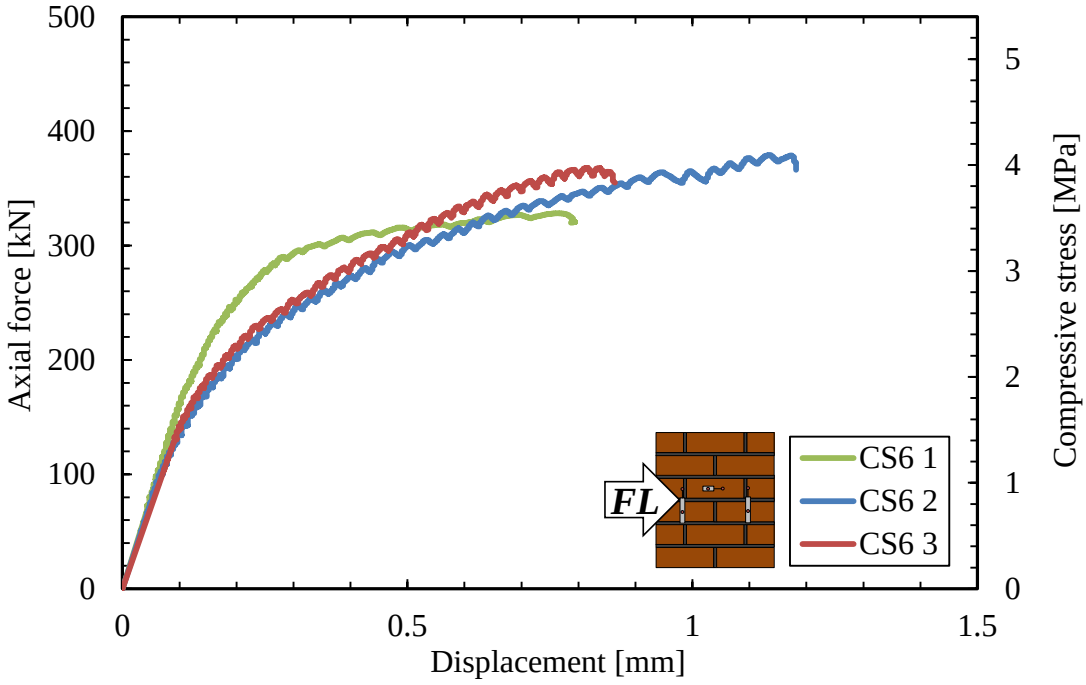

(b)

Figure E.11 Load-displacement curves from compression tests on wallettes made with CS6 blocks, front face sensors: (a) right, and (b) left.

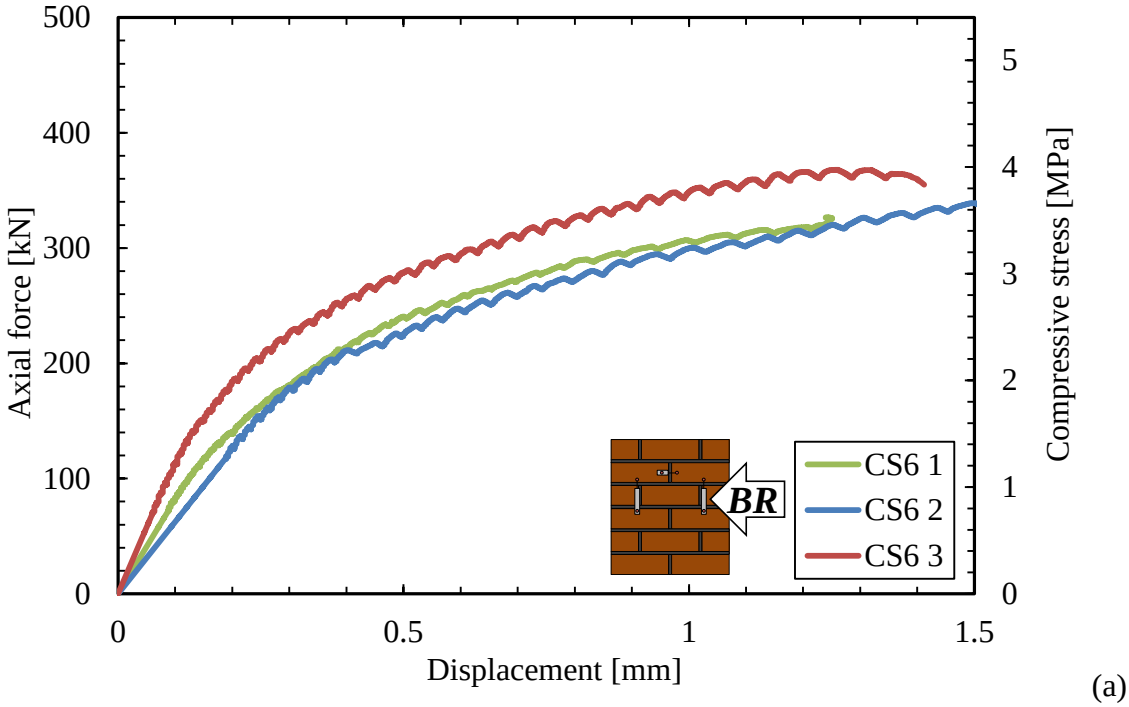

(a)

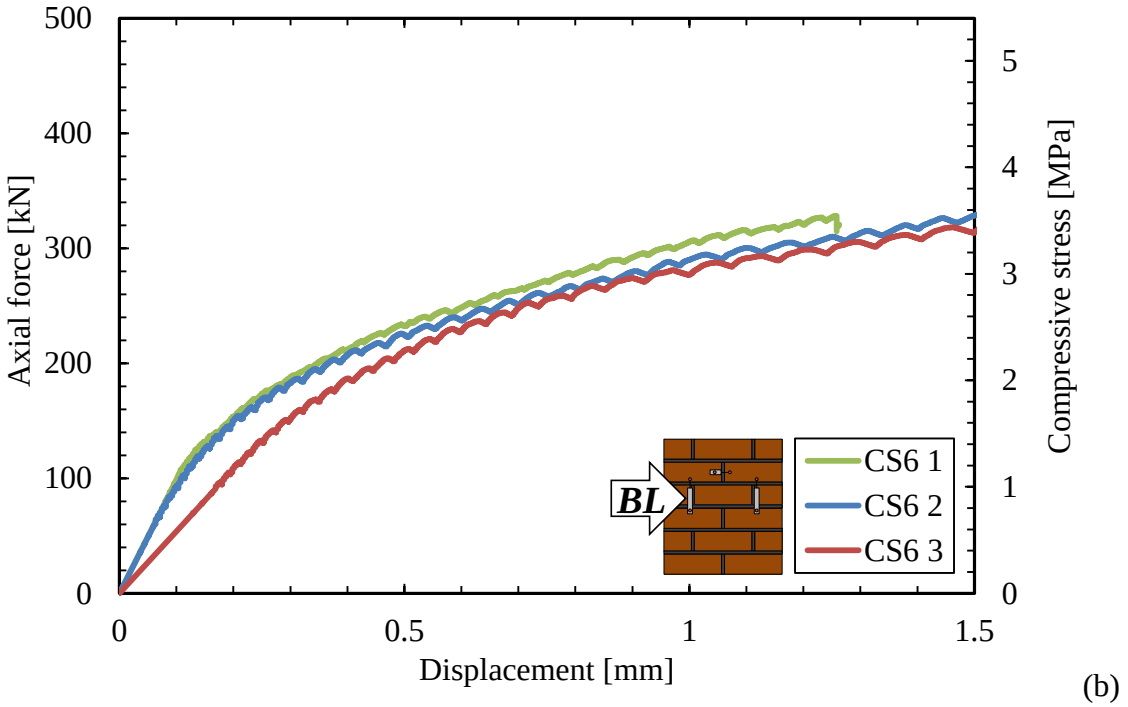

(b)

Figure E.12 Load-displacement curves from compression tests on wallettes made with CS6 blocks, back face sensors: (a) right, and (b) left.

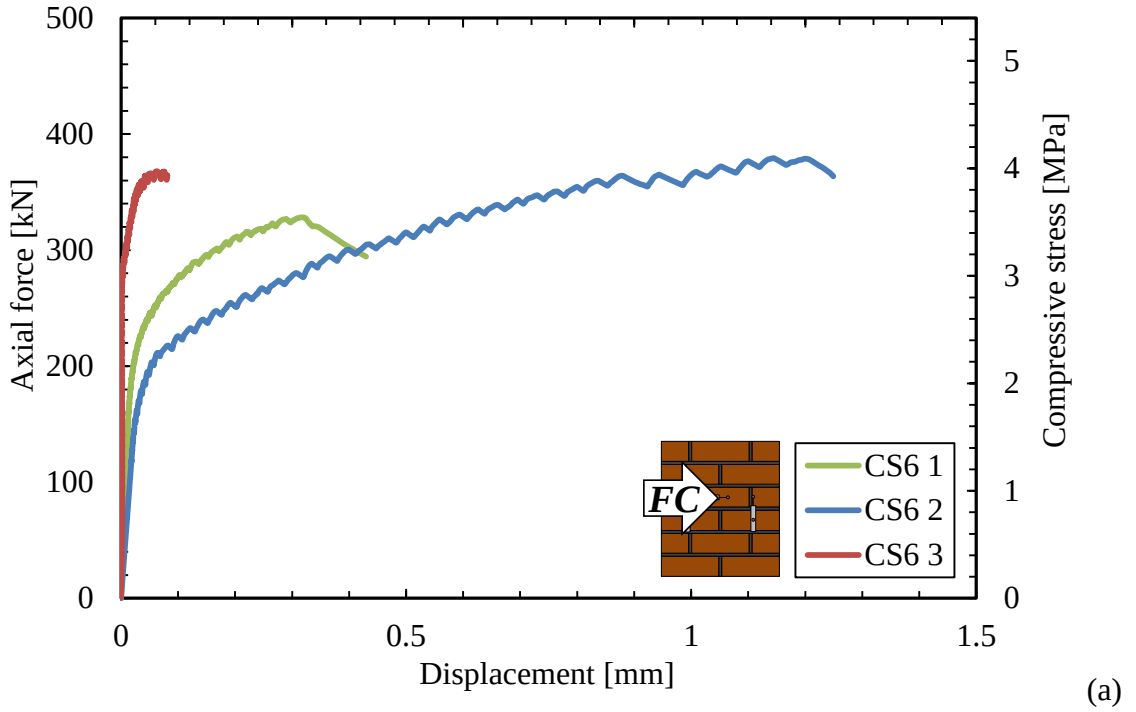

(a)

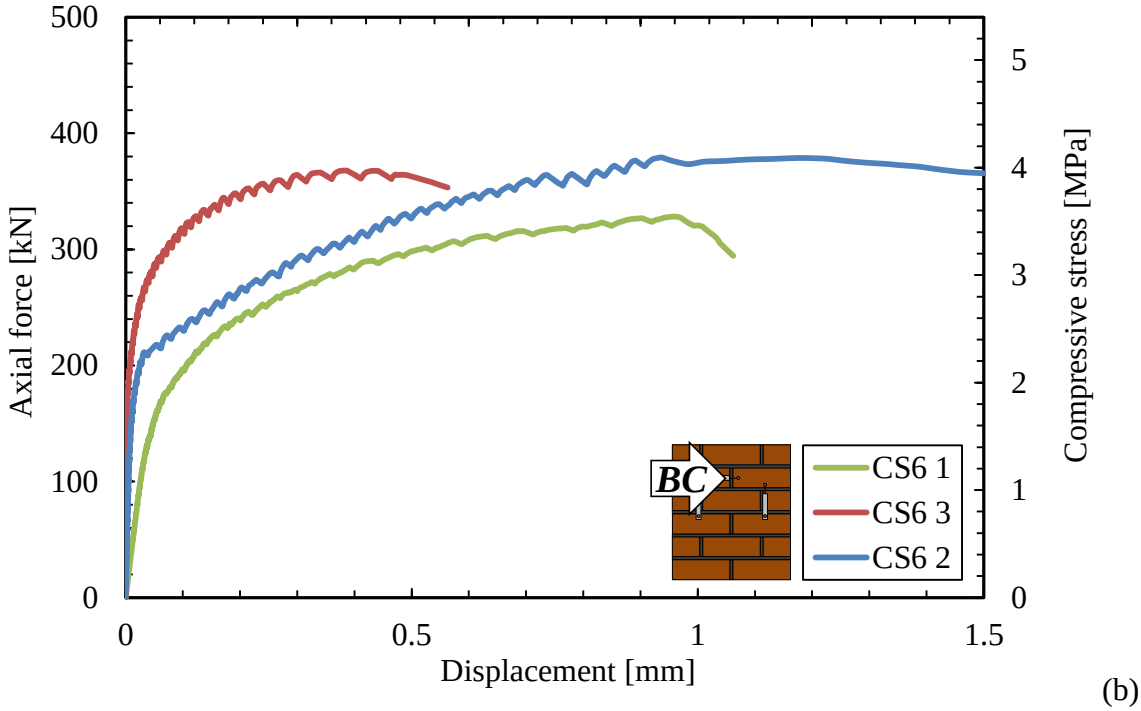

(b)

Figure E.13 Load-displacement curves from compression tests on wallettes made with CS6 blocks: (a) front face center, and (b) back face center.

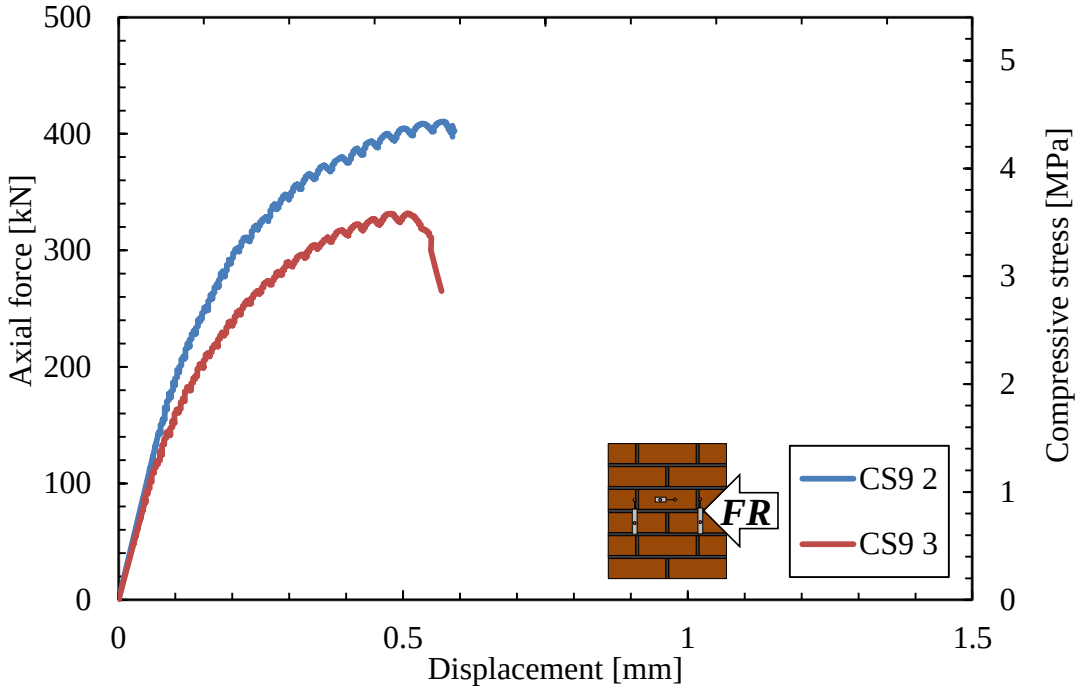

(a)

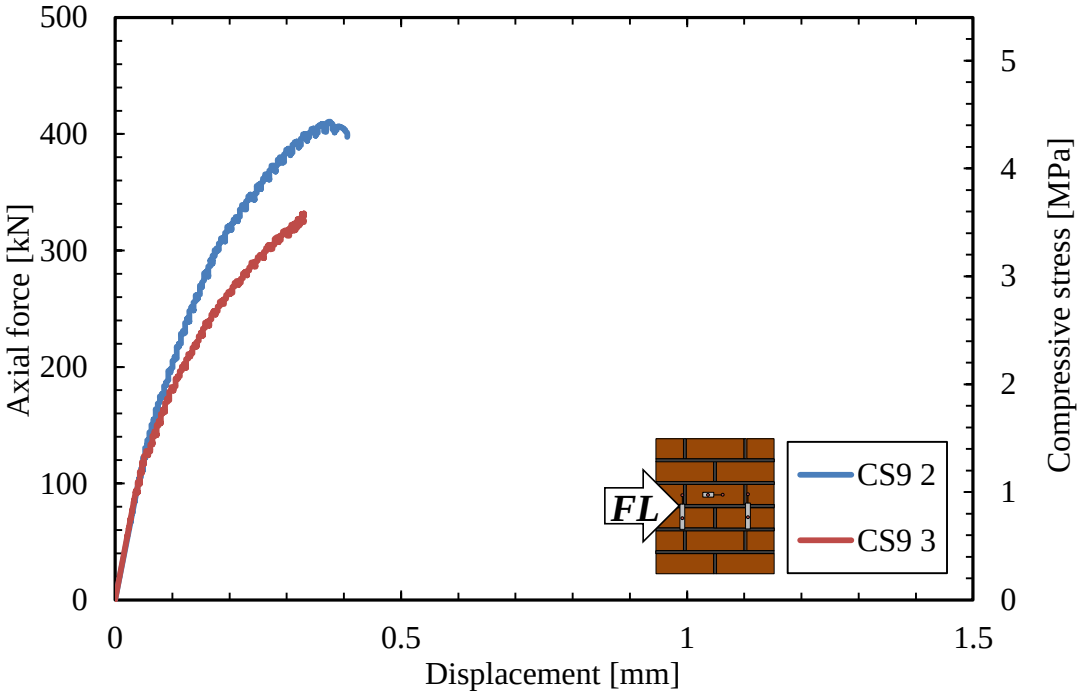

(b)

Figure E.14 Load-displacement curves from compression tests on wallettes made with CS9 blocks, front face sensors: (a) right, and (b) left.

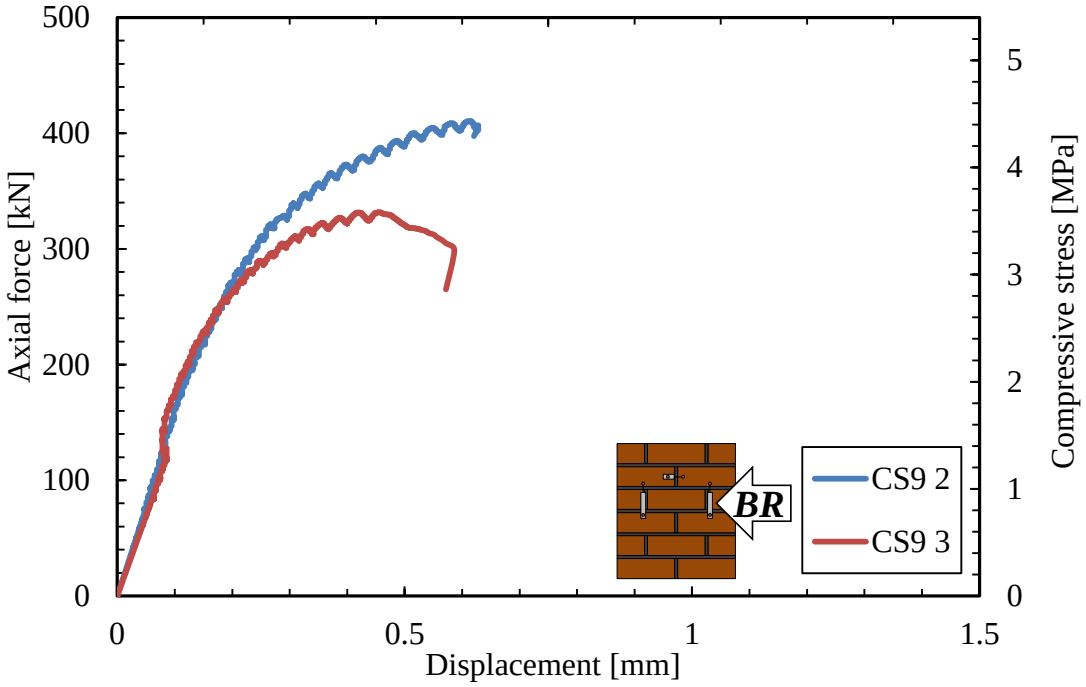

(a)

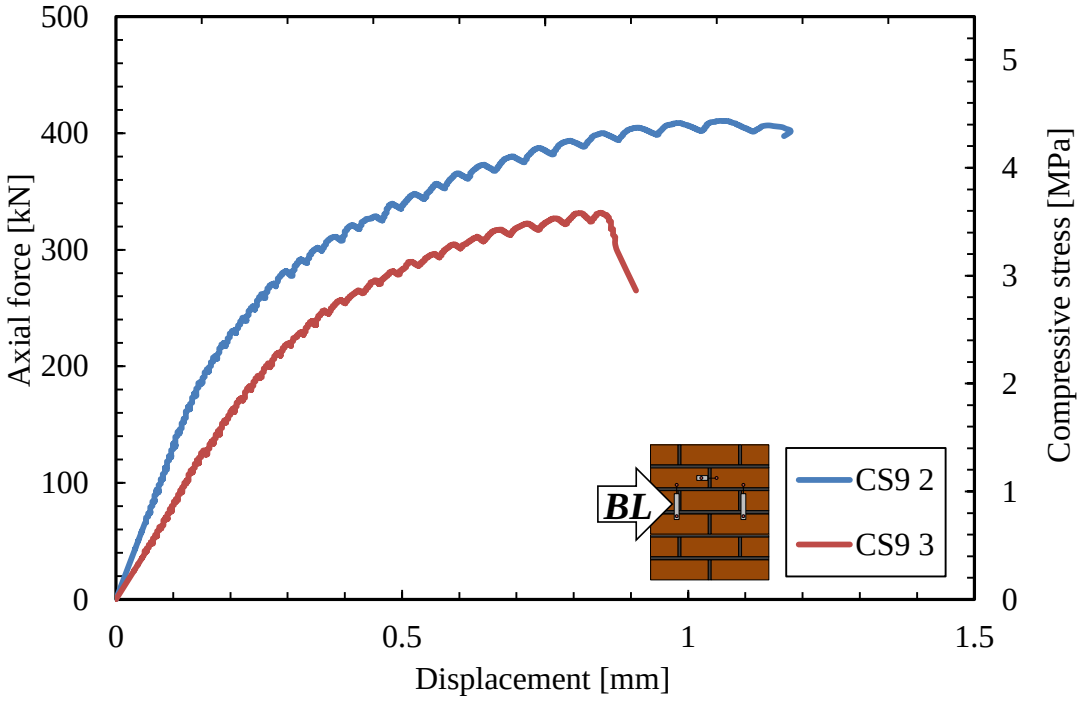

(b)

Figure E.15 Load-displacement curves from compression tests on wallettes made with CS9 blocks, back face sensors: (a) right, and (b) left.

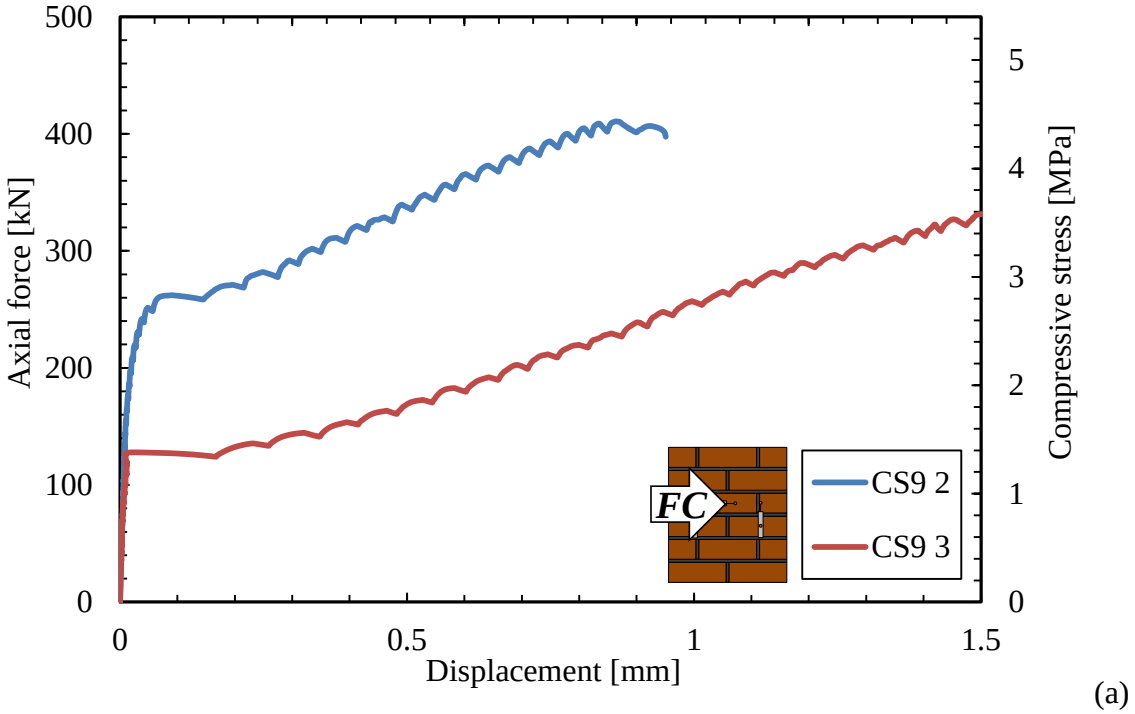

(a)

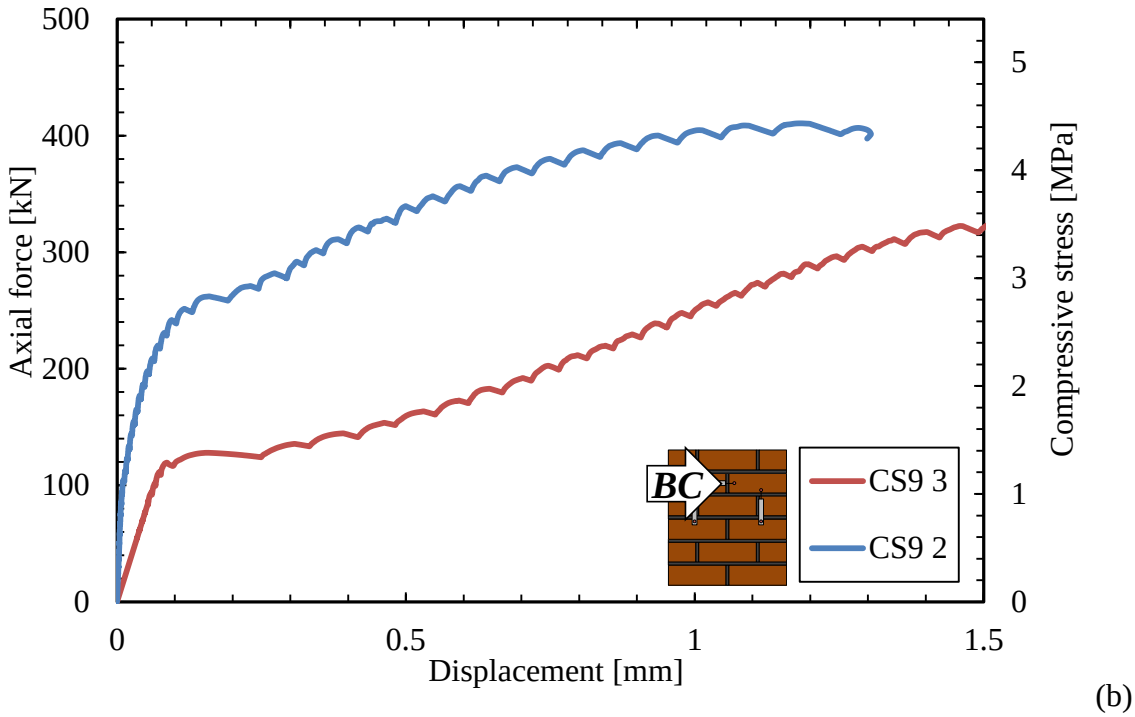

(b)

Figure E.16 Load-displacement curves from compression tests on wallettes made with CS9 blocks: (a) front face center, and (b) back face center.

APPENDIX F – SEM SHEAR STRENGTH CHARACTERIZATION: DIAGONAL COMPRESSION TEST

This appendix presents the results from diagonal compression testing for all SEM and SREM specimens.

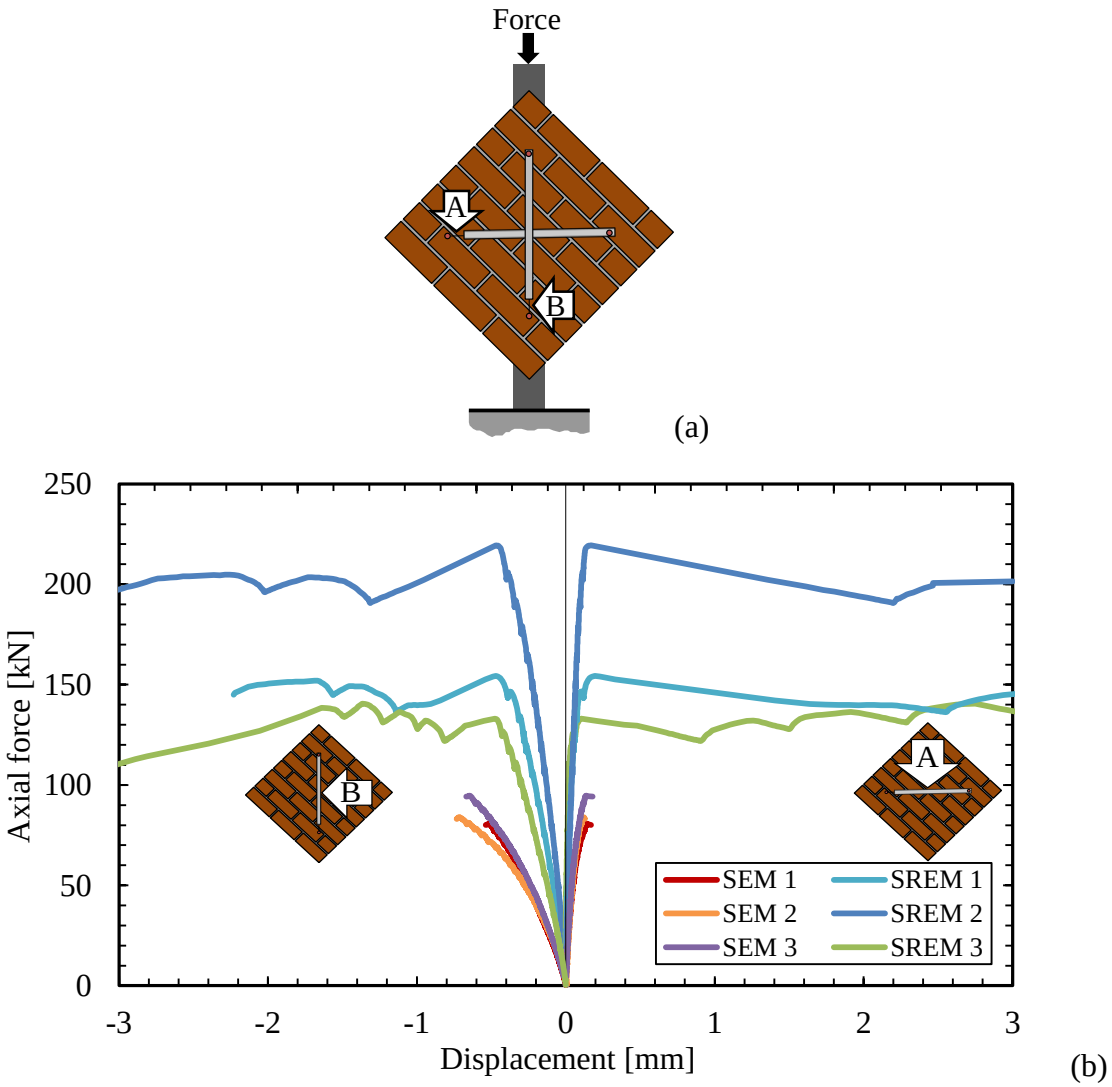

Figure F.1 Diagonal compression test: (a) arrangement of LDT sensors, (b) axial load-(vertical and horizontal) displacement curves.

APPENDIX G – SEM SHEAR STRENGTH CHARACTERIZATION: TRIPLET TEST

This appendix presents the results from direct shear (triplet) tests for all SEM and SREM specimens. Figure G.1 through Figure G.6 show the load-slip (vertical displacement) and the load-joint opening (horizontal displacement) curves based on representative LDT measurements.

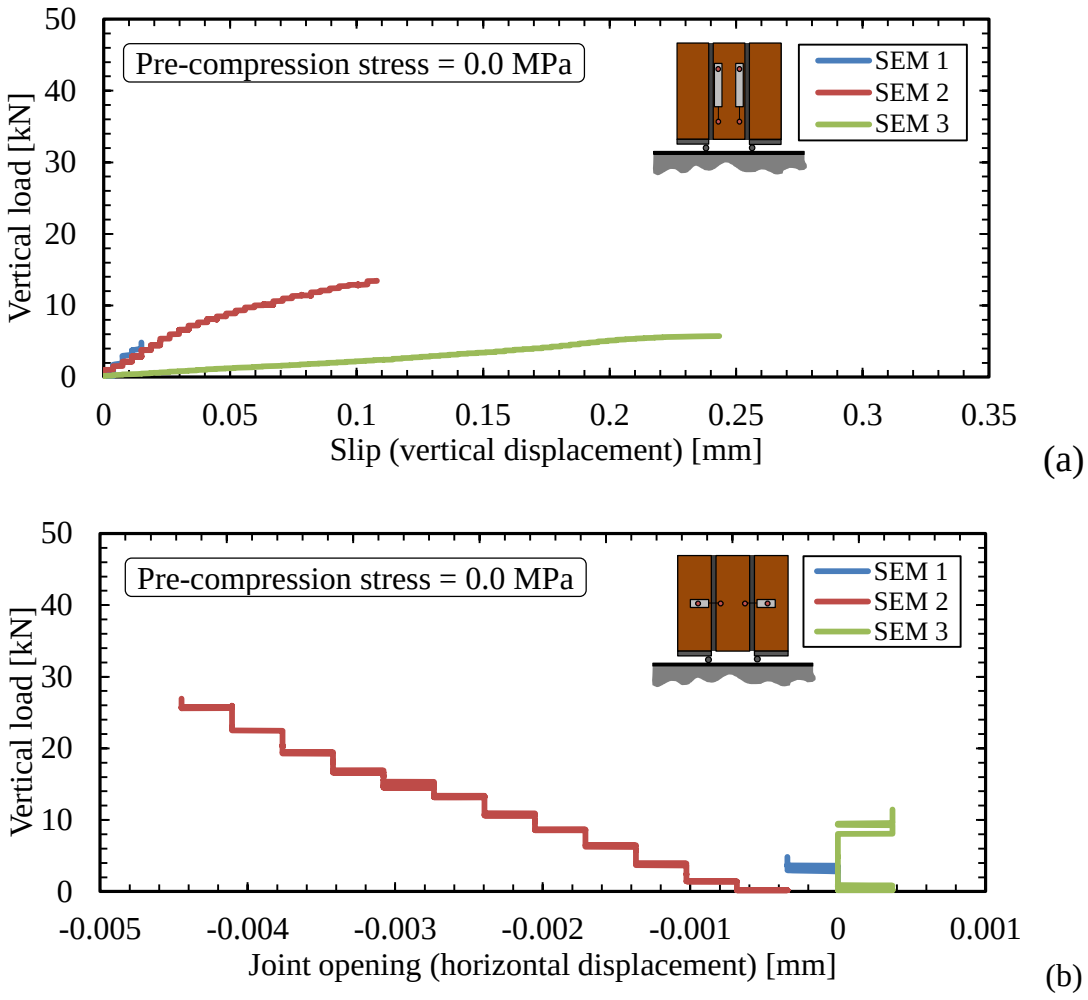

Figure G.1 Load-displacement curves from direct shear test on SEM triplets for 0.0 MPa pre-compression stress: (a) slip, and (b) joint opening (representative LDTs).

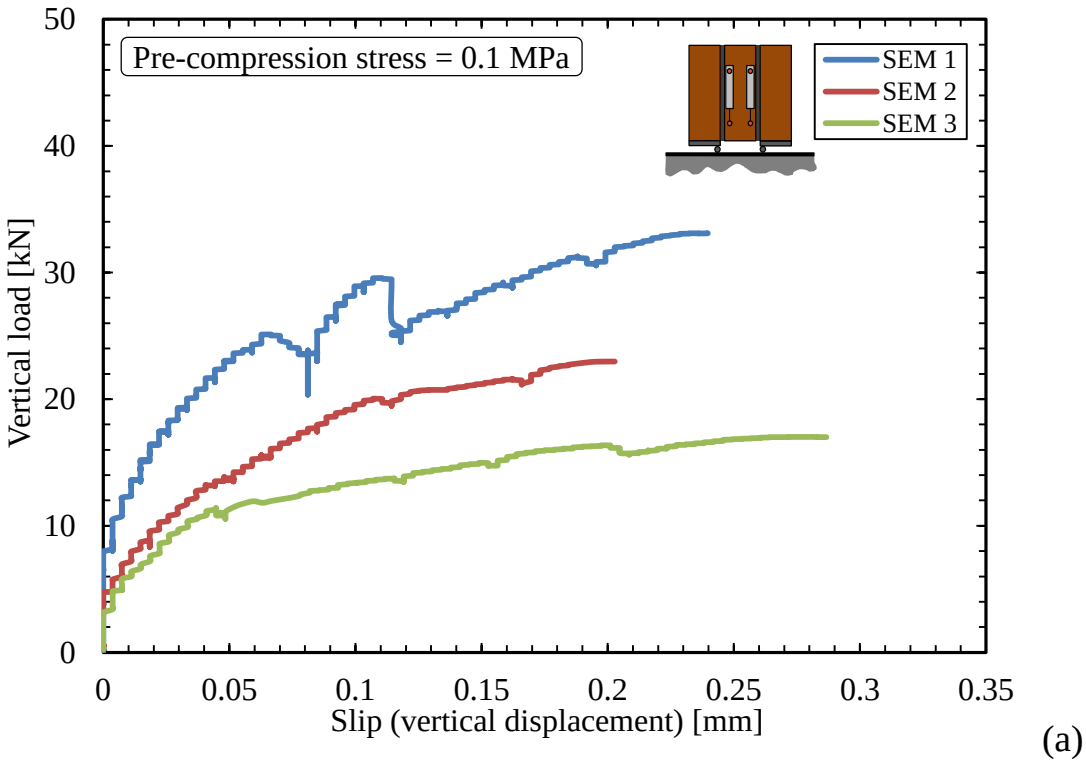

(a)

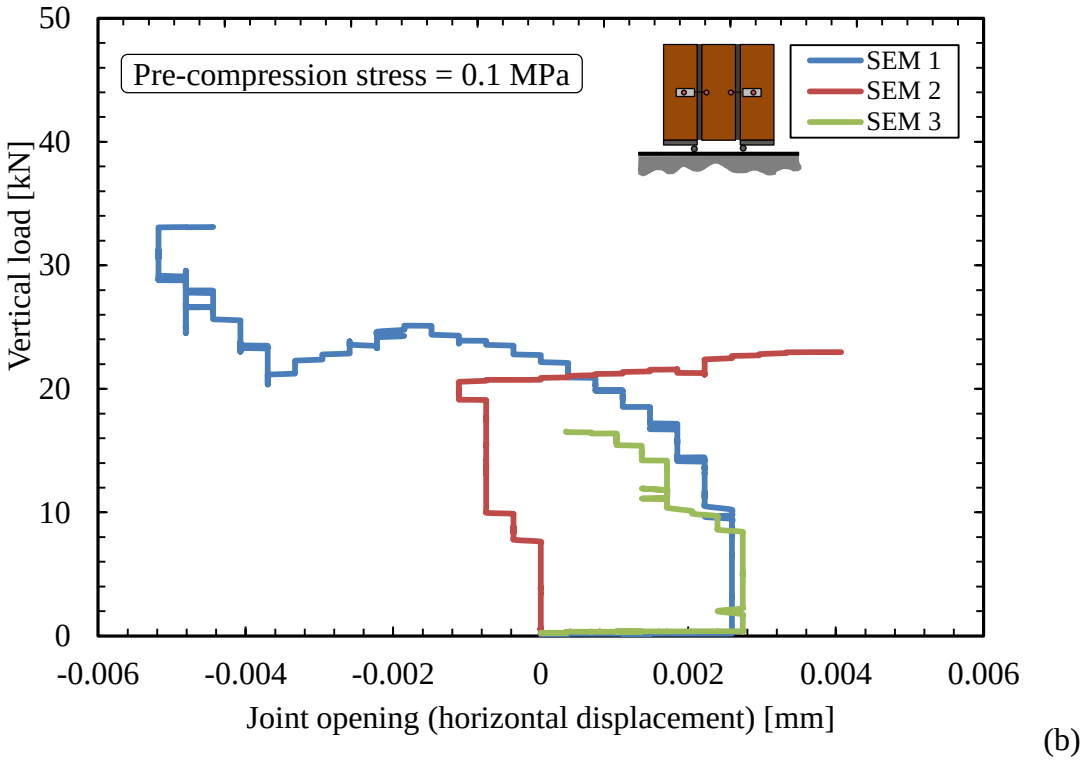

(b)

Figure G.2 Load-displacement curves from direct shear test on SEM triplets for 0.1 MPa pre-compression stress: (a) slip, and (b) joint opening (representative LDTs)

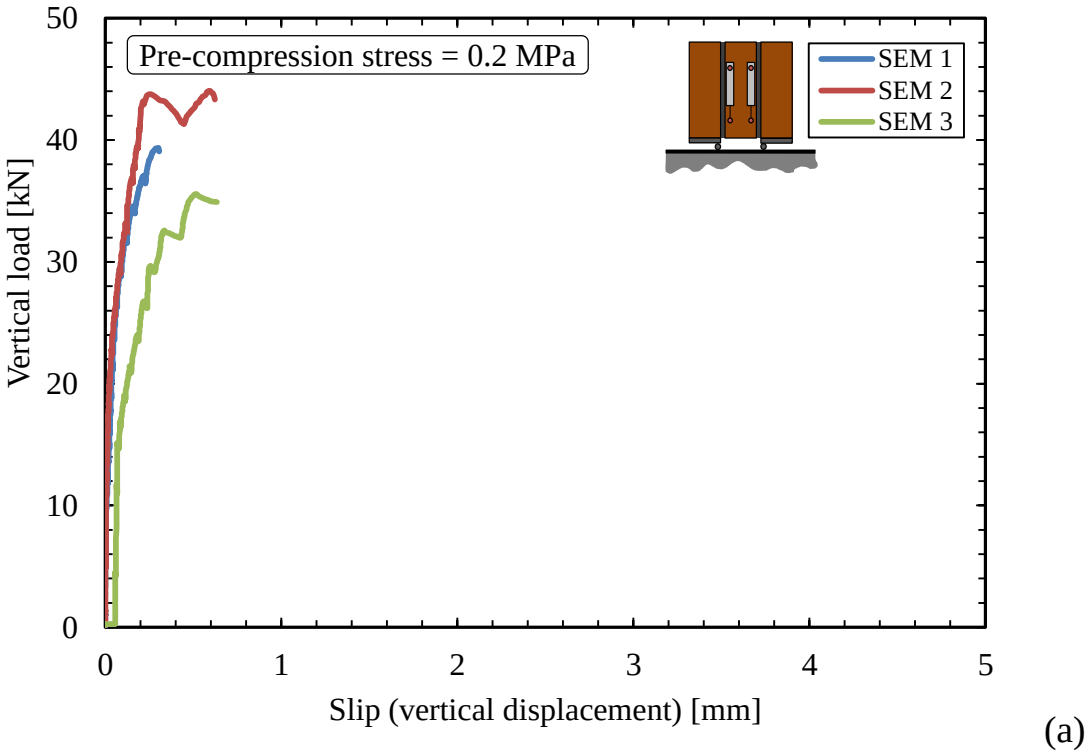

(a)

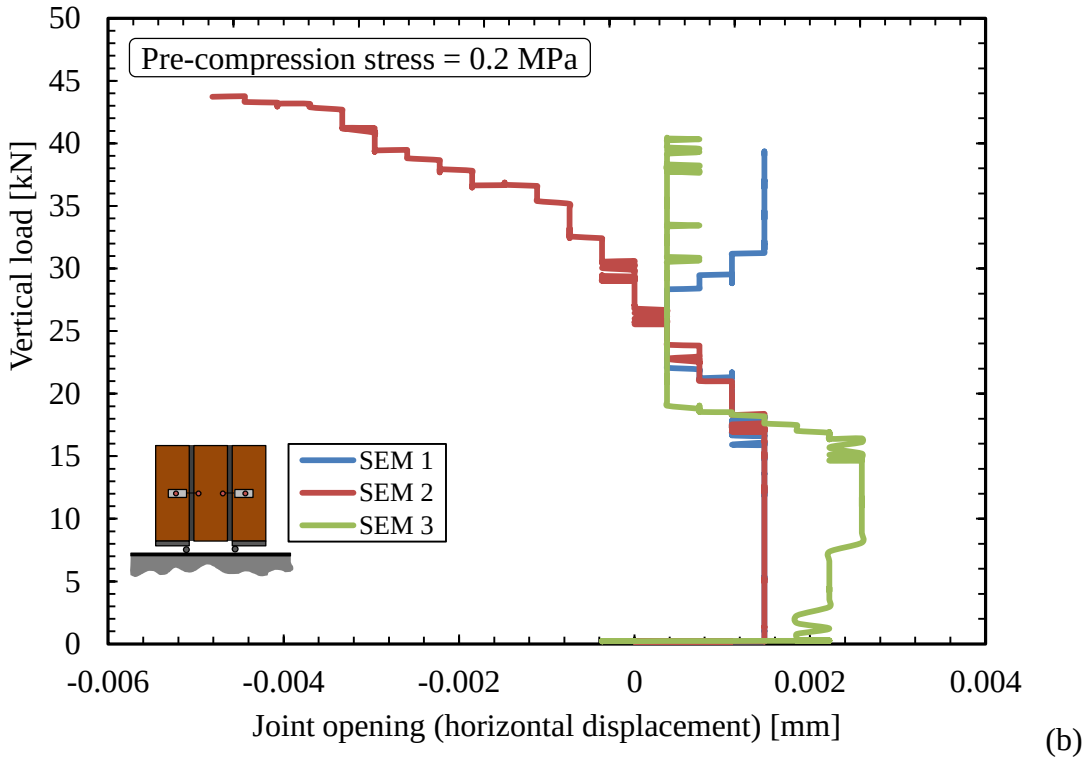

(b)

Figure G.3 Load-displacement curves from direct shear test on SEM triplets for 0.2 MPa pre-compression stress: (a) slip, and (b) joint opening (representative LDTs)

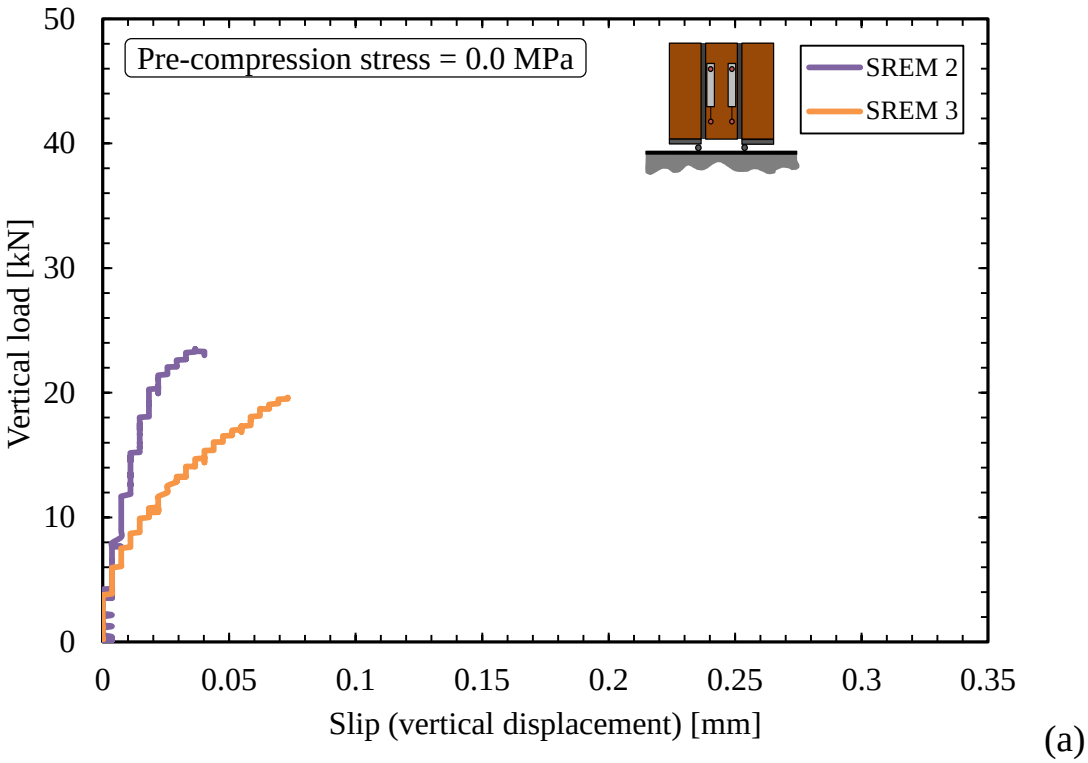

(a)

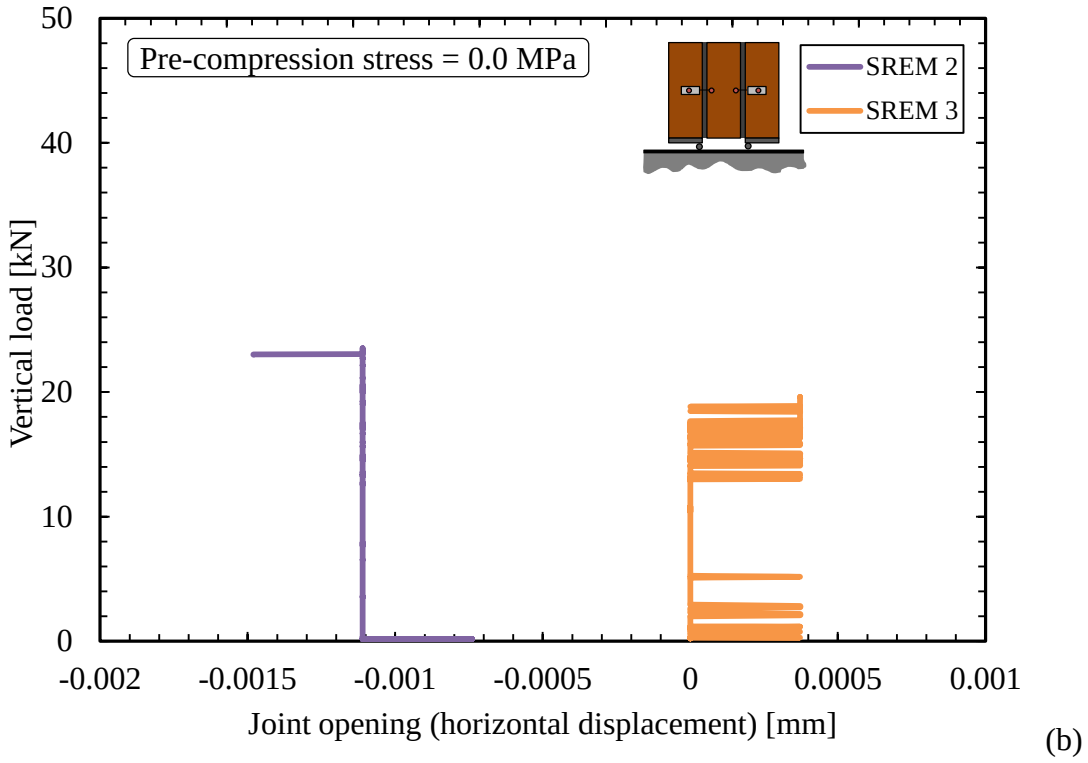

(b)

Figure G.4 Load-displacement curves from direct shear test on SREM triplets for 0.0 MPa pre-compression stress: (a) slip, and (b) joint opening (representative LDTs)

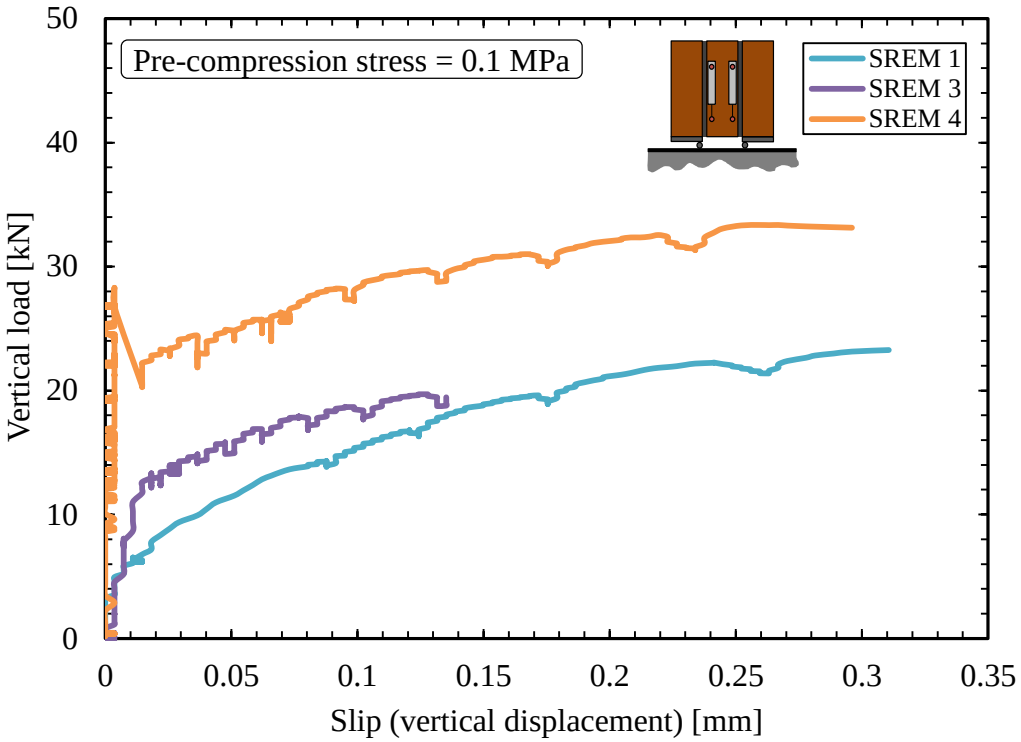

(a)

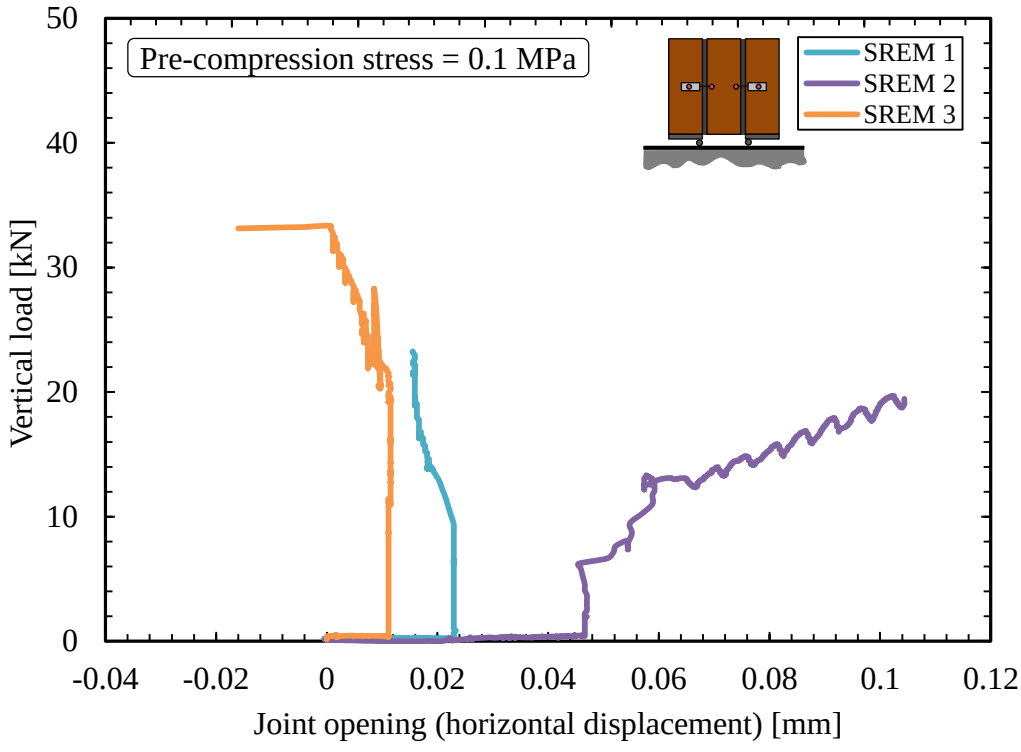

(b)

Figure G.5 Load-displacement curves from direct shear test on SREM triplets for 0.1 MPa pre-compression stress: (a) slip, and (b) joint opening (representative LDTs)

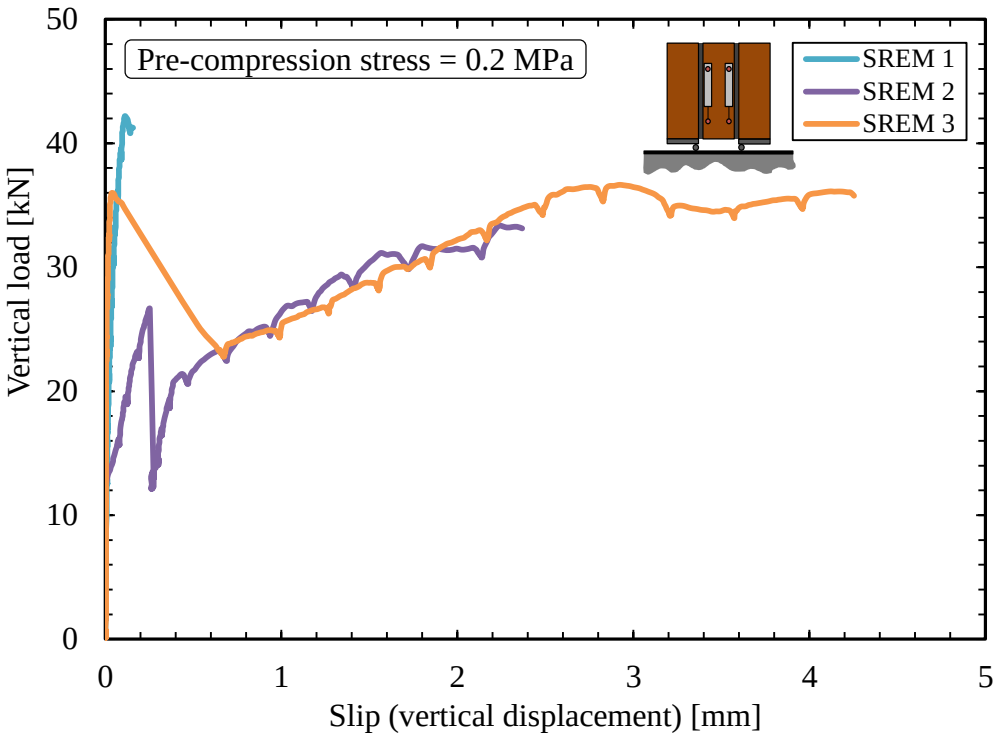

(a)

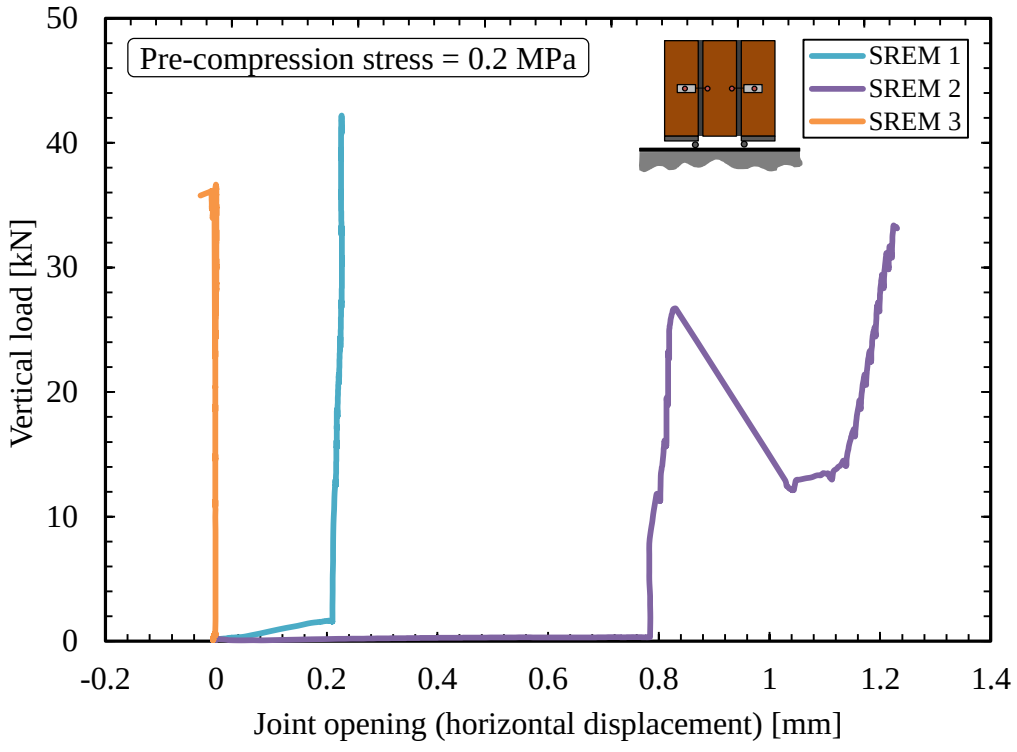

(b)

Figure G.6 Load-displacement curves from direct shear test on SREM triplets for 0.2 MPa pre-compression stress: (a) slip, and (b) joint opening (representative LDTs)